SYNTHESIS OF SUPER ABSORBENT HYDROGELS DERIVED FROM CROSS-LINKING ACTIVATED CHARCOAL AND CITRIC ACID FOR SUSTAINABLE AGRICULTURE IN SEMI-ARID REGIONS

TITUS MUNYAO KASIMU (MSC CHEMISTRY)
I84/27070/2018

Thesis Submitted in Fulfillment of the Requirements for Award of the Degree of Doctor of Philosophy (Chemistry) in the School of Pure and Applied Sciences of Kenyatta University

NOVEMBER, 2022

DECLARATION

I confirm that this thesis is my original work and has not been presented in any other university/institution for certification

Sign……..Date ……..

TITUS MUNYAO KASIMU
I84/27070/2018

SUPERVISORS

This thesis has been submitted with our approval as university supervisors

Sign……..Date ……..

Dr. Harun M Mbuvi

Department of Chemistry

Kenyatta University

Sign……..Date ……..

Dr. Francis M Maingi

Department of Science Technology and Engineering

Kibabii University

DEDICATION

I dedicate this work to my loving wife Evelyne and children Betty and Timothy for their support, encouragement and the sacrifice they gave me throughout my PhD Degree engagement.

ACKNOWLEGEDMENTS

I would like to thank the almighty God for seeing me through this journey to acquire a doctorate degree. After years of hard and difficult work, this study comes to completion. This is not through my personal effort alone but a lot of input, guidance, encouragement and suggestions from my supervisors. Without their contributions, I would have never achieved this goal today. I therefore give my sincere gratitude and appreciation to my supervisors Dr. Harun Mbuvi and Dr. Francis Maingi for their tireless efforts, encouragement, support, advice as well as valuable suggestions I received from them throughout the research period. You have carried me through, may God bless you.

I acknowledge with thanks, the assistance I got from the laboratory technician of KU, JKUAT, Mining and Geology department and Karlsruhe institute of technology (Germany), for their assistance in the laboratory. I cannot forget the support I have received from my colleagues at work for their supportive ideas and advice throughout the research period. May God bless you all. Finally, and not least, I owe my thanks and appreciation to my wife Evelyne and children Betty and Timothy. I thank you for your support, prayers and encouragement even at those times I was too occupied in my study. Your prayers and encouraging words kept me going especially when I felt frustrated and discouraged. Kindly accept my sincere appreciation.

TABLE OF CONTENTS

DECLARATION ii
DEDICATION iii
ACKNOWLEGEDMENTS iv
LIST OF TABLES x
ABSTRACT xv
CHAPTER ONE 1
INTRODUCTION 1
1.1 Background information 1
1.2 Statement of the problem 5
1.3 Justification of the study 6
1.4 Hypothesis 7
1.5 Objectives 7
1.5.1 General objective 7
1.5.2 Specific objectives 7
1.6 Significance of the study 8
1.7 Scope and limitation of study 8
CHAPTER TWO 9
LITERATURE REVIEW 9
2.1 Activated charcoal 9
2.2. Lemon juice as source of citric acid 11
2.3 Super absorbent hydrogels 11
2.4 Classification of hydrogel 12
2.4.1 Homopolymer and copolymeric hydrogels 12
2.4.2 Interpenetrating polymer networks (IPNs) 13
2.4.3 Ionic and nonionic hydrogels 14
2.5. Applications of super absorbent hydrogel 14
2.5.1. Application in human hygiene 14
2.5.2. Biomedical application of the hydrogels 15
2.5 3 Application of hydrogels in agriculture 16
2.6. Effect of hydrogel on growth parameters of maize 17
2.7 Effect of hydrogel on plant yields 18

2.8 Effect of super absorbent hydrogel on soil moisture content 19
2.9 Effect of superabsorbent hydrogels on soil 20
2.10 Synthesis of super absorbent hydrogels 21
2.10.1 Chemically cross-linked super absorbent hydrogels 22
2.10.2 Physically cross-linked hydrogel 23
2.11 Characterization of hydrogels 24
2.12. Scanning electron microscopy (SEM) 24
2.12.1 Working principle 24
2.12.2 Instrumentation 25
2.13 Fourier transform infrared (FT-IR) spectroscopy 26
2.13.1 Working principle 26
2.13.2 Instrumentation 27
2.14. X-ray diffraction (XRD) 28
2.14.1 Working principle 28
2.14.2 Instrumentation 29
CHAPTER THREE 30
MATERIALS AND METHODS 30
3.1 Research design 30
3.2 Collection of sample materials 30
3.3 Chemicals and reagents 31
3.4 Preparation of activated carbon 31
3.5 Extraction of lemon juice (LJ) from lemons as source of citric acid 32
3.6 Preparation of super absorbent hydrogel polymers 32
3.6.1 Synthesis of hydrogel from activated charcoal and glycerol (HCG-1) 32
3.6.2 Synthesis of Cross-linked hydrogel (HCG-2) 32
3.6.3. Synthesis of hydrogel from activated charcoal and ethylenediamine (HCE-1) 33
3.6.4 Crosslinking hydrogel with maleic acid (HCE-2) 34
3.6 5 Preparation of hydrogel from citric acid and glycerol (HLG-1) 35
3.6 6 Preparation of cross-linked hydrogels HLG-2 36
3.6.7 Preparation of hydrogel from lemon juice and ethylenediamine (HLE-1) 36
3.6.8 Preparation of cross-linked hydrogels (HLE-2) 37
3.7 Characterization of the hydrogel 38
3.7.1 Fourier transform infrared (FT-IR) 38

3.7.2 X-ray diffraction (XRD).....38
3.7.3 Scanning electron microscopy (SEM).....39
3.8 Percentage swelling.....40
9 Field preparation and crop management.....40
3.9.1 Field preparation.....40
3.9.2 Field study experiment.....41
3.9.3 Cultural operation and care.....42
3.10 Pre-harvest studies.....42
3.10.1 Percentage moisture in plant.....42
3.10.2 Growth height.....43
3.10.3 Number of leafs per crop.....43
3.10.4 Leaf surface index (LSI).....43
3.10.5 Dry matter accumulation per plant.....44
3.10.6 Rate of crop growth (CGR) (g m^{-2} day^{-1}).....44
3.11 Post harvest studies.....45
3.11.1 Number of cobs per plant.....45
3.11.2 Length of cob determination.....45
3.11.3 Girth of cob.....45
3.11.4 Number of grains per cob.....46
.3.11.5 Mass of grains per cob and cob without maize.....46
3.11.6 Shelling percentage.....46
3.12 Yield of maize.....46
3.12.1 Mean Grain and cob yield per plot.....46
3.12.2 Stover yield.....47
3.12.3 Biological yield.....47
3.13 Harvest index (%).....47
3.14 Statistical analysis.....48
CHAPTER FOUR.....49
RESULTS AND DISCUSSION.....49
4.1 Introductions.....49
4.2 Synthesis of super absorbent hydrogels HCE-1 and HCE-2.....49
4.2.1 Fourier transform infrared of HCE-1 and HCE-2 superabsorbent hydrogel.....50
4.2.2 Phase composition of (HCE-1) and (HCE-2) super absorbent hydrogels.....53

4.2.3 Scanning electron microscopy of (HCE-1) and (HCE-2) super absorbent hydrogels...55

4.3 Synthesis of super absorbent hydrogels HCG-1 and HCG-2.....56

4.3.1 Fourier transform infrared of HCG-1 and HCG-2 super absorbent hydrogels.....57

4.3.2 Phase composition of HCG-1 and HCG-2 super absorbent hydrogels.....59

4.3.3 Scanning electron microscopy (SEM) of HCG-1 and HCG-2 super absorbent hydrogels.....62

4.4 Synthesis of super absorbent hydrogels HLE-1 and HLE-2.....63

4.4.1 Fourier transform infrared of HLE-1 and HLE-2 super absorbent hydrogels.....63

4.4.2 Phase composition of HLE-1 and HLE-2 super absorbent hydrogels.....66

4.4.3 Scanning electron microscope (SEM) of HLE-1 and HLE-2 super absorbent hydrogels.....68

4.5 Synthesis of super absorbent hydrogels HLG-1 and HLG-2.....69

4.5.1 Fourier transform infrared of HLG-1 and HLG-2 superabsorbent hydrogel.....69

4.5.2 Phase composition of HLG-1 and HLG-2 super absorbent hydrogels.....71

4.5.3 Scanning electron microscope (SEM) of HLG-1 and HLG-2 super absorbent hydrogels.....74

4.6 Optimization of synthesis parameters for super absorbent Hydrogels.....75

4.6.1 Effect of citric acid (CA) dosage on the swelling capacity of HLG-2 and HLE-2 hydrogels.....75

4.6.2 Optimization of amount of activated charcoal used on HCG-2 and HCE-2 hydrogels.....78

4.6.3 Optimization of maleic acid dosage on HLG-2, HLE-2, HCG-2, and HCE-2 hydrogels.....80

4.6.4 Optimization of contact time on HLG-2, HLE-2, HCG-2, and HCE-2 hydrogels.....86

4.7 Effect of HCE-2, HCG-2, HLE-2, and HLG-2 super absorbent hydrogels on the growth parameters of maize crops.....91

4.7.1 Effect of hydrogels dosage on moisture content percentage at flowering stage.....92

4.7.2 Effect of super absorbent hydrogels dosage on plant height.....94

4.7.3 Effect of hydrogel dosage on number of leaves.....98

4.7.4 Effect of super absorbent hydrogel dose on plant leave area index in cm^2.....103

4.7.5 Effect of super absorbent hydrogel dose on dry matter accumulation (DMA).....107

4.7.6 Effect of super absorbent hydrogel dose on crop growth rate (g/m^2/day) (CGR).....111

4.8 Effects of super absorbent hydrogel on post-harvest parameters.....116

4.8.1 The effect of hydrogels on number of Cob per plant.....117

4.8.2 The effect of hydrogels on number of Grains per cob.....118

4.8.3 The effect of hydrogels on girth of the Cob (cm).....119
4.8.4 The effect of hydrogels on cob length (cm).....120
4.8.5 The effect of hydrogels on grains weight per cob (g).....122
4.8.6 The effect of hydrogels on weight of the cob (g).....123
4.9 The effect of hydrogels on shelling % 124
4.10. The effect of super absorbent hydrogels dose on Yield and harvest index.....125
4.10.1 The effect of hydrogels on grain yield (kg/ha).....125
4.10.2 The effect of hydrogels on stover yield (kg/ha).....127
4.10.3 The effect of hydrogels on cob yield (kg/ha).....128
4.10.4 The effect of hydrogels on biological yield (Kg/ha).....129
4.10.5 The effect of hydrogels on harvest index %.....130
CHAPTER FIVE 132
CONCLUSIONS AND RECOMMENDATIONS.....133
5.1 Conclusions.....133
5.2 Recommendations.....134
5.2.1 Recommendation from this work.....134
5.2.2 Recommendation for further research.....135
REFERENCES.....136
APPENDICES.....154

LIST OF TABLES

Table 2.1: Selected hydrogel absorbents applied in agriculture. 17
Table 2.2: Selected methods for hydrogel preparations..... 21
Table 3.1: Shows the randomized block design used in application of the hydrogels 41

LIST OF FIGURES

Figure 2.1: Chemical structure of Carbon 10
Figure 2.2: Schematic diagram for scanning electron microscope (NI, 2016). 25
Figure 2.3: Block diagram for FT-IR spectrometer 27
Figure 2.4: Schematic diagram for X-ray diffraction (XRD) (Source NI, 2016) 29
Figure 3.1: Scheme of preparation of HCG-1and HCG-2 hydrogel 33
Figure 3.2: Scheme of preparation of HCE-1and HCE-2hydrogel 35
Figure 3.3: Scheme of preparation of HLG-2 hydrogel 36
Figure 3.4: Scheme of preparation of HLE-2 hydrogel 37
Figure 4.2.1: FT-IR spectrum of HCE-1 50
Figure 4.2.2: FT-IR spectrum of HCE-2 52
Figure 4.2.3: Powdered diffraction pattern of HCE-1. 53
Figure 4.2.4: shows the powdered diffraction pattern of cross-linked HCE-2. 54
Figure 4.3.1: FT-IR spectrum of HCG-1 57
Figure 4.3.2: FT-IR spectrum of HCG-2 58
Figure 4.3.3: Powdered diffraction pattern of HCG-1. 59
Figure 4.3.4: Powdered diffraction pattern of HCG-2. 60
Figure 4.4.1: FT-IR spectrum of HLE-1 64
Figure 4.4.2: FT-IR spectrum of HLE-2 65
Figure 4.4.3: Powdered diffraction pattern of HLE-1. 66
Figure 4.4.4: Powdered diffraction pattern of HLE-2 67
Figure 4.4.5: SEM micrographs of the (A) HLE-1 and (B) HLE-2 hydrogel 68
Figure 4.5.1: FT-IR spectrum of HLG-1 69
Figure 4.5.2: FT-IR spectrum of HLG-2 70
Figure 4.5.3: Powdered diffraction pattern of uncross linked HLG-1. 72
Figure 4.5.4: Powdered diffraction pattern of cross-linked HLG-2. 73
Figure 4.5.5: SEM micrographs for (A) HLG-1 and (B) HLG-2 74
Figure 4.6.1: The effect of amount of citric acid used on the percentage swelling of 2.0 g of HLG-1 (at 5 g glycerol, 2 g maleic acid, 1 g NaOH) 76
Figure 4.6.2: The effect of amount of citric acid used on the percentage swelling of 2.0 g of HLE-2 (at 5 g ethylenediamine, 2 g maleic acid, 1 g NaOH) 77
Figure 4.6.3: The effect of amount of activated charcoal on the percentage swelling of 2.0 g HCG-2 (at 5 g glycerol, 2 g maleic acid, 1 g NaOH) 78
Figure 4.6.4: The effect of amount of activated charcoal on the percentage swelling of 2.0 g HCE-2 (at 5 g Ethylenediamine, 2 g maleic acid, 1 g NaOH) 79
Figure 4.6.5: The effect of amount of maleic acid on the percentage swelling of 2.0 g HLG-2 hydrogel immersed in 500 mL of distilled water and contact time of 24 hours (at 6 g CA, 5 g G, 1 g NaOH) 81
Figure 4.6.6: The effect of amount of maleic acid on the percentage swelling of 2.0 g HCG-2 hydrogel immersed in 500 mL of distilled water and contact time of 24 hours (at 6 g AC, 5 g EA, 1 g NaOH) 82
Figure 4.6.7: The effect of amount of maleic acid on the percentage swelling of 2.0 g HCE-2 hydrogel immersed in 500 mL of distilled water and contact time of 24 hours (at 6 g AC, 5 g EA, 1 g NaOH) 84

Figure 4.6.8: The effect of amount of maleic acid on the percentage swelling of 2.0 g of HLE-2 hydrogel immersed in 500 mL of distilled water and contact time of 24 hours (at 8 g CA and 5 g EA, 1 g NaOH) 85
Figure 4.6.9: The effect of contact time on the percentage swelling of 2.0 g HLG-2 hydrogel prepared at optimum conditions reacting volume CA: G: MA of (5.4: 3.75: 3.75) immersed in 500 mL of distilled water..... 87
Figure 4.6.10: The effect of contact time on the percentage swelling of 2.0 g of HLE-2 hydrogel prepared using CA, EDA, and MA at a volume ratio of 144:90:75 respectively immersed in 500 mL of distilled water. 88
Figure 4.6.11: The effect of contact time on the percentage swelling of 2.0 g HCE-2 hydrogel prepared at optimum conditions of AC: EDA: MA of 6:5:2 immersed in 500 mL of distilled water..... 89
Figure 4.6.12: The effect of contact time on the percentage swelling of 2.0 g HCG-2 hydrogel prepared at optimum conditions of AC: G: MA of 6:5:1 immersed in 500 mL of distilled water 91
Figure 4.7.1: Effect of super absorbent hydrogels dose on average moisture percentage 93
Figure 4.7.2(a): Effect of hydrogel dose on plant height using 15kg/ha of HCE-2, HCG-2, HLE-2 and HLG-2 hydrogels..... 94
Figure 4.7.2(b): Effect of hydrogel dose on plant height using 30kg/ha of HCE-2, HCG-2, HLE-2 and HLG-2 hydrogels..... 95
Figure 4.7.2(c): Effect of hydrogel dose on plant height using HCE-2, HCG-2, HLE-2 and HLG-2 hydrogels when 45kg/ha was applied 96
Figure 4.7.2(d): Effect of hydrogel dose on plant height using HCE-2, HCG-2, HLE-2, and HLG-2 hydrogels when 60kg/ha was applied. 97
Figure 4.7.3(a): Effect of hydrogel dose on number of leaves using HCG-2, HLE-2, HLG-2 and HCE-2 hydrogels when 15 kg/ha was applied..... 99
Figure 4.7.3(b): Effect of hydrogel dose on number of leaves using HCG-2, HLE-2, HLG-2 and HCE-2 hydrogels when 30 kg/ha was applied..... 100
Figure 4.7.3(c): Effect of hydrogel dose on number of plant leaves using HCG-2, HLE-2, HLG-2 and HCE-2 hydrogels when 45 kg/ha was applied 101
Figure 4.7.4(a): Effect of super absorbent hydrogels dose (15 kg/ ha) of HCG-2, HLE-2, HLG-2 and HCE-2 on leaf area index (LAI) (cm^2)..... 103
Figure 4.7.4((b): Effect of super absorbent hydrogels dose (30 kg/ ha) HCG-2, HLE-2, HLG-2 and HCE-2 hydrogels on leaf area index (LAI) (cm^2)..... 104
Figure 4.7.4(c): Effect of super absorbent hydrogels dose (45 kg/ ha) HCG-2, HLE-2, HLG-2 and HCE-2 hydrogels on leaf area index (cm^2)..... 105
Figure 4.7.4(d): Effect of super absorbent hydrogels dose (15 kg/ ha) of HCG-2, HLE-2, HLG-2 and HCE-2 hydrogels on leaf area index (cm^2) 106
Figure 4.7.5(a): Effect of super absorbent hydrogels dose (15 kg/ ha) dry matter accumulation in grams when HCG-2, HLE-2, HLG-2 and HCE-2 hydrogels were applied..... 107
Figure 4.7.5(b): Effect of super absorbent hydrogels dose (30 kg/ ha) on dry matter accumulation in grams when HCG-2, HLE-2, HLG-2 and HCE-2 hydrogels were applied..... 108
Figure 4.7.5(c): Effect of on dry matter super absorbent hydrogels dose (45 kg/ ha) accumulation in grams when HCG-2, HLE-2, HLG-2 and HCE-2 hydrogels were applied..... 109

Figure 4.7.5(d): Effect of super absorbent hydrogels dose (60 kg/ ha) on dry matter accumulation in grams when HCG-2, HLE-2, HLG-2 and HCE-2 hydrogels were applied 110
Figure 4.7.6(a): Effect of super absorbent hydrogels dose (15 kg/ ha) on crop growth rate (g/m^2/day) when HCG-2, HLE-2, HLG-2 and HCE-2 hydrogels were applied..... 112
Figure 4.7.6(b): Effect of super absorbent hydrogels dose (30 kg/ ha) on crop growth rate (g/m^2/day) when HCG-2, HLE-2, HLG-2 and HCE-2 hydrogels were applied..... 113
Figure 4.7.6(c): Effect of super absorbent hydrogels dose (45 kg/ ha) on crop growth rate (g/m^2/day) when HCG-2, HLE-2, HLG-2 and HCE-2 hydrogels were applied..... 114
Figure 4.7.6(d): Effect of super absorbent hydrogels dose (60 kg/ ha) on crop growth rate (g/m^2/day) when HCG-2, HLE-2, HLG-2 and HCE-2 hydrogels were applied..... 115
Figure 4.8.1: The effect of dosage (kg/ha) of hydrogels on the mean number of maize cobs per plant 117
Figure 4.8.2: The effect of dosage (kg/ha) of hydrogels on mean number of grains per cob 118
Figure 4.8.3: The effect of dosage (kg/ha) of hydrogels on mean girth of the cob (cm) 120
Figure 4.8.4: The effect of dosage (kg/ha) of hydrogels on mean cob length (cm)..... 121
Figure 4.8.5: The effect of dosage (kg/ha) of hydrogels on cob grain weight per cob (g)..... 122
Figure 4.8.6: The effect of dosage (kg/ha) of hydrogels on mean weight of the cob (g)..... 123
Figure 4.9.1: The effect of dosage (kg/ha) of hydrogels on weight percentage shelling 124
Figure 4.10.1: The effect of dosage (kg/ha) of hydrogels on mean grain yield (kg/ha) 126
Figure 4.10.2: The effect of dosage (kg/ha) of hydrogels on mean Stover yield (kg/ha) 127
Figure 4.10.3: The effect of dosage of hydrogels (kg/ha) on the mean cob yield (kg/ha) 128
Figure 4.10.4: The effect of dosage (kg/ha) of hydrogels on mean biological yield (kg/ha)..... 129
Figure 4.10.5: The effect of hydrogels dosage (kg/ha) on mean harvest index (%) 130

ABBREVIATIONS AND ACRONYMS

AC	Activated charcoal
CA	Citric acid
DH	Double haploid
EWC	Equilibrium Water Content
EDA	Ethylenediamine
FTIR	Fourier transform infrared Spectrum
GF	Gel fraction
HLE-1	Uncrosslinked citric acid -ethylenediamine hydrogel
HLE-2	Cross-linked citric acid ethylenediamine hydrogel
HLG-1	Uncrosslinked citric acid-glycerol hydrogel
HLG-2	Crosslinked citric acid -glycerol hydrogel
HCE-1	Uncrosslinked activated charcoal-ethylenediamine hydrogel
HCE-2	Crosslinked activated charcoal-ethylenediamine hydrogel
HCG-2	Uncrosslinked activated charcoal-glycerol hydrogel
HCG-2	Crosslinked activated charcoal-glycerol hydrogel
G	Glycerol
LAI	Leaf area index
LJ	lemon juice
LWC	Local wood charcoal
MA	Maleic acid
PAM	Polyacrylamide
pH	Potential of Hydrogen
SAHs	Super absorbent hydrogel
SAP	Synthetic polyacrylamide
SEM	Scanning Electron Microscopy
SDG	Sustainable development goal
UN	United Nations
XRD	X-ray diffraction

ABSTRACT

Superabsorbent hydrogels represent a set of polymeric materials with three-dimensional structure. They are capable of holding huge amounts of water and due to the hydrophilic nature in the structure. Their applications in industries and environment are of prime importance. Currently application of polyacrylic and polyacrylamide super absorbers hydrogel in irrigation farming has been reported in western countries making farming economically viable. However, these hydrogels are non-biodegradable, toxic and expensive. Therefore, the pursuit of cheap and biodegradable hydrogels is desirable. Hence this study reports the synthesis and characterization of super absorbent hydrogels derived from activated charcoal (AC) and citric acid from lemon juice (LJ) which are locally available. This involved crosslinking activated charcoal (AC) and lemon juice (LJ) with ethylenediamine (EDA) or glycerol (G) in the absence and presence of maleic acid as a cross linker. Effects of hydrogels dosage on growth and yield parameters were investigated on DH 02 maize crop grown in semi- arid region of Mwala Machakos County during the April - July 2020 rains. Characterization of the hydrogels was done using Fourier transform infrared (FT-IR) spectroscopy, scanning electron microscope (SEM), and X-ray diffraction (XRD). The synthesis conditions that produced optimal swelling conditions were determined by varying contact time and dosage of activated carbon, lemon juice and maleic acid respectively. The FT-IR results showed absorption peaks at 1591.34, 1079.83, 1590.99, 1639.48 cm^{-1} for crosslinked superabsorbent hydrogel of Citric acid Glycerol (HLG-2), Citric acid Ethylenediamine (HLE-2), Activated carbon Ethylenediamine (HCE-2) and Activated carbon Glycerol (HCG-2). The peaks were associated with –COO- stretching vibration, -COO- strong symmetric stretching, C-N- stretching vibration, and -COO- bending in non-conjugated ester respectively which were a proof of successful ester crosslink upon addition of maleic acid during the synthesis process. XRD analysis showed that upon crosslinking the phase polymer network changed from amorphous to crystalline form. SEM analysis showed clear pores with large surface area in cross linked hydrogels compared with rigid and constricted surface of uncross linked hydrogels. Superabsorbent hydrogels for maximum swelling capacity were prepared using the following ratios. Swelling capacity of hydrogels prepared at optimum conditions of volume ratio CA: G: MA (5.4: 3.75: 3.75) HLG-2, CA: EDA: MA (144: 90: 75) HLE-2 while a mass ratio of AC: G: MA (6: 5:1) HCG-2 and AC: EA: MA (6:5:2) HCE-2 show that activated carbon functionalized with glycerol and cross linked with maleic acid has higher swelling percentage of 1255.80±0.70 % when subjected to a contact time of 12 hours. The application of 60 kg/ha of Activated carbon Glycerol showed highest mean growth and yield parameters compared to other superabsorbent hydrogels. This indicates that the prepared hydrogels have potential of reducing moisture stress in maize crops grown in semi-arid region. Super absorbent hydrogels synthesized from Activated charcoal and citric acid have potential application in agriculture owing to their high swelling capacities.

CHAPTER ONE

INTRODUCTION

1.1 Background information

Super absorbent hydrogels are polymer materials with the ability to absorb and retain water or nutrients more than 400 times their original weight, then release them when the zone area is under stress conditions (Li *et al*., 2004, Laftah *et al*., 2011). The presence of a 3D hydrophilic structure with (OH, $CONH_2$, COOH, and SO_3H) functional groups attached to the polymer backbone helps in water absorption capacity (Chen *et al*., 2015, Gandini *et al*., 2016). Hydrogels are usually prepared from polar materials and are classified as physically and chemically cross-linked gels. Physically, cross-linked gels have their networks held together by physical forces, including ionic, H- bonding, or hydrophobic forces, while chemically cross-linked gels have covalently crosslinked networks (Koetting *et al*., 2015). Crosslinking the polymer increases water absorption capacity, physical integrity, and the mechanical strength in the network structure of the polymer (Rowley *et al*., 1999).

Currently, developed hydrogels are applied mostly in technological fields including medicine (Koetting *et al*., 2015), agriculture and horticulture (Senna *et al*., 2015), food packaging (Farris *et al*., 2009), and wastewater treatment (Khan and Lo, 2016). These materials can absorb water 400 times more than their weight and are therefore referred to as super-absorbent (Meng and Ye, 2017). Most of the superabsorbent hydrogels currently in use are synthetically prepared or from petroleum by-products crosslinked with organic cross-linkers (Guilherme *et al*., 2015). Mostly, synthetic cross-linkers used in super-

absorbent hydrogels are poly (vinyl alcohol) (Martens *et al*., 2003), poly (amido-amine) (Ferruti *et al*., 2005), polyacrylamide (Gao *et al*., 2007), poly (N-isopropyl acrylamide) (Nayak *et al*., 2004) and poly (ethylene glycol) (Nagahama *et al*., 2008). These are non-biodegradable and are bound to remain in the environment for long. Super absorbent hydrogels recommended for use in sustainable agriculture must be biodegradable to non-toxic degradation products and be able to avail moisture to plants during growth period (Mahmoudian and Ganji, 2017). This becomes baseline for researchers develop super absorbent hydrogels from locally available renewable green materials which are cost-effective and degradable especially natural materials such as starch and chitosan among others (Khan and Lo, 2016). Low cost with high swelling capacity hydrogels has attracted more emphasis in the field of agriculture (Ma *et al*., 2015, Cruz *et al.*, 2019). There is a need to design and develop super absorbent hydrogels from natural locally available materials that are eco-friendly.

Maize farming is practiced in most parts of the world. The cereals produced by the crop are used as the staple food for human beings in the developing world. About 80% of livestock and poultry feeds composed of maize (Shi *et al*., 2010). Due to its high contents of carbohydrates and other valuable micronutrients, commercially it has been used as a raw material in industries for brewing, manufacturing soft drinks, oil, and protein extraction (Muna *et al*., 2016). About 90 percent of the Kenyan population uses maize as a source of carbohydrates in form of githeri, ugali, or popcorns (Nyoro *et al*., 2004). Statistically, maize production has been varying since 1972 to date in Kenya (Nyoro *et al*., 2004). About 20 million Kenyans both on a large and small scale depend on Maize

farming as the source of income while the production is unable to sustain the fast-growing population.

About 90 % of the mass composition of plants and animals comprises water which is the baseline for all metabolic processes for growth. Agricultural practices are the backbone of the economy for developing and developed countries (Ogutunde *et al*., 2006). In addition, a large part of Africa is arid and semi-arid with inadequate and unreliable rainfall, poor methods of farming. The outbreak of diseases and pests has affected maize production and it is projected to worsen as the rainfall patterns changes due to global warming (Han *et al*., 2018). Inadequate rainfall and poor soil structure in arid and semi-arid regions are making farming of maize vulnerable affecting food production (Han *et al*., 2018). Sandy soil has low water holding capacity and a high rate of water drainage which is below the root zone of crops, resulting in poor water and fertilizer absorption (Wei and Durian, 2014). This hurts health and crop growth rate and by the year 2050 food production is projected to reduce by 50 % (Wei and Durian, 2014). This has motivated researchers to look for alternative methods of using super absorbent hydrogel from locally available resources to store extra water during rains and release it to the soil for use by the crop during dry period intervals (Bouman *et al*., 2002, Ullah *et al*., 2015).

Coconut shells are the products obtained after processing the soft part (fruit) and dumped as agricultural waste which is available in large quantities in tropical climates. In Kenya, coconut shells are adequately found along the coastal region and are usually disposed of through burning (Foo *et al.,* 2010). Coconut shells can undergo carbonization under

suitable conditions to form activated charcoal. Lemon juice can be used as a source of citric acid on large scale through the processing of lemons which are largely produced in semi-arid regions. Activated carbon from coconut shell and citric acid can be cross-linked with polyglycerol or polyamide in presence of maleic acid to form super absorbent hydrogel (Ma *et al*., 2015). Superabsorbent polymer hydrogels are 3D hydrophilic materials with a high ability of water absorption, retainability and have the capacity to release the moisture when the zone is dried up. These hydrogels when placed in water can swell at least more than 400 times their original size and make at least 95 percent of their stored water available for absorption (Gandini *et al*, 2016). During dry periods of crop growth, hydrogel release moisture to its zone area creating free pores in the soil promoting root growth as well as free air and water circulation activating healthy crop growth.

Free radical polymerization has been used by many researchers (Abedi-Koupai *et al*. 2004, Tong *et al*. 2007, Yazdani *et al*. 2007). The method is cheaper, easy, reduces the generation of by-products, is environmentally friendly and economically viable. It was therefore employed to synthesize hydrogels in preference to other conventional methods (Ekezie *et al*., 2017). So far, there is no study reported on activated charcoal or lemon juice cross-linked with either ethylenediamine or glycerol in the presence of maleic acid to form HCE-2, HCG-2, HLG-2, and HLE-2 hydrogels and their application in agriculture. The present study reports on synthesis, optimization, characterization, and swelling capacity of superabsorbent hydrogels derived from activated carbon and citric acid from lemon juice with glycerol or ethylenediamine. Maleic acid was used as a cross

linker to improve the network of hydrogel structure for maximum water absorption. In addition, the growth and yield parameters of maize DH-02 grown in the semi-arid region of Mwala Machakos County during April-July rains of 2020 were determined.

1.2 Statement of the problem

Over 80 % of the Kenyan land is arid and semi-arid and occupied by more than 20 million people (Nyoro *et al*., 2004). However, such lands are regarded as unproductive mainly due to unreliable rains which cannot sustain agriculture. Global warming and anticipated changes in rainfall patterns have decreased maize production (Han *et al*., 2018). The absence of water for irrigation in semi-arid environments further complicates the ability of food production. Poor soil structure has greatly contributed to a high rate of water and nutrient leaching below the crop root zone leading to poor productivity of maize crops (Wei and Durian, 2014). This resulted in famine, malnutrition, and violence among communities in Africa fighting for limited greener agricultural land. Farming is the major income generating activity in most developing countries but the gross domestic product is rapidly decreasing due to inadequate rainfall and poor water management practices (Shi *et al*., 2010). The most widely used methods for sustainable farming are irrigation, mulching or water harvesting. These methods prove to be expensive, time consuming, energy intensive and ineffective (Han *et al*., 2018). The use of super absorbent hydrogels to help relieve water stress in crops during farming is desirable (Senna *et al*., 2015). Most of the super absorbent hydrogels available are synthetic polymers such as acrylic acid, methacrylic acid, polyethylene glycol, vinyl acetate, polyvinyl alcohol and various acrylates which are expensive, and non-biodegradable

(Guilherme *et al*., 2015). While few super absorbent hydrogels such as alginate, chitosan, collagen, dextran, cellulose and chitin, are biodegradable natural polymers as well as environmentally friendly and hence appropriate for use in agriculture, there are minimal reports in Africa on their use in farming (Mahmoudian and Ganji, 2017). Therefore, there is a need to pursue ways of soil moisture conservation and water retainability in semi and arid regions through the use of super absorbent hydrogels. The present study cross-linked activated coconut shells charcoal and citric acid with ethylenediamine or glycerol to synthesize hydrogels for use in agriculture.

1.3 Justification of the study

Super absorbent polymers have been applied to reduce the effects of degraded soils which has a direct influence on demand for food and energy production. Water-soluble polymers have been in use as they are effective soil conditioners. The polymers contain hydrophilic functional groups that bind to water molecules thus retain the soil moisture for long period. Polymers have more enhanced hydrophilicity, which promotes water and nutrients retention of the soil promoting drought resistance of the crops. Thus, use of Coconut shells activated charcoal which are agricultural waste and lemon fruits as a source of citric acid which are locally available in semi-arid regions, can be utilized in the synthesis of biodegradable super absorbent hydrogels. The method used to synthesize natural super absorbent hydrogels is simple, less expensive, energy and time saving. However, application of the SAHs to the crops results in a high rate of water absorption, retention, aeration, infiltration as well as moisture release to root zone area when dries up during crop growth. This influences growth and yield parameters of plant and is the

baseline for increasing food production in arid and semi-arid region leading to affordable economy.

1.4 Hypothesis

i. Activated charcoal and citric acid can be cross-linked with ethylenediamine or glycerol in the synthesis of super-absorbent that for sustainable agriculture of the arid and semi-arid regions.

ii. Optimizing synthesis conditions of super-absorbent hydrogel enhances water absorption capacity

1.5 Objectives

1.5.1 General objective

To evaluate the performance of synthesized super absorbent hydrogels derived from activated charcoal and citric acid on the growth and yield parameters of maize in a semi-arid region

1.5.2 Specific objectives

i. To Synthesize and characterize super absorbent hydrogels from activated charcoal and citric acid interlinked with glycerol or ethylenediamine with maleic acid as cross linker using FTIR, SEM and XRD

ii. To optimize monomers cross-linker ratios for best swelling capacities

iii. To determine the required dosage of the super absorbent hydrogels for optimum growth and yield parameters of maize crops grown in semi-arid region of mwala Machakos county Kenya

1.6 Significance of the study

The research resulted in synthesizing potential super absorbent hydrogels from citric acid and activated charcoal, using locally available material for sustainable farming in semi-arid regions. This is expected to increase the rate of food production in arid and semi-arid regions, ensuring food security, enhanced health, increased employment opportunities, and an affordable economy.

1.7 Scope and limitation of study

i. The study was restricted to lemon juice as a source of citric acid and activated coconut shells charcoal during synthesis, characterization, efficiency, and absorption capacity of superabsorbent hydrogels.
ii. Only maleic acid was used as cross linker
iii. Ethylenediamine and glycerol was used as monomers for hydrogel synthesizes
iv. This research focused on randomized complete block design application of the synthesized super absorbent hydrogels to DH-02 hybrid maize crop plants in semi-arid farm plots at Mwala Machakos sub-county and not the whole county. Other crops were not considered.

CHAPTER TWO

LITERATURE REVIEW

2.1 Activated charcoal

Activated charcoal/carbon is carbonaceous material with a highly developed small porous structure and large surface area and different types have been prepared worldwide. Activated charcoal materials are characterized by the following features, microcrystalline structure, great thermal stability and large surface areas of highly disordered carbon (Ahmad, 2018). The unique morphological structure of carbon upon activation consists of aromatic sheets, strips, and micropores due to voids and gaps of molecular dimensions. This has increased its demand in technologies mainly as energy storage, energy conversion, security sensors, environmental pollution control, as a reagent in chemical production and catalysis (Santana, *et al.,* 2017).

In addition, activated carbon is for sorption and catalytic application due to the presence of (carboxylic, phenolic, and lactones) hydrophilic surface functional group. This makes them find application in oil and natural gas purification, food and pharmaceuticals industries, water treatment, hydrometallurgy, gold recovery, and carbon-in-pulp process (Okamoto *et al.,* 1999). The increasing demand for activated carbon inspired researchers to come up with cheaper, biodegradable, non-toxic activated carbon from locally available material compared to commercial activated carbon from coal. (Omri *et al.,* 2013). Figure 2.1 shows the structure of activated carbon unit.

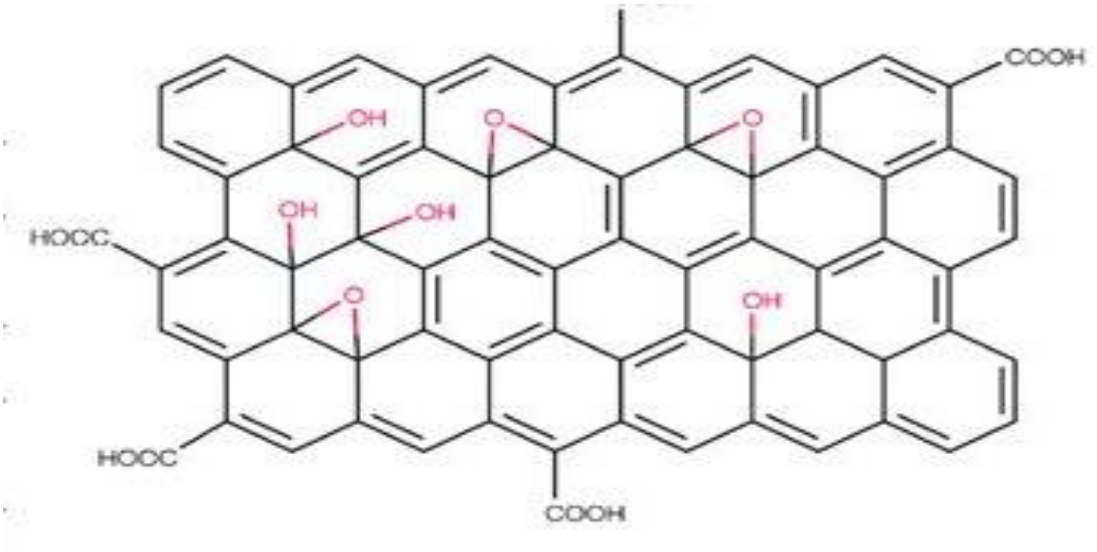

Figure 2.1: Chemical structure of Activated carbon

Activated charcoal has a permeable structure with different sizes of pores which can be modified through crosslinking to be an effective super absorbent hydrogel (Cetinkaya *et al.,* 2003). Coconut shell is referred to as a waste material obtained after processing mature coconut fruit. The shells are rich in proteins, carbohydrates, and phenolic compounds which contain carboxyl, hydroxyl, sulfate phosphate, and amino groups (Chandra *et al.,* 2009). The shell forms adjacent tetrahedral joined via a common oxygen atom resulting in an inorganic macromolecule with a structurally distinct three-dimensional framework (Shah and Jadav, 2012). Varying active groups (oxygen, hydrogen and nitrogen) are found on the surface area of most activated carbons, which are heterogeneous. High oxygen content in the activated carbon has a prominent effect on the crystalline nature of the material and the size of the pores generated (Cuhadar, 2005). Anionic activated shell charcoal containing functional groups (carboxylic, phenolic, and lactones) can undergo polymerization reaction with glycerol or ethylenediamine to form

cheaper, locally available, and renewable super absorbent hydrogels with maximum water absorption capacity.

2.2. Lemon juice as source of citric acid

The locally available lemon fruits were used to extract citric acid. Commercially, citric acid is prepared through glucose fermentation in the presence of yeast (Cuadro *et al*., 2015). Citric acid is used mostly in food as an anti-oxidant, industrially for the manufacture of soft drinks, and as a sequestering agent for metal ions due to its high affinity for metal (Demitri et al., 2008). Citric acid has been reported in the literature as a crosslinking agent in the different syntheses of cellulose-based polymers (Capanema *et al.*, 2018). Cellulose-based hydrogels cross-linked with citric acid are biodegradable and non-toxic with moderate swelling capacity (Demitri et al., 2008).

2.3 Super absorbent hydrogels

Super absorbent hydrogels are 3-dimensional hydrophilic polymers, with ability to absorb and retain a high amount of water and then releasing it under stress conditions (Cheng *et al*., 2015). Presence of hydrophilic groups on the hydrogel polymer chain, such as OH, COOH, CONH, $CONH_2$ and SO_3H give them water absorbance abilities (Cheng *et al*., 2015). They are also reported to be sensitive to ionic strength and pH of solution (Li *et al*., 2014). Superabsorbents hydrogel can be prepared from natural and synthetic polymers, depending on the charge, mechanical and structural features (Chan *et al*., 2009). The synthetic polymers such as acrylonitrile, acrylic acid (AA) and acrylamide,

were restricted for use due to their non-degradable, non- renewable and environmentally unfriendly nature.

Natural polymers such as cellulose, starch and chitosan are eco-friendly. Consequently, they have attracted much attention due to their cost-effectiveness, degradability and availability (Mahmoudian and Ganji, 2017). Superabsorbent hydrogels are widely used in various fields such as hygiene napkins, disposal diapers, soil for horticulture and agriculture, water purification, food, construction and building, corneal, tendons, implant, substitute of skin, ligaments, cartilage, bones and biomedical applications such as the controlled release of drugs (Wang *et al*., 2008). Nowadays, researchers have focused on the development of hydrogels for tissue engineering (Khan *et al*., 2011), sensors (Sorber *et al*., 2008) and drug delivery (Wu *et al*., 2008). Super-porous hydrogels (an exclusive class of hydrogels) have been used as pesticide release devices (Rudzinski *et al*., 2002), soil conditioners/improvers (Abd El-Rehim *et al*., 2004), slow- release fertilizer (Teodorescu *et al*., 2016).

2.4 Classification of hydrogel

2.4.1 Homopolymer and copolymeric hydrogels

Homopolymer is made of the same kind of monomers and may have either cross-linked or uncross-linked morphological networks. The mechanical stability and water absorption ability of cross-linked homopolymer hydrogels are high compared with the uncrosslinked polymer. Cross-linked polymers are mainly used to develop sustainable and controlled drug- delivery devices and contact lenses. Examples of cross-linked polymers currently in

use are poly(hydroxyalkyl methacrylate) derivatives, poly (3-hydroxypropyl methacrylate (PHPMA), poly(glyceryl methacrylate) (PGMA), and poly(2-hydroxyethyl methacrylate) (PHEMA) (Hennink and van 2002). Uncrosslinked homopolymers have also been used in forming hydrogels, such as poly (N-vinyl-2-pyrrolidinone) (PNVP) (El-Din *et al*., 2004), poly(acrylamide) (PAM), poly(ethylene glycol) (PEG), and poly(vinyl alcohol) (PVA). Copolymeric hydrogel is made of two or more different monomers in their networks like N-vinyl-2-pyrrolidone (NVP) and polyethylene glycol diacrylate (PAC) (El-Din *et al*., 2004). Moreover, in agriculture, super absorbent hydrogels are used as granules for holding soil moisture in semi-arid areas but proved to be non-biodegradable as well as lowering soil pH (Khan *et al*., 2011).

2.4.2 Interpenetrating polymer networks (IPNs)

Interpenetrating polymer networks (IPN) is a process of forming a single polymer hydrogel by combining two different polymer networks. For a successful IPN to be formed the two polymers to be cross-linked should possess the same characteristics of chemical kinetics biodegradable and inseparable structures. IPNs have a high ability to retain the original characteristics of each polymer network (Kojima *et al*., 2000). However, the addition of crosslinks during the synthesis of IPN provides gelation precedes facilitating phase separation during polymerization which increases apparent miscibility. This type of hydrogel is commonly used in industries but restricted from being used in agriculture due to being non-degradable, non- renewable and environmentally unfriendly (Mahmoudian and Ganji, 2017).

2.4.3 Ionic and nonionic hydrogels

Ionic hydrogels are prepared from either positive or negatively charged monomers and are also known as polyelectrolytes or polyampholytes (Demosthenous *et al*., 2002). They are classified as cationic or anionic hydrogels and are very sensitive to pH changes. The swelling capacity of polyelectrolyte is affected by an interaction between charged polymer network and free ions in the solution (Hennink and van 2002). Hydrogels with carboxylate groups in their network can absorb a larger amount of water at a pH higher than its pKa due to the increased concentration of hydrophilic groups (Kojima *et al*., 2000). Neutral hydrogels do not have charged groups in their networks and their swelling is due to the osmotic pressure of the solvent and elastic polymer stretching energy in the network (Kojima *et al*., 2000). Ionic hydrogels have been used as controlled drugs due to the increased residence time of the hydrogel at the target site (Cheng *et al*., 2015). Polyacrylic acid (PAA) and chitosan (CS) have also been reported to be used for sustained release of amoxicillin in the stomach (Filho *et al*., 2018).

2.5. Applications of super absorbent hydrogel

2.5.1. Application in human hygiene

Due to increasing advancements in technology, special super absorbent hydrogel materials are currently employed in the improvement of human hygiene both at household and hospital levels. About 90 % of the world's population is using disposable diapers and female napkins manufactured using super hydrogel absorbents. Most hospitals and health centers use disposable diapers to reduce the risk of the spread of gastrointestinal illnesses as they are more effective compared to double cloth diapers and

plastic over pants (Filho *et al*., 2018). Currently, due to the emergence of new superabsorbent materials, thinner high-performance diapers, high retention capacity reducing leakage, and diaper rashes are in place (Sannino *et al*., 2004). Most of the hydrogels in the market are synthetically made with low absorption ability and are non-biodegradable. There is a need therefore for research on the synthesis of biodegradable hydrogels with high absorption ability.

2.5.2. Biomedical application of the hydrogels

Super absorbent hydrogels were used in wound dressing to prevent infection and promote healing (Filho *et al*., 2018). Hydrogels provide a solution to wounds that do not heal properly like ulcers as they require a moist environment for fast healing. Hydrogel mixed with antiseptic maintains a moist environment which allows fast healing. Amorphous hydrogels act as dehydrating agents (Filho *et al*., 2018). They are prepared and designed to facilitate the correct moisture balance in the wound surface. In addition, they are transparent for easy monitoring of wound while providing non-adherent dressings which is easily removed without damaging the wound (El-Din *et al*., 2004). The most common methods of hydrogel dressings currently in use include antimicrobial agents, such as silver ions, in their formulation (Ma *et al*., 2015).

In the field of regenerative medicine, hydrogels are used due to their high-water absorption ability, and rubbery mechanical property to that of soft tissue (Rimmer, 2011). For maximum tissue regeneration, the scaffold should have a slow but same biodegradation rate as that of the biological process of interest to reduce premature

resorption (Amhed *et al*., 2016). Cellulose and its derivatives are currently used as biomaterials for tissue engineering scaffolds design due to their biocompatibility and good mechanical properties (Mishra *et al*., 2008).

2.5 3 Application of hydrogels in agriculture

Water and minerals are the basic needs for the healthy growth of crops (Orosz *et al.*, 2009). Currently, the high rate of industrialization has continued to pollute soil and water affecting agricultural produce (Hui *et al.*, 2005). There are various methods in place for applying hydrogel absorbers effectively to crops in the soil which include seed treatment, soil application, broadcasting, dibbling, deep placement, row application, wet patch application (Khadem *et al*., 2010). Application of zeolite hydrogel in millet has provided an environment for crop growth, increased leaf number, and the dry weight of millet as compared to control (Khadem *et al*., 2010). The high rate of gel content supply caused the opening of stomata for a long time, resulting in a high fixation of carbon dioxide gas leading to an increase in the dry matter in the crop (Liu *et al*., 2009).

Proper and timely application of hydrogel absorber ensures adequate moisture is stored during rains to be released during dry intervals of crop development, ensuring a high yield of maize crop, which is a major, staple food worldwide. Application of Polyethylene oxide hydrogel, polyacrylamide hydrogel, and cross-linked polyethylene oxide co-polyurethane hydrogel controls plant damage that resulted from salt-induced and water-scarce stress, (Kim *et al.*, 2004; Shi *et al.*, 2010). Spraying the hydrogels as dry granules or mixing them with the entire root zone is not effective (Flannery and

Busscher, 1982). Better results are obtained when the hydrogels are layered, preferably a few inches below the soil surface. The amount of gel for better performance may be affected by many factors including climate, substance type, soil type, and crop species. Systematic field studies under arid and semi-arid conditions of Machakos are needed to develop an appropriate dose of hydrogel needed. Table 2.1 shows some selected hydrogels used in agriculture.

Table 2.1: Selected hydrogel absorbents applied in agriculture

Hydrogel	**Crop used**	**Reference**
Starch-graft co-polymers	Tomato	(Tong *et al*. 2007)
Polyacrylates	Tomato	(Abedi-Koupai *et al*. 2004)
Acrylamide-acrylate	Soyabean	(Yazdani *et al*. 2007)
Co-polymers Polyethylene	barley and wheat	(Akhter *et al*. 2004)
Oxide hydrogel,	Wheatgrass	(Kreye *et al.*, 2009)
Polyacrylamide hydrogel	cotton and maize	(Jin *et al.*, 2007)
Poly-glycerol sebacate	Wheat	(Wang *et al*., 2003
Tri-block dendrimer	Rice	(Naeini *et al* 2010).
Polyethylene oxide hydrogel	Barley	(Shi *et al.*, 2010).

2.6. Effect of hydrogel on growth parameters of maize

Studies have shown that application of super absorbent hydrogel to maize plant improved the rate of growth, as they have the potential of absorbing water and other essential micronutrients required by the crop and release them at the root zone area (Boatright *et al.*, 1997; Namazi *et al.*, 2011). Application of the right ratio of hydrogel in the soil leads to high-quality leaves, fast plant growth resulting in a high yield of maize in arid areas (Kramer, 1988; Bouman *et al*., 2005). Water preservation by hydrogel ensures the surrounding environment is efficient in short-term drought tension and losses reduction in the establishment phase (Woodhouse and Johnson, 1991). Application of SAH in crops served as carrier and regulator of moisture and nutrient release, are helpful in reducing

fertilizer losses and sustaining vigorous crop growth (Mikkelsen, 1994; Yazdani *et al*., 2007). Application of gel to the fertilizer increased rate of seedlings growth, increased absorption of nitrogen and reducing leakage up to 45 % as compared to Nitrogen fertilizer alone (; Mikkelsen *et al*. 1993, Martinez *et al*., 2004; Yazdani *et al*., 2008).

2.7 Effect of hydrogel on plant yields

The impact of perlite on water use efficiency and grain yield in winter wheat (*Zarrin cultivar*) was investigated by (Moghimi *et al*., 2011). The research was carried out in an open field using a complete random block design (CRBD) with seven treatments (S0, S1, S2, S3, S4, S5 and S6), 75, 150, 300, 600, 1200 and 2400 kg ha^{-1} with four replicates. The result from the statistical analysis shows that by the addition of perlite to the soil, there was an increase of about 39.9 and 31.5 % of biological yield and grain yield wheat, which is statistically significant at 1 % confidence level. The result from the study also revealed that in the treatment of applying 2400 kg ha^{-1} perlite, there was an increase up to 40.12 % of water use efficiency. The incorporation of K400 stockabsorbant hydrogels in 0.4 to 0.6 % weights showed a significant increase in buttonwood (*Conocarpus erectus*) seedlings in an arid region of Saudi Arabia (Al Humaid and Moftah, 2007). Al Harbi *et al*. (1999) reported that the addition of SAH up to 0.3 % had a positive effect on the plant, compared to 0.4 % concentration, however, the effect was reversed.

The increase in hydrogel at high doses increased significantly the growth parameters (plant height, leaf area, stem diameter) of maize in the arid areas of China (Islam *et al*., 2011). The highest yield was obtained at 30 kg ha^{-1} of the SAH. At 10 and 20 kg ha^{-1}, the yield was lower, due to insufficient hydrogels. Maize yield increased following superabsorbent polymer application at 15 kg ha^{-1} with half the amount (150 kg ha^{-1}) of fertilizer by 11.2 % under low, 18.8 % under medium, and 29.2 % under high dose as compared to control receiving conventional fertilizer dose (300 kg ha^{-1}). The use of SAH served as a conveyor and regulator of nutrients release, which helped in limiting manure loss (Mikkelsen, 1994). The retained water and nutrients are released to the plants slowly to improve growth (Yazdani *et al*., 2007). The leaf area and the number of leaves of cucumber increased by incorporating SAH with soil (Mamun *et al*., 2017). The dry matter productions of tomatoes and cotton (Wallace and Wallace, 1986), and maize (El Hady *et al*., 1981) significantly increased with an increase in SAH as compared to control. Application of the correct hydrogel dose along with recommended doses of fertilizers to maize crops increased seed yield by 12 % as compared to control (Mondal, 2011). When the minimum and maximum dose of the super absorbent polymer was applied, maize yield increased by 11.2 % and 18.8 % respectively (Islam *et al*., 2011).

2.8 Effect of super absorbent hydrogel on soil moisture content

Moisture content in the soil is responsible for dissolving essential crop nutritious elements for crop absorption. The measure of the Moisture content is a major factor in evaluating yield percentage production in crops (Shahbeig *et al.,* 2013). The availability of polymer absorbers ensures the presence of moisture in the soil for longer periods after

rains during cropping seasons (Ghaiour, 2000; Sivapalan, 2006). Sandy soil mixed with hydrogel revealed high retainability of moisture and nutrients equal to 23 and 95 % by applying 0.03 and 0.07 % of its weight, respectively. The available water content of loamy and clay soil showed a highly significant increase (108 and 105 %, respectively) (Akhtar *et al*. 2004; Uz *et al*., 2008). Absorbers hydrogel can retain more amount available moisture in all soils except black cotton soil (Abedi-Koupai *et al*., 2004; Allahdadi *et al*., 2005). Different types of hydrogel have different holding capacities for moisture. Applying 28 kg/ha of Bhagiratha polymer together with fertilizer showed a high rate of moisture absorption in sandy loam soil as compared to the control (Mondal, 2011). Vegetable crops grown in alluvial and red sandy loam soils mixed with gel increased by 150 –200 % respectively compared to the control (Mondal, 2011).

2.9 Effect of superabsorbent hydrogels on soil

The ability of the super absorbent hydrogel to store moisture and other micronutrients of plants depends on the soil profile (Han *et al*., 2010). Sandy soils have low water retention ability due to their large soil particle resulting in the leaching of irrigation water, drainage of rain, and plant nutrients below the root zone of crops (Viera *et al*., 2007). This leads to water and fertilizer being inadequate for plant growth. The hydrogels improve soil physical properties such as water holding capacity and nutrient retention, thereby enhancing the plant life cycle under difficult conditions (El- Amir *et al*., 1993; Sendur *et al*., 2001; Karimi *et al*., 2009). Most of the SAHs reported in the literature that is derived synthetically from petroleum products are known to be toxic, non-degradable and non-biocompatible and therefore not suitable for use in agriculture (Shang *et al*., 2008, Thakur

et al., 2019). Incorporation of SAHs in the soil improves its texture, structure of soil and water penetration (Helalia and Latey, 1988), water retention of soil (Tayel and El-hady, 1981), and ease water maintenance in soil (Shooshtarian *et al*., 2011). Currently designing and synthesizing SAHs that are eco-friendly, especially from natural materials such as cellulose, starch and chitosan have attracted much attention due to their cost-effectiveness, degradability and availability (Mahmoudian and Ganji, 2017).

2.10 Synthesis of super absorbent hydrogels

The polymerization process is used to synthesize different types of super absorbent hydrogels by either chemical or physical crosslinking techniques. The type of cross linker used during synthesis determines the type of SAHs synthesized (Alemzadeh and Vossoughi, 2002). Some commonly used methods for the synthesis of the hydrogel are as shown in table 2.2.

Table 2.2: Selected methods for hydrogel preparations

Chemically Crosslinking	**Physically crosslinking**
Radical polymerization	Ionic interactions
Chemical reaction of complementary groups	Crystallization
Addition reactions	Crystallization in homopolymer systems
Condensation reactions	Stereo complex formation
High energy radiation	Physically cross-linked hydrogels from amphiphilic block and graft copolymers
Enzymes	Crosslinking by hydrogen bonds Crosslinking by protein interactions Use of genetically engineered proteins Crosslinking by antigen–antibody interactions

2.10.1 Chemically cross-linked super absorbent hydrogels

Chemically cross-linked hydrogels are prepared using a non-toxic cross-linker to maintain their biocompatibility and structural stability in the network. Various polymerization methods of hydrogel synthesis through chemical cross-linking include; chain growth, addition and condensation, gamma, and electron beam polymerization (Shang *et al*., 2008). Polymer chains are formed by the chemical reaction of complementary groups in the gel network through functional groups and complementary reactive groups -OH/NH_2 (Alemzadeh and Vossoughi, 2002). Chain-growth polymerization involves free radical, controlled free radical, anionic, and cationic polymerization, which involves three stages; initiation, propagation, and termination (Bakravi *et al*., 2018).

The initiation stage generates a free radical, which activates the addition reaction of monomers to occur. Poly (*N*-isopropyl acrylamide) hydrogel are synthesized through free radical polymerization while PVA is cross-linked with methacrylic acid using ethylene glycol di-methacrylate (EGDMA) as a cross-linking agent and benzoyl peroxide as reaction initiator by a free radical copolymerization (Thakur *et al*., 2019). Controlled living radical polymerizations have an advantage over free-radical polymerizations. It offers the benefits of longer growing chain life for macromolecular engineering (Hennink and Nostrum, 2002). Gamma and electron beam polymerization take place at high-energy electromagnetic irradiation (Hennink and Nostrum, 2002).

2.10.2 Physically cross-linked hydrogel

Physically cross-linked hydrogels use non-covalent interactions within their networks. This process reduces the toxicity effect caused by chemical crosslinking agents, reducing water absorption in the hydrogel (Hennink and Nostrum, 2002). This process of hydrogel synthesis involves ionic interaction, crystallization, stereo- complex formation, hydrophobized polysaccharides, protein interaction, and hydrogen bond formation. The ionic interaction process occurs under warm conditions, at room temperature, and at a physiological pH to form hydrogel and does not require the presence of ionic groups (Hennink and Nostrum, 2002). A stereo complex reaction occurs through crosslinking between lactic acid oligomers of opposite chirality to form hydrogel while Hydrophobic interactions result in the polymer swelling and uptake of water that forms the hydrogel (Thakur *et al*., 2019).

The ionic interactions can cause hydrogel formation, such as alginate (Bakravi *et al*., 2018). Chitosan-based hydrogels have been formed with glycerol-phosphate disodium (Alves *et al*., 2019). The crystallization method including alternate freezing and thawing is also one of the ways of forming hydrogels. Stereo complex formation between enantiomeric oligomeric lactic acid chains can form a hydrogel. Polylactic acid (PLA) is one such polymer that can form a stereo complex (Ikada *et al*. 2010). Examples include PLLA–PEG–PLLA and PDLA–PEG– PDLA stereo complex (Alves *et al*., 2019), pHEMA (poly(HEMA-*g*-oligolactate)s). Crosslinking by protein interactions is another way of preparing physically cross-linked SAHs (Yokoyama *et al*., 1986).

2.11 Characterization of hydrogels

Synthesized super absorbent hydrogels have been characterized by Fourier transform infrared (FTIR) spectroscopy, for functional group identification. X-ray diffraction (XRD) is used to determine crystalline materials, and scanning electron microscopy (SEM) is used in studying the surface morphology.

2.12. Scanning electron microscopy (SEM)

2.12.1 Working principle

Scanning electron microscopy is an instrument used in studying the surface morphology of a material with a highly magnified image that is similar to what would be visually seen (Hossain *et al*., 2012). SEM provides information about the composition of near-surface regions, and crystallographic information as well as exhibit grain structure surfaces (fracture surfaces, etched, or decorated surfaces) being characterized as to grain size and shape (Anandkumar and Mendal, 2012). The surface morphology and porosity of natural fiber have been reported as significant factors for composite interfaces and their effects on the performance have been investigated (Han and Choi, 2010). Microscopy is used to observe the morphology, pore size, and porosity of cross-linked and uncross linked hydrogel. The changes in swelling capacity can be explained by changes observed on the surface of the hydrogel absorbent. Therefore, the surface morphology and microstructure of the green hydrogel adsorbents are best studied by SEM and it is essential to coat the sample with a conductor material such as gold, platinum or with a layer of carbon when investigating biomass. This is due to the slow electron conductivity of the kind of material which may affect the image quality (Kumar *et al*., 2014).

2.12.2 Instrumentation

The main components of SEM include: Source of electrons, Column down which electrons travel with electromagnetic lenses, Electron detector, Sample chamber and Computer to display and view the images. Figure 2.2 shows the schematic diagram of SEM.

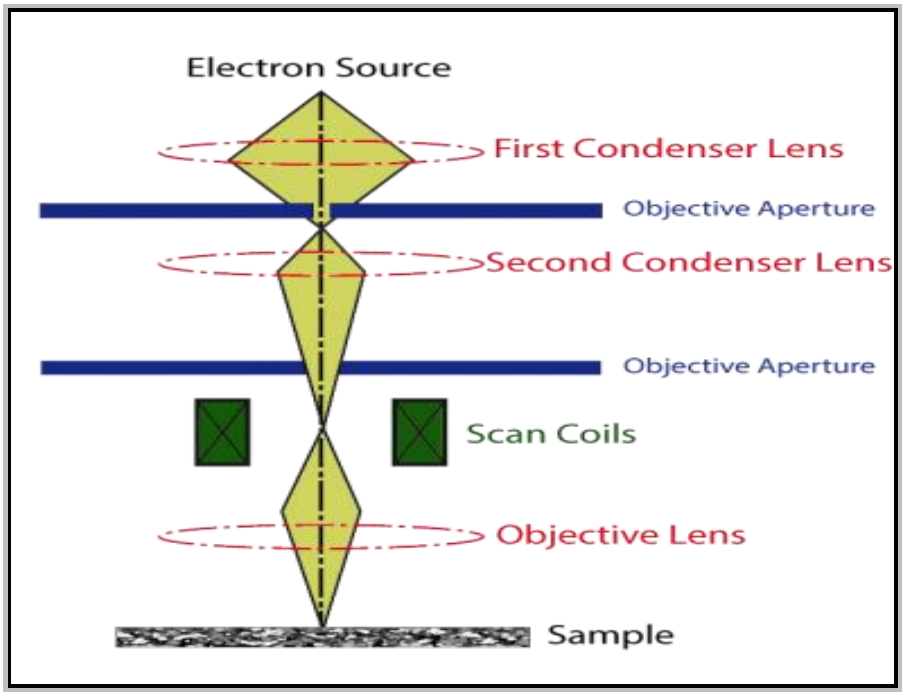

Figure 2.2: Schematic diagram for scanning electron microscope (NI, 2016).

The scanning process involves shooting an electron beam at a specimen and observing the reactions on the specimen surface. When the electron hits a molecule on the surface, its energy is absorbed by the molecule which in turns emits a lower amount of energy. This energy can be in the form of a secondary, less energetic electron, a photon of light, or x-rays (Liu *et al*., 2010). Differentiation between these emissions is used to produce

image contrast. However, in order to produce a coherent image, the sample must often be prepared with a conductive coating or by embedding resin.

2.13 Fourier transform infrared (FT-IR) spectroscopy

2.13.1 Working principle

FT-IR is a high commonly method for characterizing the chemical composition of materials by using a technique based on the vibrations of the atoms of a molecule. IR spectrum is obtained by passing incident radiation rays through a sample and determining what fraction of the radiation is absorbed in particular energy (Ferreira *et al.*, 2012). The aim is to determine infrared radiation change of intensity as a function of wavelength or frequency. The energy at any peak in an absorption spectrum corresponds to the frequency of vibration of a sample molecule (Liang *et al.*, 2009). The wavelength at which absorption occurs enables the determination of functional groups responsible for the reactions and present in the material (Ferreira *et al.*, 2012).

The IR spectrum operates within a range of (4,000-500 cm^{-1}), the vibrations can either involve a change in bond length (stretching) or bond angle (bending). Infrared spectroscopy is used to analyze the chemical treatment effect on the surface structure of biomass and the broadening of the hydroxyl band (Barreto *et al.*, 2011). The IR helps in the characterization of the axial vibration of hydroxyls from cellulose (carbons 2, 3, and 6 of the glucose) as a function of the chemical treatment with sodium hydroxide and due to changes of the inter-and intra-molecular hydrogen bonding in polysaccharides (Esmeraldo *et al*., 2010). Upon lignin acid treatment, the IR showed removal or decrease

in intensities and modes in absorptions due to C–Hn (alkyl and aromatic) stretching, C=O stretching modes, and aromatic skeleton vibration of (Ferreira *et al*., 2012). Therefore, IR spectroscopy is an important tool widely used to investigate functional groups of hydrogels and give information about the structural arrangement of crosslinked and uncrosslinked hydrogels (Selling *et al*., 2015). Studies have shown that maleic acid has a carboxylic group which has the ability to crosslink with the hydroxyl group to form ester linkage (Selling *et al*., 2015).

2.13.2 Instrumentation

A FT-IR spectrometer consists of a source, interferometer, sample compartment, detector, amplifier, A/D convertor and a computer. Figure 2.2 shows FT-IR spectrometer

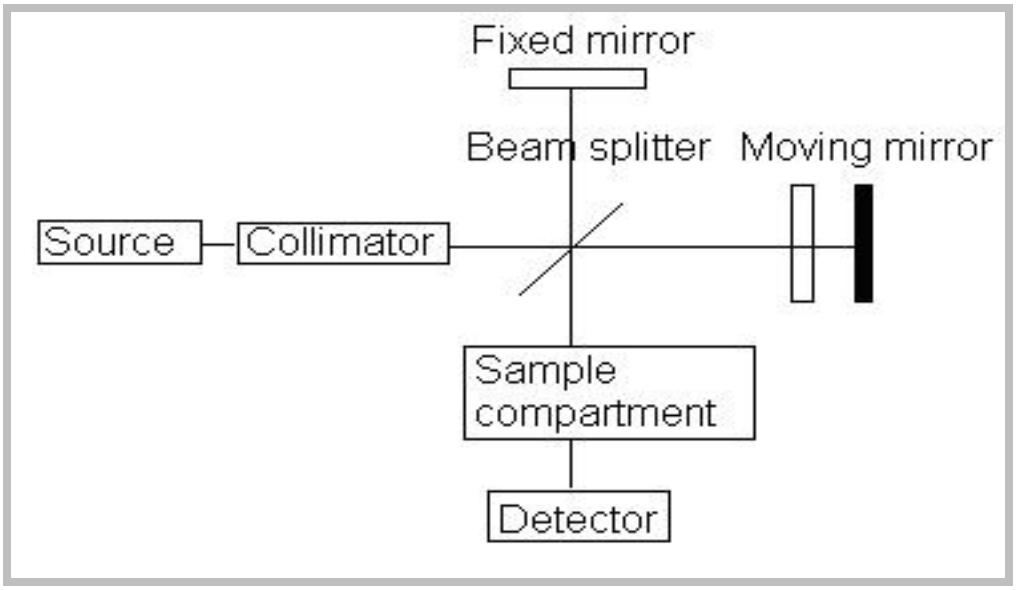

Figure 2.3: Block diagram for FT-IR spectrometer

Fourier transforms infrared consist of the interferometer at centre where the IR-beam enters the then directed towards the beam splitter. The split beam is directed towards fixed and moving mirror respectively then towards the sample after recombining followed by obtaining the spectra information of all wavelengths simultaneously. Omnic software was used to process spectra wavelength at a range between 500 and 4000 cm^{-1} at 25 °C. A scientific function called a Fourier transform was used to change over intensity versus- time range into a power versus- recurrence range (Naja *et al.*, 2005).

2.14. X-ray diffraction (XRD)

2.14.1 Working principle

X-rays are high-energy electromagnetic waves with short wavelengths, in the order of atomic spacing. Diffraction patterns from powder samples are mainly used for sample identification and phase analysis due to unique diffracted intensities for a particular phase (Passerini *et al.*, 2006). Diffraction mainly occurs when a propagating X-ray wave encounters regularly spaced solid particles with the same magnitude as the wavelength of spacing between the particles (Callister and Rethwisch, 2013). Not all diffracted waves appear, however, in the interference pattern due to destructive interference (the resultant of out-of-phase waves). Bragg's law gives a condition for the intensity of the diffracted beam related to the angle between the diffracted beam and the solid.

X-ray diffraction has been reported used in hydrogels to show the crystalline structure of the amoxicillin drug, as demonstrated by sharp and intense diffraction peaks close to 2-theta 6, 7.5, and a range of peaks between 10 and 30 2-theta (Passerini *et al.*, 2006). Upon

transformation of the chitosan into the form of hydrogel membranes, the crystalline structure changes from amorphous to crystalline phase (Cheng *et al.,* 2010). In conclusion, X-ray diffraction analysis can be of help to determine phase modification of green superabsorbent hydrogel after and before crosslinking with maleic acid.

2.14.2 Instrumentation

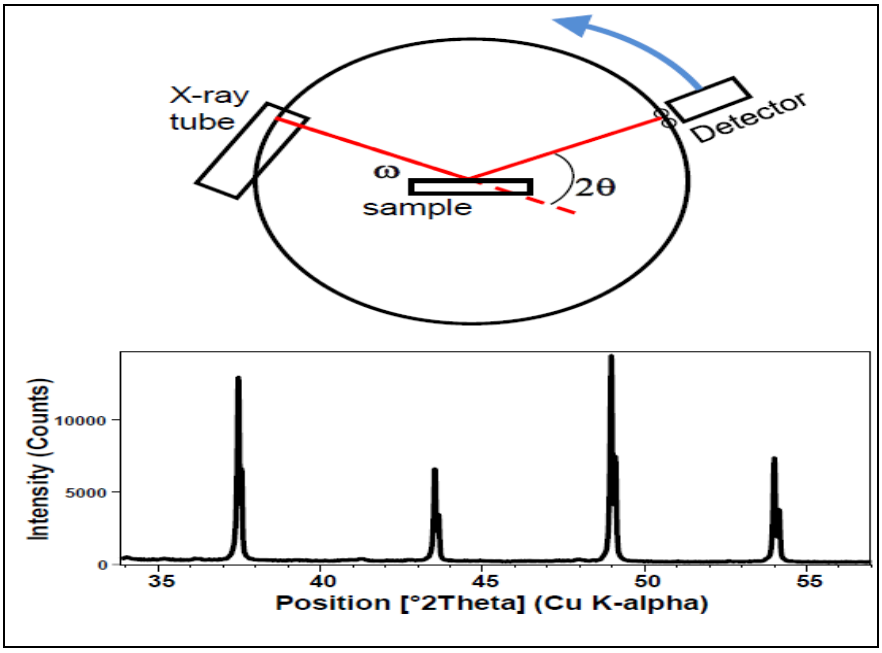

Figure 2.4: Schematic diagram for X-ray diffraction (XRD) (Source NI, 2016).

The detector moves in a circle around the sample position and is recorded as the angle 2theta (2θ) while intensity is usually recorded as counts or as counts per second using the Bragg-Brentano Para focusing geometry. To ensure a properly focused X-ray, the incident angle omega changes in conjunction with 2theta through either rotating the sample or the X-ray.

CHAPTER THREE

MATERIALS AND METHODS

3.1 Research design

This study utilized an experimental design that involved preparation of activated charcoal from coconut shells, extraction of citric acid from lemon fruits. Synthesis of super absorbent hydrogel by polymerizing AC or citric acid with ethylenediamine and glycerol then crosslinking with maleic acid. Optimization of AC, citric acid and maleic dosage to synthesize SAHs with optimum swelling capacity. monomers and crosslinkers of HLG-2, HLE-2, HCG-2 and HCE-2 super absorbent hydrogels done in Kenyatta university laboratories. Characterization of super absorbent hydrogels by SEM, XRD and FTIR while Application of the synthesized SAHs in the growing of maize (*Zea mays*) plants in farm plots at Mwala Machakos Sub County and measuring growth and yield parameters.

3.2 Collection of sample materials

Coconut shells for charcoal preparation were obtained from Changamwe Sub-County Mombasa County and then transported to the Kenyatta University laboratory. The shells were broken into smaller pieces 5 centimeters in length and then cleaned using deionized water to remove earthy materials followed by sun drying for three weeks. Lemon fruits used as a source of citric acid were purchased from local farmers in Wamunyu market Mwala sub County, Machakos County. Lemon fruits were transported to the Kenyatta University laboratory, feels removed and soft part blender using electric blender to extract citric acid.

3.3 Chemicals and reagents

All the chemicals used were of analytical grade and were used as purchased. Ethylenediamine used was obtained from Merck Chemical Co (Darmstadt, Germany), potassium manganate VII, sodium hydroxide, and sulphuric acid were obtained from Kenya science chemical limited Kenya, while maleic acid was obtained from Sigma Aldrich Company (Germany).

3.4 Preparation of activated carbon

The preparation procedure of activated charcoal was adopted from Papita (2010). Pieces of dry coconut shells were placed in a 20 L aluminum container and excess air was removed by warming. The container was then tightly closed and heated at a temperature of 473 to 553 K for 8 hours after which cooling was done for 24 hours to obtain charcoal (Papita, 2010). The charcoal was crushed and ground into fine powder using a Sheller machine (Honda ESB 501). A sample of 20 g of the powdered charcoal was then put in a 1 L Erlenmeyer flask and 500 mL of 2 M solution of acidified potassium permanganate was added. The mixture was allowed to stand for 12 hours to oxidize carbon. Oxidative reaction introduces oxygen functional groups on the surface of carbon materials to enhance cross-linking ability with ethylenediamine (Meng and Ye, 2017). The mixture was then filtered and the residue was washed with deionized water to remove the purple color of the oxidizing agent and air-dried in the open to a constant weight to obtain activated carbon.

3.5 Extraction of lemon juice (LJ) from lemons as source of citric acid

During extraction of citric acid used in the synthesis of super absorbent hydrogel, the lemons were peeled to obtain the fleshy inner part. The fresh soft part of the fruit was obtained then cut into smaller sizes followed by blending using an electric blender (CSZ 910) to obtain juice. The mixture was then sieved using standard sieve of 14-16 micro pores to obtain citric acid (CA) (Coolman *et al.*, 2008). Titration reaction between extracted citric acid and 1 M of sodium hydroxide solution was carried out to determine concentration of citric acid in the juice. The results obtained shows that citric acid in lemon fruits was 0.3 molar per litre (0.58 grams per 10 mL of citric acid extracted).

3.6 Preparation of super absorbent hydrogel polymers

3.6.1 Synthesis of hydrogel from activated charcoal and glycerol (HCG-1)

The synthesis of HCG-1 from AC and glycerol was adopted from Lakshmi (2011). An electronic weighing balance (CZ 200) was used to accurately weigh 80.0 g of powdered activated carbon which was transferred into 1000 mL Erlenmeyer flask. Addition of 100 mL of distilled water was done as stirring was continued until a gel was formed. The resultant gel was heated to boiling followed by adding 37.5 mL of 13.6 M glycerol and 10 mL of 5.0 M Sodium hydroxide as activator with stirring. The mixture was then heated until it became viscous, after which it was allowed to cool to room temperature to form 123 g of solid hydrogel polymer.

3.6.2 Synthesis of Cross-linked hydrogel (HCG-2)

The process of HCG-2 synthesis was carried out by preparing HCG-1 as per the procedure described in section 3.6.1. To the viscous gel obtained in section 3.6.1, 25.0

mL of 3.5 M maleic acid were added with stirring. The stirring and heating of the mixture was done continuously at a temperature of 373 K to 423 K until a viscous gel was formed followed by cooling to obtain 125 g solid HCG-2 hydrogel. Figure 3.1 shows the preparation scheme of HCG-2 hydrogel. The structure of activated charcoal was adopted from (Sugumaran *et al.* 2012).

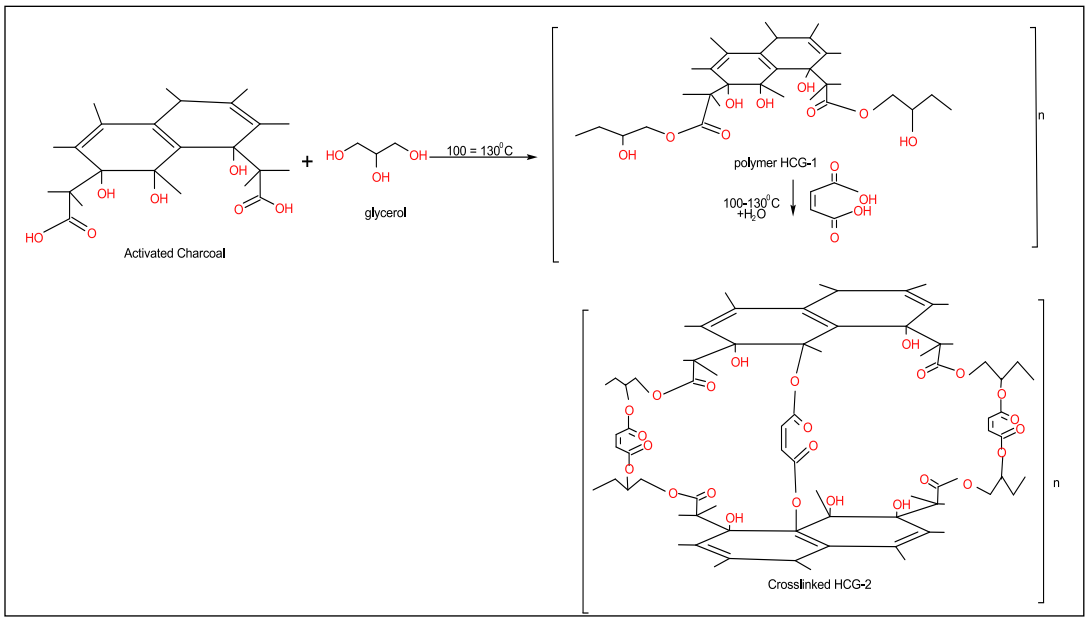

Figure 3.1: Scheme of preparation of HCG-1and HCG-2 hydrogel

3.6.3. Synthesis of hydrogel from activated charcoal and ethylenediamine (HCE-1)

The synthesis procedure of the hydrogel from activated charcoal and ethylenediamine (EA) was adopted from (Basri *et al*. 2020) with slight modification. The process occurred through interlinking the carboxylic acid group in AC and the amine group on EA to form monomeric unit through amide linkage. Accurately weighed 80.0 g of powdered (AC) using a weighing balance with precision (CZ 200) was transferred into a 1000 mL

Erlenmeyer flask. 150 mL of deionized water was then added while stirring to form carbon suspension. The mixture obtained was heated to a temperature of 100 °C for 5 minutes followed by the addition of 50.0 g of ethylenediamine and 2.0 g of sodium hydroxide pellets as the activator. The resultant mixture was heated at a temperature of 150 °C until a paste formed, after which it was allowed to cool to room temperature to form118.0 g of solid hydrogel polymer labeled HCE-1.

3.6.4 Crosslinking hydrogel with maleic acid (HCE-2)

The cross-linked HCE-2 superabsorbent hydrogel was prepared by adding 10.0 g of maleic acid to boiling paste of HCE-1. Stirring and heating of the mixture were done continuously at a temperature of 150 °C until viscous gel was formed. The gel was then cooled at room temperature to form 122.0 g of super absorbent hydrogel labeled HCE-2. Ester linkage was facilitated by the availability of hydroxyl groups in the polymeric material HCE-1 and carboxylate groups in maleic acid. Figure 3.2 shows the preparation scheme of HCE-2 hydrogel (Sugumaran *et al.,* 2012, Njoku *et al.,* 2014).

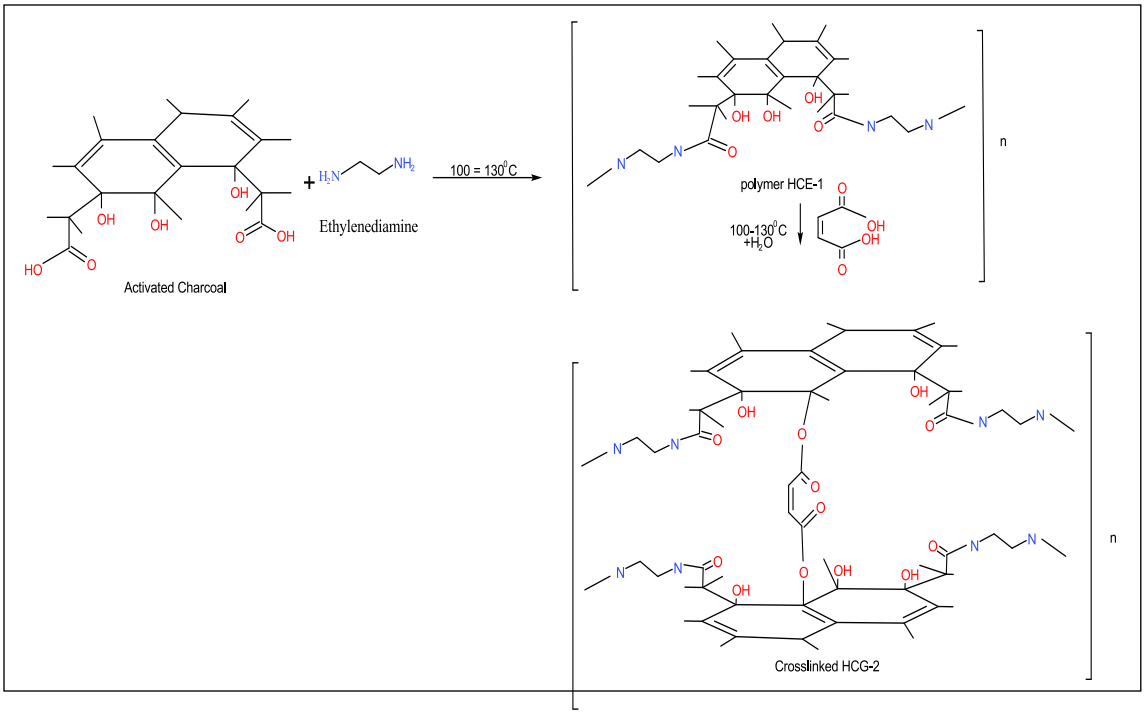

Figure 3.2: Scheme of preparation of HCE-1and HCE-2hydrogel

3.6 5 Preparation of hydrogel from citric acid and glycerol (HLG-1)

To prepare the lemon juice (citric acid)-glycerol polymer (HLG-1). A sample of 72.0 mL of 0.3 M lemon juice (citric acid), and 45.0 mL of 13.6 M glycerol measured with precision were put into evaporating dish. While 5.0 M sodium hydroxide were added to the mixture as activator with stirring. The mixture was then heated in the oven at a temperature of 363 K under stirring condition to facilitate water removal and polymerization reaction to occur. The heating was stopped when viscous gel was formed and the gel cooled to form 75 g solid of HLG-1 hydrogel (Coolman *et al.*, 2008).

3.6 6 Preparation of cross-linked hydrogels HLG-2

During the process of polymer gel HLG-2 preparation, hydrogel gel HLG-1 prepared in section 3.6.5 was cut into smaller pieces and placed in a 2 L aluminum container and heated in an oven to melt. 50.0 mL of 3.5 M maleic acid was then added as a cross-linker and the mixture was heated continuously with stirring at a temperature of 373 K until a viscous gel was formed. The mixture was then removed from the oven and cooled to form (HLG-2) hydrogel. Figure 3.3 shows the diagrammatic scheme for preparation of HLG-2 hydrogel

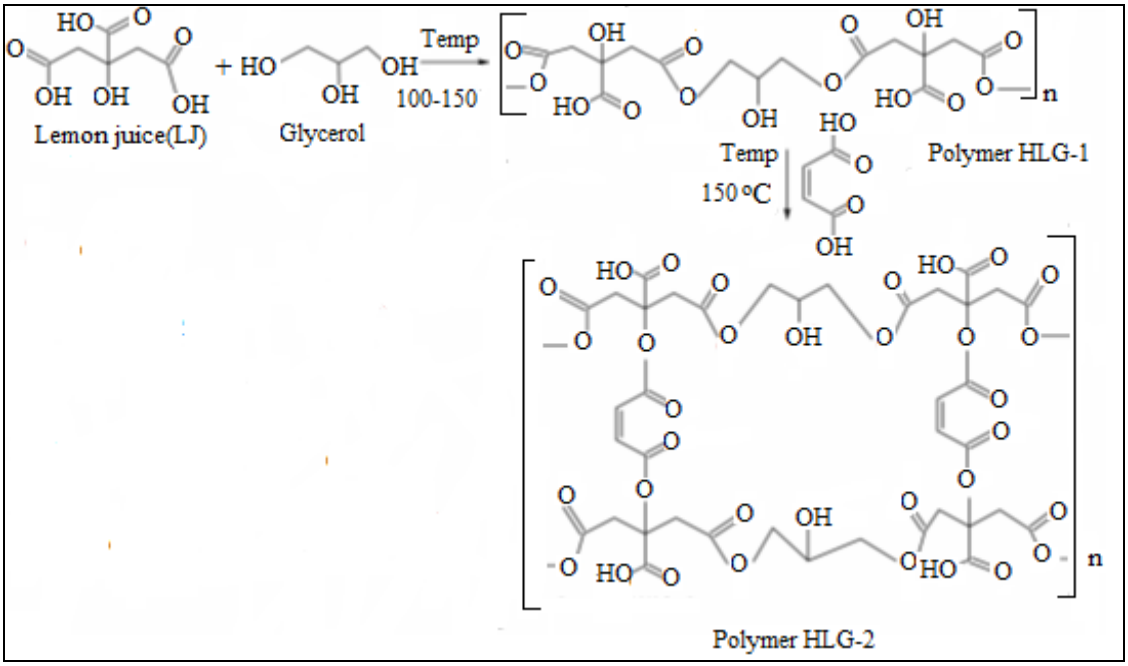

Figure 3.3: Scheme of preparation of HLG-2 hydrogel

3.6.7 Preparation of hydrogel from lemon juice and ethylenediamine (HLE-1)

During preparation of uncrosslinked super absorbent hydrogel HLE-1. A sample of 145.0 mL of (CA) from lemon juice and 90.0 mL of ethylenediamine (14.8M) were measured using a volumetric flask and put in a 5.0 L aluminum container. 100 mL of distilled water

was added to the mixture as solvent. The mixture was then heated at a temperature of 373 K to 405 K in an oven until the gel was viscous. This was a proof of complete polymerization reaction, and the gel was allowed to cool to form 95 g of solid hydrogel HLE-1.

3.6.8 Preparation of cross-linked hydrogels (HLE-2)

Cross-linked HLE-2 superabsorbent hydrogel was prepared by adding 75.0 mL of 3.5 M maleic acid to boiling HLE-1. The mixture was stirred and heated continuously at a temperature of 373 K to 405 K to form a viscous gel. The mixture was then cooled to form 110 g of HLE-2 hydrogel. Figure 3.4 shows the preparation scheme of HLE-2 hydrogel.

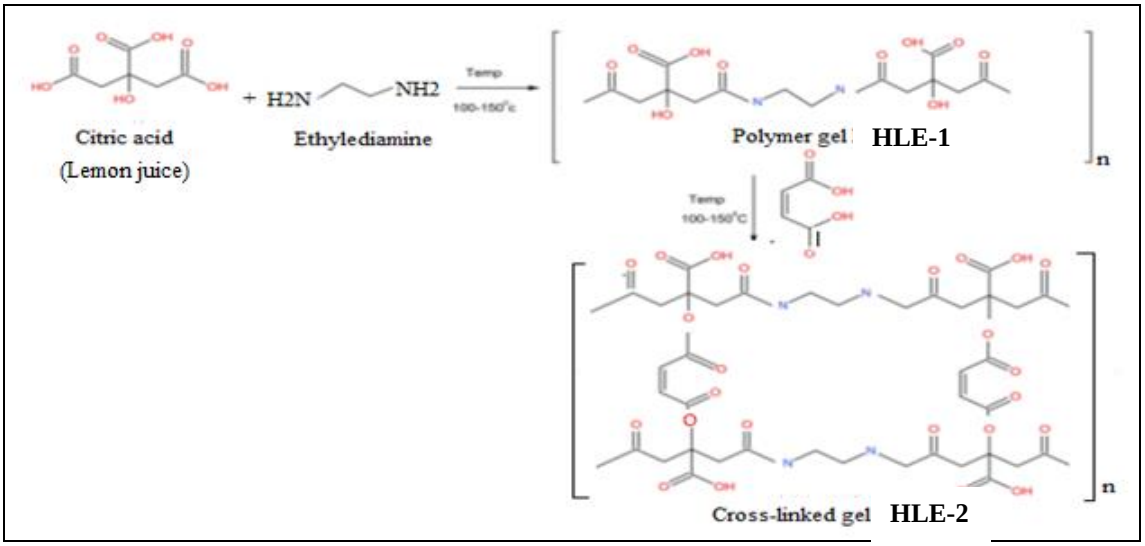

Figure 3.4: Scheme of preparation of HLE-2 hydrogel

3.7 Characterization of the hydrogel

3.7.1 Fourier transform infrared (FT-IR)

The procedure for determination of functional groups present in the crystal of HLG-2, HLE-2, HCG-2, and HCE-2 super absorbent hydrogel was adopted from (Krauklis *et al*., 2018) using (Shimadzu IR Tracer -100 German). The FTIR analysis samples with and without crosslinker were obtained by mixing 1 mg of the dried sample of material with 25 mg KBr (1:25) (Hammond *et al*., 2005). Grinding of the mixture done using mortar and pestle to form fine powder then compressed into a thin pellet. The analysis of the pellet was done using FTIR spectrophotometer followed by measurement of spectra within the range of 400–4000 cm^{-1}. The spectra were plotted using the same scale on the transmittance axis of cross linked and uncrosslinked hydrogel.

3.7.2 X-ray diffraction (XRD)

The phase composition of the Samples of HLG-2, HLE-2, HCG-2, and HCE-2 superabsorbent hydrogel was carried out using (Hossein beygin German) diffractometer with Cu Kα radiation, λ=1.5418 Å and an applied voltage and current 45 kV, 40 mA, respectively. Scanned 2 theta range was 10-90 with step size of 0.017 degrees 2 theta. Anton Paar HTK1200 high temperature furnace was used for non-ambient temperature measurements. Calibration of Internal thermocouple chamber was regularly done in comparison with the use of the external thermocouple, since large (up to 700 °C) discrepancies between internal thermocouple and actual temperatures were confirmed to be regular by the manufacturer at temperatures below 500-6000 °C. The quality of data

required was determined by different collection time, phase characterization and analysis were set at a rate of 10 seconds per step while quantitative phase and composition analysis time per step of up to 50 seconds were used.

Single crystal analysis results into various parasitic secondary reflections, to overcome this effect highly parallel and focused beam was used at mirror stage to produces regular clear pattern. Instrumental peak broadening was measured using LaB6 as a standard and detailed techniques of crystalline size measured. Powders were ground using mortar and pestle to obtain similar particle size distribution followed by obtaining diffraction patterns at room temperature. The samples were done in triplicate at the same amount and conditions for absolute comparison of peak intensities while Philips X'Pert Plus software was utilized to perform Reitveld refinements of the unknown phases.

3.7.3 Scanning electron microscopy (SEM)

The surface morphologies of the HLG-2, HLE-2, HCG-2, and HCE-2 superabsorbent hydrogels were determined using Scanning Electron Microscope (ZEISS SUPRA 60 German) bright microscope at an accelerating voltage of 250 kV. Powdered prepared samples were dried in the oven at 45 °C for 6 hours until a constant weight was attained followed by coating with gold then placing them in an enclosed glass slide to obtain micrographs (Zhu *et al*., 2017).

3.8 Percentage swelling

The procedure for determining percentage swelling of the super absorbent hydrogel was adopted from (Zhu *et al*., 2017). A sample of 2.0 g of the SAHs polymers were put in permeable polyester bags of 5 cm long. The weight of the hydrogels and polyester bags was determined and recorded as (Ws). The polyester bags containing hydrogels were then immersed in 500 mL of distilled water and allowed to absorb water for 24 hours. After the contact period, the samples were removed and excess water on the surface of polyester bags was removed using filter paper (blotting) and their weight determined and recorded as (Wd) (Zhu *et al*., 2017). Equation 1 was used to determine the equilibrium water content.

$$EWC\ (\%) = \frac{Q_t - Q_x}{Q_x} \times 100 \quad \text{...} 1$$

Where Q_x is the initial weight of hydrogel before swelling and Q_t the final mass of the swollen hydrogel HLG-2, HLE-2, HCG-2, and HCE-2.

3.9 Field preparation and crop management

3.9.1 Field preparation

Land clearing was done on month of January 2020 using panga, jembe and axe to easy primary cultivation, chase rodents and any other dangerous animals, which may be available. Primary cultivation on gross plots was done before rains on April using oxen plough to kill weeds, soil borne pathogens by exposing them to radiant heat from sun and allow water infiltration in the soil. Secondary cultivation carried out after 14 days using

hallows to break large clods of soil to increase rate of water infiltration, easy planting and root penetration in the soil. Tertiary cultivation practices were done using jembe and spade to ensure proper levelling of the plots followed by preparation of holes for planting as per the recommended spacing of 90 cm by 30 cm in semiarid regions.

3.9.2 Field study experiment

Experimental design was used in the synthesis of super absorbent hydrogel. Maize hybrid seeds DH 02 were planted in 52 plots. Application of the cross-linked superabsorbent hydrogel was carried out in split plot arrangement of size 4.2 x 3.6 m^2 using randomized complete block design with three replicates. The effects of four types of superabsorbent hydrogels HLG-2, HLE-2, HCG-2, and HCE-2 were the main blocks. Plots coded 1, 2, 3 and 4 were treated with hydrogel dosage of (15, 30, 45 and 60 kg/ha) respectively while zero was used as control experiment.

Table 3.1: Shows the randomized block design used in application of the hydrogels

Hydrogel	**Plots (4.2 x 3.6 m^2)**												
HCG-2	0	1	2	3	4	1	2	3	4	1	2	3	4
HCE-2	1	2	3	0	1	4	3	2	1	4	3	4	2
HLE-2	3	0	1	4	3	2	1	4	3	2	1	2	4
HLG-2	2	4	4	2	2	3	4	1	1	3	1	3	0

Parameters measured and recorded included percentage moisture content at flowering, plant height, the number of leaves, leaf surface index, dry matter accumulation, and rate of crop growth after 15, 30, 45 and 60 days. Harvesting of maize was at 120 days (after matured), and maize stalks were cut using a sickle. The maize cobs were dried by spreading them on a mat. The post-harvest parameters determined included the number of

cobs per plant, cob length, the girth of the cob, the number of grains per cob, the mass of grain per cob, and mass per grain shelling percentage were determined using an electronic analytical balance. The yield parameters per plot determined included grain yield, stover yield, cob yield, biological yield and harvest index percentage were determined using an electronic analytical balance and computed in kg/ha.

3.9.3 Cultural operation and care

During planting time, half dose of Nitrogenous and full dose of P_2O_5 and K_2O fertilizer was applied in form of urea, DAP and Muriate of Potash. Remaining half-nitrogenous fertilizer applied in two split applications, at knee high and tasseling stages. Folia tango sprayed at 15 and 45 days to control maize stalk borers throughout the research period while weeds control by hand digging using jembe was conducted at 15 and 45 days. Harvesting using sickle was performed per the maturity of each plot followed by proper drying of the yields in the sun. Actelic dudu dust was sprayed on harvested maize cobs to control weevils then threshing, shelling, and winnowing done manually on yields. Finally, the weights of pure clean grains, stover, and cobs were obtained by use of electronic balance per plot followed by mean determination then recorded.

3.10 Pre-harvest studies

3.10.1 Percentage moisture in plant

During experimentation period, gravimetric technique was employed to determine the moisture content of maize crop in each plot at the flowering stage. Weight of three random complete uprooted maize crop taken and recorded when fresh and after drying at

298 K for 5 days until they attained constant weight. Mean values of the weight obtained as fresh weight (Wf) and dry weight (Wd) while moisture content percentage of plant calculated by using equation 2.

$$moisture\ content\ \% = \frac{(W_f - W_d)}{(W_d)} \times 100 \quad \ldots\ldots 2$$

3.10.2 Growth height

A meter rule was used to measure the height of three selected maize crop in each plot randomly, starting from ground level to the growing tip of each crop at 15, 30, 45 and 60 days of the growth period. Mean values for each plot determined and expressed in centimeters.

3.10.3 Number of leafs per crop

The leaves of three randomly selected maize crops from each plot counted at 15, 30, 45, 60 days of the growth period and flowering stage. Mean leaf values for each growth stage per plot obtained and recorded.

3.10.4 Leaf surface index (LSI)

Leaf surface index is the ratio of leafs surface area per crop to the size of the land occupied by the maize crop. To determine LSI, the maize crops from the bordering rows of each plot were taken for study at 15, 30, 45, and 60 days of the growth period. The leaves of the maize crop were separated; each leaf's surface area was determined using a planimeter, and a sum of the surface area of leaves per plant was obtained.

Determinations of LSI were done (Watson, 1956; Yao *et al*., 2010; Musa and Usman, 2016).

$$LSI = \frac{\textbf{Leaf area per plant } (cm^2)}{\textbf{Land area occupied by the plant } (cm^2)} \quad \text{.....3}$$

3.10.5 Dry matter accumulation per plant

Dry matter accumulation at 15, 30, 45, 60 days of growth period and harvesting stage were obtained randomly by uprooting three maize crops from each plot with all leaves attached. The obtained samples of maize crop were air dried until they attained constant dry weight. The mean values of dry matter per plot determined then expressed in gram per plant.

3.10.6 Rate of crop growth (CGR) (g m^{-2} day^{-1})

This is the ratio of dry matter accumulation in the plant per unit of ground area per unit of time. The data of dry matter accumulation in grams and the land surface area occupied by crop in cm^2 obtained at sections 3.10.5 and 3.10.4 respectively were employed to obtain crop growth rates at 15, 30, 45 and 60 days of growth period using equation 4. The mean values were worked out and expressed in g m^{-2} day^{-1} (Watson 1956; Blackman 1919).

$$CGR\ (g\ m^{-2} day^{-1}) = \frac{x_2 - x_1}{t_2 - t_1} \times \frac{1}{A} \quad \text{.....4}$$

where

x_1 = Dry matter of the crop (g) at time t_1, x_2 = Dry matter of the crop (g) at time t_2, A = land surface area covered by the crop (m^2)

3.11 Post harvest studies

3.11.1 Number of cobs per plant

The procedure for determining number of cobs per plant was adopted from (Islam *et al.* 2011). Three maize plants per plot were randomly obtained at the harvesting stage, counting the number of cobs was done per plant. Mean cob per plant for each plot was determined and recorded

3.11.2 Length of cob determination

The procedure for determining length of cob was adopted from (Orosz *et al*., 2009). Three randomly selected maize cobs from each plot were used to determine the mean cob length per plot. The cob length was measured using a meter scale and recorded in centimeters.

3.11.3 Girth of cob

The procedure adopted from Khadem *et al.* (2010) was used to determine mean girth of cob per plot. Three randomly selected maize cobs per plot were obtained. The girth of each cob was determined by getting the average circumference of the three regular intervals of the cob using thread at the top, bottom, and central portions of each cob. The measurements obtained were transferred to a meter scale for reading in centimeters followed by calculating the mean girth value per cob.

3.11.4 Number of grains per cob

The procedure was adopted from (zhiming *et al.*, 2007), after the physiological maturity of maize crops, three randomly selected maize crops were harvested per plot. The total number of grains in each cob was determined by counting followed by calculating the mean number of grains on a cob per plot.

.3.11.5 Mass of grains per cob and cob without maize

The procedure was adopted from (Islam *et al.*, 2011). After harvesting, the maize cobs per plot were dried in the sun to obtain a constant mass. Three dry maize cobs per plot were randomly selected then shelling was done by hand. Mass of dry grains and cobs without grains was determined by use of electronic balance (CZ 200). The mean mass per cob and grains per cob were calculated and recorded in grams.

3.11.6 Shelling percentage

The shelling percentage of each plot was determined from three plants randomly sampled after harvest using the formula adopted from (Undie *et al.* 2012).

$$\text{Shelling percentage (\%)} = \frac{Mean\ seed\ weight\ per\ cob}{Mean\ cob\ weight} \times 100\% \quad \text{.....3}$$

3.12 Yield of maize

3.12.1 Mean Grain and cob yield per plot

Harvesting of maize cobs per net plot were done after reaching biological maturity by dehusking. The harvested cobs were air-dried until no change in weight. Shelling of the

cobs per plot done by hand then cobs and pure dry maize separated. Mass of pure maize grain and cobs per plot determined using electronic balance followed by mean grain and cob yield per plot then computed in kg per hectare.

3.12.2 Stover yield

The procedure was adopted from (zhiming *et al*., 2007). After harvesting maize cobs, the stover per plot were harvested using sickle, then air-dried in the sun until constant mass was attained. Completely dry Stover was put in bundles per plot and their mass obtained using electronic balance in kilograms per plot. Mean stover yield obtained then expressed in kg per hectare

3.12.3 Biological yield

After obtaining mean dry Stover and cob yield per plot as described in section 3.12.2 and 3.12.1, to obtain biological yield the sum mass of dry stover and cob yield per net plot was determined and expressed in kilograms per hectare. Procedure was adopted from (Islam *et al*., 2011)

3.13 Harvest index (%)

This is the mass ratio of grain yield of maize to that of biological yield. The mean grain yield and biological yield were obtained per plot as described in 3.12.1 and 3.12.3 respectively. The ratio of mean grain and biological yield were computed in percentage per hectare.

3.14 Statistical analysis

The optimizations results obtained from the studies were subjected to analysis of variance One-way ANOVA test with post hoc comparison (Tukey HSD test), using minitab software version 17, Fisher least significance difference (LSD) test to generate mean at 5 % confidence level of significance

CHAPTER FOUR

RESULTS AND DISCUSSION

4.1 Introductions

All experimental work and findings obtained in this study are discussed in this chapter. This includes results from the characterization of the cross linked and uncrosslinked hydrogels experiments results. The results on parameters such as the effect of activated charcoal, citric acid, ethylenediamine, glycerol and maleic acid dosage on the swelling capacity of hydrogel were optimized is provided. The determination of the swelling capacity of cross-linked hydrogel prepared using optimum conditions as well as the effect of dosage on growth and yield parameter of maize grown in the semi-arid region of Mwala is also provided and discussed.

4.2 Synthesis of super absorbent hydrogels HCE-1 and HCE-2

The process involved carbon suspension formation under heating of 80.0 g of powdered (AC) with 150 mL of deionized water in 1000 mL Erlenmeyer flask at a temperature of 100 °C for 5 minutes followed by the addition of 50.0 g of ethylenediamine and 2.0 g of sodium hydroxide pellets as the activator to form. A solid hydrogel polymer of 118.0 g was formed and labeled HCE-1. The HCE-2 super absorbent hydrogel was prepared by adding 10.0 g of maleic acid to a boiling paste of HCE-1 at a temperature of 150 °C until viscous gel was formed. The gel was then cooled to form 122.0 g of SAH labeled HCE-2 with optimum percentage swelling of 1090 %. Polymerization reaction occurs between monomer of AC and ethylenediamine forming HCE-1 hydrogel which was converted to

crosslinked hydrogel through ester linkage between OH groups of HCE-1 polymer units with carboxylate groups of maleic acid. The products were characterized by FTIR spectroscopy, XRD, and SEM as well as by determination of their percentage swelling.

4.2.1 Fourier transform infrared of HCE-1 and HCE-2 superabsorbent hydrogel

The FTIR was carried out to identify the functional groups involved in amine linkage, ester cross linkage and water absorption in super absorbent hydrogels. FTIR spectra of HCE-1 and HCE-2 were recorded in the range 4000-200 cm^{-1}. The IR spectrums are shown in figures 4.2.1 and 4.2.2 while functional groups summarized in (appendix 1A) respectively.

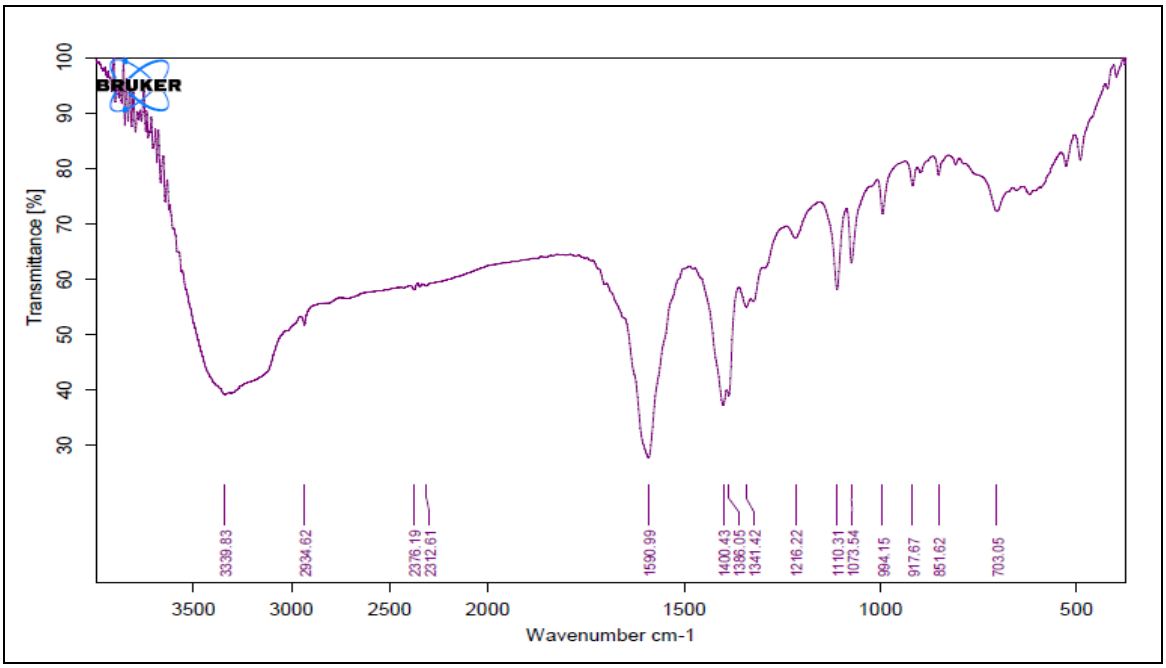

Figure 4.2.1: FT-IR spectrum of HCE-1

Figure 4.2.1 shows an FT-IR spectrum of HCE-1 super absorbent hydrogel. The absorption peaks in HCE-1 observed at around 3339.83 cm^{-1} and 2934.62 cm^{-1} were

attributed to -OH stretching vibration and C-H asymmetric stretching of methylene in AC. Similar results have been reported by (Kono and Fujita, 2012). However sharp spectra bands at 1590.99 cm^{-1}, and 1216.2 cm^{-1} in HCE-1 were associated with C-N-stretching vibration and N-H bending bond, indicating interlink between AC and EA monomers. Similar results were obtained by (Gupta *et al.,* 2013). Peaks appearing at around 1341.4 cm^{-1}, and 1073.5 cm^{-1} are due to –OH bending and C-O- stretching vibration in HCE-1 respectively. Similar results were obtained by (Yeasmin and Mondal, 2015). In addition, IR peaks at 1400.43 cm^{-1} and 1386.05 cm^{-1} are assigned to -COO^{-} carboxylate associated with AC in the gel. The peaks at 1110 cm^{-1}, 994 cm^{-1}, 917.7 cm^{-1}, and 703 cm^{-1} are due to alkyl substitute in ether C-O stretching, vinyl C-H out of plane bending, bending -OH vibration and bonding deformation vibration respectively (Merkel *et al*., 2014). The bands at around 851.6 cm^{-1} and 703.05 cm^{-1} were a relatively pure ring stretching mode associated with aromatic ether C-O–O^{-} and H bond deformation in AC. A similar finding has been reported by (Jiang *et al.*, 2004; Parikh and Chorover, 2005). Figure 4.2.2 shows the FT-IR spectrum of HCE- 2 super absorbent hydrogel

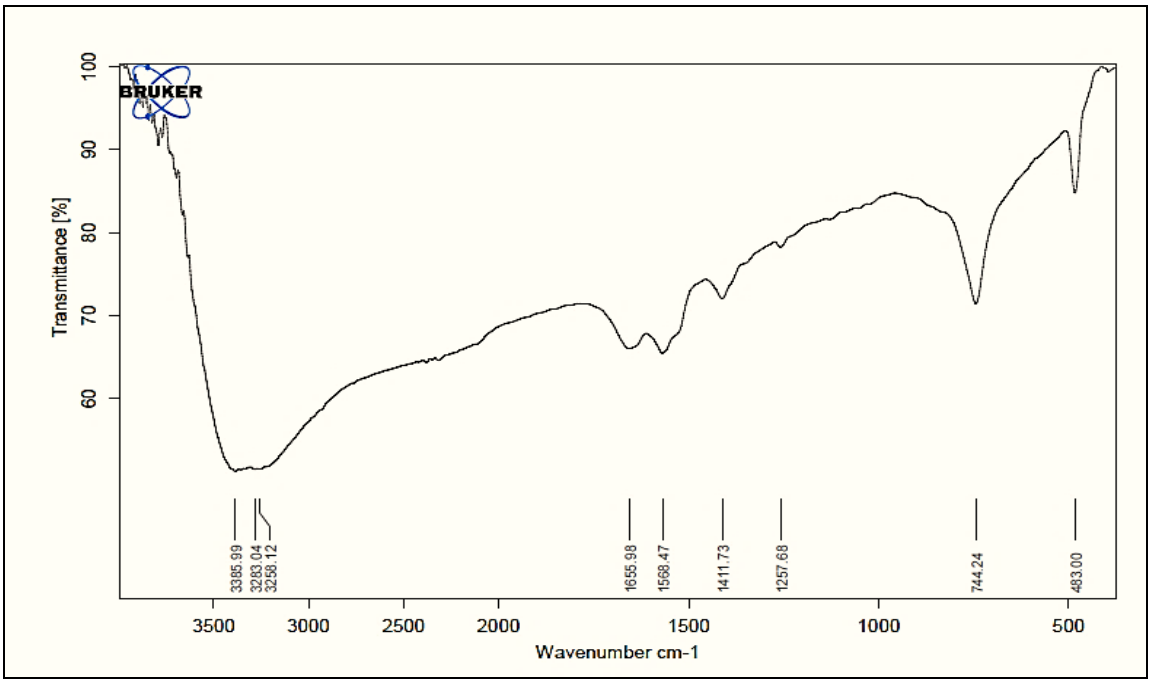

Figure 4.2.2: **FT-IR spectrum of HCE-2**

Figure 4.2.2 shows FT-IR spectrum of cross-linked HCE-2 super absorbent hydrogel with maleic acid and their functional groups associated with peaks. Functional group of the cross-linked hydrogel was analyzed after maleic acid was incorporated in the hydrogel and coded as HCE-2. New peaks appeared at 3283.04 cm^{-1}, 3258.12 cm^{-1} associated with normal polymeric –OH stretching in (AC) overlapping with asymmetric strong H bond interaction in EA. Similar results were obtained by Kono and Fujita, (2012). Appearance of broad peaks at 3385.99, 1257.68 cm^{-1} and 744.24 cm^{-1} were attributed to broad -OH stretching vibration, –OH phenolic bending and –OH bending in carboxylate respectively (Capanema *et al.*, 2018). The increased presence of hydrophilic groups, shows increased water affinity on the surface of HCE-2. On the other hand most significant change between HCE-1 and HCE-2 is the appearance of the peak at 1655.98 cm^{-1} associated with CO stretching in amide and the shift of $-COO^{-}$ stretching vibration from 1386.05 to

1411.73 cm^{-1} (Singh and Kaur, 2013). This indicates ester crosslink between the polymer chains HCE-1 gel to form HCE-2 super absorbent hydrogel as reported in a similar study by (Singh and Kaur, 2013).

4.2.2 Phase composition of (HCE-1) and (HCE-2) super absorbent hydrogels

The XRD diffraction pattern of HCE-1 is shown in figure 4.2.3. The sharp peaks represent the crystalline phases present in the studied samples while the hallo/broad peaks represent the amorphous phase. Similar findings have been reported for by (Teodorescu *et al*., 2016).

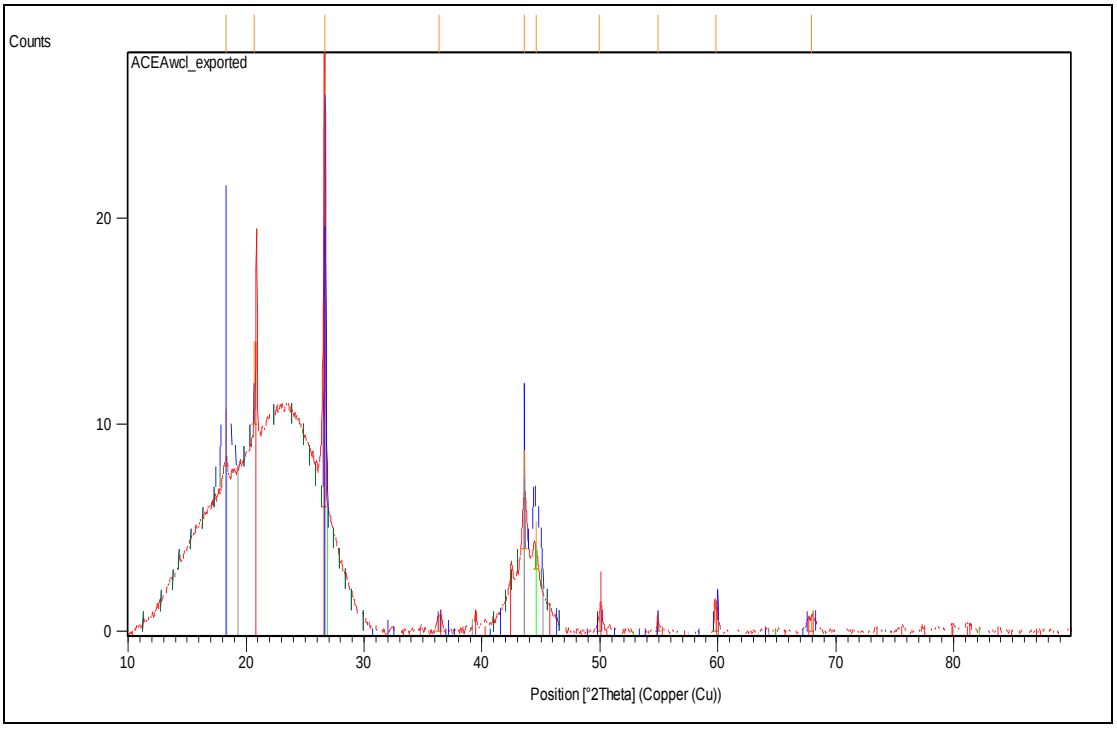

Figure 4.2.3: Powdered diffraction pattern of HCE-1.

Strong reflection intensities peaks were observed at (2θ) values of 20.6, 26.68, 43.59, 44.58, and 49.96 representing semi crystalline phases of the polymer network, S-triazine

($C_3H_3N_3$), graphite, carbon, and amine (NH_2) phases respectively (Mohamood *et al.*, 2018). The peak bands in the hump between 10 and 31° (2θ) revealed the presence of a carboxylate phase on the surface of activated carbon and the amorphous nature of HCE-1. Similar results were obtained by (Teodorescu *et al*. 2016). Figure 4.2.4 shows the diffraction pattern of the HCE-2.

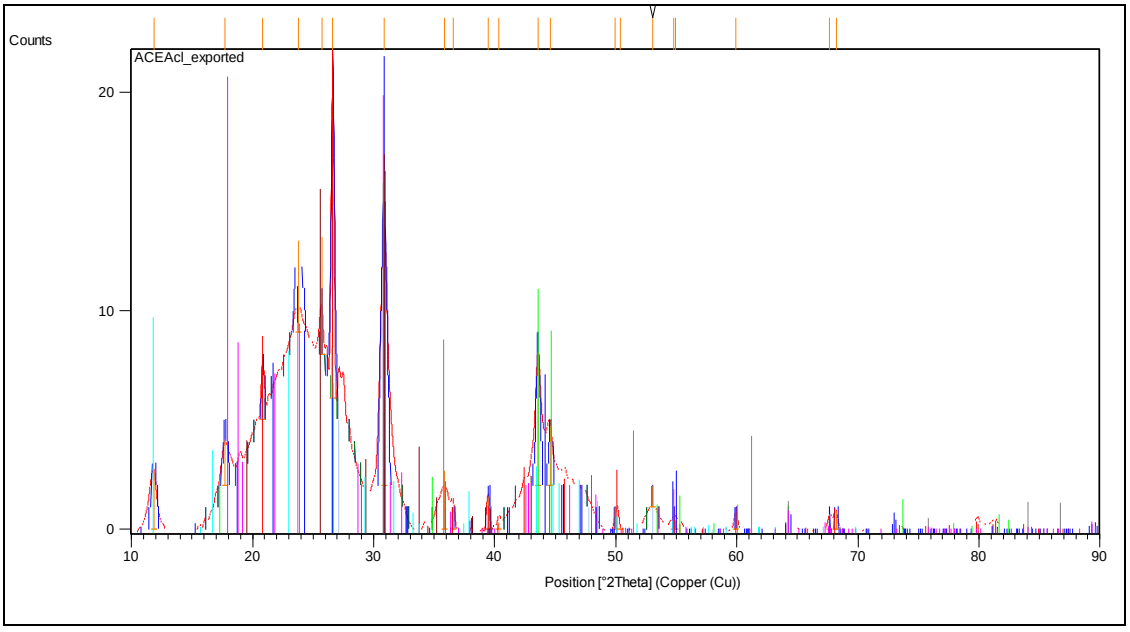

Figure 4.2.4: shows the powdered diffraction pattern of cross-linked HCE-2.

New peaks appeared on HCE-2 hydrogel at 2θ values of 23.81 and 25.71 due to the tubular structure of carbon atoms in the hydrogel (Bouchelta *et al*., 2008). The sharp, well-resolved peaks at angle 2θ 30.84, 35.88, 39.45 confirmed crystalline phases of graphite, carboxylate, and amine respectively. The peaks at an angle (2θ) of 40.33 and 50.37 were due to the crystalline phase structure of the hydrogel (Varaprasad *et al*., 2010). The peak at 18.27(2θ) (Figure 4.2.3) associated with a crystalline phase of N-C=O in HCE-1 disappeared upon cross-linking. This could be attributed to the fact that there

were inter and intramolecular interactions between –COOH in AC and –NH_2 group from EA forming a strong crystalline phase network in HCE-2 super absorbent hydrogel as reported in a similar study by (Busselez *et al*., 2012). A higher degree of crystallinity was observed in HCE-2 super hydrogel as compared to HCE-1. XRD analysis shows an increase in crystallinity of HCE-2 and this is key towards hydrogel degradability, water uptake, and swelling ratio as reported in a similar study of hydrogel by (Ou *et al*., 2005).

4.2.3 Scanning electron microscopy of (HCE-1) and (HCE-2) super absorbent hydrogels

The microstructure and morphology analysis of the SAHs of HCE-1 and HCE-2 was done using a scanning electron microscope (model Zeiss supra 60) at an accelerating voltage of 2.50 kV. This is a powerful method commonly used to capture the characteristic network structure in hydrogels (Aouada *et al*., 2005; El Fray *et al*., 2007; Pourjavadi and Kurdtabar, 2007). The SEM images of powdered hydrogels (HCE-1 and HCE-2) are shown in figure 4.2.5

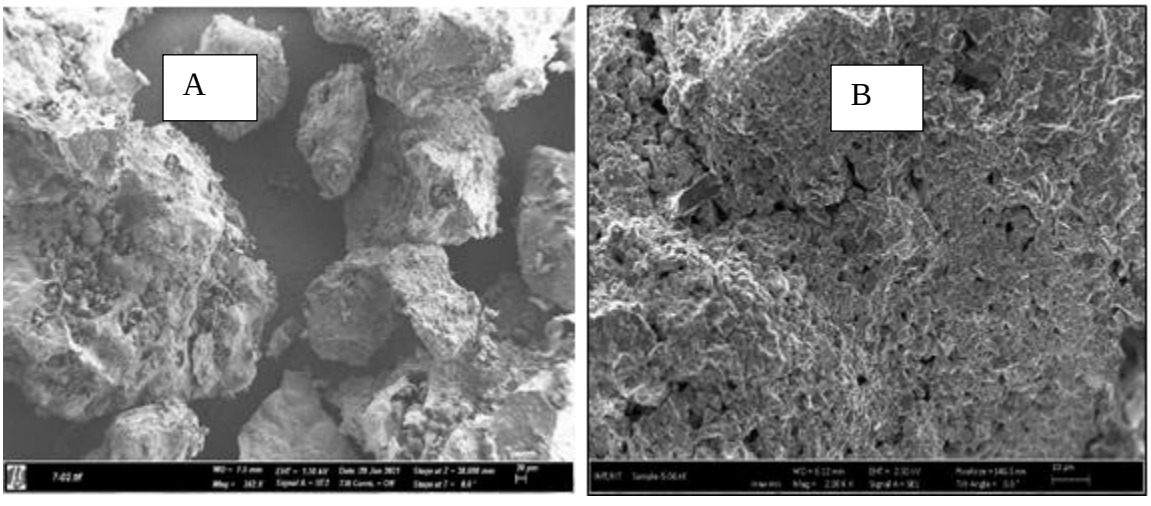

Figure 4.2.5: SEM micrographs of (A) HCE-1 and (B) HCE-2 super absorbent hydrogels

The micrographs show the presence of voids due to the irregular continuous mass of particles that are compacted in the gels. The micrograph of HCE-2 shows dense mast homogenous morphology compared with the rigid rough morphology of HCE-1. This could be attributed to complete polymerization that occurred upon the addition of the cross linker (Lu *et al*., 2009, Kumar *et al*., 2014). This revealed that the addition of cross linker facilitated polymerization reaction via formation of ester links, more cross linker points, and increased crosslinking density on hydrogel resulting in the formation of rough and protrusions surfaces throughout the micrographs which are responsible for water absorption (Luo *et al*., 2009).

4.3 Synthesis of super absorbent hydrogels HCG-1 and HCG-2

The carbon suspension was formed by heating 80.0 g of powdered AC with 100 mL of distilled water into a 1000 mL Erlenmeyer flask followed by adding 37.5 mL of 13.6 M glycerol and 10 mL of 5.0 M Sodium hydroxide to form 123 g of solid hydrogel polymer HCG-1. The process of HCG-2 synthesis was carried out by preparing HCG-1 and then adding 25.0 mL of 3.5 M maleic acid. Stirring and heating were done at a temperature of 373 K to 423 K until a viscous gel was formed, followed by cooling to obtain 125 g solid HCG-2 hydrogel with the highest percentage swelling of 1255 %. The products were characterized by FTIR spectroscopy, XRD, and SEM as well as by determination of their percentage swelling.

4.3.1 Fourier transform infrared of HCG-1 and HCG-2 super absorbent hydrogels

Figure 4.3.1 shows the FT-IR spectrum of HCG-1 super absorbent hydrogel and functional groups associated with peaks before crosslinking with maleic acid appendix 1B

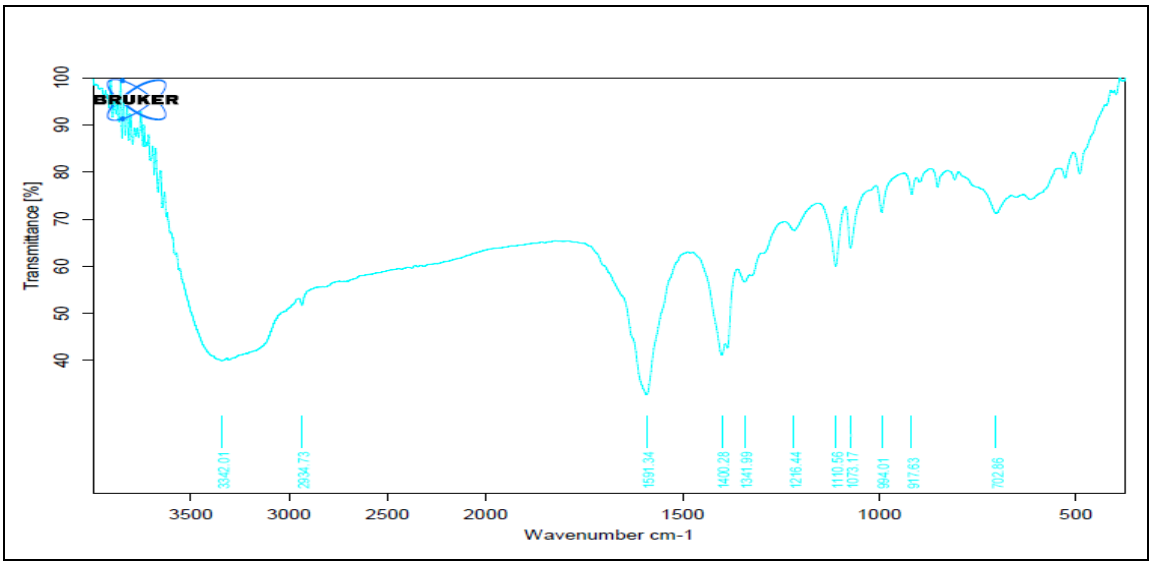

Figure 4.3.1: FT-IR spectrum of HCG-1

The spectrum in figure 4.3.1 shows uncross linked network of HCG-1 with broad peak absorption band at 3342.01 cm^{-1} indicating bending vibration of –OH on the surface of activated charcoal while C-H asymmetric stretch of methylene at of 2934.73 cm^{-1} (Kondo 1997; Viera *et al*., 2007). Strong peaks at 1591.34 cm^{-1} and 1400.28 cm^{-1} are attributed to symmetric stretching and asymmetric bending vibration bands of COO^{-} while C–O stretch vibration, alkyl substituted ether C–O stretching vibration and C–O– C stretch of ring ether vibration appeared at 1341.99 cm^{-1}, 1110.56 cm^{-1} and 1073.17 cm^{-1} respectively. Further small intense peaks at 1216.44 cm^{-1}, 994.01 cm^{-1}, 917.63 cm^{-1} and 702 cm^{-1} were associated with –OH bending in phenol, vinyl C-H out of plane bending,

Vinylidene C-H out of plane bending and H-bond deformation respectively (Silverstein and Bassler, 1966).

Figure 4.3.2 shows the FTIR spectrum and functional groups of HCG-2 super absorbent hydrogel after crosslinking with maleic acid (appendix 1B). As shown, new peaks rise upon crosslinking at 2108.49 cm^{-1}, 1639.48 cm^{-1}, 1409.36 cm^{-1}, 1255.84 cm^{-1} and 619.57 cm^{-1} associated with CN bending, COO^{-} bending in non-conjugated ester, phenol –OH stretch in ester, aromatic ether stretching and alcohol OH out of plane bend indicating successful esterification (Coma *et al*., 2003).

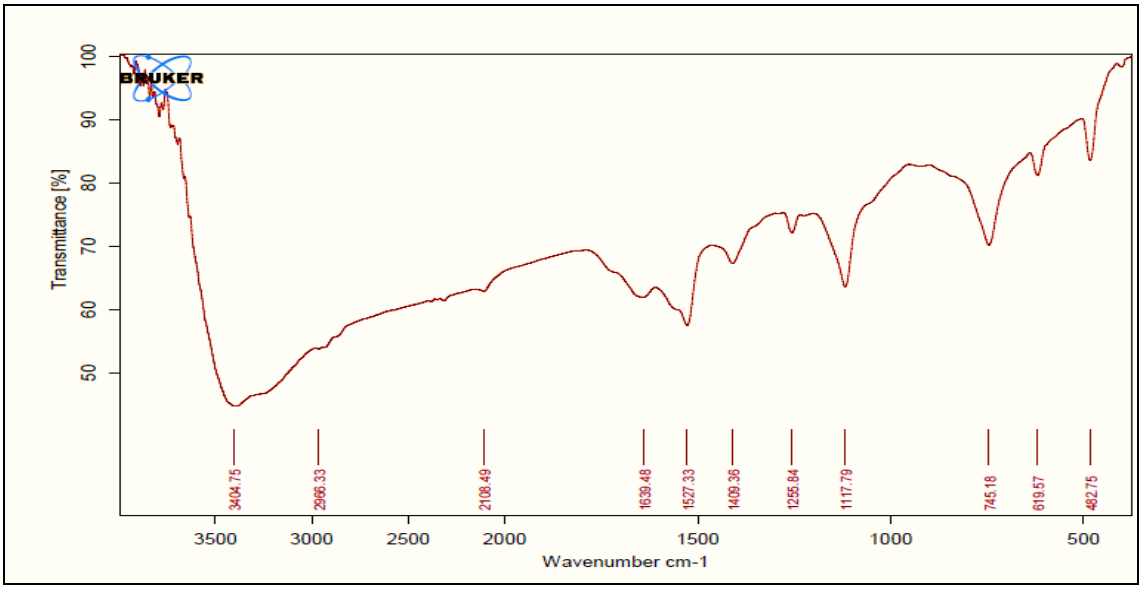

Figure 4.3.2: FT-IR spectrum of HCG-2

There was a significant shift in wavelength of HCG-1 as compared with HCG-2, alcohol –OH stretching mode shifts from 3342.01 cm^{-1} to 3404.75 cm^{-1}, asymmetric C-H stretch shifts from 2934.73 cm^{-1} to 2966.33 cm^{-1}, symmetric stretching of COO^{-} shifts from 1591.34 cm^{-1} to 1527.33 cm^{-1}. Consequently, alky substituted ether C–O stretch vibration

shifts from 1110.56 cm^{-1} to 1117.79 cm^{-1} while H bond deformation shifts from 702.86 cm^{-1} to 745 cm^{-1}. Again IR spectrum of HCG-1 shows peaks at 1400.28 cm^{-1}, 1341.99 cm^{-1}, 1073.17 cm^{-1}, 994.01 cm^{-1} and 917.63 cm^{-1} disappeared completely as compared with spectrum of HCG-2. The above information shows clearly, there was hydrogen bonds formation, intramolecular and intermolecular hydrogen bond formation in HCG-2 super hydrogel as reported in the similar work by (Wingerson and Richard, 2002)

4.3.2 Phase composition of HCG-1 and HCG-2 super absorbent hydrogels

Figure 4.3.3 and 4.3.4 represents the diffraction patterns of the HCG-1and HCG-2 hydrogel respectively. Diffraction patterns obtained during the analysis of the super absorbent hydrogel. The sharp peaks represent the crystalline phases present in the studied samples while the hallo/broad peaks represent the semi crystalline phase.

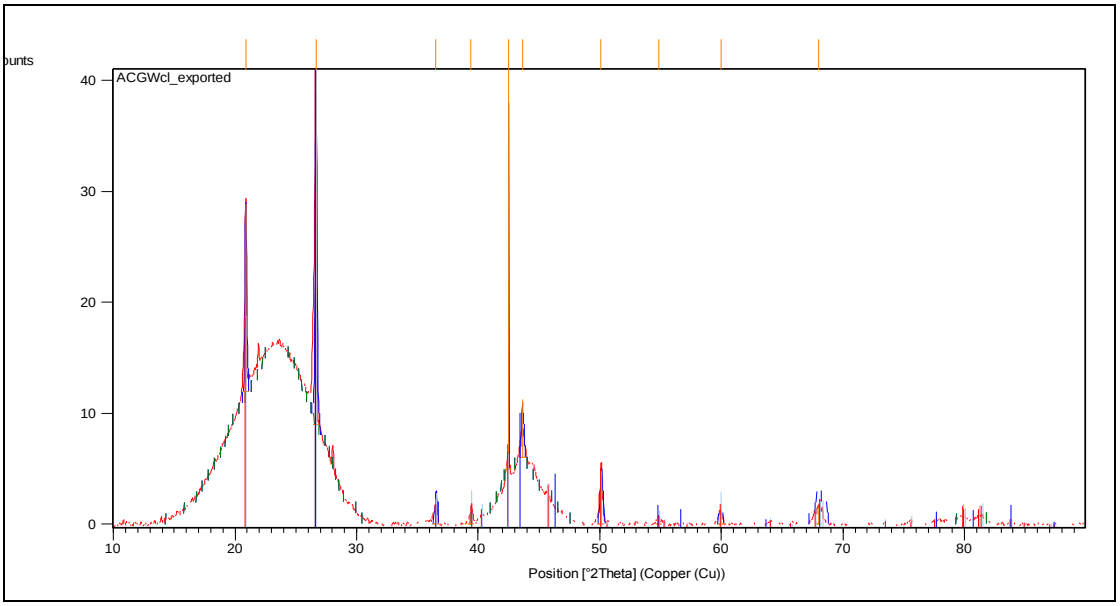

Figure 4.3.3: Powdered diffraction pattern of HCG-1.

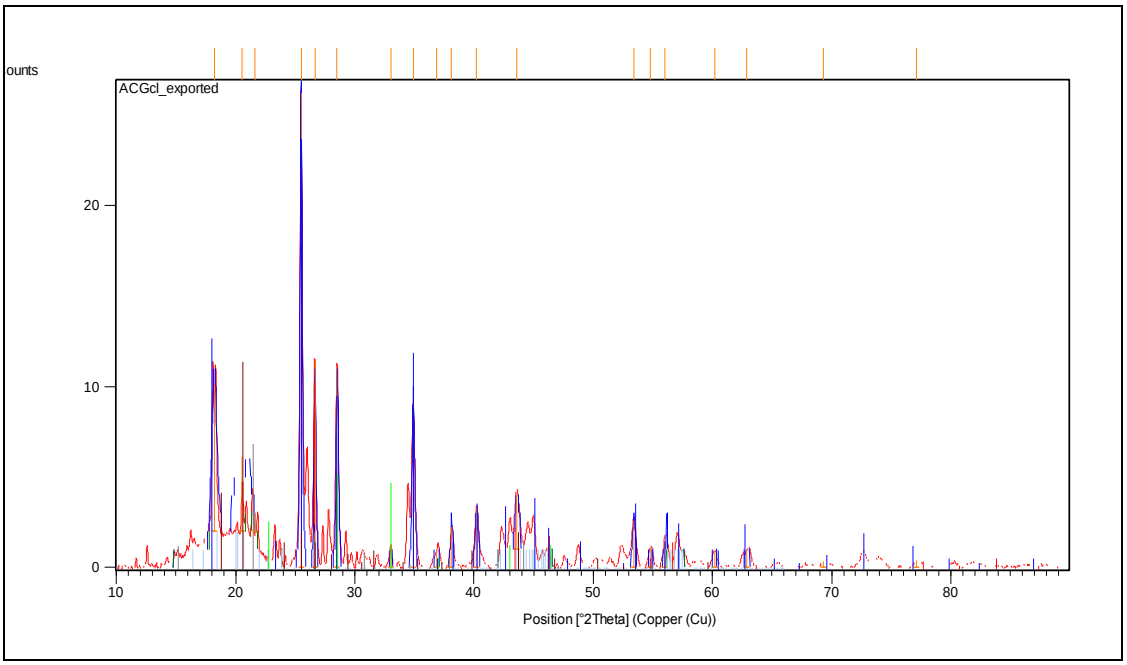

Figure 4.3.4: Powdered diffraction pattern of HCG-2.

Figure 4.3.3 and 4.3.4 shows X-ray diffraction patterns of HCG-1 and HCG-2. The phases changed significantly as the 2θ angle peaks of HCG-1 at 39.37, 42.52, 50.09, 59.96 and 68.01° disappeared as compared with HCG-2. This may be attributed to the polymerization reaction initiated by cross linker between crystalline phases of carbon (-COOH) and glycerol –OH. Similar results were obtained by Silva *et al*. (2007). The sharp well-resolved new peaks appeared on HCG-2 at (2θ) 18.21, 21.59 and 25.48 identified as crystalline phases of ($CaC_2O_4.H_2O$), graphite and unburned carbon respectively (Bouchelta *et al*.,2008). An increased number of sharp peaks in HCG-2 are proof of crystalline phase formation with the addition of binder. The crystalline phases of peaks between the 2θ angle of 33.04 to 40.19, 56.0 to 60.17 were identified as $C_{10}H_{14}O$ and $Na_2C_2O_4.8H_2O$. This information confirms polymer formation in HCG-2 super hydrogel that is crystalline. Similar results were reported by (Hajimohammadi *et al*.,

2011). The diffraction peaks at 2θ between 62.88 and 77.11 in HCG-2 were associated with face-centered cubic packing of graphite while angle 2θ at 28.8 was due to graphite peak arising on the tubular structure of carbon atoms was clear proof of crystalline structure (Bouchelta *et al*., 2008).

Additionally, there was a slight peak shift noticed in the pattern at 2θ values of HCG-1 compared to HCG-1 from 2θ of 20.87 to 20.56°, 26.65 to 26.64°, 43.63 to 43.57° and 36.52 to 36.86° respectively. This shows increase in the crystallinity of the HCG-2 phase compared to HCG-1 hydrogel after addition of cross linker. A similar result was reported by (Pal and Pal, 2006). The result reveals that peak intensity of HCG-1 is two times greater than that of HCG-2 super hydrogel. This could have been attributed to the fact that HCG-1 was converted to a crystalline 3-dimensional structure on addition of maleic acid (Hajimohammadi *et al*., 2011). There was a significant decrease on full width at half-maximum FWHM 2θ from HCG-1 to HCG-2 (Appendices 2C and 2D). This decrease is an indication that HCG-2 has high tensile stress and larger crystal size with high water absorption and retention capacities than HCG-1 (Silva *et al*., 2007).

4.3.3 Scanning electron microscopy (SEM) of HCG-1 and HCG-2 super absorbent hydrogels

The results from the SEM analysis are as shown in figure 4.3.5

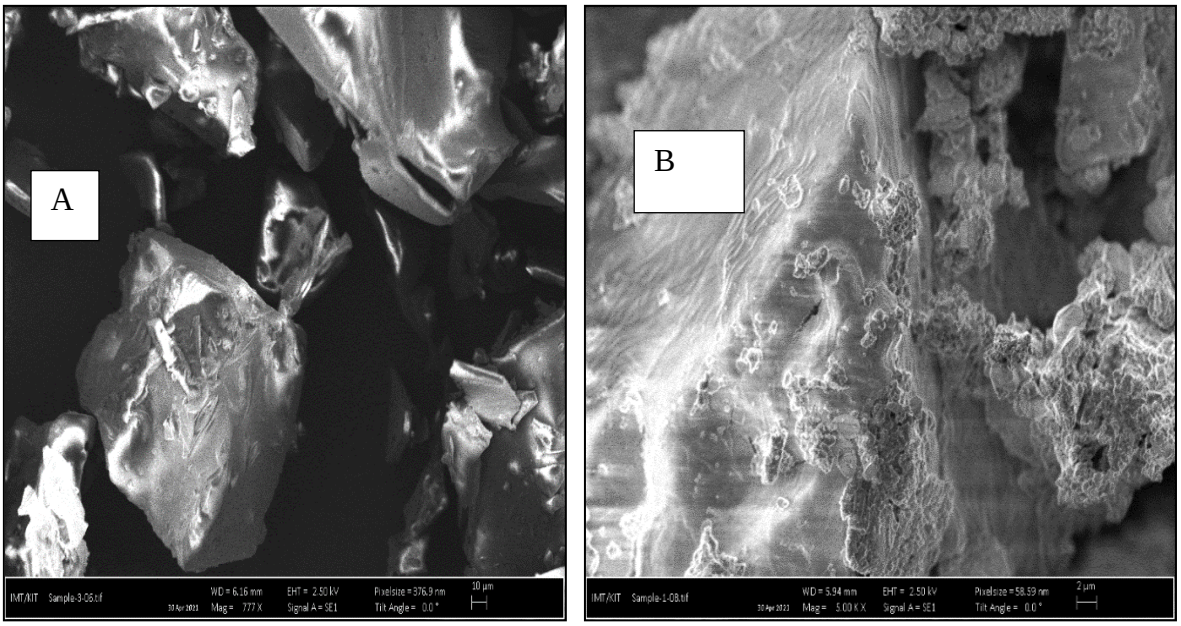

Figure 4.3.5: SEM micrographs of the (A) HCG-1 and (B) HCG-2 hydrogels

From the images, it is clear that super absorbent hydrogel HCG-1 showed crystalline intact and rigid structure without voids and pore on its surface figure 4.3.5(a). This may be associated with the conditions that polymerization between activated charcoal and glycerol was successful. However, after crosslinking with maleic acid HCG-2 showed surface modification different from that of HCG-1. A well-developed fibrous with smooth irregular pores and lamina structural nature occurred on the surface of the powdered HCG-2 super absorbent hydrogel as shown in figure 4.3.5(b). This clearly showed the formation of a 3-dimensional crystalline structure as a result of maleic acid joining carboxylate groups of activated charcoal with hydroxyl groups of glycerol

forming HCG-2 polymer. A similar finding was reported by (Mohan *et al*., 2010, Buikliskii *et al*.,2012).

4.4 Synthesis of super absorbent hydrogels HLE-1 and HLE-2

The reaction of 145.0 mL of (CA) and 90.0 mL of ethylenediamine (14.8 M) with 10 mL 5.0 M NaOH under heating at a temperature of 373 K to 405 K in an oven, formed 95 g of solid hydrogel HLE-1. Super absorbent hydrogel HLE-2 was prepared by adding 75.0 mL of 3.5 M maleic acid to the viscus gel of HLE-1 as heating and stirring were done forming 110.0 g of HLE-2 super absorbent hydrogel with the highest percentage swelling of 925 %. The products were characterized by FTIR spectroscopy, XRD, and SEM as well as by determination of their percentage swelling.

4.4.1 Fourier transform infrared of HLE-1 and HLE-2 super absorbent hydrogels

FT-IR was used to determine the functional groups present in the super absorbent hydrogel before and after cross-linking with maleic acid. Figure 4.4.1 shows the IR spectrum of the hydrogel before crosslinking. The hydrogel was coded as HLE-1.

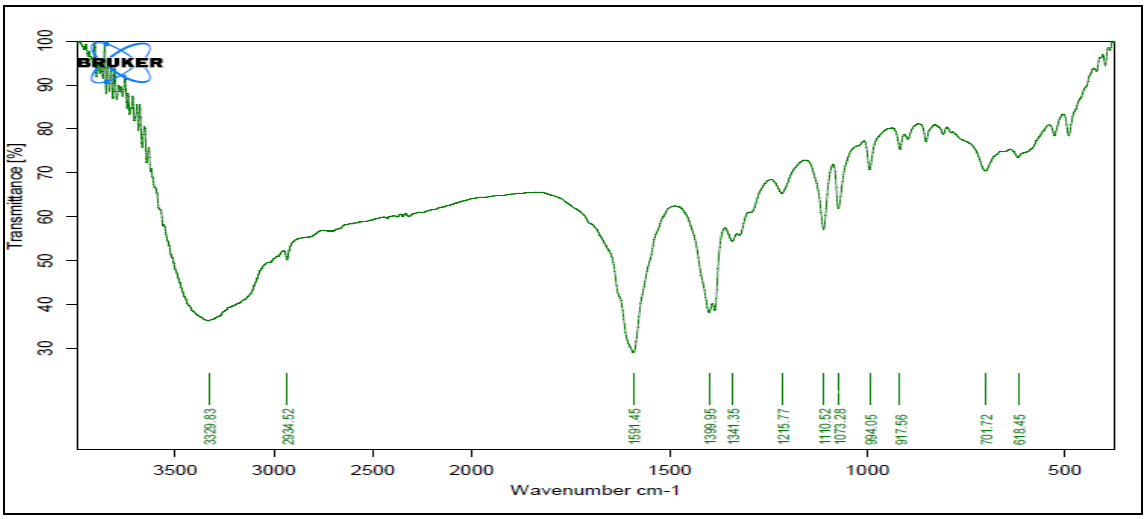

Figure 4.4.1: FT-IR spectrum of HLE-1

The broad band at 3329.83 cm^{-1} is a characteristic of the aliphatic secondary amine NH stretching vibration while the band at 2934.52 cm^{-1} represents the C–H stretching asymmetric vibration in the methyl group in lemon juice. This was also observed by (Mishra *et al*., 2008). The absorptions bands at 1591.45 cm^{-1}, 1399.95 cm^{-1}, and 1341.35 cm^{-1} are assigned to aromatic ring stretching, tertiary alcohol -OH bending, and primary -OH in-plane bending respectively (Bakravi *et al*., 2018). In addition, the absorption band at a wavelength of 1215.77 cm^{-1}, 1073.28 cm^{-1},1110.52 cm^{-1}, 701.72 cm^{-1} and 618.45 cm^{-1}, represents aromatic secondary amine CN stretching, cyanate –OCN, C-OCN stretch, and primary amine CN stretch respectively while 994.05 cm^{-1}, and 917.56 cm^{-1} represents C-O bend associated with lemon juice, and Vinylidene C-H out of plane bend (Bakravi *et al*., 2018). Figure 4.4.2 shows the spectrum of the HLE-2.

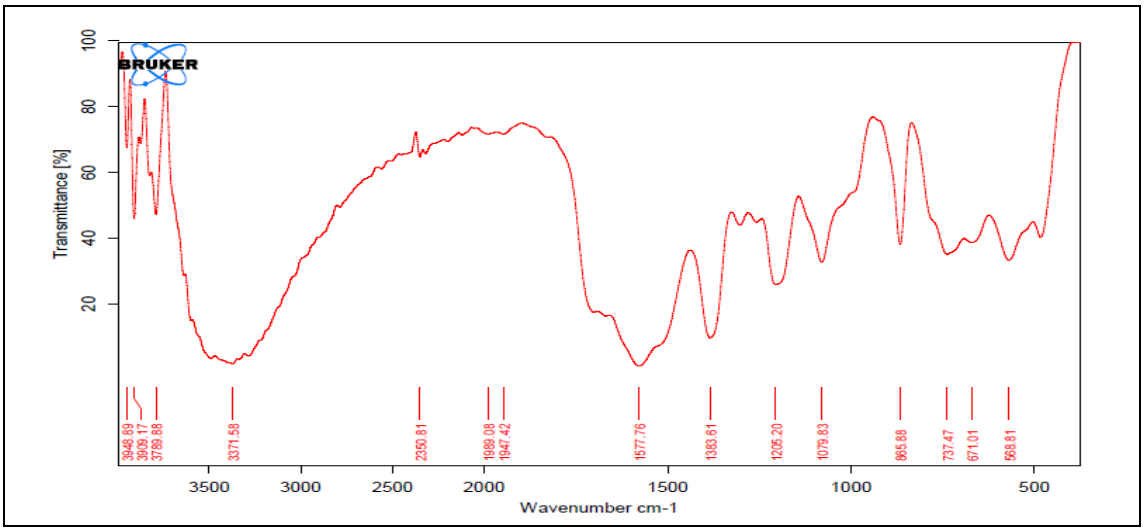

Figure 4.4.2: FT-IR spectrum of HLE-2

The results show two new sharp peaks at a wavelength of 3948.89 cm^{-1} and 3909.17 cm^{-1}. They are associated with the stretching frequency of the –OH group as well as intramolecular and intermolecular hydrogen bonds (Yeasmin and Mondal, 2015). The band at 3787.88 cm^{-1} is assigned to amide interlink between carboxylate and amine groups from citric acid and ethylenediamine respectively. This was also reported by (Mishra *et al.*, 2008). In addition, the new small absorption band at 3371.58 cm^{-1} is attributed to the presence of strong H-OH interaction. The spectra bands around 1989.08 cm^{-1} and 1947.47 cm^{-1} are attributed to –CN bending and ($–CONH_2$) amide functional groups as well as decreased bending vibration of −OH from 701.72 cm^{-1} to 671 cm^{-1}, showing amide linkage between citric acid and ethylenediamine in HLE-2 hydrogel. A similar result was reported by (Yeasmin and Mondal, 2015).

The new broad bands around 2371.58 cm^{-1}, 1577.76 cm^{-1}, 1383.61 cm^{-1}, 1205.20 cm^{-1}, and 885 cm^{-1} are due to C=O stretching in ester aldehyde, primary amine -NH bending, -

OH bending in ester, phenol C-O stretching and C-O-C stretching respectively. The presence of those functional groups illustrates that there was an ester cross-link between the hydrogel HLE-1 and maleic acid. This was also reported by (Khan *et al.*, 2011). In addition, IR spectra in figure 4.4.2 showed a new strong symmetric stretching $-COO^-$ peak at 1079.83 cm^{-1} indicating successful ester linkage formation (Thombare *et al.*, 2018).

4.4.2 Phase composition of HLE-1 and HLE-2 super absorbent hydrogels

Figure 4.4.3 and 4.4.4 represents the diffraction patterns of HLE-1 and HLE-2 super absorbent hydrogels respectively.

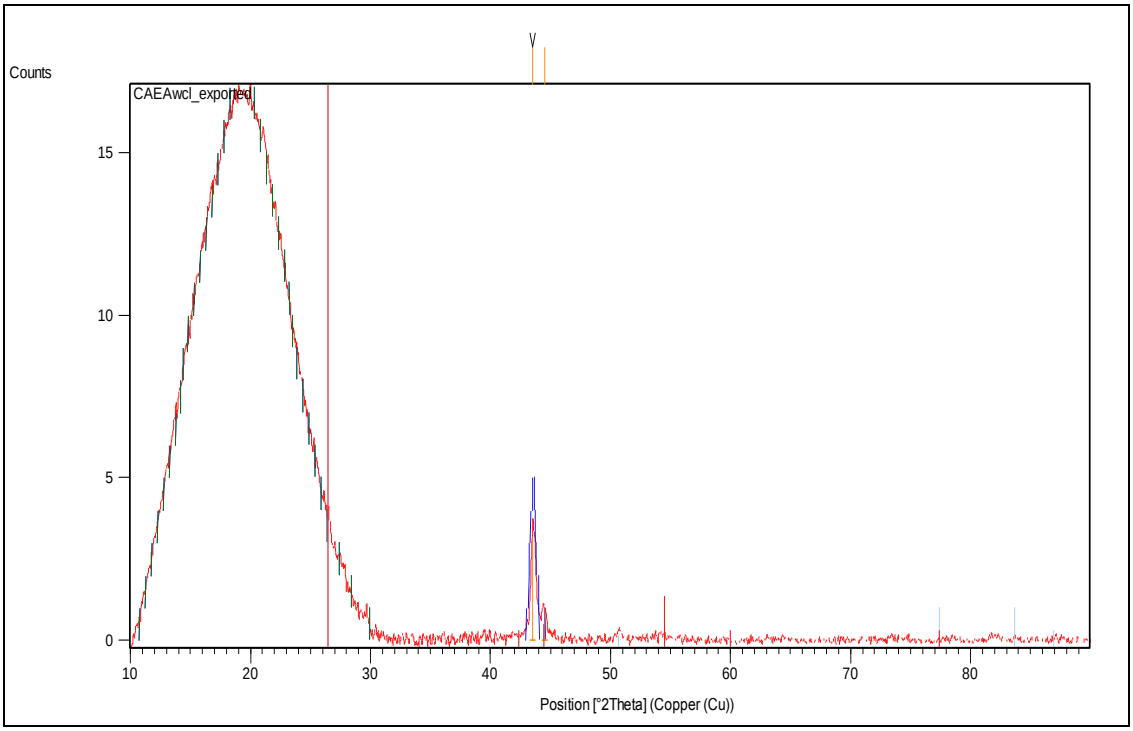

Figure 4.4.3: Powdered diffraction pattern of HLE-1.

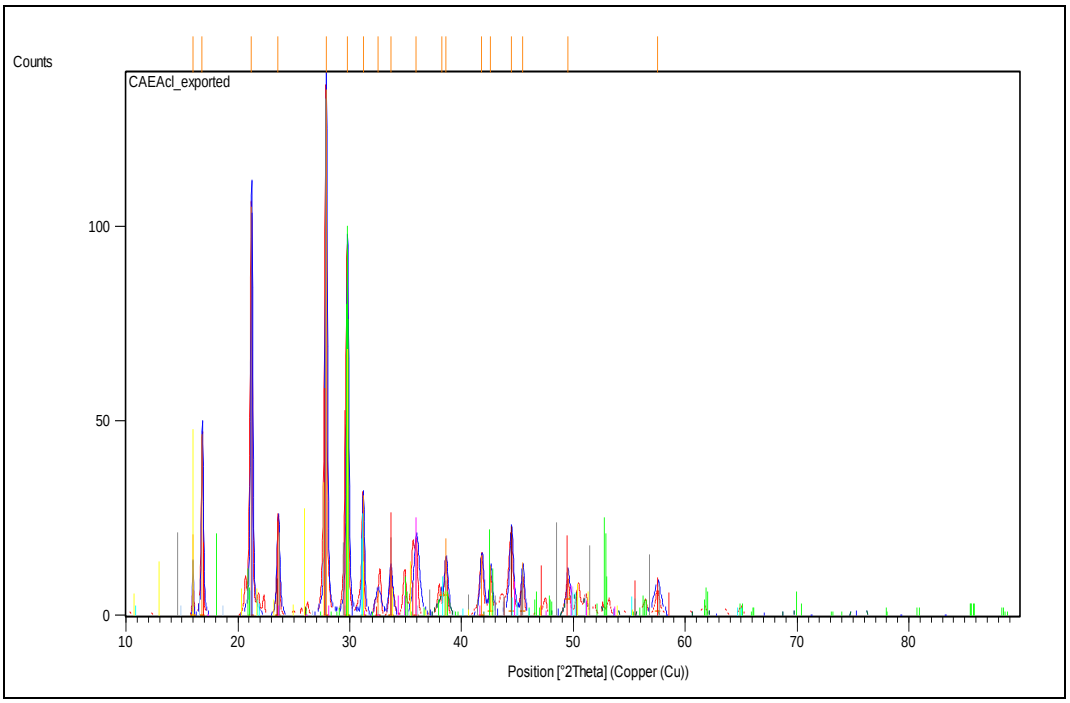

Figure 4.4.4: Powdered diffraction pattern of HLE-2

Diffraction pattern in figure 4.4.3 shows a broad hump between 11 – 32° (2θ) associated with amorphous nature of the hydrogel. Sharp two peaks at 2θ 43.49 and 44.51° were identified as graphite crystalline phases and attributed to amide interlink between citric acid and ethylenediamine polymer network in HLE-1 hydrogel. Similar results were reported by (Li and Liu, 2007). Figure 4.4.4 shows the appearance of new sharp peaks with relatively high intensity at 15.96, 21.21, 23.59 and 29.77 (2θ) identified as crystalline phase of $Ca(NH_2\text{-}OH)$, $(C_8H_6O_2)4H_2O$, graphite and $MgCH_3.4NH_3$ respectively (Wang *et al*. 2015). The peaks between (2θ) 31.20 to 38.24 and 41.78 to 49.49 are in plane of 100 and 101 reflection of carbon crystalline phases respectively (Hassan *et al*., 2000). This reveals ester cross-linkage reaction in HLE-2 in presence of maleic acid resulting to high crystalline three-dimensional structure super absorber hydrogel. Similar findings were reported by (Guo *et al*. 2010).

4.4.3 Scanning electron microscope (SEM) of HLE-1 and HLE-2 super absorbent hydrogels

The microstructural analysis of the hydrogels was carried out using a scanning electron microscope. Figure 4.4.5 (A and B) shows the images of both the and HLE-1 and HLE-2 respectively.

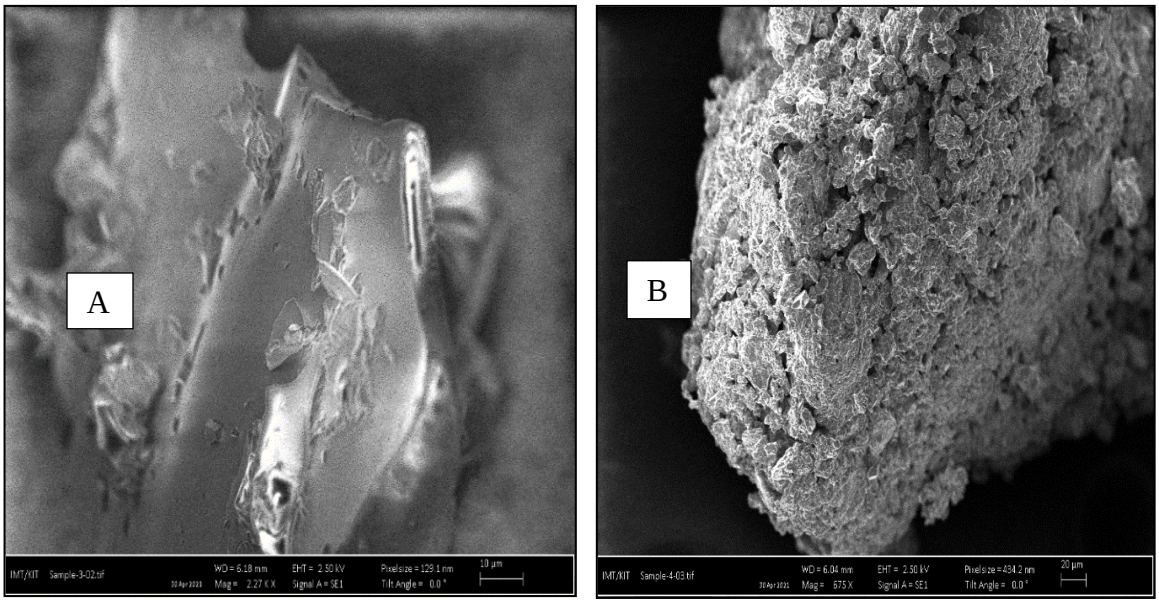

Figure 4.4.5: **SEM micrographs of the (A) HLE-1 and (B) HLE-2 hydrogel**

A rigid, concrete and smooth surface was observed in HLE-1 (Figure 4.4.5(A). Upon cross-linking, the microstructure of the hydrogel changed to an uneven surface indicating dispersal of the polar phase (Figure 4.4.5(B). The spherical and spindle shaped structures on the surface of HLE-1 indicate a copolymerization reaction between citric acid with ethylenediamine. Similar findings were reported by (Pandey and Negi, 2015). The SEM micrograph of HLE-2 contains pores of different sizes and shapes with an external surface full of cavities which may have occurred due to the presence of maleic acid as a cross-linker between different monomers during polymerization reaction.

4.5 Synthesis of super absorbent hydrogels HLG-1 and HLG-2

The reaction of 72.0 mL of 0.3 M (CA) and 45.0 mL of 13.6 M glycerol with 10 mL 5.0 M NaOH under heating at a temperature of 363 K in an oven gave 75 g of solid Super absorbent hydrogel HLG-1. While synthesis of HLG-2 SAH was done by adding 50.0 mL of 3.5 M maleic acid to the viscous gel of HLG-1 as heating and stirring were done until a viscous gel was formed followed by cooling, gave 80.0 g of HLG-2 Super absorbent hydrogel with highest percentage swelling of 910 %. The products were characterized by FTIR spectroscopy, XRD, and SEM as well as by determination of their percentage swelling.

4.5.1 Fourier transform infrared of HLG-1 and HLG-2 superabsorbent hydrogel

FT-IR analysis was carried out to identify the functional groups present in the super absorbent hydrogel before and after cross-linking. Figure 4.5.1 shows IR spectra of the HLG-1 sample and their corresponding functional groups.

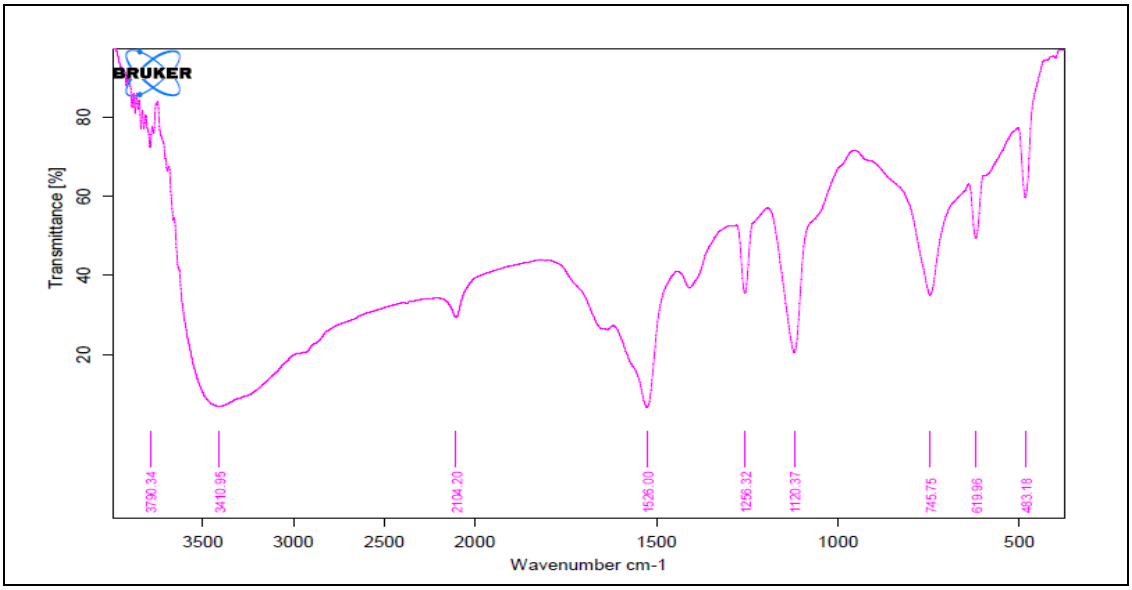

Figure 4.5.1: FT-IR spectrum of HLG-1

The absorption peaks observed at around 3790.34 cm^{-1} are a result of the presence of isolated -OH groups in citric acid while the broad peak of H-OH appeared at 3410.95 cm^{-1} (Wingerson and Richard,2002). The sharp spectra peaks at around 1528 cm^{-1} and 619.96 cm^{-1} are assigned to –COO- stretching and –OH out of plane bend respectively (Costa-Junior *et al*., 2009). The peak at 1528 cm^{-1} assigned to –COO- is a clear indication of the formation of ester linkage between citric acid in lemon juice and glycerol monomers. Similar results were reported by (Costa-Junior *et al*., 2009). The peaks at 1256.32 cm^{-1}, 1120.37 cm^{-1}, and 745.75 cm^{-1} are attributed to C-O stretching in ether, C-O stretch in alky, and C-H out of plane bending respectively (Abdulhameed *et al*., 2019).

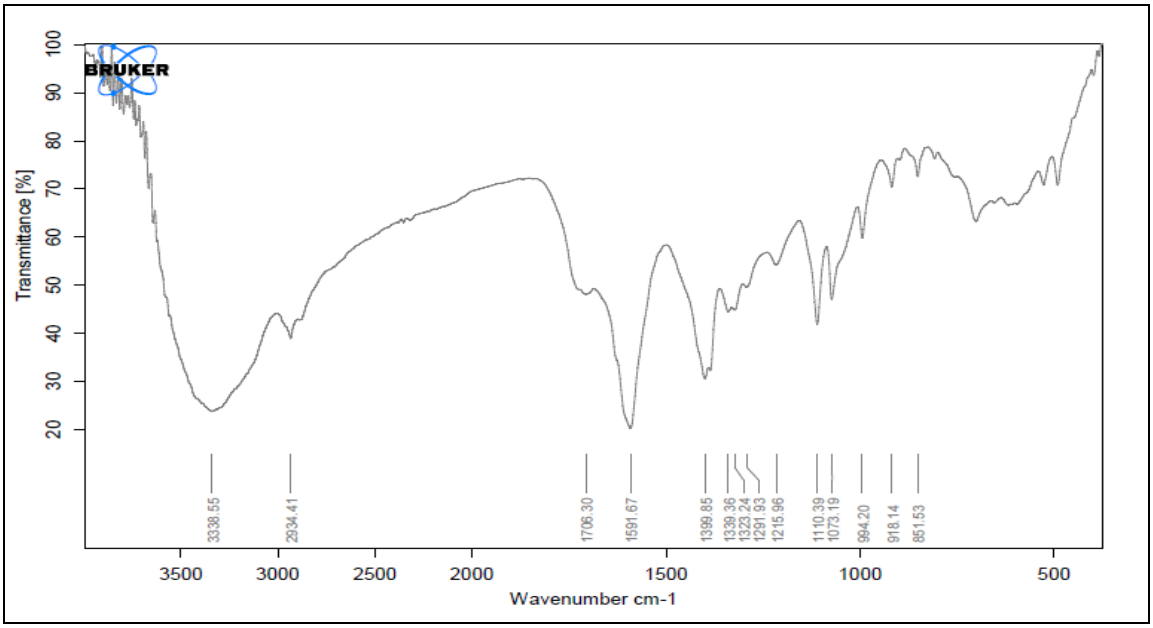

Figure 4.5.2: FT-IR spectrum of HLG-2

Figure 4.5.2 shows IR spectrum of the HLG-2 super hydrogel cross-linked with maleic acid. Occurrence of new broad peak at a wavelength of 3338.55 cm^{-1} of HLG-2 is due to

overlap peaks of –OH group stretching in citric acid with strong H bonded peak observed at around 2934.41 cm^{-1} in glycerol. Similar findings were reported by (Bakravi *et al*., 2017). In addition, peak at around 1706.30 cm^{-1} is associated C=O carbonyl stretching showing ester formation was successful while tertiary –OH bending in alcohol, primary –OH in plane bending, secondary –OH in plane bending appeared at 1399.85 cm^{-1}, 1339.36 cm^{-1} and 1323.24 cm^{-1} respectively. Similar results were reported by (Wingerson and Richard,2002).

The peaks appearing at around 1073.19 cm^{-1}, 994.20 cm^{-1} is associated with COO^{-} symmetric stretching, and C-O bending associated with alcohol (Mishra *et al*., 2008). There was significant shift in wavelength in figure 4.5.1 as compared to figure 4.5.2. Alcohol C-O stretching in ether shifts from 1256.32 cm^{-1} to 1215.96 cm^{-1}, ether C-O stretch in alkyl shifts from 1120.37 cm^{-1} to 1110.39 cm^{-1} while –OH bending in alcohol shifts from 745.75 cm^{-1} to 918.14 cm^{-1} confirming ester formation (Kondo, 1997). The spectra band observed at 1591.34 cm^{-1} is a result of the presence of –COO- asymmetric stretching associated with successful ester crosslinking between –OH in the polymeric unit (HLG-1) and –COOH group in the maleic acid binder. Furthermore, disappearance of IR peaks at around 3790.34 cm^{-1} 3410.95 cm^{-1} and 2104 cm^{-1} is another proof of successful esterification. Similar results were reported by (Kondo, 1997).

4.5.2 Phase composition of HLG-1 and HLG-2 super absorbent hydrogels

Figure 4.5.3 and 4.5.4 shows the powdered diffraction patterns of the HLG-1 and HLG-2 hydrogel respectively. The amorphous characteristics of uncross linked HCG-1 hydrogel

is highly noticeable due to presence of broad halo peak at angle between 11–31 (2θ). The XRD analysis shows that the HLG-1 hydrogel is mainly amorphous. Similar findings were reported by (Varaprasad *et al.*, 2010).

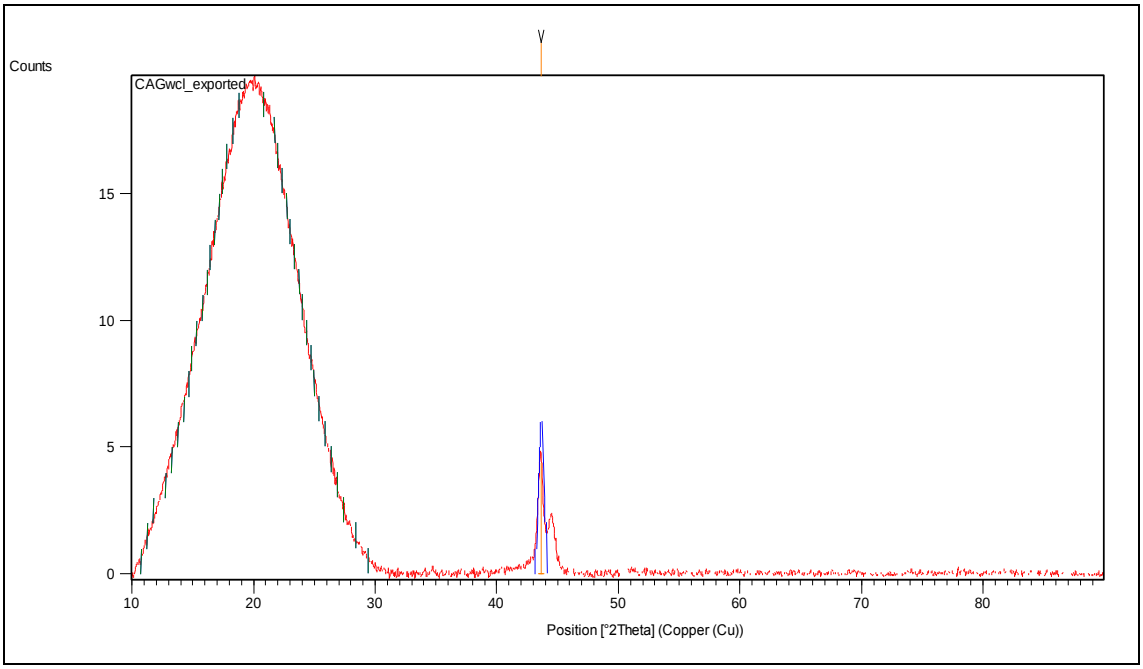

Figure 4.5.3: Powdered diffraction pattern of uncross linked HLG-1.

Figure 4.5.3 shows clearly HLG-1 hydrogel is mainly amorphous. This is due to presence of broad halo peak at angle 2θ between 11–31 attributed to polymer network. Similar results were reported by (Varapsad *et al.*, 2010). The only sharp peak in XRD pattern at angle (2θ) 43.5 is associated with graphite phase (Varapsad *et al.*, 2010). Figure 4.5.4 shows the diffraction pattern of the HLG-2.

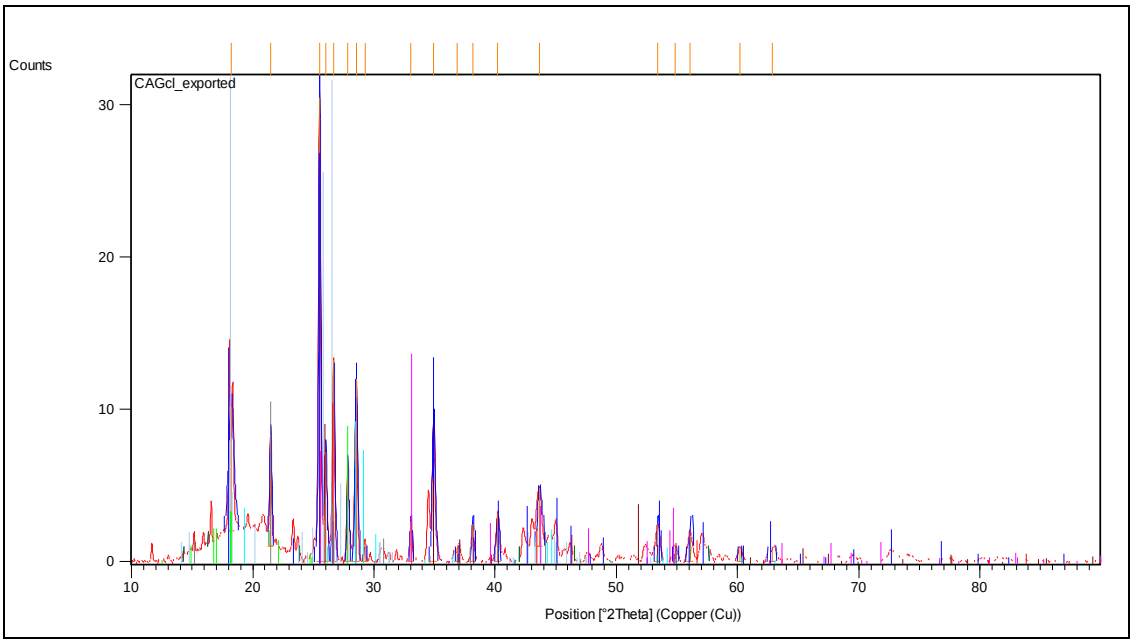

Figure 4.5.4: Powdered diffraction pattern of cross-linked HLG-2.

The peaks at an angle (2θ) 18.21 and 21.47 were observed due to the presence of carboxylate phases on the polymer network an indication of the semi-crystalline nature of hydrogel HLG-2 (Mohamood *et al.*, 2018). The peaks appearing at an angle (2θ) 25.52 and 27.83 were due to the tubular structure of carbon atoms in the hydrogel network of HLG-2 compared to an amorphous structure in HLG-1 Similar findings were reported by (Mohamood *et al.*, 2018). The increased number of sharp peaks at (2θ) of 38.18, 40.19, 53.42, 54.88, and 62.48° may be attributed to the increased crystalline phase of in HLG-2, (Naohara *et al.*, 2017). The peak at 26.68° (2θ) arises due to the tubular structure of carbon atoms (Karadağ and Üzüm, 2012). Crosslinking the hydrogel showed conversion of the hydrogel from amorphous to crystalline. The increase in ester linkages upon crosslinking resulted in the formation of a three-dimensional crystalline polymer structure with high water absorption capacity.

4.5.3 Scanning electron microscope (SEM) of HLG-1 and HLG-2 super absorbent hydrogels

The microstructure and morphological analysis of the superabsorbent hydrogel of HLG-1 and HLG-2 was done by scanning electron microscopy (SEM) (Zeiss supra 60) at an accelerating voltage of 2.50 kV

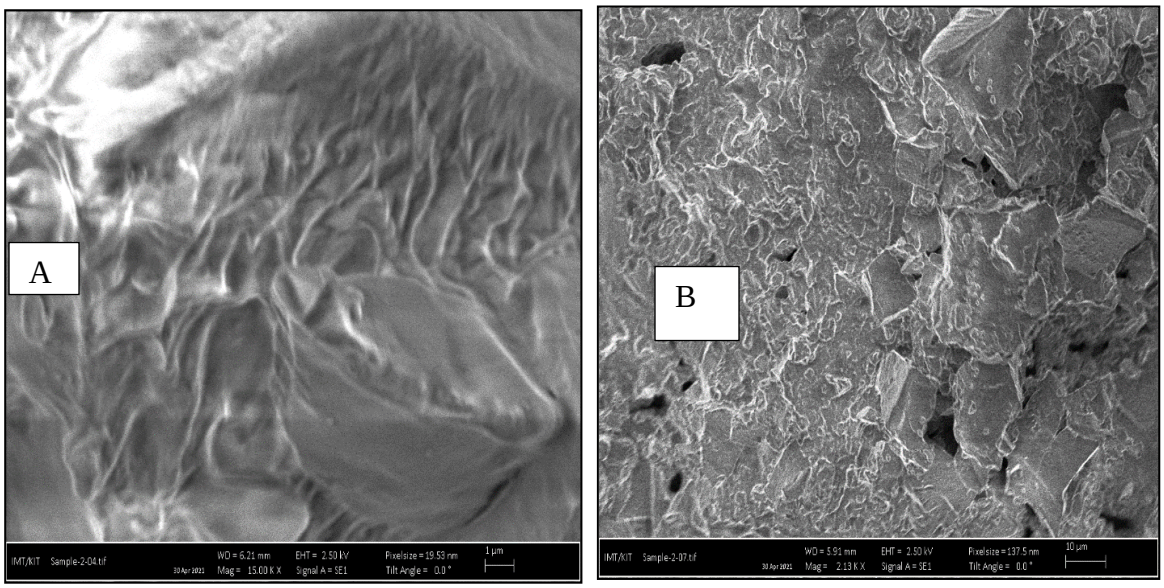

Figure 4.5.5: SEM micrographs for (A) HLG-1 and (B) HLG-2

The SEM micrograph in figure 4.5.5(A) clearly shows that the HLG-1 super absorbent hydrogel as rigid, rough, and constricted surface while HLG-2 has a roughness morphological surfaces with clear pores throughout its structure. This reveals the maximum surface area for water absorption properties of the hydrogel. Similar results were reported by (Habib-ur-Rehman *et al*., 2006). The lamina structural nature will enhance the absorption of water into the hydrogel pores as shown in figure 4.5.5(B) compared with the rigid structure in figure 4.4.5(A). This was possible due to intermolecular hydrogen bonding or intramolecular hydrogen bonding between the side

chains and its backbones in HLG-2 super hydrogel. Similar findings were reported by (Guo *et al*., 2010).

4.6 Optimization of synthesis parameters for super absorbent Hydrogels

Studies were carried out to investigate the optimal conditions of swelling time, dosage ratio between monomers, and cross-linker mass required for the production of most desirable, stable, and high-water absorptive hydrogels through water absorption capacity in deionized water. The results obtained are used to give information on the effects of these reaction conditions and different formulations on green hydrogel performance and are presented in figures 4.6.1 to 4.6.12

4.6.1 Effect of citric acid (CA) dosage on the swelling capacity of HLG-2 and HLE-2 hydrogels

Figure 4.6.1 shows the percentage swelling obtained when 2.0 g of prepared hydrogel was immersed in distilled water.

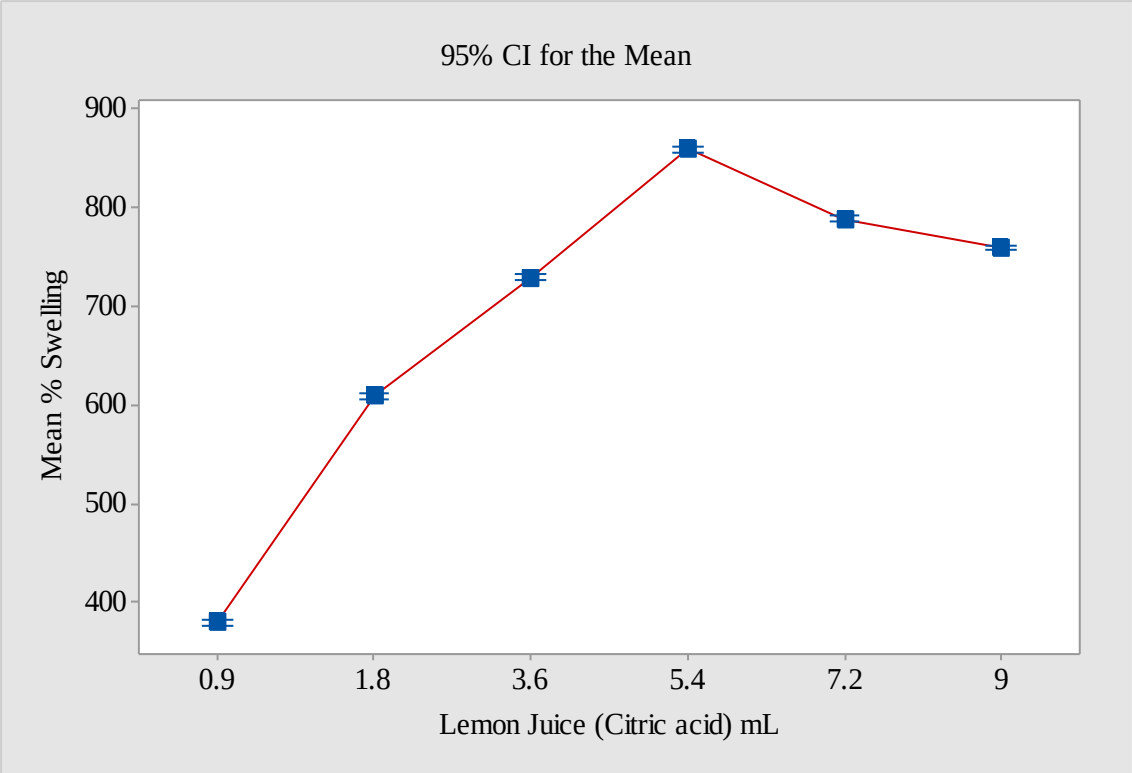

Figure 4.6.1: The effect of amount of citric acid used on the percentage swelling of 2.0 g of HLG-(at 5 g glycerol, 2 g maleic acid, 1 g NaOH)

The graph in figure 4.6.1 shows that as the dose of (CA) was increased from 0.9-5.4 mL, the percentage swelling of hydrogel increased from 380 % to 860 %, followed by a decrease at a dose of (CA) above 5.4 mL. The increase in swelling capacity as the dosage of citric acid was increased could be associated with the increased number of anionic hydroxyl groups that leads to increased grafting between the functional groups of the monomers forming a crystalline structure in HLG-2. Similar results were reported by (Yazdani *et al.*, 2000; Parvathy and Jyothi, 2012). Decreased percentage swelling after obtaining optimal swelling capacity could be attributed to the termination of disproportionation reaction between carboxylate and hydroxyl functional groups instead of coupling as ratio dosage of (CA) exceeded that of glycerol. Similar results were reported by (Lanthong *et al.*, 2006).

Figure 4.6.1, clearly showed that volume ratio 5.4: 3.75 of CA: G should be cross linked with maleic acid to prepare polymer gel with maximum water absorption capacity.

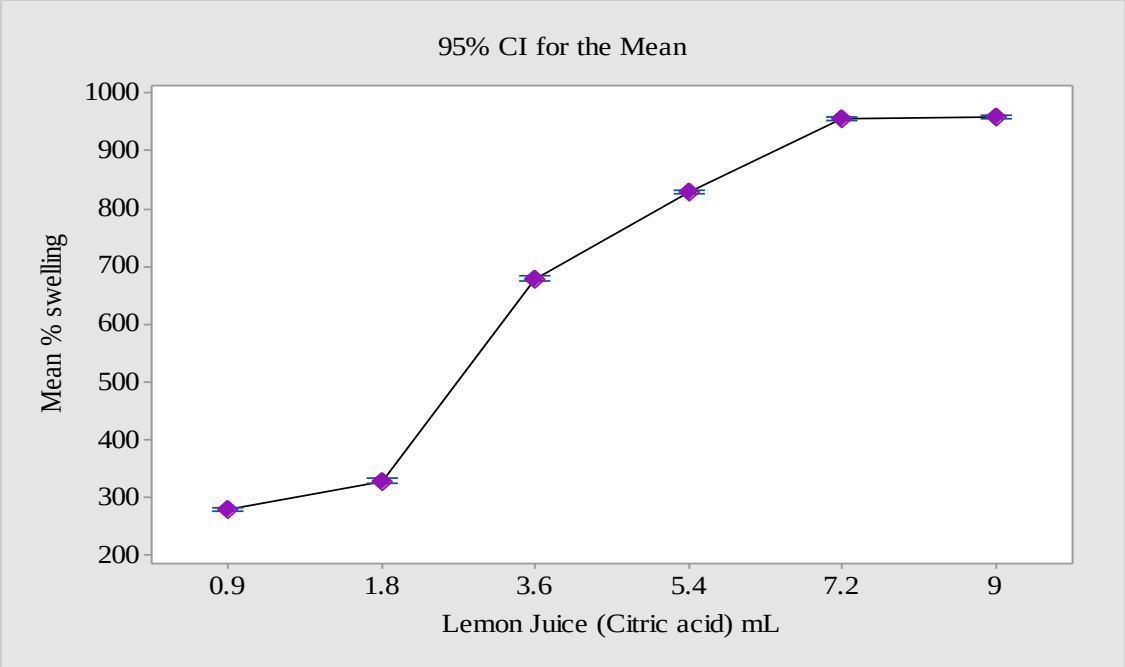

Figure 4.6.2: The effect of amount of citric acid used on the percentage swelling of 2.0 g of HLE-2 (at 5 g ethylenediamine, 2 g maleic acid, 1 g NaOH)

The percentage swelling of HLE-2 (Figure 4.6.2) increased from 280 % to 955 % when citric acid dosage was increased from 0.9 to 7.2 mL then remained fairly constant. The increased swelling percentage may be associated with increased hydrophilic nature and ionic pressure effect due to increased dosage of citric acid. Similar findings were reported by (Parvathy *et al*., 2014). On the other hand, a decrease in the swelling capacity after the optimal dosage of citric acid may be as a result of the inadequate entropy and internal energy caused by the shielding effect of increased hydroxyl groups from citric acid, leading to a low rate of diffusion of water molecules into the hydrogel (Harsh and Gebrke, 1991; Witono *et al*., 2014). A volume of 7.2 mL lemon juice (citric acid) produced HLE-2 hydrogel with the optimal water absorption capacity.

4.6.2 Optimization of amount of activated charcoal used on HCG-2 and HCE-2 hydrogels

During optimization process, HCG-2 and HCE-2 super absorbent hydrogels used were prepared by varying amount of activated charcoal (AC) from (1, 2, 4, 6, 8, and 10 g) while maintaining 3.75 mL of 13.6 M glycerol, 4.5 mL of 14.8 M ethylenediamine, 5.0 mL of 3.5 M maleic acid as cross linker and 10 mL of 5 M NaOH as activator constant. Figure 4.6.3 and 4.6.4 shows the percentage swelling of 2 g of each prepared hydrogel immersed in 100 mL distilled water for 24 hours.

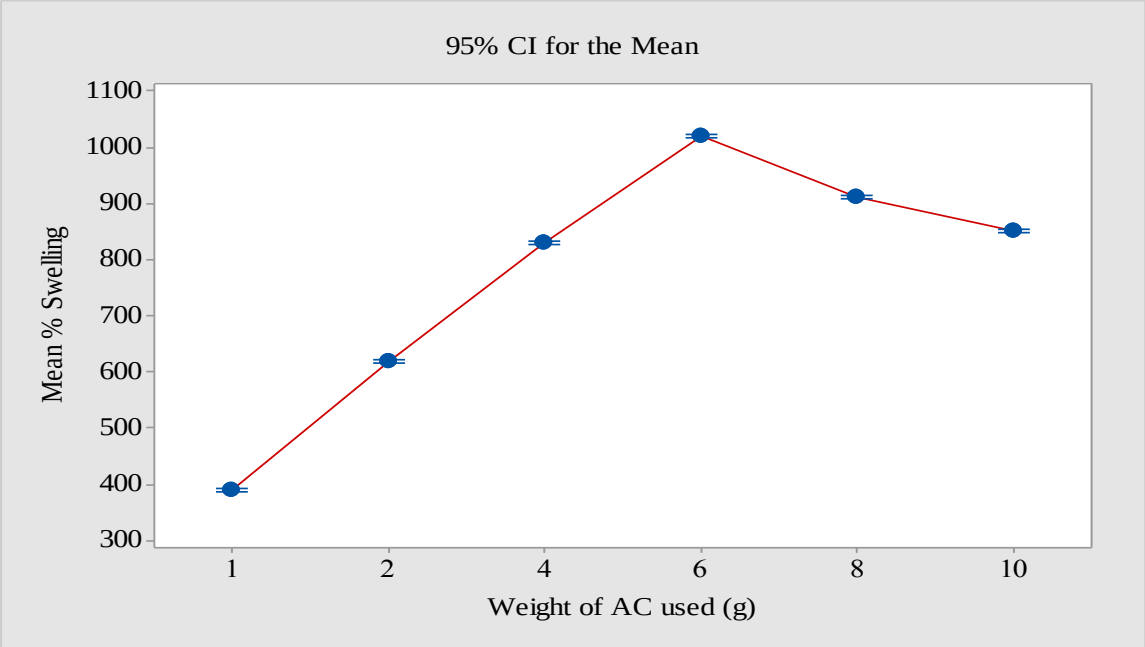

Figure 4.6.3: The effect of amount of activated charcoal on the percentage swelling of 2.0 g HCG-2 (at 5 g glycerol, 2 g maleic acid, 1 g NaOH)

From figure 4.6.3, it is evident that increasing the amount of AC in synthesis of HCG-2 from 1 g to 6 g recorded a rapid increase in percentage swelling of HCG-2 hydrogel from 390 % to 1020 % followed by a decrease to 923 1 % in the percentage swelling as the

dosage increased to 10 g. Mainly increasing the swelling ability of HCG-2 as the dosage of AC increases may be due to the high ionization constant of increasing carboxylate groups, the hydrophilic properties of the gel in deionized water, and improved chain expansion of the gel. Similar findings were reported by (Zain *et al*., 2018). Decreased percentage swelling as the dosage of AC increases is attributed with highly branched arrangement which lowers the physical entanglements in the structure of HCG-2 gel is formed and probably breakdown of the H-bonds or may be ionization of the extra-functional groups which affects H-bonds within the network of HCG-2 gel lowering it swelling ability. Similar results were reported by (Zheng *et al*., 2012). It's noted that mass ratio 6: 5 of AC: G should be used to prepare HCG-2 polymer gel with maximum absorption capacity.

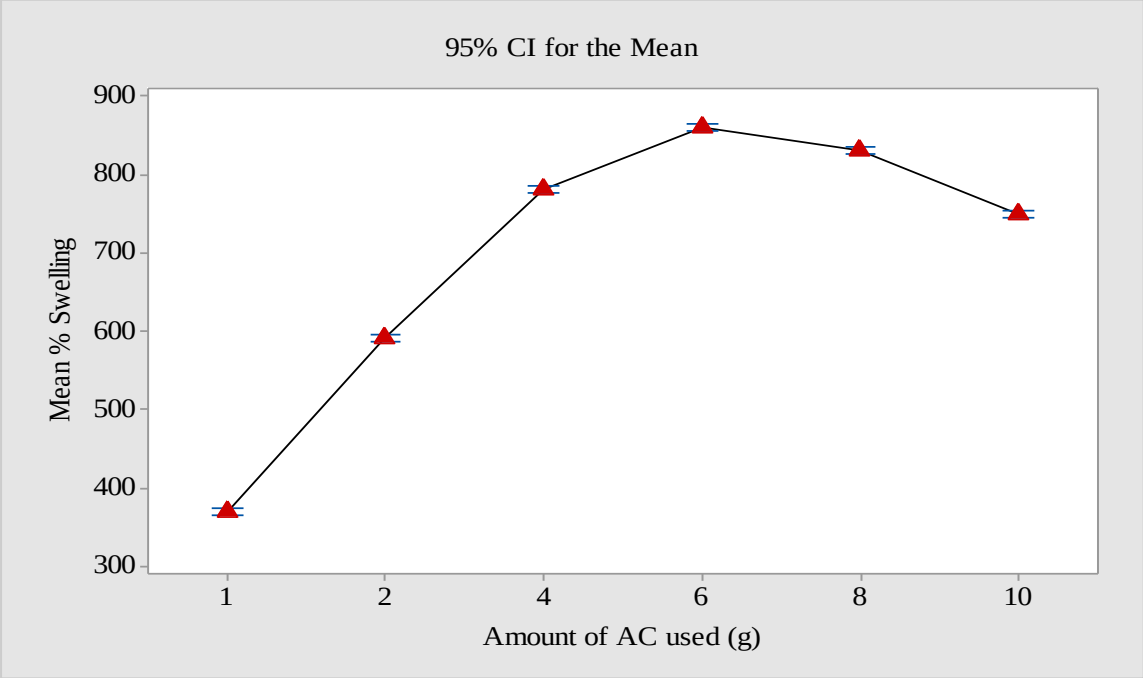

Figure 4.6.4: The effect of amount of activated charcoal on the percentage swelling of 2.0 g HCE-2 (at 5 g Ethylenediamine, 2 g maleic acid, 1 g NaOH)

From figure 4.6.4, the swelling capacity of HCE-2 super absorbent hydrogel generally increased from 370 %, reaching maximum capacity at 860 % when AC dosage increased from 1.g to 6 g. The reason for increased hydrogel swelling capacity relates to increased net charges of carboxylate ions in the polymer network which promotes the copolymer's chain expansion (Jyothi *et al*., 2010). A decrease in swelling capacity to 750 % is observed as the amount of AC monomer increases up to 10 g during hydrogel preparation. This was due to increased interactions between amine groups and increasing carboxylate groups resulting in decreased desorption in HCE-2 hydrogel. Similar findings were reported by (Jyothi *et al*., 2010). The decreased swelling percentage capacity was also associated with the bridging effect of the primary amides and increasing electrostatic repulsion of the increased carboxylate groups in HCE-2 hydrogel forcing conformational changes in super absorbent hydrogel. Similar results were reported by (Song *et al*., 2009). Results revealed that AC should be crosslinked with ethylenediamine in a mass ratio of 6: 5 to prepare HCE-2 super hydrogel with maximum water absorption capacity.

4.6.3 Optimization of maleic acid dosage on HLG-2, HLE-2, HCG-2, and HCE-2 hydrogels

The effect of the maleic acid (cross-linker) concentration was studied by varying dosage (1.25, 2.5, 3.75, 5.0, 6.25, and 7.5 mL). super absorbent Hydrogels were prepared as outlined in section 3.6. The addition of a chemical cross- linker is important to improve both the integrity of the gel and the predictability of mechanical properties (Durrani and Donald, 1995). Figure 4.6.5 shows the effect of varying dosages of maleic acid cross linker on the swelling capacity of superabsorbent hydrogel HLG-2.

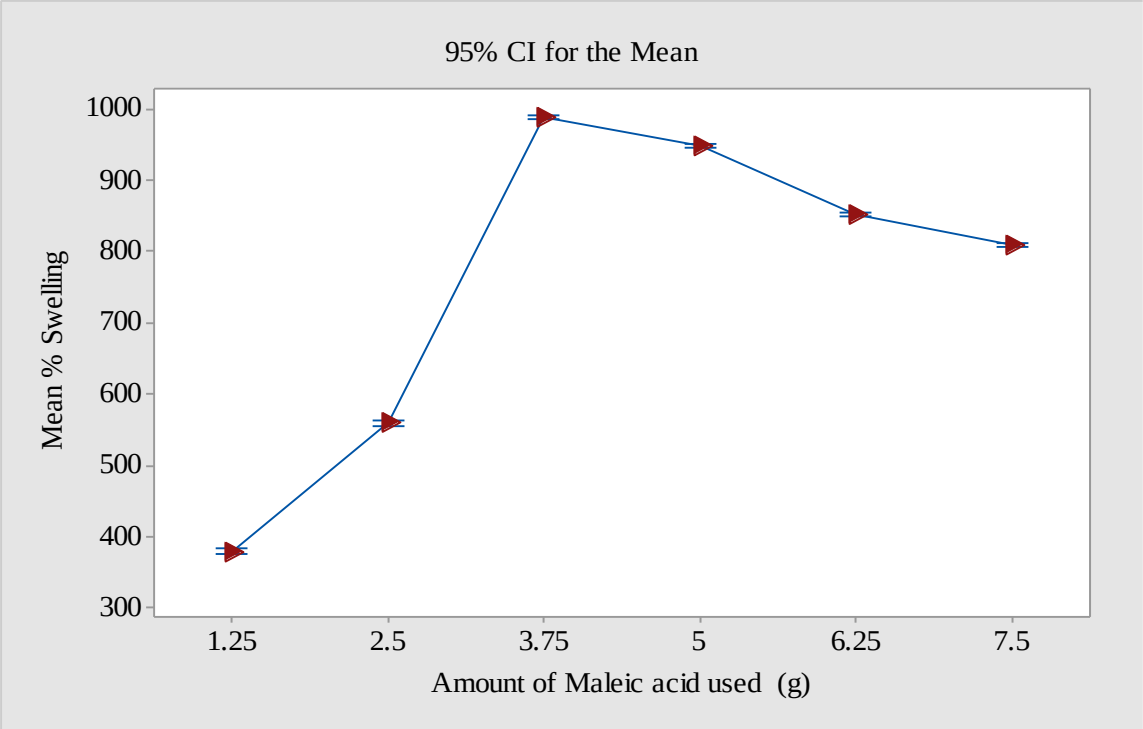

Figure 4.6.5: The effect of amount of maleic acid on the percentage swelling of 2.0 g HLG-2 hydrogel immersed in 500 mL of distilled water and contact time of 24 hours (at 6 g CA, 5 g G, 1 g NaOH)

Figure 4.6.5 shows that the percentage swelling of HLG-2 hydrogel increased from 380 to 990 % when cross-linker dosage increased from 1.25 to 3.75 mL. The results showed that a lower mass ratio between citric acid and glycerol resulted in larger pores with low strength to absorb larger quantities of water. On the other hand, the mechanical strength of hydrogel increases with increased dosage of cross-linker due to the formation of smaller well-cross-linked pore networks with increased hydrophilic groups for water absorption. Similar findings were reported by (Kabiri *et al*., 2003). It was also noted that further increase of maleic acid dosage above 3.75 mL decreased the percentage swelling capacity of HLG-2 to 810 %. The increase in the cross-linker mass above the optimal caused the swelling capacity of hydrogel to decrease due to the increasing crosslinking density resulting in a rough and rigid network with low water absorption and expansion

rate (Kabiri *et al*., 2003). Incorporation of chemical cross linker in hydrogel preparation improves its mechanical properties as well as the integrity of gel (Durrani and Donald, 1995), however there is need to determine the optimal cross-linker dosage that will not reduce the swelling capacity of the gel affecting its economic application. A volume ratio of CA: G: MA (5.4: 3.75: 3.75) was used to prepare HLG-2 gel with optimum swelling capacity.

Figure 4.6.6 shows the effect of varying dosages of maleic acid cross linker on the swelling capacity of super absorbent hydrogel HCG-2.

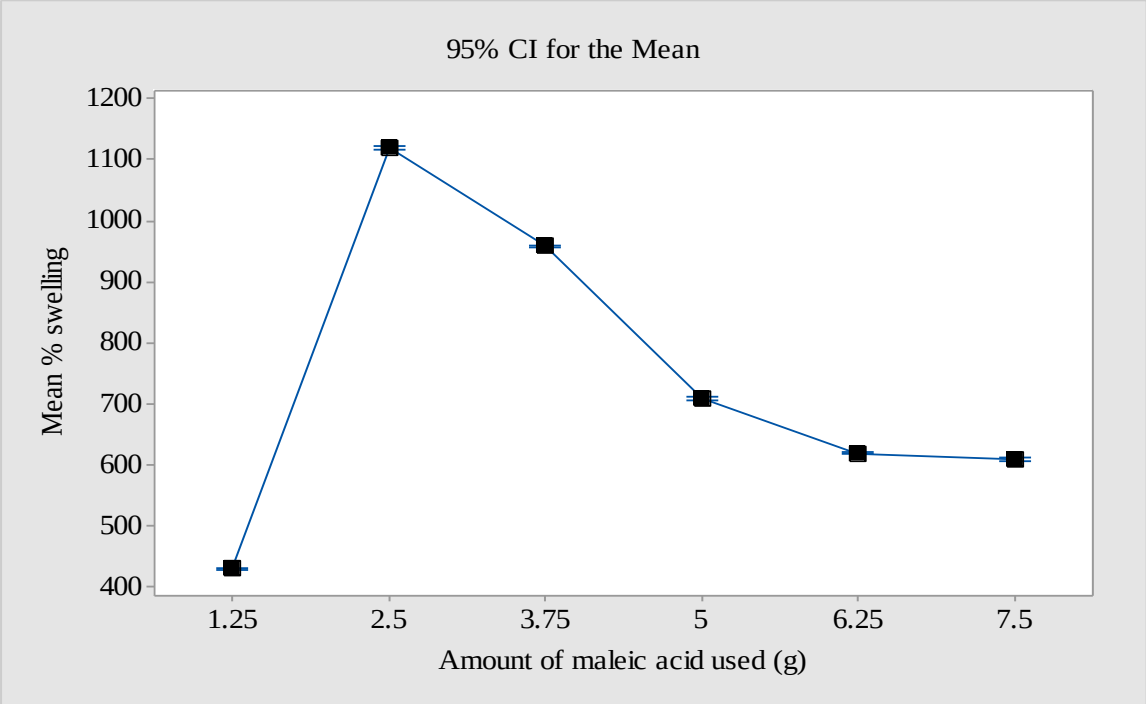

Figure 4.6.6: The effect of amount of maleic acid on the percentage swelling of 2.0 g HCG-2 hydrogel immersed in 500 mL of distilled water and contact time of 24 hours (at 6 g AC, 5 g EA, 1 g NaOH)

Figure 4.6.6 shows that an increase in cross linker dosage from 1.25 to 2.5 mL increased the percentage swelling capacity of HCG-2 super hydrogel from 430 to 1120 %. The

increased high rate of swelling capacity reveals that an increased dosage of maleic acid increased rate of ester crosslink between carboxylate and hydroxyl group of AC and glycerol. Cross linker also increases the number of pores per unit area in hydrogel network for water absorption ability. Similar results were reported by (Katime and Mendizábal, 2010). The decreased swelling capacity of HCG-2 hydrogel after a crosslinker dosage of 2.5 mL was recorded. It is assumed that over crosslinking reinforces the hydrogel structure with amphiphilic groups resulting to increased pressure between smaller newly formed inter-phases in the structure of hydrogel decreasing its absorption ability. Similar findings were reported by (Katime and Mendizábal, 2010). A mass ratio of 6: 5:1 of AC: G: MA was used to prepare HCG-2 gel with optimum swelling capacity.

Figure 4.6.7 shows the effect of varying dosages of maleic acid cross linker on the swelling capacity of super absorber hydrogel HCE-2.

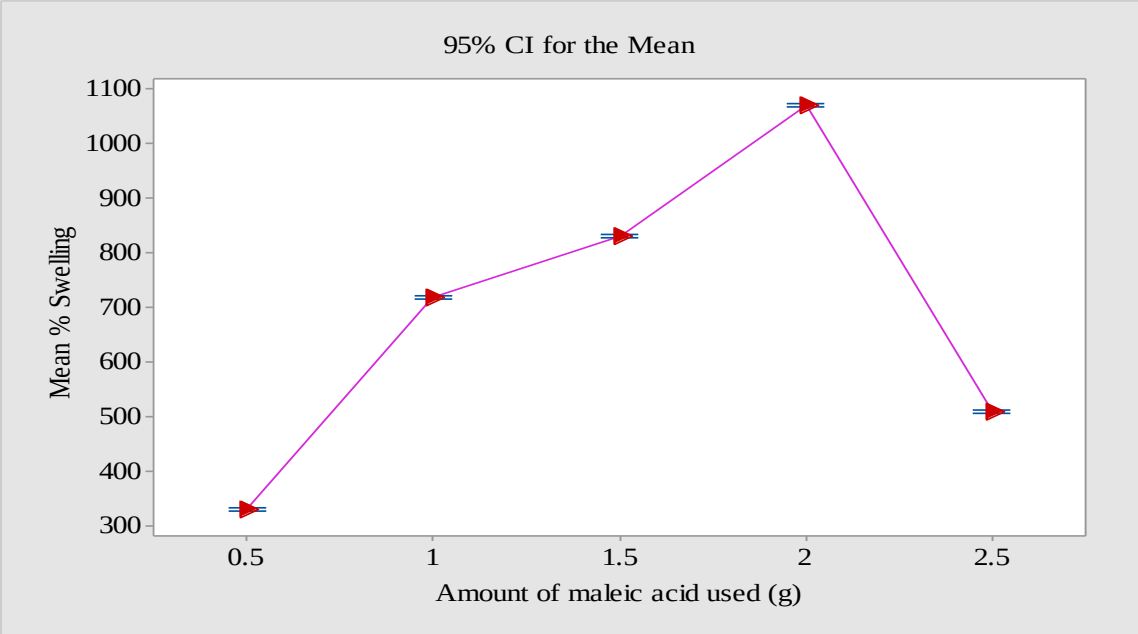

Figure 4.6.7: The effect of amount of maleic acid on the percentage swelling of 2.0 g HCE-2 hydrogel immersed in 500 mL of distilled water and contact time of 24 hours (at 6 g AC, 5 g EA, 1 g NaOH)

A steady increase in the percentage swelling capacity of HCE-2 hydrogel from 330 to 1070 % was noticed when the cross-linker mass was increased from 0.5 to 2.0 g (appendix 3c). Hydrogels with a lower mass of cross-linker concentration are flexible with a larger network of pores which facilitates high absorption of water while higher cross linker concentration forms hydrogels with rigid and smaller network sizes of pore shielding water absorption (Katime and Mendizábal, 2010). On the other hand, a percentage decrease in the swelling ability of the gel from 1070 to 510 % was noted as the mass of cross linker ratio to that of monomers increased above 2.0 g. This could be attributed to the fact that the over cross-linking hinders the mobility of polymeric chains thus lowering the swelling of hydrogel. Similar findings were reported by (Katime and Mendizábal, 2010). A mass ratio of AC: EA: MA of 6:5:2 gave the highest swelling capacity of 1070 %. A chemical cross-linker is important in improving both the integrity

of the gel and the predictability of its mechanical properties (Durrani and Donald, 1995). Figure 4.6.8 shows the effect of varying dosages of maleic acid cross linker on the swelling capacity of super absorber hydrogel HLE-2.

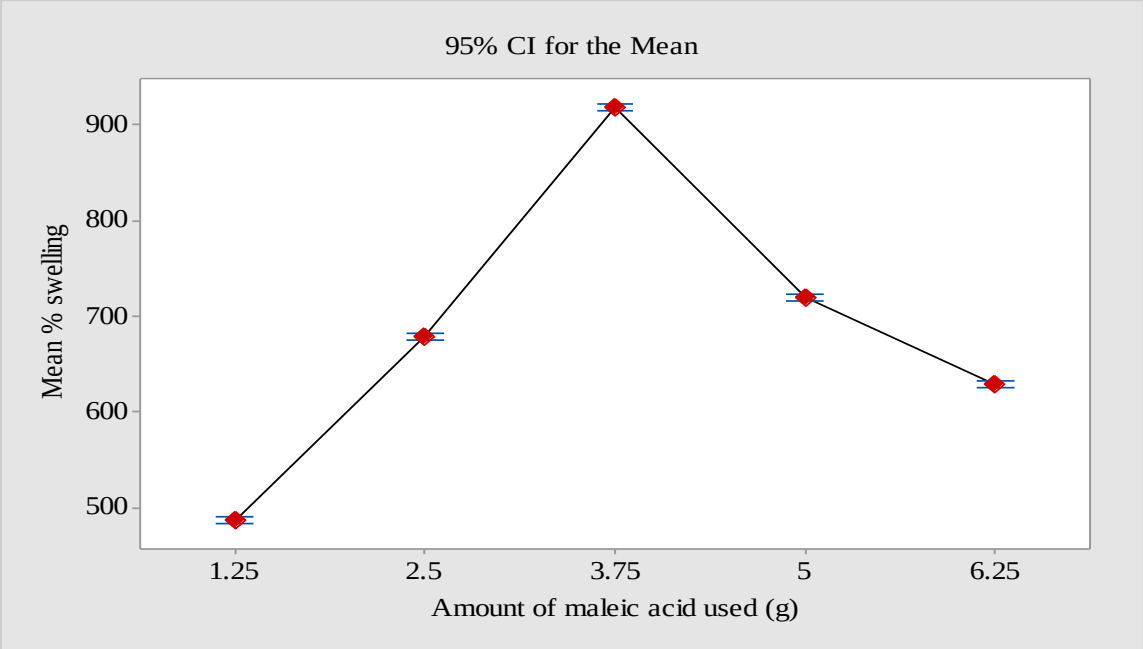

Figure 4.6.8: The effect of amount of maleic acid on the percentage swelling of 2.0 g of HLE-2 hydrogel immersed in 500 mL of distilled water and contact time of 24 hours (at 8 g CA and 5 g EA, 1 g NaOH)

Figure 4.6.8 indicated that an increase in cross linker dosage from 1.25 to 3.75 mL gradually increased the percentage swelling capacity of HLE-2 super absorbent hydrogel from 490 to 920 %. The increased swelling capacity suggested that an increased dosage of maleic acid increased the number of hydrophilic groups in the hydrogel. Swelling occurs through electrostatic repulsion between anions inside the hydrogel network and its elasticity. Similar results were reported by (Mahdavinia *et al*., 2012). The decreased swelling capacity of HLE-2 hydrogel after a cross linker dosage of 3.75 mL was

observed. The decrease in swelling capacity after the optimal cross linker dosage of 3.75 mL could be as a result of the decrease in an expansion of the hydrogel structure caused by increased crosslinking points. The decreased expansion of the hydrogel leads to shielding of the water molecules from being absorbed into the three-dimensional structure of hydrogel (Mahdavinia *et al*., 2012). The addition of a chemical cross-linker is important to improve both the integrity of the gel and the predictability of mechanical properties (Durrani and Donald, 1995). A volume ratio of CA: EDA:MA at 144:,90:,75 respectively were used to synthesis superabsorbent with highest swelling percentage.

4.6.4 Optimization of contact time on HLG-2, HLE-2, HCG-2, and HCE-2 hydrogels

The effect of contact time on the percentage swelling of super absorbent hydrogels at (0.5, 1, 2, 4, 6, 12, and 24 hours) was investigated by immersing 2.0 g of each hydrogel prepared at optimum conditions in 500 mL of distilled water in 1000 mL beaker as described in section 3.10 of this thesis. Figure 4.6.9 shows the effect of contact time on the percentage swelling of superabsorbent hydrogel HLG-2 at different contact times.

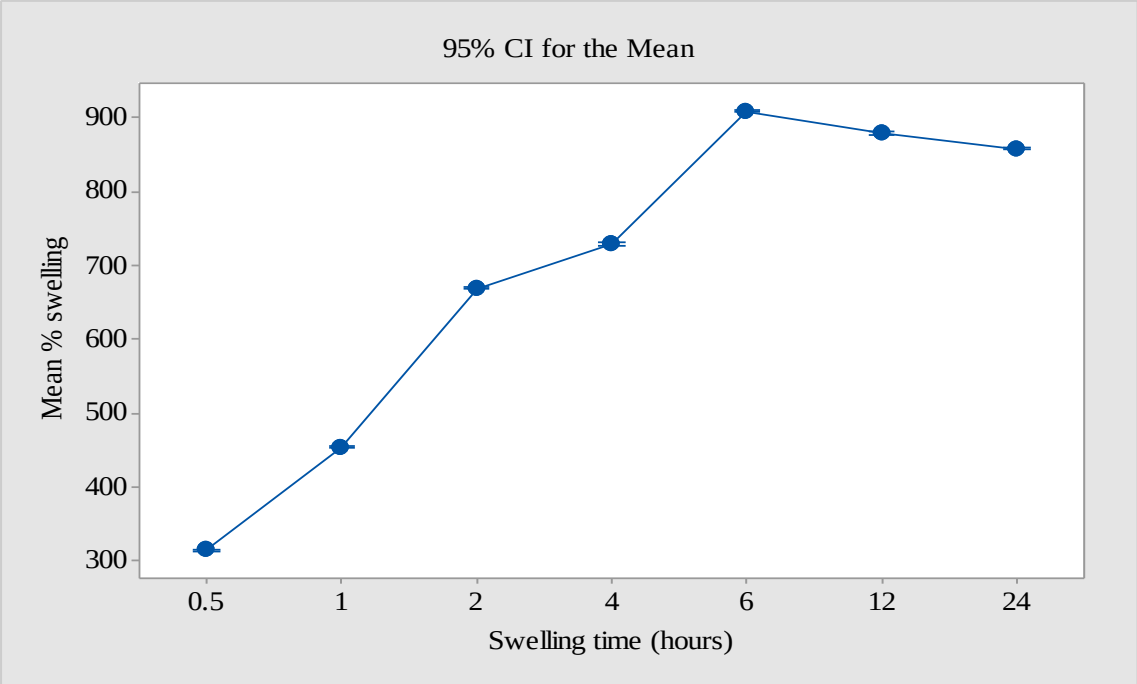

Figure 4.6.9: The effect of contact time on the percentage swelling of 2.0 g HLG-2 hydrogel prepared at optimum conditions reacting volume CA: G: MA of (5.4: 3.75: 3.75) immersed in 500 mL of distilled water

Figure 4.6.9 showed that percentage swelling of HLG-2 hydrogel increased steadily from 315 % to 910 % with the increase in contact time, from 0.5 to 6 hours followed by a gradual decrease in the rate of swelling to 860 % as time increased to 24 hours. The increase in the swelling capacity could be as a result of water penetrating the polymer gel through capillary and diffusion in the glassy state and is absorbed by hydrophilic groups such as carboxylate through the formation of hydrogen bonds. Similar findings were reported by (Ji, *et al*., 2018). The swelling is driven by the repulsion of hydrophilic groups inside the network and the osmotic pressure difference in the hydrogel. Decreased water absorption rate may be attributed to the porous network of the polymer getting saturated hence no vacant spaces for more water molecules (Parvathy and Jyothi, 2014). Again decreased percentage swelling may be associated with desorption of water due to

turgor pressure (Ji, *et al*., 2018). Moreover, during the swelling process hydrogels expand and then dissociate releasing acidic molecules in water which decreases water absorption into the functional group (Ji, *et al*., 2018).

Figure 4.6.10 shows the effect of contact time on the swelling capacity of super absorbent hydrogels HLE-2 at different contact times.

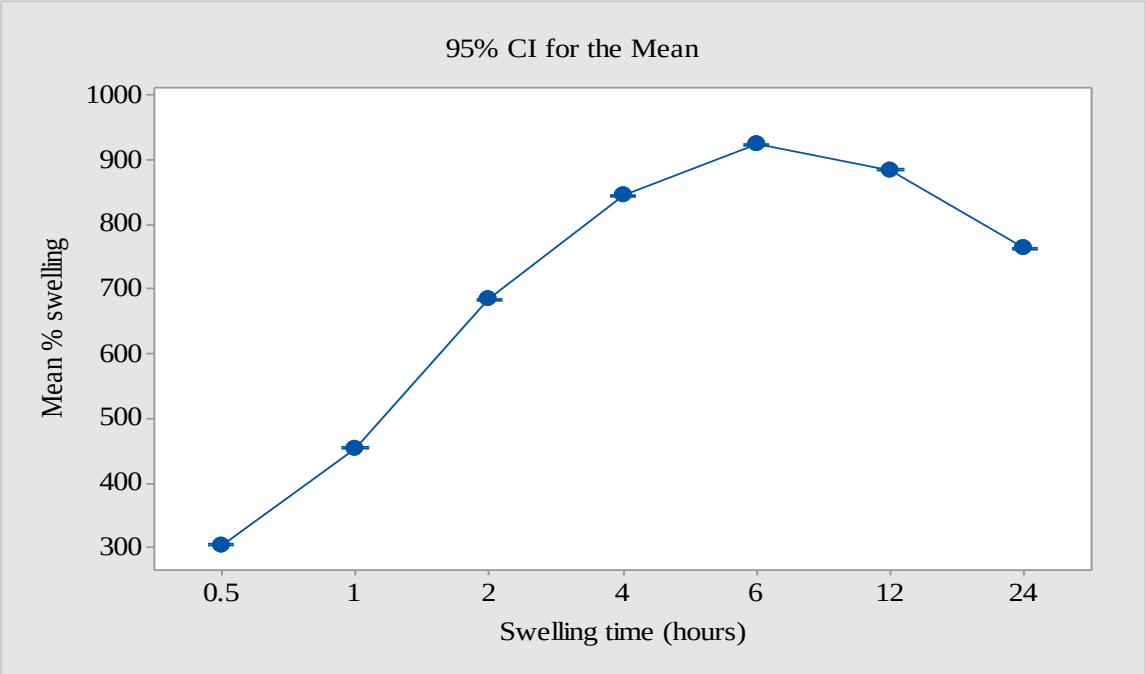

Figure 4.6.10: The effect of contact time on the percentage swelling of 2.0 g of HLE-2 hydrogel prepared using CA, EDA, and MA at a volume ratio of 144:90:75 respectively immersed in 500 mL of distilled water.

Figure 4.6.10 show that the percentage swelling of hydrogel increased from 305 % to 925 % for HLE-2 when the contact time was increased from 0.5 to 6 hours followed by a decrease to 640 % after 6 hours. The increase in swelling capacity may be as a result of water penetration in the hydrogel through capillary and diffusion in the glassy state and then absorbed by hydrophilic groups such as carboxylate through the formation of

hydrogen bonds. Similar results were reported by (Ji, *et al*., 2018). The swelling of the hydrogel is driven by the repulsion of hydrophilic groups inside the network and the osmotic pressure difference between the hydrogel and the surrounding environment. The decreased rate of water absorption after the optimal contact time may be attributed to saturation of the porous network hence the unavailability of vacant sites for water molecules (Gharekhani *et al*., 2017). However, excess water in the gel diffuses out to attain equilibrium state (Vimala *et al*., 2009).

Figure 4.6.11 shows the effect of contact time on the swelling capacity of green super absorbent hydrogels HCE-2 at different contact times.

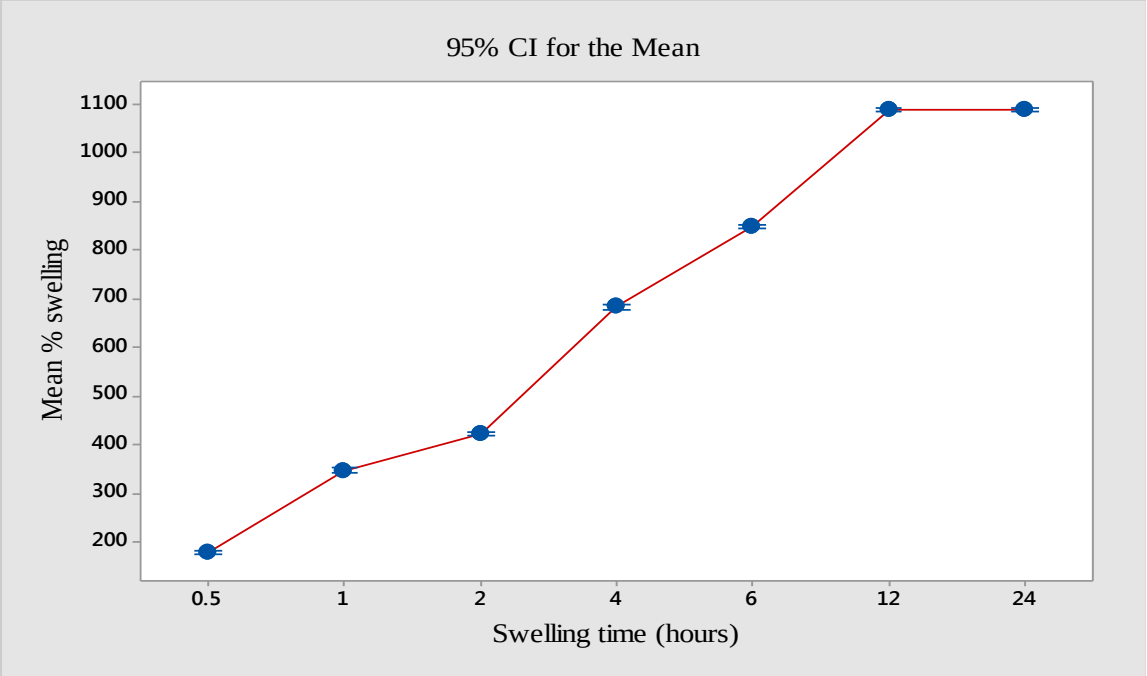

Figure 4.6.11: The effect of contact time on the percentage swelling of 2.0 g HCE-2 hydrogel prepared at optimum conditions of AC: EDA: MA of 6:5:2 immersed in 500 mL of distilled water

From figure 4.6.11, the percentage swelling increased steadily from 180 % to 1090 % within the first 12 hours and remained constant an indication it had attained its maximum swelling capacity. After the optimum contact time, the porous network of the polymer gel gets saturated with water hence no vacant spaces for the water molecules to occupy (Vimala *et al*., 2009). The results show that HCE-2 green superabsorbent hydrogel is more hydrophilic due to the presence of hydrogen bond between carboxylate ions in AC and amine groups in polyamine facilitating water absorption. Similar findings were reported by (Ravichandran *et al*., 1997). Currently reported swelling percentages on hydrogels are 580.00 % for AAP (Ravichandran *et al*., 1997), 850.00 % at pH 7.0 for PAA-based complex (Jafari and Hamid, 2005). Therefore, apart from hydrogel HCE-2 being biodegradable and cheaper it has the ability to absorb water more than 1000 times its weight, so it's a potential hydrogel.

Figure 4.6.12 shows the effect of contact time on the swelling capacity of green super absorbent hydrogels HCG-2 at different contact times.

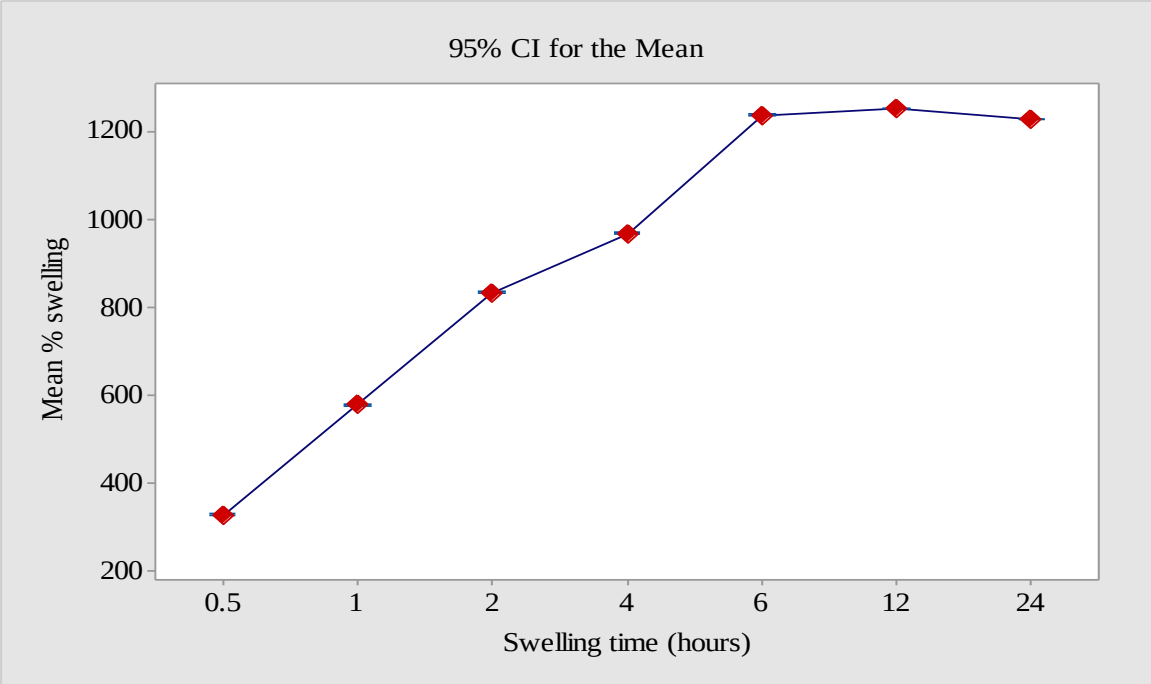

Figure 4.6.12: The effect of contact time on the percentage swelling of 2.0 g HCG-2 hydrogel prepared at optimum conditions of AC: G: MA of 6:5:1 immersed in 500 mL of distilled water

Figure 4.6.12 showed that percentage swelling increased steadily from 330 % to 1255 % within 12 hours followed by a slight decrease in the rate of swelling to 1230 % at 24 hours. This is because, as the time interval increases, the porous network of the polymer gets saturated water hence no vacant spaces for the water molecules. Subsequently, the rate of swelling gradually slows to an equilibration Similar findings were reported by (Vimala *et al*., 2009).

4.7 Effect of HCE-2, HCG-2, HLE-2, and HLG-2 super absorbent hydrogels on the growth parameters of maize crops

To evaluate the effect of HCE-2, HCG-2, HLE-2, and HLG-2 super absorbent hydrogels on growth and yield parameters, maize crop DH-02 were grown in plots with the same

conditions but with varying hydrogel dosage applications. Growth parameters were monitored at regular intervals for a period of 60 days while yield parameters were measured at harvesting after 120 days. The results and discussions on the variations of the specific growth and yield parameters of maize under different SAH treatments are presented in the subsections that follow. It is important to note that growth period starts as soon as crops germinate, 7 days after the first rain.

4.7.1 Effect of hydrogels dosage on moisture content percentage at flowering stage

The figure 4.7.1 shows dosages effect of HCG-2, HLE-2, HLG-2, and HCE-2 hydrogels in the mean moisture content percentage of maize plant at flowering stage. Maize was grown under similar climatic conditions but with a varying dosage of hydrogels applied to range from zero for control, 15, 30, 45 and 60 kg/ha. Moisture content percentage was obtained in triplicate at 50 days after germination of the maize crops followed by mean determination. Moisture content is essential morphological parameter for grain setting as well as maturity in maize crops leading to high grain yield per hectare.

Figure 4.7.1 shows effect of super absorbent hydrogels dose on mean moisture percentage of DH-02 maize plants at flowering stage.

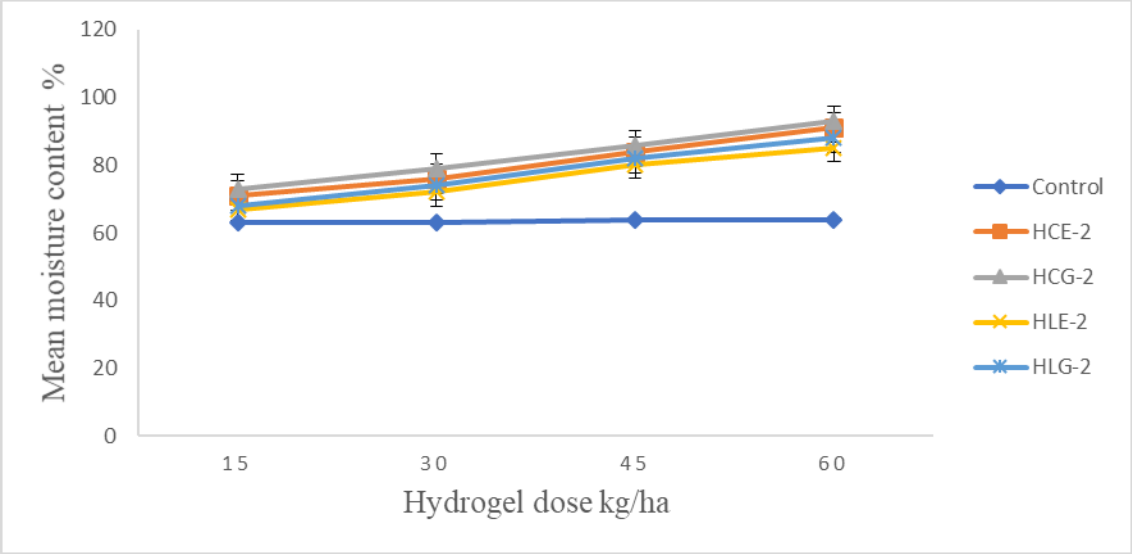

Figure 4.7.1: Effect of super absorbent hydrogels dose on average moisture percentage

The results in figure 4.7.1 shows that the mean moisture content percentage increased as follows 71.60±0.10 to 91.80±0.30 HCE-2, 73.97±0.12 to 93.20±0.10 HCG-2, 67.53±0.06 to 85.47±0.31 HLE-2, and 68.90±0.10 to 88.20±0.17 HLG-2 when dosage increased from 15 to 60 kg/ha, respectively. The mean moisture content percentage of plants treated with HCG-2 and HCE-2 were significantly different ($p < 0.05$) while those with HLE-2 and HLG-2 were not significantly different ($p > 0.05$) when 15 kg/ha were applied (appendix 4a). On the other hand, results indicate that as dosage of HCE-2, HCG-2, HLE-2, and HLG-2 SAHs increases from 30-60 kg/ha mean moisture percentage differed significantly ($p < 0.05$) and as compared to control (appendix 4a.). Results revealed that maize plant treated with super absorbent hydrogel HCG-2 had highest mean moisture content percentage compared to other superabsorbent hydrogels at different dosages during flowering stage. This implies that super absorbent hydrogel HCG-2 performed better as compared to other super absorbent at different hydrogel dosages. It may be concluded that addition of super absorbent hydrogel in the soil absorbs moisture during

rain session then releases it to the plants during flowering and grain filling stage plays major role which is characterized with dry period (Shoa-Hoseini *et al*., 2005) Again low moisture content leads to delayed flowering and maturity of maize crops leading to reduction in the yield per hectare (Shoa-Hoseini *et al*., 2005).

4.7.2 Effect of super absorbent hydrogels dosage on plant height

The performances of the dosage of HCE-2, HCG-2, HLE-2, and HLG-2 super absorbent hydrogels were evaluated through the determination of the mean heights of maize plants at different growth stages. Maize was grown under similar conditions but at a varying dosage of the hydrogels varied that ranged from zero (control), 15, 30, 45, and 60 kg/ha. The height of maize was obtained in triplicate at 15, 30, 45, and 60 days after planting. The mean heights of maize plants obtained and dosage effect of HCE-2, HCG-2, HLE-2 and HLG-2 hydrogels compared to control are presented in figure 4.7.2(a, b, c, and d) respectively.

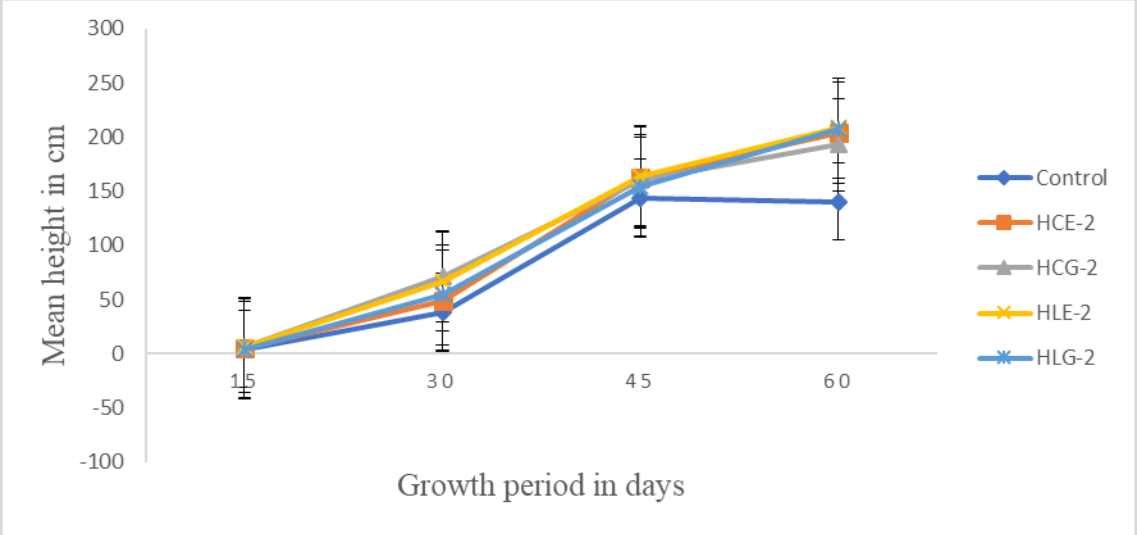

Figure 4.7.2(a): Effect of hydrogel dose on plant height using 15 kg/ha of HCE-2, HCG-2, HLE-2 and HLG-2 hydrogels

Figure 4.7.2(a) shows that, the mean height for maize plants plots treated with (15 kg/ha) increased progressively up to a period of 60 days. Mean maximum heights attained at 60 days were 203.53 ±0.25, 192.93 ±0.25, 208.40 ±0.20 and 208.03 ±0.21 cm for HCE-2, HCG-2, HLE-2-2 and HLG-2, respectively. The results differed significantly ($p < 0.05$) over control with maximum height of 140.60±0.53 cm at 60 days. Mean plant heights differed significantly ($p < 0.05$) from 15 to 45 days for all types of super absorbent hydrogels. On the other hand, mean heights of plots treated with 15 kg/ha of HCE-2 and HCG-2 were significantly different ($p < 0.05$) while those with HLE-2 and HLG-2 were not significantly different ($p > 0.05$) at a growth period of 60 days (appendix 4b).

Figure 4.7.2(b) shows the results of the effect of growth period on plant height using 30 kg/ha of HCE-2, HCG-2, HLE-2 and HLG-2 hydrogels.

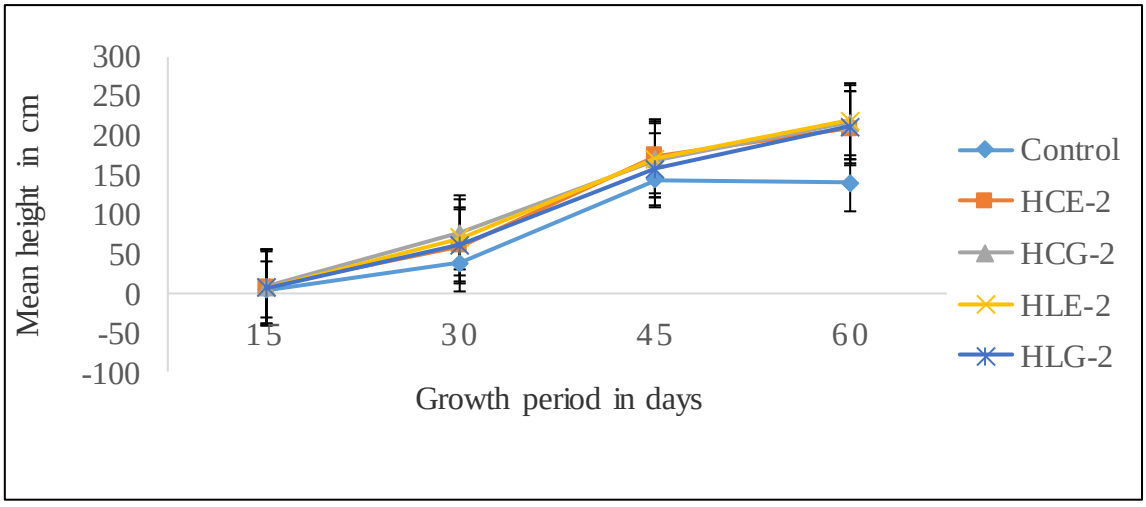

Figure 4.7.2(b): Effect of hydrogel dose on plant height using 30 kg/ha of HCE-2, HCG-2, HLE-2 and HLG-2 hydrogels**.**

From figure 4.7.2(b), application of (30 kg/ha) plants gave maximum mean heights of 208.57±0.25, 216.50±0.27, 218.67±0.38, and 211.47±0.31 cm at the 60th day for HCE-2, HCG-2, HLE-2, and HLG-2, respectively. The mean plant heights differed significantly ($p < 0.05$) as SAHs applied varies and as compared to the mean of the control at the same growth period (see appendix 4B). Figure 4.7.2(c) shows the results of effect of growth period on plant height using 45 kg/ha of HCE-2, HCG-2, HLE-2, and HLG-2 hydrogels.

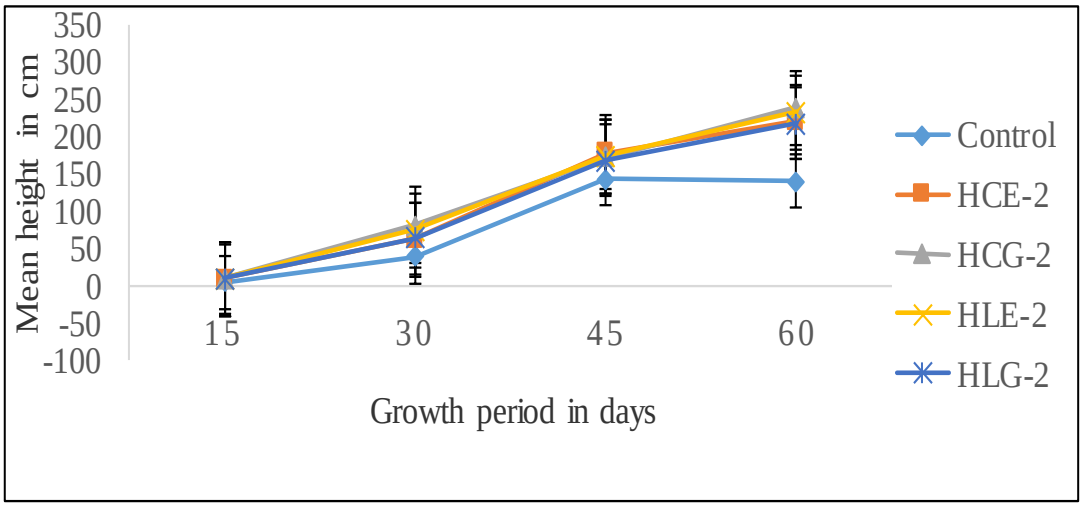

Figure 4.7.2(c): Effect of hydrogel dose on plant height using HCE-2, HCG-2, HLE-2 and HLG-2 hydrogels when 45 kg/ha was applied

As shown in figure 4.7.2(c), the mean height for maize plants plots treated with (45 kg/ha) but varying the type of hydrogel applied increased progressively up to a period of 60 days. Mean maximum heights attained at 15 days were found to be 8.27±0.21, 8.53±0.15, 8.50±0.10, and 8.23±0.06 cm for HCE-2, HCG-2, HLE-2, and HLG-2, respectively. The plant's heights were not significant difference ($p > 0.05$) as the type of hydrogel varies but differed significantly ($p < 0.05$) as compared to control with a maximum height of 4.10±0.20 cm. These mean heights increased to 220.30±0.20,

239.27±0.15, 233.67±0.15, and 218.27±0.21 cm for HCE-2, HCG-2, HLE-2, and HLG-2 at the 60th day, respectively. As the type of hydrogel applied varies, plant heights differed significantly ($p < 0.05$) and as compared to the control with a maximum height of 140.27±0.15 cm at 60 days of the growth period (see appendices 4b).

Figure 4.7.2(d) shows the results of the effect of super absorbent hydrogel on plant height using 60 kg/ha of HCE-2, HCG-2, HLE-2 and HLG-2 hydrogels.

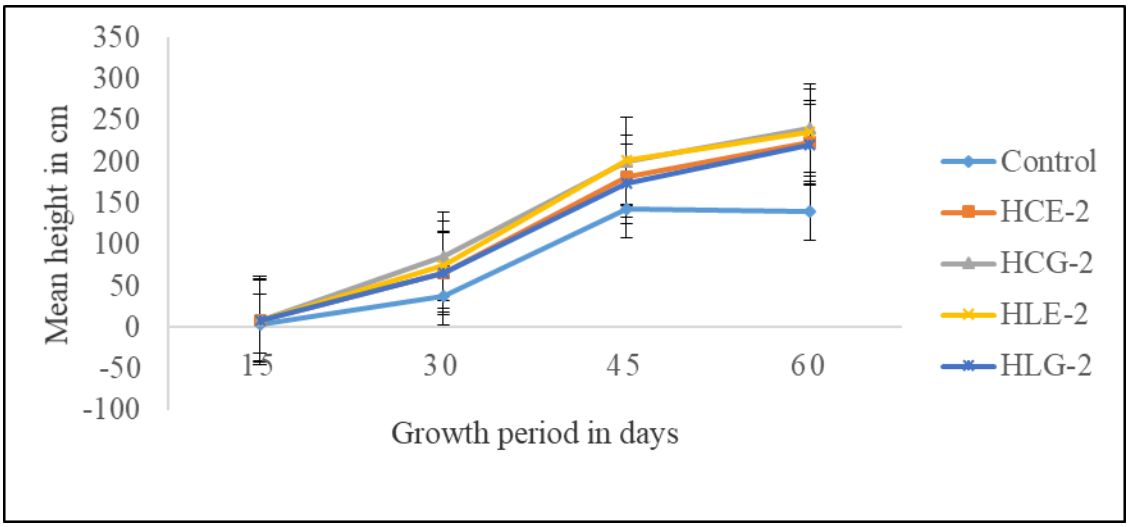

Figure 4.7.2(d): Effect of hydrogel dose on plant height using HCE-2, HCG-2, HLE-2, and HLG-2 hydrogels when 60 kg/ha was applied.

Figure 4.7.2(d) reveals that the mean height for maize plants plots treated with (60 kg/ha) but varying the type of hydrogel applied increased up to a period of 60 days. Mean maximum heights attained at 15 days were found to be 8.63±0.15, 8.50±0.20, 8.37±0.25, and 8.47±0.21 cm of HCE-2, HCG-2, HLE-2, and HLG-2, respectively and were not significant difference ($p > 0.05$) (see appendix 4B). On the other hand, mean heights increased to 223.30±0.20, 240.47±0.25, 235.23±0.15, and 220.57±0.15 cm of HCE-2,

HCG-2, HLE-2, and HLG-2, respectively at 60^{th}. The plant heights differed significantly ($p < 0.05$) as the type of hydrogel varied and as compare to control. Super absorbent hydrogel HCG-2 performed better as compared to HCE-2, HLE-2 and HLG-2 at different hydrogel dosages with the highest mean plant height of 240.47±0.25 cm when (60 kg/ha) of hydrogel were applied (see appendix 4b).

The results obtained revealed that each successive increase in levels of polymer from 15 to 60 kg/ha brought a significant increase in mean plant height up to a growth period of 60 days. An increase in plant height is due to the high potential of super absorbent hydrogel to absorb, and conserve water in the soil, availability and indirectly nutrients provided by super absorbent polymer (Nnadi and Brave 2013). These results in an increased rate of cell division, cell expansion, and cell elongation (Tong-Chao *et al*. 2007, Al-Harbi *et al*. 1999).

4.7.3 Effect of hydrogel dosage on number of leaves

The figure 4.7.3(a, b, c and d) shows dosages effect of HCG-2, HLE-2, HLG-2, and HCE-2 hydrogels on the mean number of leaves per maize plant at different growth periods. Maize was grown under similar climatic conditions but with a varying dosage of hydrogels applied to range from zero for control, 15, 30, 45 and 60 kg/ha. The number of leaves per plant was obtained in triplicate at 15, 30, 45 and 60 days after planting followed by mean determination.

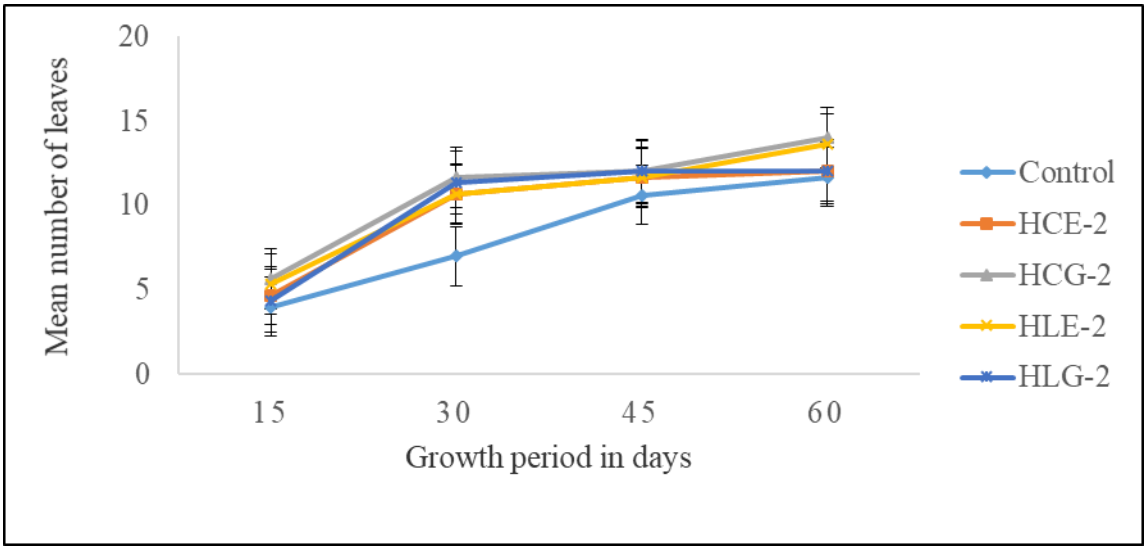

Figure 4.7.3(a): Effect of hydrogel dose on number of leaves using HCG-2, HLE-2, HLG-2 and HCE-2 hydrogels when 15 kg/ha was applied

Figure 4.7.3(a) shows the mean number of leaves for DH-02 maize plants plots treated with (15 kg/ha) but varying the type of hydrogel applied showed a progressive increase up to 60 days. The mean number of leaves increased from 15 to 60 days as follows 4.67±0.58 to 12.00±1.00 HCE-2, 5.67±0.58 to 14.00±0.00 HCG-2, 5.33±0.58 to 13.67±0.58 HLE-2, and 4.33±0.58 to 12.00±1.00 HLG-2, respectively. The results differed significantly ($p < 0.05$) as compared to control which increased from 4.00±0.00 to 11.67±0.58 (appendix 4c). The mean number of leaves of plants treated with HCG-2 and HLE-2 were significantly different ($p < 0.05$) while those with HCE-2 and HLG-2 were not significantly different ($p > 0.05$) at 60th days (see appendix 4c).

Figure 4.7.3b shows the results of the effect of the hydrogel dose on a plant's mean number of leaves using 30 kg/ha of HCE-2, HCG-2, HLE-2, and HLG-2 hydrogels.

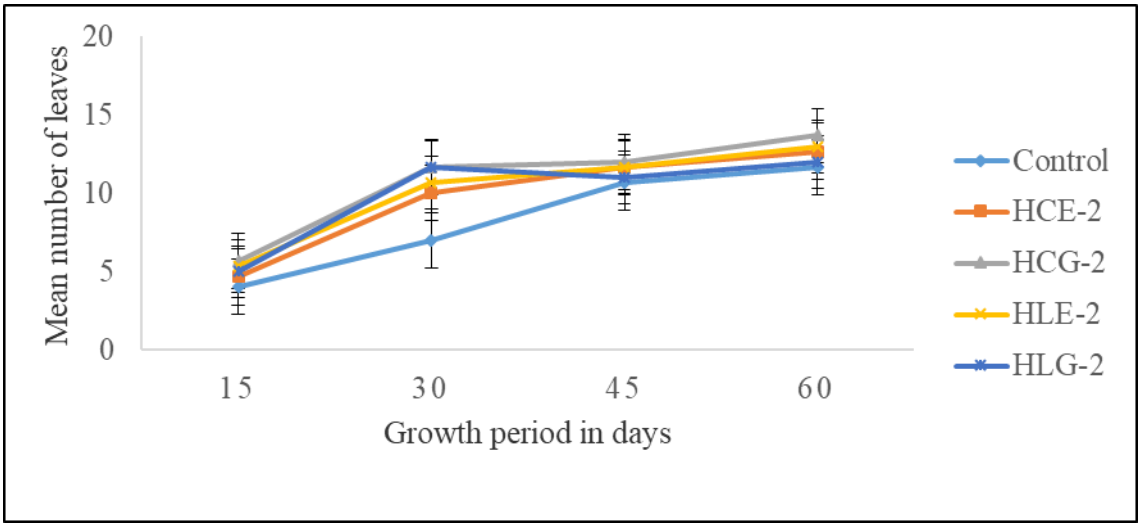

Figure 4.7.3(b): Effect of hydrogel dose on number of leaves using HCG-2, HLE-2, HLG-2 and HCE-2 hydrogels when 30 kg/ha was applied

Figure 4.7.3(b) revealed that the mean number of leaves of plots treated with 30 kg/ha of the super absorbent hydrogels increased during the growth period. The results indicate that HCE-2, HCG-2, HLE-2, HLG-2 increased from 4.67±0.58 to 12.67±0.58, 5.67±0.58to 13.67±0.58, 5.33±0.58 to 13.00±1.00, and 13.00±1.00 to 12.00±1.00, respectively from 15th to 60th day. There was no significant difference ($p > 0.05$) in the plant number of leaves as the type of hydrogel varied as well as compared to control at 15th and 60th day of growth period (see appendix 4c).

Figure 4.7.3c shows the results of the effect of the hydrogel dose on a plant's mean number of leaves using 45 kg/ha of HCE-2, HCG-2, HLE-2, and HLG-2 hydrogels.

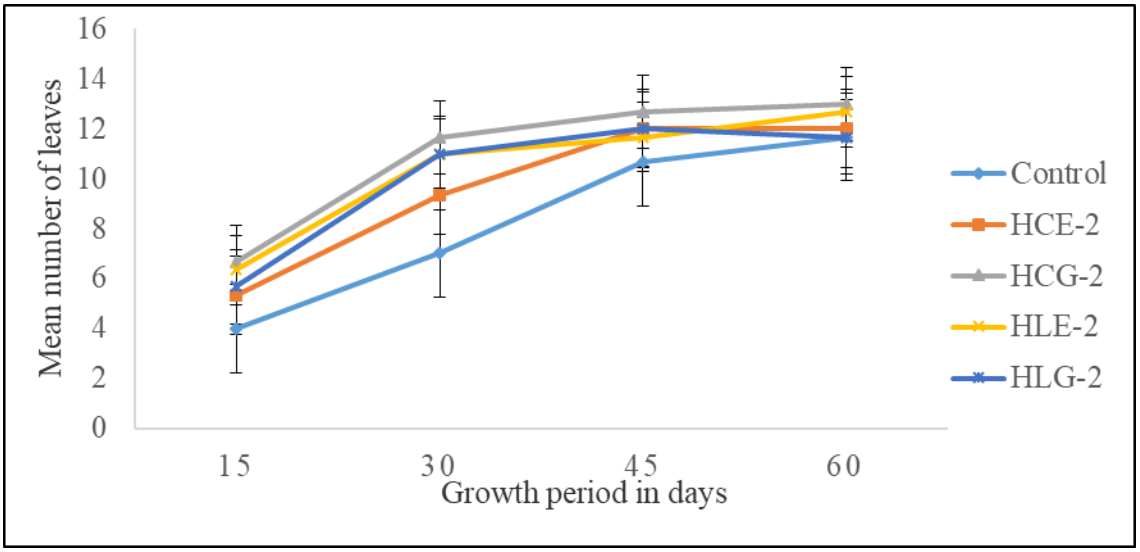

Figure 4.7.3(c): Effect of hydrogel dose on number of plant leaves using HCG-2, HLE-2, HLG-2 and HCE-2 hydrogels when 45 kg/ha was applied

Results in figure 4.7.3(c) indicate that, on the application of 45 kg/ha of HCG-2, HLE-2, HLG-2 and HCE-2 hydrogels mean number of leaves increased as the growth period increases. The mean number of leaves increased from 5.33±0.58 to 12.00±1.00, 6.67±0.58 to 13.00±1.00, 6.33±0.58 to 12.67±0.58, and 5.67±0.58 to 11.67±0.58 for HCE-2, HCG-2, HLE-2, and HLG-2, respectively from 15^{th} to 60^{th} day of growth period. Results showed no significantly difference ($p > 0.05$) as the type of hydrogel was varied as well as compared to control (see appendix 4c).

Figure 4.7.3(d) shows the results of the effect of the hydrogel dose on the plant mean number of leaves using 60 kg/ha of HCE-2, HCG-2, HLE-2 and HLG-2 hydrogels.

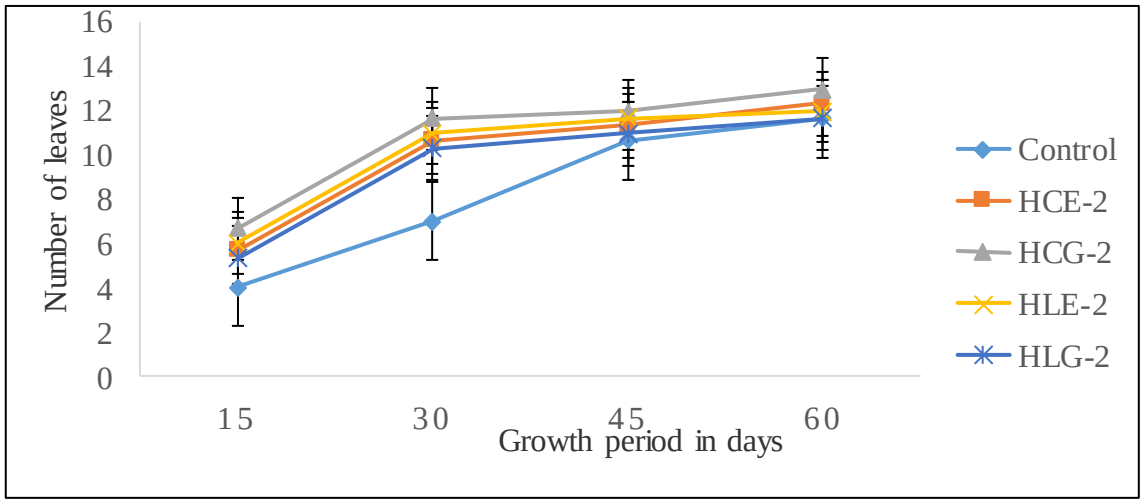

Figure 4.7.3(d): Effect of hydrogel dose on number of leaves using HCG-2, HLE-2, HLG-2, and HCE-2 hydrogels when 60 kg/ha was applied

Figure 4.7.3(d) shows that the average number of leaves for plots treated with 60 kg/ha HCE-2, HCG-2, HLE-2 and HLG-2 hydrogel at 60 days were 12.33±0.58, 13.00±1.00, 12.00±0.00 and 11.67±0.58, respectively. The mean leaves values showed no significantly different ($p > 0.05$) as the type of hydrogels vary as well as compared to that of control (see appendix 4c). The results revealed that HCG-2 performed better than other hydrogels on the mean number of leaves. This may be attributed to its higher ability of water absorption than other superabsorbent hydrogels (Stern *et al.*, 1992). In addition, increased mean number of leaves per plant as the dosage of hydrogel increase shows a significant amount of water absorption in the hydrogel structure. Successively this ensures enough water was absorbed and stored into the soil around plant roots to be released during dry periods of crop growth (Johnson and Woodhouse, 1991; Hayat and Ali 2004).

4.7.4 Effect of super absorbent hydrogel dose on plant leave area index in cm^2

The performances of the dosage of HCE-2, HCG-2, HLE-2, and HLG-2 super absorbent hydrogels were evaluated by determining the mean heights of maize plants at different growth stages. The maize crop was grown under similar conditions but at varying dosage of the hydrogels, (0, 15, 30, 45, and 60 kg/ha). The plant leave area index of maize was measured in triplicates at 15, 30, 45, and 60 days after planting. The effect of super absorbent hydrogels dose on plant leave area index are shown in figure 4.7.4(a, b, c and d). Figure 4.7.4(a) Effect of super absorbent hydrogels dose (15 kg/ha) HCG-2, HLE-2, HLG-2 and HCE-2 on leaf area index (LAI) (cm^2.

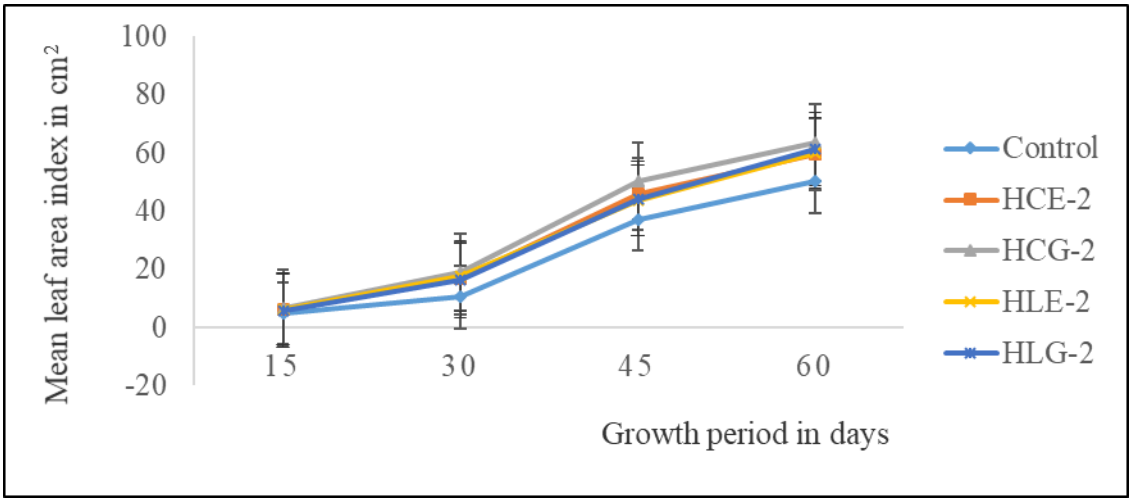

Figure 4.7.4(a): Effect of super absorbent hydrogels dose (15 kg/ha) of HCG-2, HLE-2, HLG-2 and HCE-2 on leaf area index (LAI) (cm^2)

Figure 4.7.4(a), showed the influence of hydrogel on mean leaf area index (LAI) for DH-02 maize plants grown in plots treated with 15 kg/ha of HCE-2, HCG-2, HLE-2 and HLG-2 increased progressively from 15 to 60 days of the growth period. It was noted that the mean LAI increased from 6.30±0.20 to 59.57±0.32, 6.77±0.25 to 63.47±0.35, 6.23±0.15 to 60.03±0.31 and 5.97±0.15 to 61.27±0.25 for HCE-2, HCE-2, HLE-2 cm^2,

respectively as growth period increased from 15th to 60th day. The mean LAI of maize plants treated with HCG-2 and HLG-2 differed significantly ($p < 0.05$) while those with HCE-2 and HLG-2 were not significantly different ($p > 0.05$) at 60th day (see appendix 4d).

Figure 4.7.4(b) Effect of super absorbent hydrogels dose (30 kg/ha) HCG-2, HLE-2, HLG-2 and HCE-2 on leaf area index (LAI) (cm^2).

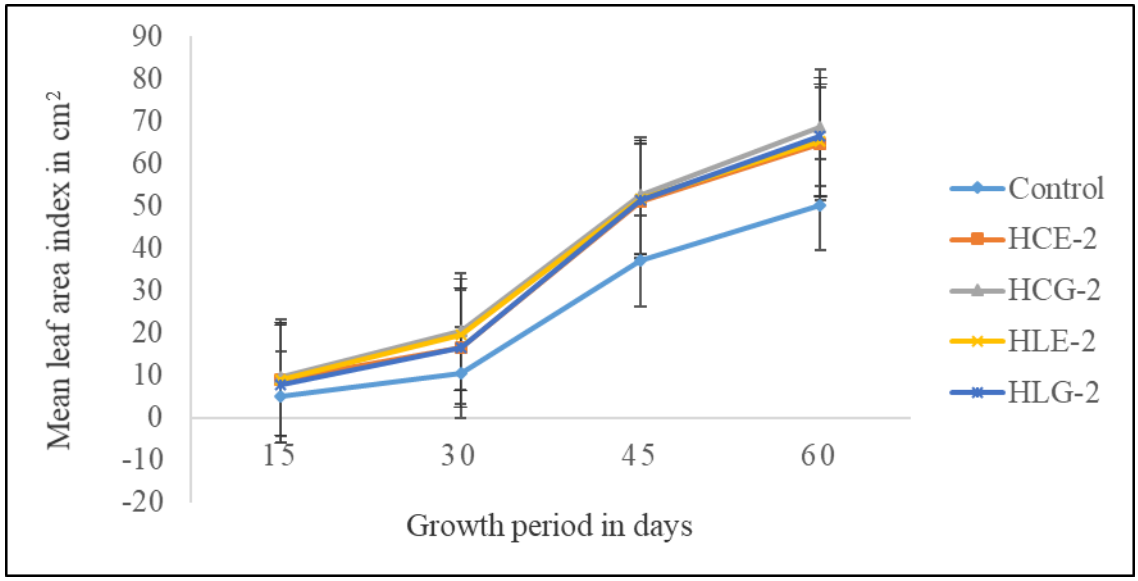

Figure 4.7.4((b): Effect of super absorbent hydrogels dose (30 kg/ha) HCG-2, HLE-2, HLG-2 and HCE-2 hydrogels on leaf area index (LAI) (cm^2)

Figure 4.7.4(b) shows that the mean leaf surface area for maize plants plots treated with (30 kg/ha) increased progressively up to 60 days. Mean maximum LAI increased from 8.93±0.15 to 64.57±0.25, 64.57±0.25 to 68.50±0.30, 9.07±0.25 to 65.33±0.15, and 7.87±0.25 and 66.40±0.20 cm^2 for HCE-2, HCG-2, HLE-2, and HLG-2, respectively as growth period increased from 15th to 60th day. The results that LAI differed significantly

($p < 0.05$) as type of super absorbent hydrogel applied varies as well as compared to control with maximum LAI of 140.60±0.53 cm^2 at 60th day (see appendix 4d).

Figure 4.7.4(c) Effect of super absorbent hydrogels dose (45 kg/ha) HCG-2, HLE-2, HLG-2 and HCE-2 on leaf area index (LAI) (cm^2.

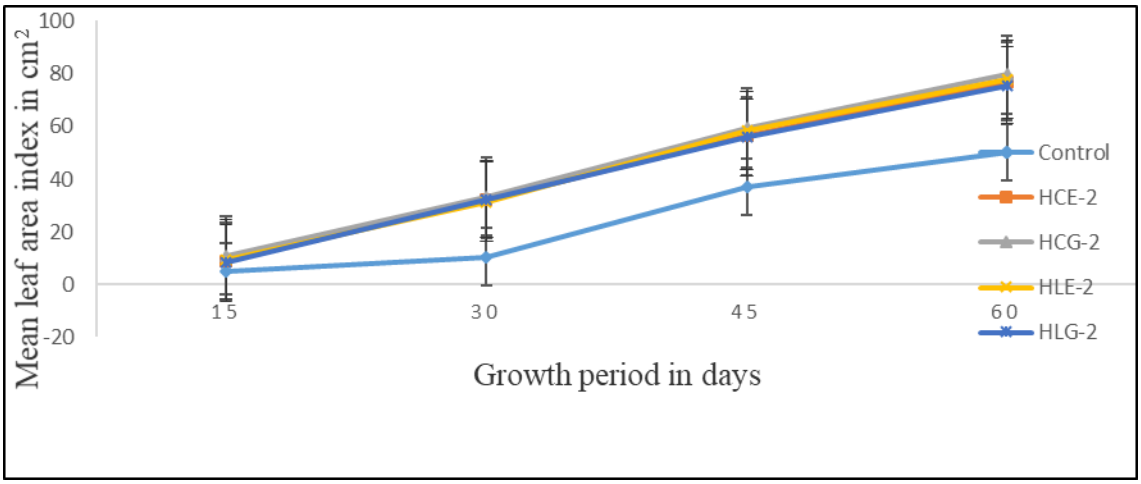

Figure 4.7.4(c): Effect of super absorbent hydrogels dose (45 kg/ha) HCG-2, HLE-2, HLG-2 and HCE-2 hydrogels on leaf area index (cm^2)

Figure 4.7.4(c) indicates clearly that, the mean LAI for maize plants plots treated with 45 kg/ha but varying the type of hydrogel applied of HCE-2, HCG-2, HLE-2 and HLG-2 at 15th day attained maximum of 8.87±0.38, 11.03±0.25, 9.60±0.17, and 8.33±0.25 cm^2, respectively. The plants LAI for treatment with HCG-2 and HLE-2 differed significantly ($p < 0.05$) while HCE-2 and HLG-2 were not significantly different ($p > 0.05$) at 15th day (appendix 4d.). The mean LAI increased progressively to 77.07±0.25, 79.63±0.15, 77.90±0.2, and 75.53±0.31 cm^2 for HCE-2, HCG-2, HLE-2 and HLG-2 at 60th day of growth period, respectively. This implies that super absorbent hydrogel HCG-2 performed better as compared to other superabsorbent (see appendix 4d).

Figure 4.7.4(d) Effect of super absorbent hydrogels dose (60 kg/ha) HCG-2, HLE-2, HLG-2 and HCE-2 on leaf area index (LAI) (cm^2.

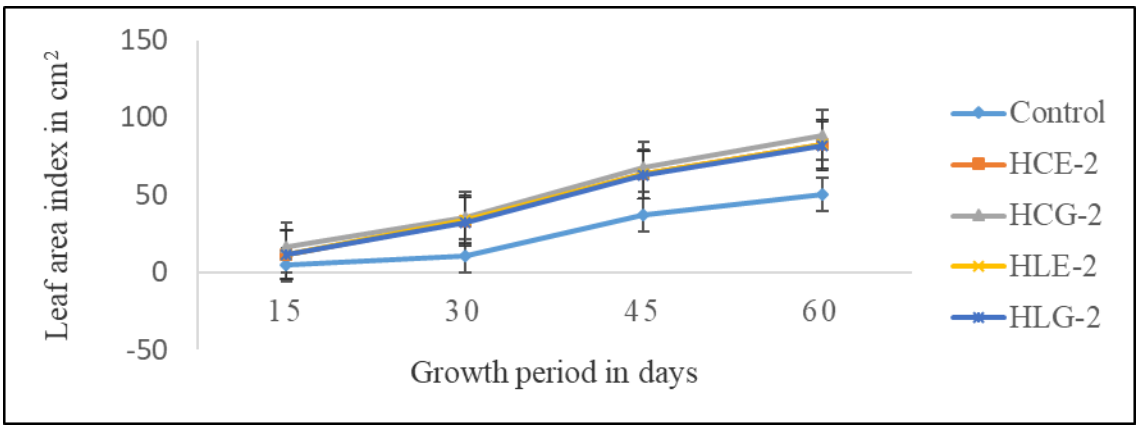

Figure 4.7.4(d): Effect of super absorbent hydrogels dose (15 kg/ha) of HCG-2, HLE-2, HLG-2 and HCE-2 hydrogels on leaf area index (cm^2)

Figure 4.7.4(d) showed the mean LAI of maize plants treated with 60 kg/ha of HCE-2, HCG-2, HLE-2 and HLG-2 super absorbent hydrogel which increased progressively from 15 to 60 days. The highest mean LAI of 82.33±0.15, 88.63±0.15, 82.77±0.32, and 81.50±0.20 cm^2 for HCE-2, HCG-2, HLE-2, and HLG-2, respectively were noted for the growth period of 60 days. The mean LAI of maize plants treated with HCG-2 and HLG-2 differed significantly ($p < 0.05$) while those with HCE-2 and HLE-2 were not significantly different ($p > 0.05$) at 60^{th} day (see appendix 4d).

This implies that superabsorbent hydrogel HCG-2 performed better as compared to other superabsorbents at different hydrogel dosages. An increase in LAI as dosage of hydrogel varies may be attributed with increased leaf relative water content due to sufficient availability of soil moisture and its supply to the crop (Volkamar and Chang 1995; Thombare *et al*., 2018). On the other hand, HCG-2 polymer has a higher ability to

conserve different amounts of water in the structure depending on the amount of dosage applied. This may be due to availability of excess pores in the polymer structure compared to other hydrogels, increasing the soil's capacity for water storage, ensuring more available water under stress condition, thus the relative water content in leaves increased (Vazdani *et al*., 2007; Mondal, 2011).

4.7.5 Effect of super absorbent hydrogel dose on dry matter accumulation (DMA)

The dosage effect of HCE-2, HCG-2, HLE-2, and HLG-2 super absorbent hydrogels was investigated through the determination of the mean dry matter accumulation of maize plants at different growth stages. Maize plants under investigation were grown under similar conditions but at a varied dosage of the hydrogel in the range from zero (control), 15, 30, 45 and 60 kg/ha. The dry matter accumulation of maize was obtained in triplicate at 15, 30, 45 and 60 days after planting. The effects of hydrogels dosage are presented in figure 4.7.5(a, b, c and d).

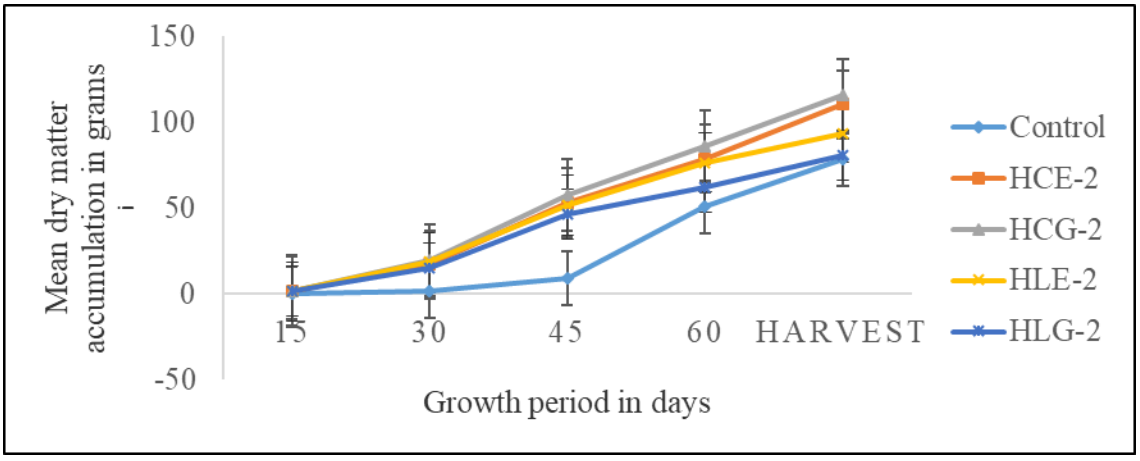

Figure 4.7.5(a): Effect of super absorbent hydrogels dose (15 kg/ha) dry matter accumulation in grams when HCG-2, HLE-2, HLG-2 and HCE-2 hydrogels were applied

Generally, results in figure 4.7.5(a) shows that, dry matter accumulation for the maize plants grown with 15kg/ha of HCE-2, HCG-2, HLE-2 and HLG-2 increased progressively as the growth period of the crop increased from 15th to harvest day (105 days). Mean maximum dry matter accumulation attained for the maize plants treated with 15 kg/ha of HCE-2, HCG-2, HLE-2 and HLG-2 increased from 1.60±0.10 to 110.37±0.21, 1.97±0.12 to 115.90±0.30, 1.57±0.06 to 93.60±0.36, and 1.90±0.10 to 80.53±0.31 g, respectively from 15th to harvest day (105 days). Dry matter accumulation differed significantly ($p < 0.05$) for the four hydrogels and as compared to that of control during harvest period. This indicates that superabsorbent hydrogel HCG-2 performed better as compared to other superabsorbent (appendix 4E). This may be due to availability of pores and hydroxyl groups facilitating high rate of water absorption and releasing it to the roots of crops during dry growth periods.

Figure 4.7.5(b) shows the results of the effect of the growth period on dry matter accumulation using 30 kg/ha of HCE-2, HCG-2, HLE-2 and HLG-2 hydrogels.

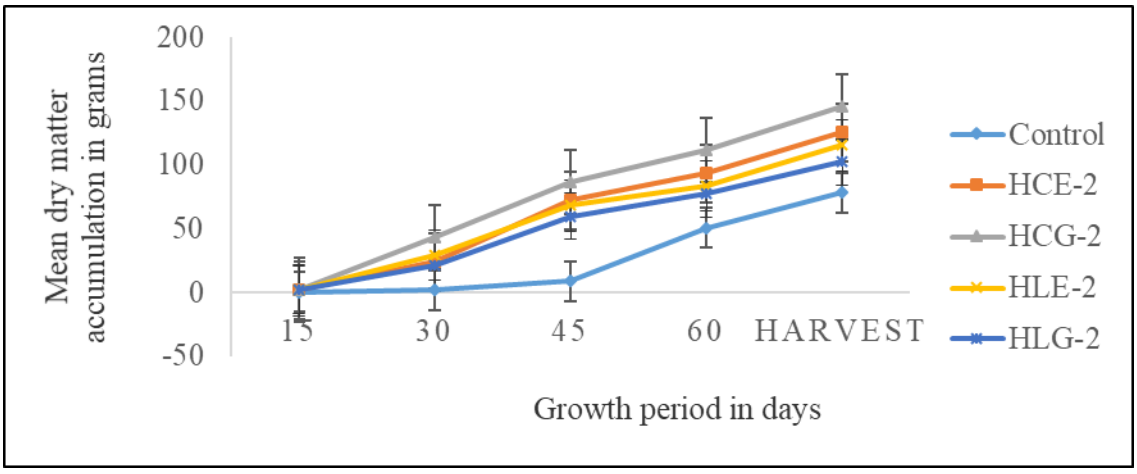

Figure 4.7.5(b): Effect of super absorbent hydrogels dose (30 kg/ha) on dry matter accumulation in grams when HCG-2, HLE-2, HLG-2 and HCE-2 hydrogels were applied

Figure 4.7.5(b) clearly indicates that, as the mean dry matter accumulation of maize plant grown in plots treated with 30 kg/ha of HCE-2, HCG-2, HLE-2 and HLG-2 super absorbent hydrogel increased from 15th to harvest day (105 days), the maximum dry matter accumulation increased from 1.73±0.06 to 125.70±0.10, 2.07±0.06 to 145.47±0.21, 1.83±0.06 to 115.57±0.25, and 2.00±0.10 to 102.47±0.15 g for HCE-2, HCG-2, HLE-2, and HLG-2 super absorbent hydrogels respectively. The results differed significantly ($p < 0.05$) for HCE-2, HCG-2, HLE-2, and HLG-2 hydrogels as growth period increases up to harvest period and as compared with control plot. Super absorbent hydrogel HCG-2 performed better than others (see appendix 4E).

Figure 4.7.5c shows the results of the effect of growth period on dry matter accumulation using 45 kg/ha of HCE-2, HCG-2, HLE-2 and HLG-2 hydrogels.

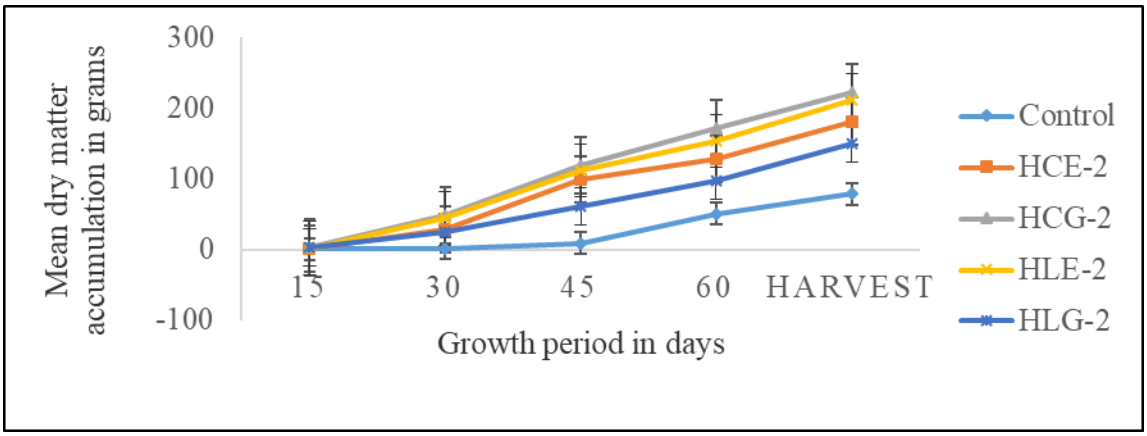

Figure 4.7.5(c): Effect of on dry matter super absorbent hydrogels dose (45 kg/ha) accumulation in grams when HCG-2, HLE-2, HLG-2 and HCE-2 hydrogels were applied

The results in figure 4.7.5(c) shows that, when maize plants were treated with the dosage of 45 kg/ha of HCE-2, HCG-2, HLE-2 and HLG-2 hydrogel there was progressive increase in dry matter accumulation from 15th to harvest day (105 days). The mean dry

matter accumulation increased from 1.87±0.06 to 181.60±0.20, 2.17±0.06 to 222.53±0.21, 2.00±0.10 to 211.60±0.20, and 2.10±0.10 to 150.50±0.20 g for HCE-2, HCG-2, HLE-2 and HLG-2, respectively. The results differed significantly ($p < 0.05$) as the type of hydrogel was varied at harvest time. Hydrogel HCG-2 performed better compared to other SAHs (see appendix 4E).

Figure 4.7.5(d) shows the results of the effect of the growth period on dry matter accumulation using 60 kg/ha of HCE-2, HCG-2, HLE-2 and HLG-2 hydrogels.

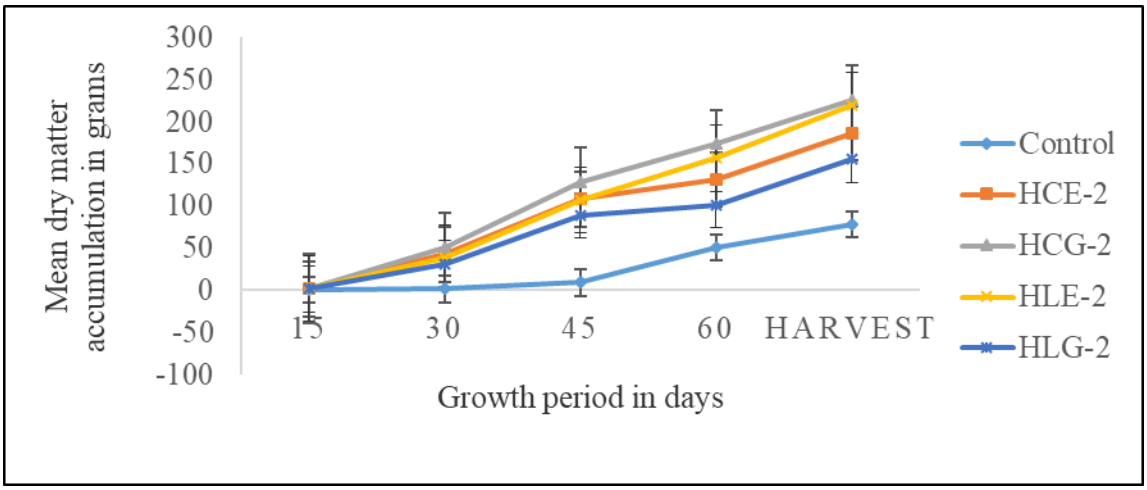

Figure 4.7.5(d): Effect of super absorbent hydrogels dose (60 kg/ha) on dry matter accumulation in grams when HCG-2, HLE-2, HLG-2 and HCE-2 hydrogels were applied

Figure 4.7.5(d) revealed that mean dry matter accumulation for maize plants grown with 60 kg/ha of HCE-2, HCG-2, HLE-2 and HLG-2 increased as the growth period increases from 15th to harvest day (105 days). The mean maximum dry matter accumulation attained increased from 1.97±0.12 to 186.33±0.25, 2.07±0.15 to 225.77±0.15, 1.83±0.06 to 219.40±0.01, and 1.70±0.10 to 155.37±0.35 g for HCE-2, HCG-2, HLE-2 and HLG-2, respectively from 15th to the harvest day (105 days). The results showed that dry matter

accumulation differed significantly ($p < 0.05$) from one hydrogel to another (appendix 4E). These results imply that super absorbent hydrogel HCG-2 performed better as compared to other SAHs, recording the highest mean dry matter of 225.77±0.15 when 60 kg/ha was applied.

This may be attributed to high number of pore and hydrophilic groups in the surface of HCG-2 increasing rate of moisture and nutrients absorption and release to crops. The use of superabsorbent hydrogel served as a carrier and regulator of nutrients release, which helped in limiting fertilizer and moisture loss (Mikkelsen, 1994; Van *et al*., 2011). The retained water and nutrients are released to the plants slowly during dry sessions leading to improve growth (Yazdani *et al*., 2007).

4.7.6 Effect of super absorbent hydrogel dose on crop growth rate (g/m^2/day) (CGR)

The dosage effect of HCE-2, HCG-2, HLE-2, and HLG-2 super absorbent hydrogels was investigated through the determination of the mean crop growth rate of maize plants at different growth stages. Maize plants under investigation were grown under similar conditions but at varying dosages of the hydrogels in the range from zero (control), 15, 30, 45, and 60 kg/ha. The crop growth rate of maize was obtained in triplicate at 15, 30, 45, and 60 days after planting followed by obtaining mean values. The dosage effect of HCE-2, HCG-2, HLE-2, and HLG-2 hydrogels compared to control are presented in figure 4.7.6(a, b, c and d).

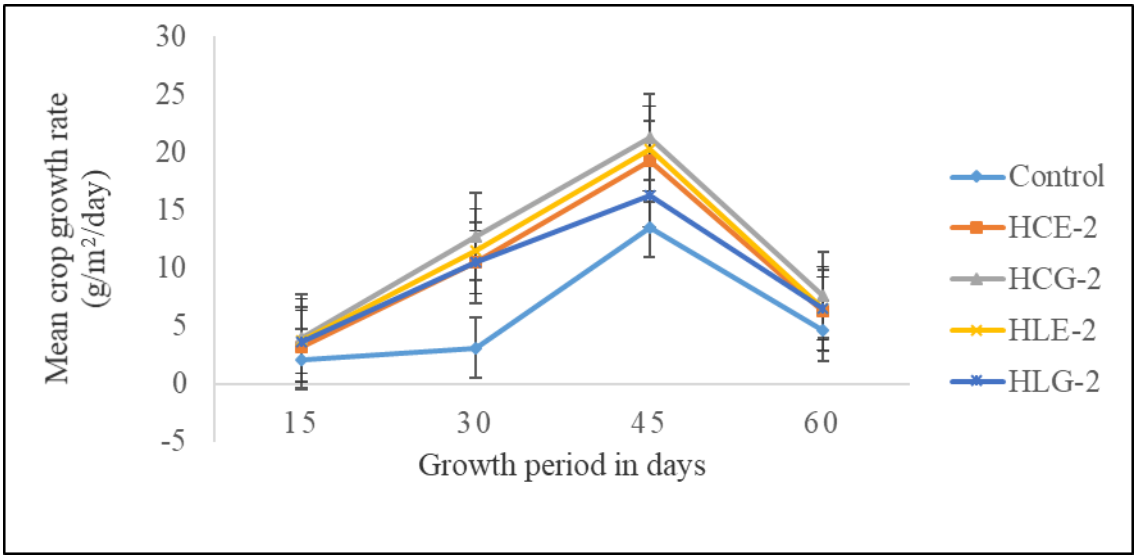

Figure 4.7.6(a): Effect of super absorbent hydrogels dose (15 kg/ha) on crop growth rate ($g/m^2/day$) when HCG-2, HLE-2, HLG-2 and HCE-2 hydrogels were applied

Figure 4.7.6(a) clearly shows that the mean crop growth rate of maize plants grown in the plots treated with 15 kg/ha of HCE-2, HCG-2, HLE-2 and HLG-2 increased to 19.23±0.12, 21.30±0.20, 20.30±0.17 and 16.30±0.10 ($g/m^2/day$) at time interval of 45 days. The results differed significantly ($p < 0.05$) as the type of hydrogel varied and as compared to control which increased to 13.53±0.31 ($g/m^2/day$). This may be attributed to availability of constants supply of moisture and nutrients during dry period of crop growth. On the other side, a slight decrease in mean crop growth rate between 45^{th} and 60^{th} day of 6.33±0.217, 6.7±0.15, 6.53±0.12 and 6.53±0.25 ($g/m^2/day$) for HCE-2, HCG-2, HLE-2 and HLG-2 were observed.

This shows that, maize crops have reached maturity stage and absorption of moisture and nutrients stored for grain filling. The mean plants' growth rate for treatments with HCE-2, HLE-2 and HLG-2were not significantly difference while HCG-2 differed significantly

($p < 0.05$) at 60th day and performed better compared to others hydrogels (see appendix 4F). This indicates that HCG-2 has high potential capacity of absorbing large amount of moisture and nutrients which were availed during water stress periods.

Figure 4.7.6(b) shows the results of the dosage effect of the growth period on mean crop growth rate using 30 kg/ha of HCE-2, HCG-2, HLE-2 and HLG-2 hydrogels.

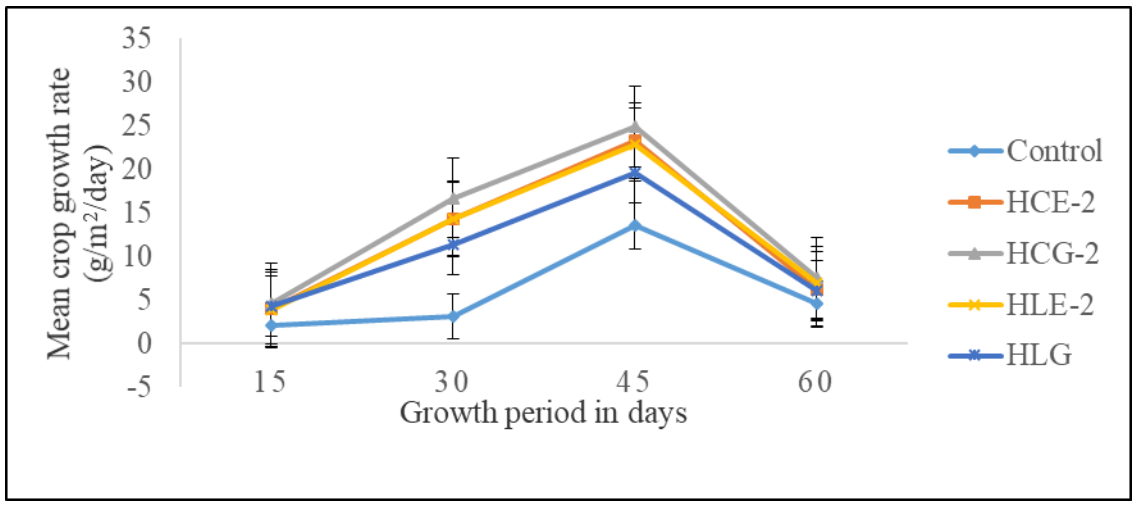

Figure 4.7.6(b): Effect of super absorbent hydrogels dose (30 kg/ha) on crop growth rate ($g/m^2/day$) when HCG-2, HLE-2, HLG-2 and HCE-2 hydrogels were applied

Figure 4.7.6(b) showed that Plots treated with 30 kg/ha of the hydrogel registered increased mean growth rate up to 45th day followed by decreased to the 60th day and differed significant ($p < 0.05$) as hydrogel varied and as compared to control. The mean crop growth rate increased to 23.30±0.10, 24.90±0.20, 22.83±0.35 and 19.57±0.21 ($g/m^2/day$) for HCE-2, HCG-2, HLE-2 and HLG-2. Mean plant growth rate for treatment of HCG-2 and HLG-2 differed significantly ($p < 0.05$) while HCE-2 and HLE-2 showed no significant difference ($p > 0.05$) at 45th day. On the other hand, results showed

decreased mean growth rate between 45th and 60th day of 6.27±0.15, 7.60±0.17 6.93±0.15 and 6.07±0.15 (g/m^2/day) for HCE-2, HCG-2, HLE-2 and HLG-2.

The mean growth rate for treatments with HCE-2 and HLG-2 showed no significantly difference ($p > 0.05$) while those with HCG-2 and HLE-2 differed significantly ($p < 0.05$) at 60th day of growth period. The increased growth rate may be due to availability of moisture and nutrients which are released during growth period while decrease in growth rate shows the crops have reached maturity rate. In addition, the results indicate that HCG-2 performed better compared to other hydrogels (appendix 4F). This revealed that HCG-2 has capacity of absorbing large quantity of water due to its crystallinity structure.

Figure 4.7.6c shows the results of dosage effect of growth period on mean crop growth rate using 45 kg/ha of HCE-2, HCG-2, HLE-2 and HLG-2 hydrogels.

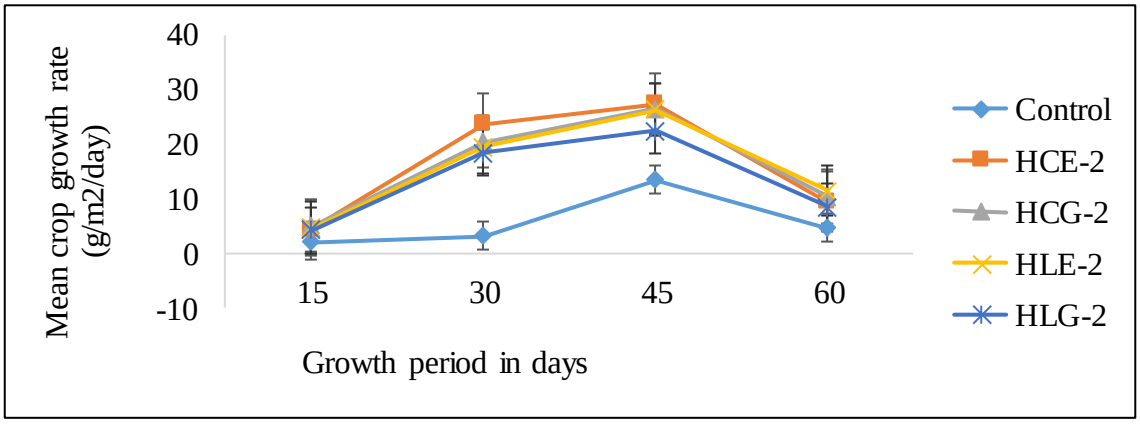

Figure 4.7.6(c): Effect of super absorbent hydrogels dose (45 kg/ha) on crop growth rate (g/m^2/day) when HCG-2, HLE-2, HLG-2 and HCE-2 hydrogels were applied

Figure 4.7.6(c) indicates that treatments of plots with 45 kg/ha of HCE-2, HCG-2, HLE-2 and HLG-2 super absorbent hydrogel increased the mean growth rate of maize plant up to 45th day followed by decrease at 60th day. The mean growth rate at 45 days were 27.37±0.32, 26.53±0.21 26.37±0.12, and 22.50±0.20 for HCE-2, HCG-2, HLE-2 and HLG-2 then decreased to 9.40±0.20, 10.40±0.27, 11.50±0.20 and 8.47±0.21, respectively. The results differed significantly ($p < 0.05$) as the type of hydrogel applied varied and as compared to control while application of HCG-2 performed better compared to other hydrogels (appendix 4F). This may be due crystalline structure with rigid pore, facilitating high water absorption rate and release it during dry periods of growth rate. Figure 4.7.6(d) shows effect of growth period on the mean crop growth rate using 60 kg/ha.

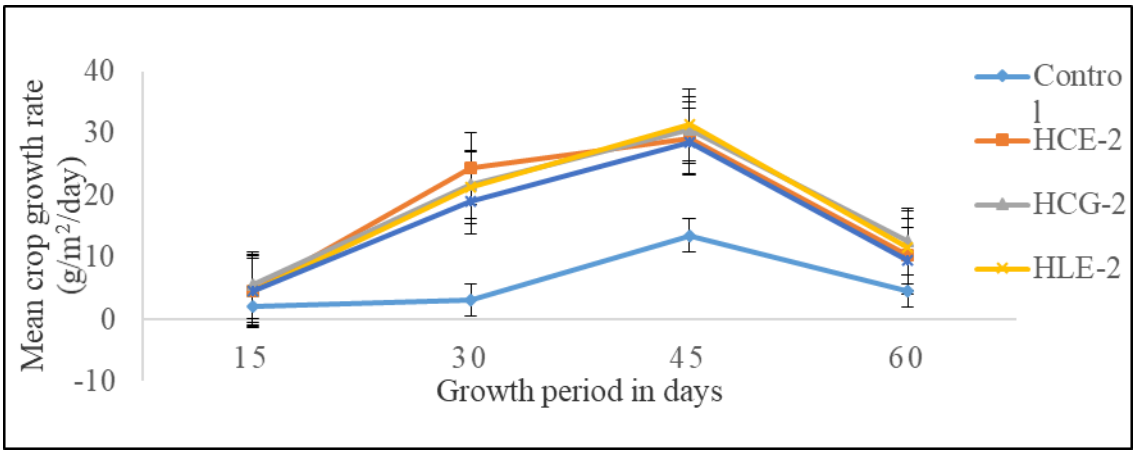

Figure 4.7.6(d): Effect of super absorbent hydrogels dose (60 kg/ha) on crop growth rate (g/m^2/day) when HCG-2, HLE-2, HLG-2 and HCE-2 hydrogels were applied

There was gradual increase in rate of crop growth rate up to 45th day and then a decrease Figure 4.7.6(d). The maximum mean growth rates were 29.17±0.15, 30.50±0.20, 31.37±0.21 and 28.63±0.31 at 45 days for HCE-2, HCG-2, HLE-2 and HLG-2 hydrogels

respectively. The plants mean crop growth rate for treatments with HCE-2 and HLG-2 were not significantly different ($p > 0.05$) while those with HCG-2 and HLE-2 differed significantly ($p < 0.05$) at 45 days of growth period (appendix 4F). Progressive decrease in growth rate was noted from 45^{th} day attaining minimum value at 60^{th} day of 10.40±0.20, 12.53±0.21, 11.60±0.30 and 9.47±0.31 for HCE-2, HCG-2, HLE-2 and HLG-2 hydrogels, respectively.

This shows that maize crops have reached maturity stage and no more growth rate despite availability of moisture and nutrients in the soil. The results revealed that super absorbent hydrogel HCG-2 performed better as compared to other hydrogels. Super absorbent hydrogels retainability of moisture and nutrients around root zone increases root length which increases rate of mineral absorption thus facilitating fast growth while decreased rate of growth indicates the plants had reached maturity stage (Dexter and Miyamoto 1995; Sendur *et al*., 2001).

4.8 Effects of super absorbent hydrogel on post-harvest parameters

The performances of the dosage of HCE-2, HCG-2, HLE-2, and HLG-2 super absorbent hydrogels were investigated through the determination of the mean number of cobs per plant, length of cob, the girth of cob, weight of grains per cob, weight of grain cop and shelling percentage compared to control. Maize plants under investigation were grown under similar conditions but at a varying dosage of the hydrogels ranging from 0 15, 30, 45, and 60 kg/ha. The yield parameters under investigation were obtained in triplicate

then the mean was determined followed by the dosage effect of HCE-2, HCG-2, HLE-2, and HLG-2 hydrogels compared to control.

4.8.1 The effect of hydrogels on number of Cob per plant

This section was to investigate the effect of super absorbent hydrogels HCE-2, HCG-2, HLE-2, and HLG-2 on the mean number of cobs of maize plants grown under similar conditions but at a varying dosage of hydrogels in the range from (0, 15, 30, 45 and 60 kg/ha. The results of the findings are presented in figure 4.8.1

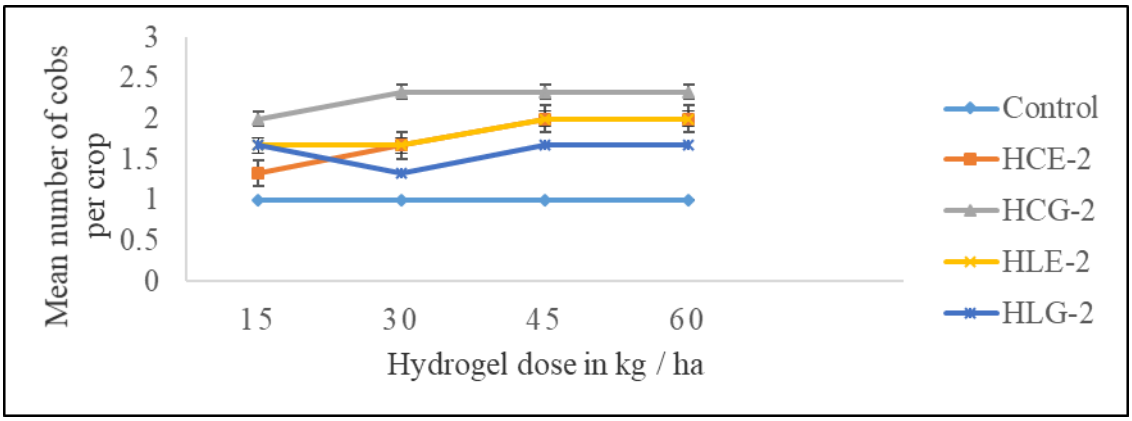

Figure 4.8.1: The effect of dosage (kg/ha) of hydrogels on the mean number of maize cobs per plant

Figure 4.8.1 show that there is a gradual increase in the mean number of cobs per maize plant as the treatment dosage of hydrogels increased and show no significant difference ($p > 0.05$) as compared to control (appendix 5A). The average of the number of cobs increased from 1.33±0.58 to 2.00±0.00, 2.00±0.00 to 2.33±0.58, 1.67±0.58 to 1.67±0.58, and 1.67±0.58 to 1.67±0.58 for HCE-2, HCG-2, HLE-2 and HLG-2, respectively as applied dosage of hydrogels increases from 15 to 45 kg/ha. The mean number of cobs for plants treated with HCE-2, HCG-2 and HLE-2 were not significantly different ($p > 0.05$)

while HLG-2 differed significantly ($p < 0.05$) when 60 kg/ha of hydrogel was applied (Appendix 5A).

The results indicated that HCG-2 performed better compared to other superabsorbent hydrogels. The increase in the number of cobs is due to the presence of moisture in the root zone of maize crop during dry sessions, which increases with the dosage of hydrogel applied. The super absorbent hydrogel increases the turgor pressure inside the plant, by providing the adequate amount of water and nutrients as required by the plant, this led to an increase in number of cobs per plant (Al-Harbi *et al*., 1999; Yazdani *et al*., 2007).

4.8.2 The effect of hydrogels on number of Grains per cob

The effect of super absorbent hydrogels (HCE-2, HCG-2, HLE-2 and HLG-2) on the mean number of grains per cob was investigated at varied doses (0, 15, 30, 45 and 60 kg/ha) and results were presented in figure 4.8.2.

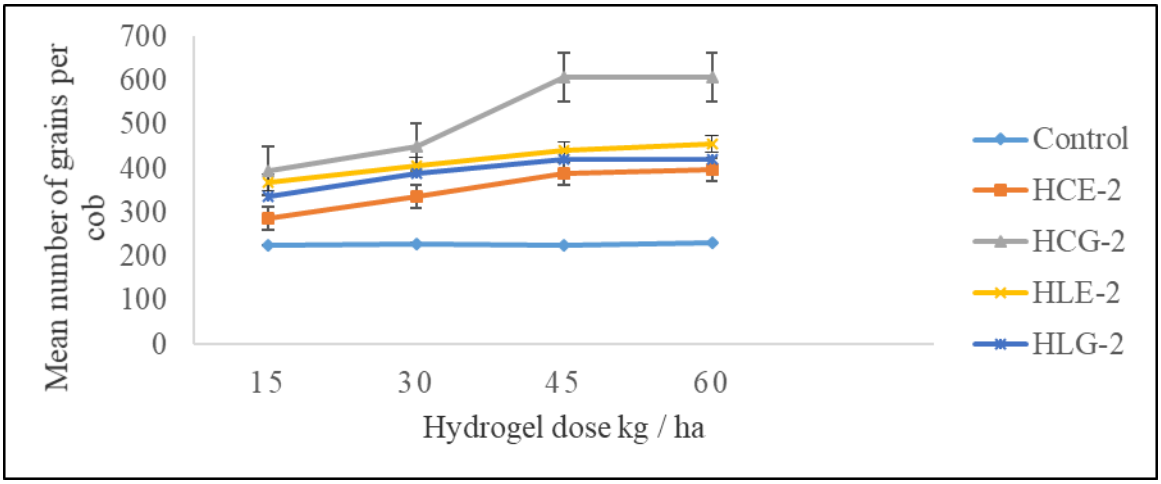

Figure 4.8.2: The effect of dosage (kg/ha) of hydrogels on mean number of grains per cob

The results presented in figure 4.8.2 show that the mean number of grains per cob increases with an increase in the dosage of hydrogel applied. The mean number of grains per cob for maize plants increased from 286.00±7.55 to 397.00±4.58, 394.33±2.52 to 607.33±5.13, 367.67±3.51 to 455.67±4.51, and 335.33±6.51 to 419.67±3.51 for HCE-2, HCG-2, HLE-2 and HLG-2 as dosage increases from 15 to 60, kg/ha respectively. The plant's mean number of grains per cob for all treatments with super absorbent hydrogels differed significantly ($p < 0.05$) when 60 kg/ha was applied and compared to that of control. Plants treated with HCG-2 were superior over others by recording 607.33±5.13 when 60 kg/ha of the hydrogel was applied (Appendix 5B). This shows that increasing the dosage of the hydrogel increases water absorption capacity during rain sessions and avail the water during dry period which occurs between 35 to 55 days after planting. This ensure high moisture content percentage in the crops leading to improved grain filling and maturity, increasing grain yields (Khadem *et al*., 2010).

4.8.3 The effect of hydrogels on girth of the Cob (cm)

The effect of super absorbent hydrogels (HCE-2, HCG-2, HLE-2 and HLG-2) on the mean girth of cob was investigated at varied doses (control, 15, 30, 45 and 60 kg/ha) and the results are presented in figure 4.8.3.

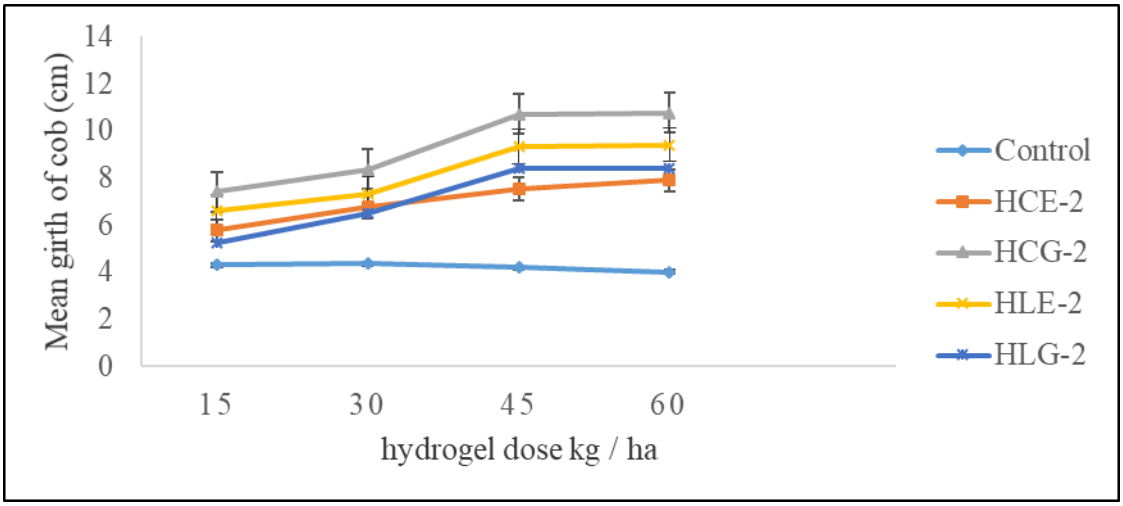

Figure 4.8.3: The effect of dosage (kg/ha) of hydrogels on mean girth of the cob (cm)

Results in figure 4.8.3 show that as the applied dose of super absorbent hydrogel increases from 15 to 60 kg/ha, the mean diameter of the cob increases from 5.77±0.15 to 7.90±0.10, 7.40±0.20 to 10.77±0.06, 6.60±0.20 to 9.40±0.20, and 5.23±0.06 to 8.40±0.10 cm for HCE-2, HCG-2, HLE-2 and HLG-2, respectively. The mean diameter of the plants treated with hydrogels differed significantly ($p < 0.05$) as compared to control (Appendix 5C). The results showed that HCG-2 recorded a higher mean diameter of the cob as compared to other types of hydrogel. The positive impact on mean girth diameter as the dosage of hydrogels increases may be associated with availability of moisture from hydrogel during flowering and grain filling stage which was normally characterized by dry period (Khadem *et al*., 2010).

4.8.4 The effect of hydrogels on cob length (cm)

The effect of super absorbent hydrogels (HCE-2, HCG-2, HLE-2 and HLG-2) on the cob length was investigated at varied doses (0, 15, 30, 45 and 60 kg/ha) and results are presented in figure 4.8.4.

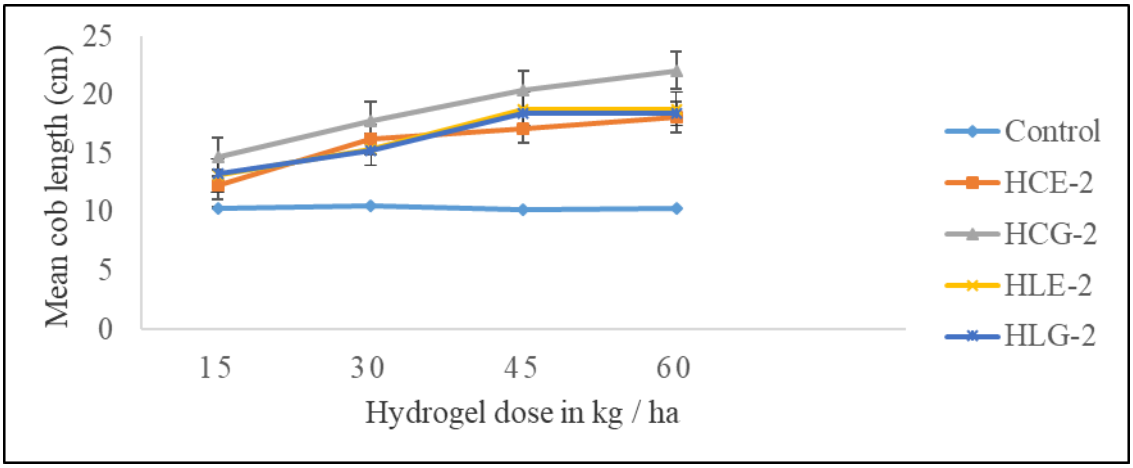

Figure 4.8.4: The effect of dosage (kg/ha) of hydrogels on mean cob length (cm)

Results in figure 4.8.4 revealed that as the applied dosage of HCE-2, HCG-2, HLE-2 and HLG-2 super absorbent hydrogel increases from 15 to 60 kg/ha, the mean cob length of maize plant increases. The highest mean cob length of the maize plants treated with 60 kg/ha of HCE-2, HCG-2, HLE-2, and HLG-2 were 18.10± 0.27, 22.10±0.10, and 18.80±0.17 and 18.43±0.12 cm. The plant cob length for plots treated with HCE-2 and HCG-2 differed significantly ($p < 0.05$) while those with HLE-2 and HLG-2 were not significantly different ($p > 0.05$) (Appendix 5D). Results showed that plots treated with super absorbent hydrogel HCG-2 performed better as compared to other super absorbent at different hydrogels dosage. The results showed significant difference ($p < 0.05$) in cob length between the plots treated with hydrogels and the control (appendix 5D). This indicates that hydrogel application influenced length of cob positively due to the constant supply of water to maize roots during flowering and grain filling stage (Hossain, 2009; Niazuddin *et al*., 2002).

4.8.5 The effect of hydrogels on grains weight per cob (g)

The effect of super absorbent hydrogels (HCE-2, HCG-2, HLE-2 and HLG-2) on the grains weight per cob was investigated at varied doses (0 15, 30, 45 and 60 kg/ha) and results are presented in figure 4.8.5.

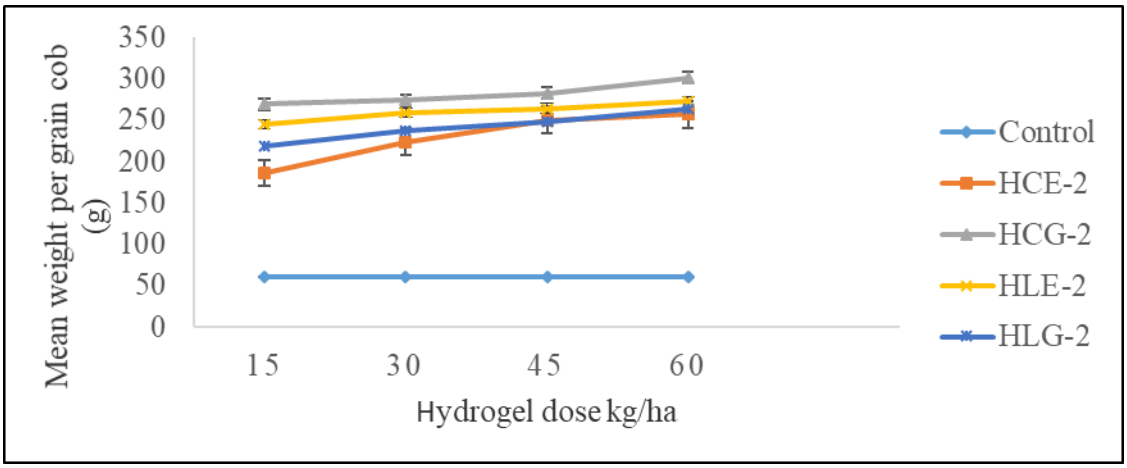

Figure 4.8.5: The effect of dosage (kg/ha) of hydrogels on cob grain weight per cob (g)

Results in figure 4.8.5 revealed that there was a progressive increase of the grain average mean weight per cob as the dosage of different types of hydrogel applied increases. The highest average mean recorded were 257.13±0.57, 301.50±1.02, 272.33±1.03, and 263.13±0.74 g for HCE-2, HCG-2, HLE-2 and HLG-2, respectively. The differed significantly ($p < 0.05$) as compared to that of control on plots treated with 60 kg/ha (appendix 5E).

Photosynthesis leads to synthesis of carbohydrates which is supplied during grain filling, high moisture content protects the grains from abnormal external temperature and bird damage leading to increased grain yield per cob (El-Hady *et al*. 2006). Application of hydrogels in the soil provides enough supply of water and essential nutrients to maize

crop during dry sessions of their growth leading to improved number grain per cob (Sivalapan, 2006). Plots applied with HCG-2 hydrogel yielded a higher number of grains per cob compared to other plots with HCE-2, HLE-2 and HLG-2. This may be attributed to more hydrophilic groups and pore networks in HCG-2 hydrogel compared to other hydrogels.

4.8.6 The effect of hydrogels on weight of the cob (g)

The effect of super absorbent hydrogels (HCE-2, HCG-2, HLE-2 and HLG-2) weight of the cob was investigated at varied doses (0l, 15, 30, 45 and 60 kg/ha) and results are presented in figure 4.8.6

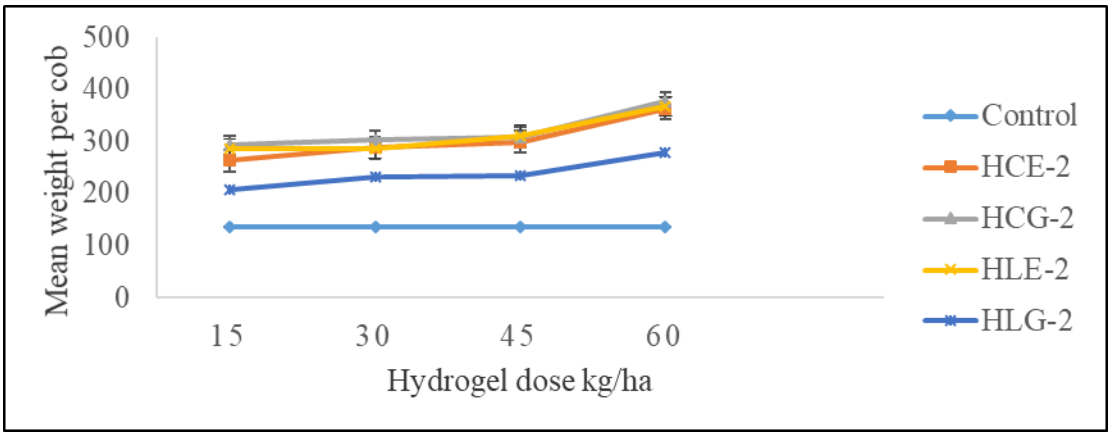

Figure 4.8.6: The effect of dosage (kg/ha) of hydrogels on mean weight of the cob (g)

Figure 4.8.6 shows that; average mean of the cob weight increases as the dosage of applied hydrogels increases from 15 to 60 kg/ha. Plots applied with HCG-2 recorded the highest mean cob weight of 376.13±0.76 g followed by HLE-2, HCE-2 and HLG-2 with 367.00±0.20, 363.00±0.56 and 279.13±0.25 g, respectively. The mean cob weight per maize plant was affected by the amount and the type of hydrogel applied and differed

significantly ($p < 0.05$) as compared to control (Appendix 5F). In addition, increased cob weights were due to the availability of water, nutrients and photo assimilates in the soil and especially during flowering stage (Sendure *et al*., 2001). The application of hydrogel polymer in the soil was able to absorb moisture during rain and release them to the soil during stress conditions (Sendure *et al*., 2001). From the results, it's clear that hydrogel polymer HCG-2 has good water absorption ability due to the presence of hydroxyl and carboxylate groups in the structure.

4.9 The effect of hydrogels on shelling %

The effect of super absorbent hydrogels (HCE-2, HCG-2, HLE-2 and HLG-2) on the shelling percentages were investigated at varied doses (control, 15, 30, 45 and 60 kg/ha) The results are presented in figure 4.9.1.

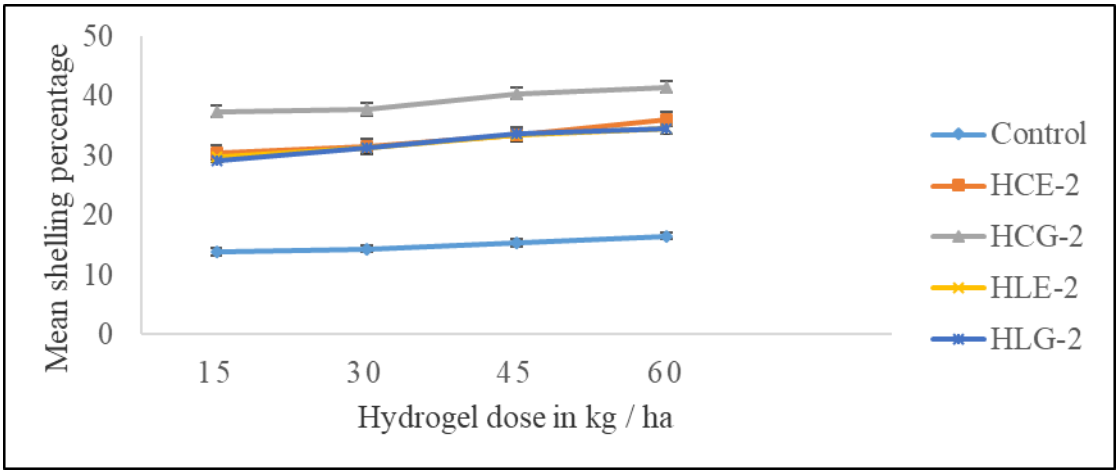

Figure 4.9.1: The effect of dosage (kg/ha) of hydrogels on weight percentage shelling

Figure 4.9.1 revealed that the mean shelling percentage of maize plants increased with increased hydrogel polymer dosage. The highest mean shelling percentage attained on

plots treated with 15 kg/ha of SAHs were found to be 44±021, 51.43±0.31, 58.43±0.47, 50.40±0.17 and 49.13±0.31 for (control, HCE-2, HCG-2, HLE-2 and HLG-2), respectively. The mean shelling percentages of treatments with HCE-2 and HCG-2 of hydrogels were significantly different ($p < 0.05$) while those treated with HLE-2 and HLG-2 were not significantly different ($p > 0.05$ (appendix 6E). At the treatment with 60 kg/ha of SAHs the shelling percentage increased to 44.70±0.17, 70.43±0.31, 76.47±0.21, 65.03±0.38, and 62.23±0.15 % for (control, HCE-2, HCG-2, HLE-2 and HLG-2) The mean shelling percentage treatments with HCE-2 and HCG-2 of hydrogels were significantly different ($p < 0.05$) while those treated with HLE-2 and HLG-2 were not significantly different ($p > 0.05$) (appendix 6E), respectively. Enough water supply in the soil results in an increased growth rate, high yield and high shelling percentage (Huttermann *et al*., 1999). Hydrogel polymers contain hydrophilic groups which are responsible for water absorption. Thus, HCG-2 SAH performed better than all the other super absorbents at different hydrogel dosage studies (appendix 6E).

4.10. The effect of super absorbent hydrogels dose on Yield and harvest index

4.10.1 The effect of hydrogels on grain yield (kg/ha)

The effect of super absorbent hydrogels (HCE-2, HCG-2, HLE-2 and HLG-2) on the grain yield in kg/ha was investigated at a varied doses (0, 15, 30, 45 and 60 kg/ha) The results are presented in figure 4.10.1

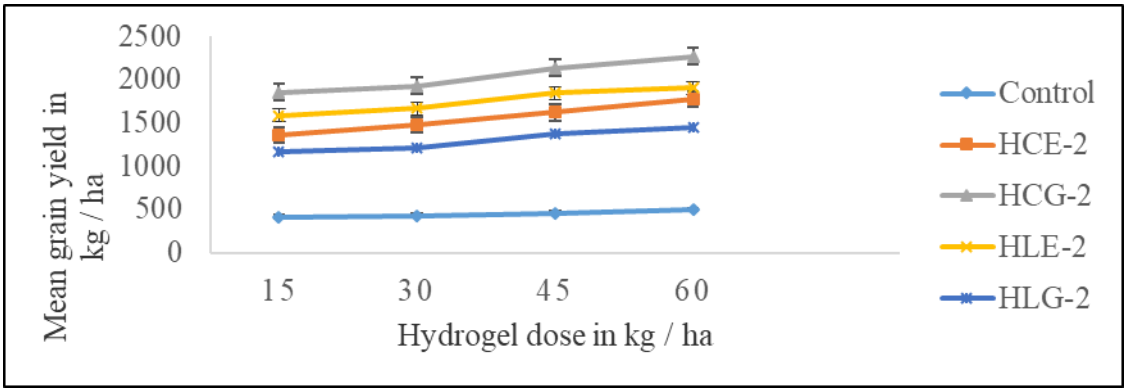

Figure 4.10.1: The effect of dosage (kg/ha) of hydrogels on mean grain yield (kg/ha)

Results in figure 4.10.1, shows that HCE-2, HCG-2, HLE-2 and HLG-2 super absorbent hydrogels significantly influenced the mean grain yield of maize plant (kg/ha) which is a function of cob length, cob weight and the number of grain rows per cob. Data indicates that as the dosage of applied hydrogel increases from 15 to 60 kg/ha, mean grain yield in kg/ha increased and were significantly difference ($p < 0.05$) as the applied dosage increases. The results increased from 1362±5.58 to 1780.13±3.42, 1855.67±4.38 to 2272.83±3.72, 1589.60±3.05 to 1905.80±3.44 and 1165.43±4.62 to 1448.93±3.97 for HCE-2, HCG-2, HLE-2 and HLG-2, respectively. The mean grain yields on plots treated with varying type of hydrogel were found significantly different ($p < 0.05$) as the type of hydrogel and dosage applied varied as well as compared to control which increased from 415.17±3.82 to 495.33±7.80 (Appendix 6A). This implies that super absorbent hydrogel HCG-2 performed better as compared to other super absorbent at different hydrogel dosages. This may be concluded that addition of hydrogel in the soil compensated for low water application in the soil during dry growth sessions resulting to increased grain yield due to the availability of stored moisture by hydrophilic polymer (Silberbush *et al*., 1993; Zhang *et al*., 2005).

4.10.2 The effect of hydrogels on stover yield (kg/ha)

The effect of super absorbent hydrogels (HCE-2, HCG-2, HLE-2 and HLG-2) on the stover yield in kg/ha was investigated at varied doses (0, 15, 30, 45 and 60 kg/ha). The results are presented in figure 4.10.2.

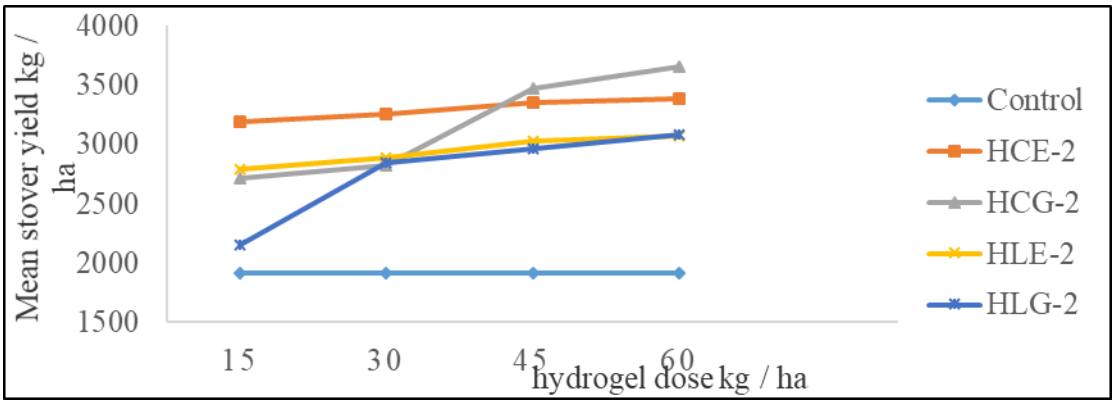

Figure 4.10.2: The effect of dosage (kg/ha) of hydrogels on mean Stover yield (kg/ha)

Figure 4.10.2, it can be deduced that increasing super absorbent hydrogel dosage increased the stover yield of maize DH - 02 per hectare. The average mean of stover yield on plots applied with HCE-2, HCG-2, HLE-2 and HLG-2 increased from 3191.57±4.84 to 3391.33±2.81, 2717.93±2.06 to 3662.83±3.98, 2787.53±3.15 to 3078.73±1.96, and 2152.23±4.23 to 3085.50±0.66, kg/ha respectively as the dosage of hydrogel applied increased from 15 to 60 kg/ha. The mean stover yield in kg/ha were significantly different ($p < 0.05$) as the dose and type of hydrogel applied varied as well as compared to control (Appendix 6B). The results indicate that HCG-2 super absorbent hydrogel performed better than other hydrogels. This may be attributed to the high rate of soil water retention and preservation ability increased with increasing hydrogel polymer application. The improved soil moisture results to a fast rate of maize growth leading to early maturity with increased Stover yield (Nazrali *et al*, 2010).

4.10.3 The effect of hydrogels on cob yield (kg/ha)

The effect of super absorbent hydrogels (HCE-2, HCG-2, HLE-2, and HLG-2) on the cob yield in kg/ha was investigated at a varied doses (0, 15, 30, 45, and 60 kg/ha). The results are presented in figure 4.10.3

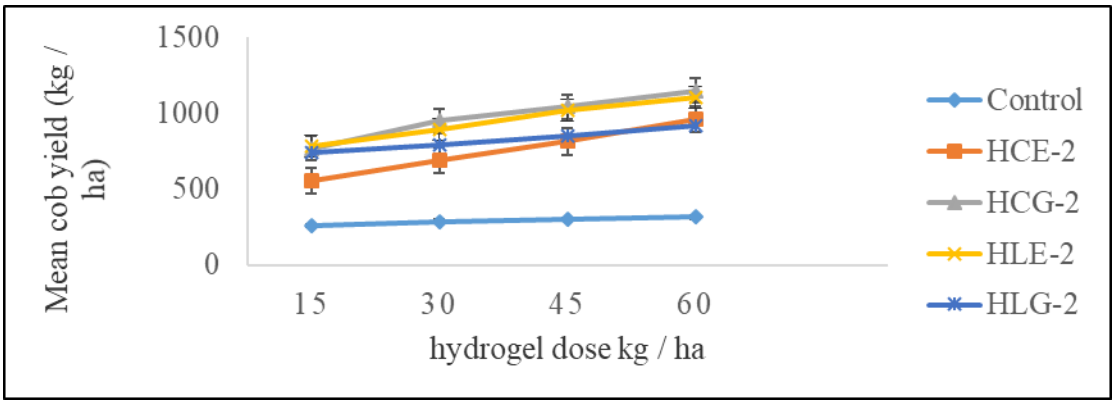

Figure 4.10.3: The effect of dosage of hydrogels (kg/ha) on the mean cob yield (kg/ha)

From figure 4.10.3 it's noted that type of hydrogel significantly influenced mean cob yield per hectare. As the hydrogel quantity applied in the soil increases from 15 to 60 kg/ha corresponding increase in mean cob yield also increases. Mean cob yield in kg/ha of maize plants treated with 15 kg/ha of HCE-2, HCG-2, HLE-2, and HLG-2 were found to be 556.53±1.32, 770.40±1.21, 785.67±0.50, and 745.60±0.98 kg, respectively. The results were found significantly different ($p < 0.05$) as type of hydrogel varies and as compare to those of control with 260.90±1 kg. These mean cob yields increased to 962±1.27, 1150.53±1.12, 1108.67±1.06, and 918.43±1.15 kg for treatments with 60 kg/ha of hydrogel, respectively, which showed significantly different ($p < 0.05$) as compared with control with 316.37±1.05 kg. The results revealed that HCG-2 hydrogel performed better than other super absorbent hydrogels (Appendix 6C). This may be due to water

availability, provided by hydrogel application to maize crops at all stages of growth catalyzing increasing cob growth rate (El-Hady *et al*., 2006).

4.10.4 The effect of hydrogels on biological yield (Kg/ha)

The effect of super absorbent hydrogels (HCE-2, HCG-2, HLE-2 and HLG-2) on the biological yield was investigated at a varied doses (0, 15, 30, 45, and 60 kg/ha) The results are presented in figure 4.10.4

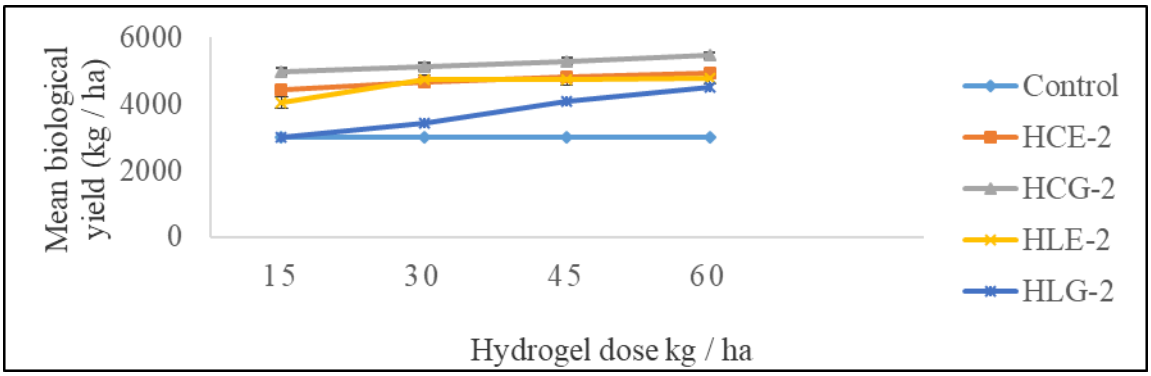

Figure 4.10.4: The effect of dosage (kg/ha) of hydrogels on mean biological yield (kg/ha)

From the figure 4.10.4, it is clear that biological yield of maize DH-02 increased with increased dosage of each hydrogel to the soil. The mean biological yield in kg/ha of maize treated with 15 kg/ha of HCE-2, HCG-2, HLE-2 and HLG-2 was found to be 4441.53±1.19, 4956.77±0.90, 4055.77±0.61, and 2988.30±1.08 kg/ha, respectively. The results differed significantly ($p < 0.05$) as the type of hydrogel varies as well as with the control (appendix 6D). Upon treatment with 60 kg/ha of SAHs of HCE-2, HCG-2, HLE-2 and HLG-2, the mean biological yields increased to 4928.73±0.42, 5455.80±0.56,

4779.13±0.21 and 4503.80±0.7 kg/ha of the yield, respectively. The results were significantly different ($p < 0.05$) with the HCG-2 SAH performing better than all the other super absorbent hydrogels doses.

The positive impact revealed that superabsorbent applications in the soil especially semi-arid regions acts as miniature water storage reservoirs and prolong evaporation of water in the soil (Bhat *et al*., 2009). Availability of hydrogel in the soil improves soil texture, facilitates high rate of root growth, and increased absorption of micro and macro nutrients which are essential for healthy growth of maize crop increasing biological yield (Azevedo *et al*., 2002).

4.10.5 The effect of hydrogels on harvest index %

The effect of super absorbent hydrogels (HCE-2, HCG-2, HLE-2 and HLG-2) on the harvest index in percentage was investigated at a varied doses (0, 15, 30, 45 and 60 kg/ha) The results are presented in figure 4.10.5

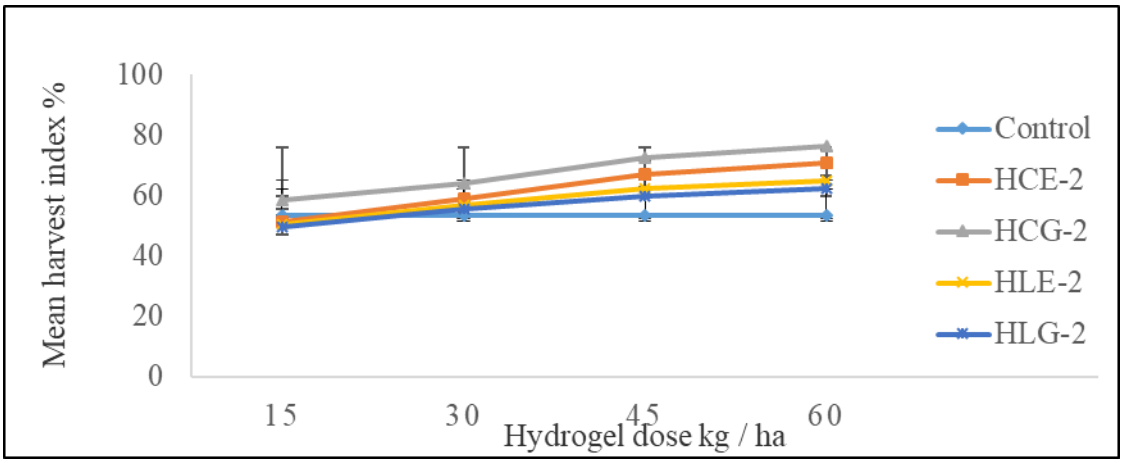

Figure 4.10.5: The effect of hydrogels dosage (kg/ha) on mean harvest index (%)

Figure 4.10.5 shows that as the dosage increased there was a significant increase in the mean harvest index of maize DH - 02 compared to control. The mean harvest index in kg/ha of maize plants treated with 15kg/ha of HCE-2, HCG-2, HLE-2 and HLG-2 was found to be 30.53±0.40, 37.20±0.46, 29.83±0.25, and 29.23±0.55 %, respectively. The mean harvest index treatments with HCE-2 and HCG-2 of hydrogels were significantly different ($p < 0.05$) while those treated with HLE-2 and HLG-2 were not significantly different ($p > 0.05$) (appendix 6E). At the treatment with 60 kg/ha of the SAHs, harvest index increased to 36.53±0.31, 41.50±0.27, 34.60±0.36, and 34.40±0.20 % for HCE-2, HCG-2, HLE-2 and HLG-2, respectively. The mean harvest index treatments with HCE-2 and HCG-2 of hydrogels were significantly different ($p < 0.05$) while those treated with HLE-2 and HLG-2 were not significantly different ($p > 0.05$) (appendix 6E), respectively. The results revealed that application of HCG-2 hydrogel to maize plants performed better than other super absorbent hydrogels. This may be attributed to the crystalline structure of the hydrogel with increased number of hydroxyl groups which facilitating high rate of water absorption, retainability as well as availing water to crop root zone when dries up.

Genetic composition of crop is the major factor determining harvest index of crop although morphological, physiological and biochemical parameters are key towards the productivity of the crop in water stress condition. This depends more on the ability of the crop production and mobilization of carbohydrates, uptake of water and nutrients from soil during cropping period (Abd *et al*., 2004). Application of superabsorbent hydrogels was able to absorb and retains water during rainy session and then releasing it to the soil

during dry seasons. This ensures continues supply of water to crops throughout growth period, leading to rapid growth parameters thus increased harvest index.

CHAPTER FIVE

CONCLUSIONS AND RECOMMENDATIONS

5.1 Conclusions

Based on the results of this study, it was concluded that synthesis of HCE-2, HCG-2, super absorbent hydrogel from activated charcoal of coconut shells with ethylenediamine and glycerol, HLE-2, HLG-2 from citric acid with ethylenediamine and glycerol respectively were successful obtained. The FT-IR spectra showed clearly, the appearance of peaks at 1568.87, 1639.48 cm^{-1} assigned to $-COO^{-}$ asymmetric stretching and bending in non-conjugated ester in HCE-2 and HCG-2. On the other hand, 1079.83, 1528 cm^{-1} assigned to $-COO^{-}$ symmetric bending and stretching for HLE-2 and HLG-2 respectively indicating successful ester formation. XRD analysis of the hydrogels showed an increased crystallinity in HCE-2, HCG-2, HLE-2 and HLG-2 polymer as compared to semi crystalline structure in HCE-1, HCG-1, HLE-1 and HLG-1. However, SEM analysis of uncross linked hydrogels showed crystalline rigid structure with fewer pores on their surface compared to the well-developed fibrous with smooth irregular pores and lamina structures in cross linked hydrogels.

Super absorbent hydrogels for maximum swelling capacity were synthesized using the following ratios. A volume ratio of CA: G: MA (5.4: 3.75: 3.75) for HLG-2, CA: EDA: MA (144: 90: 75) for HLE-2 while A mass ratio of AC: G: MA (8: 5:1) for HCG-2 and AC: EA: MA (6:5:2) for HCE-2. The hydrogels prepared at optimum conditions showed a maximum swelling capacity of 1090, 1255, 925, 910 % for HCE-2, HCG-2, HLE-2 and HLG-2, respectively. The SAHs were subjected to a contact time of 12 hours for HCE-2 and HCG-2 while HLE-2 and HLG-2 of 6 hours in 500 mL deionized water.

The increase in dosage of superabsorbent hydrogel applied, progressively increased growth and yield parameters of maize grown in semi-arid region. Maximum growth and yield parameters were recorded on application of 60 kg/ha of hydrogel. HCG-2 superabsorbent hydrogel performed better with harvest index of 87.5 % followed by HLE-2, HLG-2 and HCE-2 with 81.6, 72.4 and 66.53 %, respectively when 60 kg/ha of hydrogel were applied. The results differed significant compared to control with 53.43 % harvest index. All the super absorbent hydrogels prepared were found to be efficient in maize growing in a semi-arid region as determined from plant growth and yield parameters measured. They were able to support plant growth during dry periods and especially flowering stage The growth and yield parameters were found to be significantly influenced by type and dose of super absorbent hydrogels. The highest parameters were recorded at 60 kg/ha of SAHs dose.

5.2 Recommendations

5.2.1 Recommendation from this work

i. Activated charcoal and citric acid should be used as monomeric units for synthesizing hydrogels

ii. Super absorbent hydrogels HCE-2, HCG-2, HLE-2 and HLG-2 have potential application in agriculture owing to their high swelling capacities.

5.2.2 Recommendation for further research

i. The HCE-2, HCG-2, HLE-2 and HLG-2 super absorbent hydrogels have high water absorption capacity. However, more crops should be subjected to such trials using the hydrogels.

ii. Studies should be conducted on the efficacy of the HCE-2, HCG-2, HLE-2 and HLG-2 super absorbent hydrogels on absorption capacity and release of essential nutrients required for crop growth.

iii. Studies should be done using different types of cross linkers to find out whether the water absorption ability of the hydrogels can be improved.

iv. Further field study is needed to determine optimum dosage for maximum growth and yield parameters for maize plant by applying dosages above 60kg/ha

v. Studies should be conducted on the recycling and re-usability of the super absorbent hydrogels.

vi. Further experimentation is needed to determine dosage of the hydrogel for maize crop under different types of soil and climate condition.

vii. Studies should be conducted on economic, viability and sustainability of hydrogels use.

viii. More studies are required to establish the environmental safety of the hydrogels and their biodegradability as well as their degradation products.

ix. Pilot studies are required before they can be recommended to use in agriculture

x. studies should be conducted on shrinking rate of super absorbent hydrogels

REFERENCES

Abd, El-Rehim, H., Hegazy, E. and Abd, El-moody H. (2004). Radiation synthesis of hydrogels to enhance sandy soils water retention and increase plant performance. *Journal of applied polymer science,* **93:** 1360-1371.

Abdulhameed A., Mbuvi H. M., Changamu E. O., and Maingi F. M. (2019). Microwave synthesis of carboxymethylcellulose (CMC) from rice husks. *IOSR Journal of Applied Chemistry*, **12(12)**: 33-42.

Abedi-Koupai, J. and Mesforoush, M. (2009). Evaluation of superabsorbent polymer application on yield, water, and fertilizer use efficiency in cucumber (*C*ucumis sativus). *Journal of irrigation and drainage,* **2:** 100-111.

Abedi-Koupai, J. and Sohrab, F. (2004). Effect of super absorbent application on water retention capacity and water potential in three soil textures. *Journal of science and technology of polymers,* **17:** 163- 173.

Abedi-Koupai, J., Mesforoush, M. and Sohrab, F. (2004). Effect of super absorbent polymers on soil hydraulic properties. *Proceedings of 8th national conference on hydraulic engineering. Cold coast, Australia,* 1-12.

Ahmad, K.S. (2018). Exploring the potential of Juglans regia-derived activated carbon for the removal of adsorbed fungicide Ethaboxam from soils. *Journal of Environmental monitoring Assessment*, 190, 737.

Ahmed, M. (2016). Hydrogel: Preparation, characterization, and applications. *A review. Journal Advanced technology*, **6:** 105–121.

Aikawa, K., Matsumoto, K., Uda, H., Tanaka, S., Shimamura, H., Aramaki, Y. and Tsuchiya, S. (1998). Hydrogel formation of the pH response polymer polyvinylacetal diethylaminoacetate (AEA). *International Journal of Pharmaceutics,* **167:** 97-104.

Akhtar., Mahmood, K., Malik, K., Mardan, A., Ahmad, M. and Iqbal, M. (2004). Effects of hydrogel amendment on water storage of sandy loam and loam soils and seedling growth of barley, wheat and chickpea. *Plant, soil and environment*, **50:** 463-469.

Al, E., Güçlü, G., İyim, T., Emik, S. and Özgümüş, S. (2008). Synthesis and properties of starch-graft-acrylic acid/na-montmorillonite superabsorbent nanocomposite hydrogels. *Journal of Applied Polymer Science,* **109:** 16-22.

Alemzadeh, I. and Vossoughi, M. (2002). Controlled release of paraquat from poly vinyl alcohol hydrogel. *Chemical Engineering Process*, **41:** 707–710.

Al-Harbi., A., Omran, A., Shalaby, A. and Choudhary, M. (1999). Efficacy of a Hydrophilic polymer declines with time in green house experiments. *Horticultural Science,* **34**: 223–224.

Al-Humaid A., and Moftah A. E. (2007). Effects of hydrophilic polymer on the survival of Buttonwood seedlings grown under drought stress. *Journal of Plant Nutrition,* **30(1)**: 53-66.

Allahdadi, I., Yazdani, F., Akbari, G. and Behbahani, S. (2005). Evaluation of the effect of different rates of superabsorbent polymer (superab a200) on soybean yield and yield component (glycine max l.). *3rd specialized training course and seminar on the application of superabsorbent hydrogel in agriculture*, 20- 32.

Alves, D., Gonçalves, J., Coseglio, B., Burgo, T., Dotto, G., Pinto, L. and Cadaval, T. (2019**)**. Adsorption of phenol onto chitosan hydrogel scaffold modified with carbon nanotubes. *Journal of Environmental Chemical Engineering*, 7**:** 103460.

Anandkumar, J. and Mandal, B. (2012). Single , binary and ternary metal adsorption using acid-treated Aegle marmelos Correa shell: kinetic, mechanism and thermodynamic study.and Networks. *Chemical Engineering Process,* **3:** 1-27.

Aouada, F., Moura, M., Fernandes, P., Rubira, A. and Muniz, E. (2005). Optical and morphological characterization of polyacrylamide hydrogel and liquid crystal systems. *European Polymer Journal,* **41:** 2134-2141.

Azevedo, T., Bertonha, A. and Rezende, R. (2002). Levels of superabsorbent polymer, irrigation interval and coffee plant growth. *Acta Scientiarum,* **24:** 1239-1243.

Bakravi A., Ahamadian Y., Hashemi H. and Namazi, H. (2018). Synthesis of gelatin-based biodegradable hydrogel nanocomposite and their application as drug delivery agent. *Advanced Polymer Technology*, 1-11.

Barreto, A., Rosa, D., Fechine, P. and Mazzetto, S. (2011). Properties of sisal fibers treated by alkali solution and their application into cardanol based biocomposites. *Composites: Part A,* **42**: 492–500.

Basri, S., Zainuddin, N., Hashim, K. and Yusof, N. (2016). Preparation and characterization of irradiated carboxymethyl sago starch-acid hydrogel and its application as metal scavenger in aqueous solution. *Carbohydrate Polymer,* **138:** 34–40.

Bhat N., Suleiman M. and Abdal M. (2009): Selection of crops for sustainable utilization of Land and Water resources in Kuwait, *World Journal. of Agricultural, Science*., **5(2)**: 201-206.

Blackman, V. (1919). The compound interest law and plant growth. *Annual review of Botany* **33:** 353-360.

Boatright, J., Balint, D., Mackay, W. and Zajicek, J. (1997). Incorporation of a hydrophilic polymer into annual landscape beds. *journal of environmental horticulture*, **15:** 37-40.

Bouchelta, C., Medjram, M., Bertrand, O. and Bellat J. (2008). Preparation and characterization of activated carbon from date stones by physical activation with steam. *Journal of Analytical and Applied Pyrolysis* **82**: 70–77.

Bouman, B., Hengsdijk, H., Hardy, B., Bindraban, P., Tuong, T. and Ladha, J. (2002). Water-wise rice production. Proceedings of the International Workshop on Water-wise Rice Production. *Los Baños, Philippines. International Rice Research Institute, Los Baños, Philippines*, 333-336.

Bouman, B., Peng, S., Castaneda, A. and Visperas, R. (2005). Yield and water use of irrigated tropical aerobic rice systems. *Agricultural Water Management*, **74:** 87–105.

Buikliskii, V., Levchenko, V., Popov, F. and Sheremet, M. (2012). Borohydride reduction of Ag+in aqueous poly(acrylic acid-co-acrylamide) solutions. *Colloid Journal*, **74(1):** 7-11.

Busselez, R., Arbe, A., Cerveny, S., Capponi, S., Colmenero, J. and Frick B. (2012). Component dynamics in polyvinylpyrrolidone concentrated aqueous solutions. *Journal of chemical and physical Chemistry Research*, **137:** 084902.

Capanema, N., Mansur, A., De Jesus, A., Carvalho, S., de Oliveira, L. and Mansur, H. (2018). Superabsorbent crosslinked carboxymethyl cellulose-PEG hydrogels for potential wound dressing applications. *International Journal of Biological Macromolecules*, **106:** 1218–1234.

Cetinkaya1, S., Sakintuna, B., and Yurum, Y. (2003). Formation of Crystal Structure during Activated Carbone production from Turkish Elbistan Lignite. *Fuel Chemistry Division Preprints*, **48(1):** 67.

Chan A. W., Whitney P. A., and Neufeld R. J. (2009). Semisynthesis of a controlled stimuli-responsive alginate hydrogel. *Biomacromolecules*, **10**: 609-616.

Chandra, T., Mirna, M., Sudaryanto, Y. and Ismadji, S. (2009). Activated carbon from durian shell preparation and characterization. *Journal of Taiwan Institute Chemical Engineering*, **40:** 457-462.

Cheng W., Hu X., Wang D. and Liu G. (2015). Preparation and characteristics of corn straw-co-amps-co-aa superabsorbent hydrogel. *Polymers*, **7:** 2431-2445.

Çöle, G., Gök, M. and Güçlü, G. (2013). Removal of basic dye from aqueous solutions using a novel nanocomposite hydrogel: N-vinyl 2-pyrrolidone/itaconic acid/organo clay. *Water Air Soil Pollution*, **224(1760):** 1-16.

Coma V., Sebti J., Pardon P. Pichavant F. and Descahmps A. (2003). Film properties from crosslinking of cellulosic derivatives with a polyfunctional carboxylic acid. *Carbohydrate Polymers*, **51(3):** 265-271.

Coolman, R., Kanamori, T. and Kim, T. (2008) Biodegradable Polymers: Investigating the Reaction between Tartaric Acid and Glycerol" *Oregon State University.*

Cruz, H., Law, Y., Guest, J., Rabaey, K., Batstone, D., Laycock, B., Verstraete, W. and Pikaar, I. (2019). Mainstream Ammonium Recovery to Advance Sustainable Urban Wastewater Management, *Environmental Science Technology*, ***53*:** 11066-11079.

Cuadro, P., Belt, T., Kontturi, K., Reza, M., Kontturi, E., Vuorinen, T. and Hughes, M. (2015). Cross-linking of cellulose and poly (ethylene glycol) with citric acid. *Reactive and Functional Polymers,* 77-89.

Cuhadar, C. (2005). Production and characterization of Activated Carbone from Hazelnut shell and Hazelnut Husk. M.Sc. *Department of Chemical Engineering, Middle east Technical University*

Dalaran, M., Emik, S., Güçlü, G., İyim, T. and Özgümüş, S. (2009). Removal of acidic dye from aqueous solutions using poly (DMAEMA-AMPSHEMA) terpolymer/MMT nanocomposite hydrogels. *Polymer Bulletin,* **63:** 159-171.

Dalaran, M., Emik, S., Güçlü, G., İyim, T. and Özgümüş, S. (2011). Study on a novel polyampholyte nanocomposite superabsorbent hydrogels: Synthesis, characterization and investigation of removal of indigo carmine from aqueous solution, *Desalination,* **279:** 170-182.

Demitri, C., Sole, R. Del, Scalera, F., Sannino, A., Vasapollo, G., Maffezzoli, A., Nicolais, L. (2008). Novel Superabsorbent Cellulose-Based Hydrogels Crosslinked with Citric Acid. *Journal of Applied Polymer Science*, **110:** 2453–2460.

Demosthenous E, Hadjiyannakou S, Vamvakaki M, Patrickios C.2002. Synthesis and characterization of polyampholytic model networks: Effects of polymer composition and architecture. *Macromolecules*., **35:** 2252-2260.

Dexter S. and Miyamoto T. (1995). Acceleration of water uptake and germination of sugar beet seed balls by surface coatings of hydrophilic colloids. *Agronomy Journal*, **51:** 388–389.

Durrani, A. and Donald, M. (1995). Physical Characterization of Amylopectin Gels. *Polymer Gels and Networks,***3:** 1-27.

Ekezie F., Sun D., Han Z. and Chang J. (2017). Microwave-assited food processing technologies for enhancing product quality and process efficiency: A review of recent development. *Trend in Food Science and Technology*, **67**: 58-69.

El Fray, M., Pilaszkiewicz, A., Swieszkowski, W. and Kurzydlowski, K. (2007) Morphology assessment of chemically modified cryostructured poly(vinyl alcohol) hydrogel. *European Polymer Journal*, **43:** 2035-2040.

El-Amir, S., Helalia, A. and Shawky, M. (1993). Effects of acryhope and aquastore polymers on water regime and porosity in sandy soils. Egyptian. *Journal of Soil Science*, **4:** 395–404.

El-Din, H., Maziad, N. and El-Naggar A (2004). Radiation crosslinking and sorption properties of hydrogels based on 1-vinyl-2-pyrrolidone, hydroxyethyl methacrylate, and their copolymers. *Journal of Applied Polymer Science*, **91:** 3274-3280.

El-Hady O. A., Tayel M. Y., and Lofty A. A. (1981). Super gel as a soil conditioner: its effect on plant growth, enzymes activity, water use efficiency and nutrient uptake. *Acta Horticulturae,* **119(2)**: 257–265.

El-Hady, O. and Abo-Sedera, A. (2006). Conditioning effect of composts and acrylamide hydrogels on a sandy calcareous soil. II - Physico-bio-chemical properties of the soil. *International Journal of Agriculture and Biology*, **8:** 876-884.

Esmeraldo, M., Barreto, A, Freitas, J, Fechine, P, Sombra, A. Corradini, E., Mele, G, Maffezzoli, A. and Mazzetto, S. (2010). Dwarf-green coconut fibers: a versatile natural renewable raw bioresource. Treatment morphology and physicochemical properties. *Journal of Bioresources***, 5(4):** 2478–2501.

Farris, S., Schaich, K., Liu, L., Piergiovanni, L., and Yam, K. (2009). Development of polyion-complex hydrogels as an alternative approach for the production of bio-based polymers for food packaging applications: a review. *Trends in Food Science & Technology*, **20(8):** 316-332.

Ferreira, R., Sousa, F,. Oliveira, V., Neto, S., Basílio, P. and Fechine, A. (2012). Biomass adsorbent for Removal of Toxic Metal Ions From Electroplating Industry Wastewater. *Posted in http://www.interchopen.com. Accessed on 5/10/2014.*

Ferruti P., Bianchi S., Ranucci E., Chiellini F. and Piras A. (2005). Novel agmatine-containing poly (amidoamine) hydrogels as scaffolds for tissue engineering. *Biomacromolecules.* **6**: 2229–2235.

Filho, C; Bueno, P; Matsushita, A; Rubira, A; Muniz, E Durães, L.; Murtinho, D and Valente, A (2018). Synthesis, characterization and sorption studies of aromatic compounds by hydrogels of chitosan blended with _-cyclodextrin- and PVA-functionalized pectin. *Chemical Engineering Journal*, **8:** 14609–14622.

Flannery, R. and Busscher, W. (1982). use of a synthetic polymer in potting soils to improve water holding capacity. *communications in soil science and plant analysis,* **13 (2):** 103 -111.

Foo, K. and Hameed, B. (2010). Insights into the modeling of adsorption isotherm systems. *Chemical Engineering Journal*, **156:** 2–10.

Gandini, A., Lacerda, T., Carvalho, A. and Trovatti, E. (2016). Progress of Polymers from Renewable Resources: Furans, Vegetable Oils, and Polysaccharides. *Chemistry Review*, **116(3):** 1637-1669.

Gao D., Xu H., Philbert M. and Kopelman R. (2007). Ultrafine hydrogel nanoparticles: synthetic approach and therapeutic application in living cells. *Chemical Engineering Journal*, **46:** 2224–2227.

Ghaiour, F. (2000). effect of moisture absorbent materials on soil water holding potential. *ministry of agriculture. Isfahan research, center of animal and natural resources. Isfahan, Iran*, 515-517.

Gharekhani, H., Olad, A., Mirmohseni, A. and Bybordi, A. (2017). Superabsorbent hydrogel made of NaAlg-g-poly(AAco- AAm) and rice husk ash: Synthesis, characterization, and swelling kinetic studies. *Carbohydrate Polymer*, **168:** 1–13.

Guilherme, M., Aouada, F., Fajardo, A., Martins, A., Paulino, A., Davi, M., Rubira, A. and Muniz, E. (2015). Superabsorbent hydrogels based on polysaccharides for application in agriculture as soil conditioner and nutrient carrier: A review. *European Polymer Journal*, **72:** 365-385.

Guo, X; Shi, H. and Dick, W. (2010). Compressive strength and microstructural characteristics of class C fly ash geopolymer. *Cement and Concrete Composites*, **32:** 142–147.

Gupta, V.K and Rastogi, A. (2013). Biosorption of lead from aqueous solutions by green algae Spirogyra species: kinetics and equilibrium studies. *Journal of Hazardous Materials*. **152:**407–414.

Hajimohammadi, A; Provis, J. and Van Deventer, J. (2011). The effect of silica availability on the mechanism of geopolymerisation. *Cement and Concrete Research*, **41:** 210–216.

Hammond, P., Ali, D. and Cumming, R. (2005). A system on chip digital pH meter for use in a wireless diagnostic capsule. *Biomedical Engineering*, **4:** 687-694.

Han B., Benner S. G., and Flores A. N. (2018). Evaluating impacts of climate change on future water scarcity in an intensively managed semi-arid region using a coupled model of biophysical processes and water rights. *Hydrology and Earth System Sciences Discussions*, 153.

Han, S. O. and Choi, H. Y. (2010). Morphology and surface properties of natural fiber treated with electron beam. *Microscopy: Science, Technology, Applications and Education*, **3:**1880-1887.

Harsh, D. and Gebrke, S. (1991). Controlling the swelling characteristics of temperature sensitive cellulose ether hydrogels. *Journal of controlled release*, **17:** 175-186.

Hassan, C. and Peppas, N. (2000). Structure and Morphology of Freeze/Thawed PVA Hydrogels. *Macromolecules*, ***33*:** 2472-2479.

Hayat, R. and Ali, S. (2004). Water absorption by synthetic polymer (Aquasorb) and its effect on soil properties and tomato yield. International. *Journal of Agriculture and Biology*, **6:** 998–1002.

He, X., Wu, S., Fu, D. and Ni J. (2009). Preparation of sodium carboxymethylcellulose from paper sludge. *Journal of Chemical Technology and Biotechnology*, **84**: 427-434.

Helalia A., and Letey J. (1988). Cationic polymer effects on infiltration rates with a rainfall simulator. *Soil Science Society of America Journal,* **52(1)**: 247-250.

Hennink, W. and Nostrum, C. (2002). Advanced Drug Deliveries Review. Volume 54, January 2002, 13-36. *Department of Pharmaceutics, Utrecht University*, **54:** 13–36.

Hossain M. S. (2009). Effect of deficit irrigation on yield and water productivity of maize. M.S Thesis (Agricultural. Engineering.). *Department of Irrigation and Water Management*, 26-38.

Hossain, M., Ngo, H., Guo, W. and Nguyen, T. (2012). Biosorption of Cu (II) from water by banana peels based biosorbent. experiments and models of adsorption and desorption. *Journal of Water Sustainability*, **2(1):** 87–104.

Hu, C., Delgado, J., Zhang, X. and Ma, L. (2005). Assessment of groundwater use by wheat (Triticum aestivum L.) in the Luancheng Xian region and potential implications for water conservation in the northwestern North China Plain. *Journal of Soil and Water Conservation*, **60:** 80–88.

Humphreys, E., Meisner, C., Gupta, R., Timsina, J., Beecher, H., Lu, T., Singh, Y., Gill, M., Masih, I., Guo, Z. and Thompson, J. (2005). Water savings in rice-wheat systems. *Plant Production Science*, **8:** 242–258.

Huttermann, A., Zommorodi, M. and Reise, K. (1999). Addition of hydrogels to soil for prolonging the survival of Pinus halepensis seedlings subjected to drought Soil Tillage. *Journal of Soil and Water Conservation*, **50**: 295-304.

Ikada, Y., Jamshidi, K., Tsuji H and Hyon S. (2010). Stereocomplex formation between IPN hydrogel. *International Journal of biological and macromolecular*, **46(2):** 237- 244

Islam, M., Hu, Y., Mao, S., Jia, P., Eneji, A. and Xue, X. (2011). Effects of water saving superabsorbent polymer on antioxidant enzyme activities and lipid peroxidation in corn (Zea mays L.) under drought stress. *Journal of the Science of Food and Agriculture*, **91:** 813–819.

Jafari, S. and Hamid, M. (2005). A study on swelling and complex formation of acrylic acid and methacrylic acid hydrogels with polyethylene glycol. *Iran Polymer Journal*, **14:** 863–873.

Ji, H., Song, X., Shi, Z., Tang, C., Xiong, L., Zhao, W. and Zhao, C. (2018). Reinforced-Concrete Structured Hydrogel Microspheres with Ultrahigh Mechanical Strength, Restricted Water Uptake, and Superior Adsorption Capacity. *Sustainable Chemical Engineering*, **6:** 5950–5958.

Jiang, W., Saxena A., Song, B., Beveridge, T. and Myneni, S. (2004). Elucidation of functional groups on Gram-positive and Gram-negative bacterial surfaces using infrared spectroscopy. *Langmuir*, **20:** 11433–11442.

Jin, H., Hongwen, L., Kuhn, N., Xuemin, Z. and Wenying, L. (2007). Soil loosening on permanent raised-beds in arid northwest China. *Soil and Tillage Research*, **97:** 172–183.

Jyothi Alummoottil, N., Sreekumar, J., Moorthy Subramoney, N. and Sajeev Moothandaserry, S. (2010). Response Surface Methodology for the Optimization and Characterization of Cassava Starch- graft- Poly(acrylamide). *Sustainable Chemical Engineering*, **62(1):** 18-27.

Kabiri K, Omidian H, Hashemi SA, Zohuriaan-Mehr MJ. (2003). Synthesis of fast-swelling superabsorbent hydrogels: effect of crosslinker type and concentration on porosity and absorption rate. *European Polymer Journal*, **39:** 1341–1348.

Karadağ, E. and Üzüm, Ö. (2012). A study on water and dye sorption capacities of novel ternary acrylamide/sodium acrylate/PEG semi IPN hydrogels. *Polymer. Bulletin*, **68:** 1357-1368.

Karimi, A., Noshadi, M. and Ahmadzadeh, M. (2009). Effects of superabsorbent polymer (igeta) on crop, soil water and irrigation interval. *Journal of Science and Technology of Agriculture and Natural Resources*, **12:** 415–420.

Katime, I. and Mendizábal, E. (2010). Swelling Properties of New Hydrogels Based on the Dimethyl Amino Ethyl Acrylate Methyl Chloride Quaternary Salt with Acrylic Acid and 2-Methylene Butane-1,4-Dioic Acid Monomers in Aqueous Solutions. *Materials Sciences and Applications*. **1(03):** 162-167.

Khadem, S., Galavi, M., Ramrodi, S., Mousavi, M., Rousta. S and Rezvanimoghadam, P. (2010). Effect of animal manure and super absorbent polymer on corn leaf relative water content, cell membrane stability and leaf chlorophyll content under dry condition. *Australian Journal of Crop Science*, **4:** 642-647.

Khan, A., El-Toni, A. M., Alrokayan, S., Alsalhi, M., Alhoshan, M., and Aldwayyan, A. (2011). Microwave assisted synthesis of silver nanoparticles using poly-N-isopropylacrylamide/acrylic acid microgel particles. *Colloidal Surface Physicochemical Engineering Aspects*, **377:** 356-360.

Khan, M. and Lo, I. (2016). A holistic review of hydrogel applications in the adsorptive removal of aqueous pollutants: Recent progress, challenges, and perspectives. *Water Research*, **106:** 259-271.

Kim, I., Seo, S. and Moon, H. (2008). Chitosan and its derivatives for tissue engineering applications. *Biotechnology Advanced*, ***26*:** 1–21.

Koetting, M., Peters, J., Steichen, S. and Peppas, N. (2015). Stimulus-responsive hydrogels: Theory, modern advances, and applications. *Material Science Engeering Research*, **93:** 1-49.

Kojima, C., Kono, K., Maruyama, K. and Takagishi, T. (2000). Synthesis of polyamidoamine dendrimers having poly(ethylene glycol) grafts and their ability to encapsulate anticancer drugs. *Bioconjugate Chemistry,* **11:** 910-917.

Kondo T. (1997). The assignment of IR absorption bands due to free hydroxyl groups in cellulose. *Cellulose*, **4(4):** 281–292.

Kono, H. and Fujita, S. (2012). Biodegradable superabsorbent hydrogels derived from cellulose by esterification crosslinking with 1, 2, 3, 4-butanetetracarboxylic dianhydride. *Carbohydrate Polymers*, **87(4):** 2582–2588.

Kramer, P. (1988). Measurement of plant water status: Historical perspectives and current concerns. *Irrigation Science*, **9:** 275–287.

Krauklis, A., Gagani, A. and Echtermeyer, A. (2018). Near infrared spectroscopic method for monitoring water content in epoxy resins and fiber reinforced composite. *Journal of Environmental Chemical Engineering,**11***: 586–599.

Kreye, C., Bouman, B., Castaneda, A., Lampayan, R., Faronilo, J., Lactaoen, A. and Fernandez, L. (2009). Possible causes of yield failure in tropical aerobic rice. *Field Crops Research*, **111:** 197–206.

Kumar, R., Mudhoo, A., Lofrano, G. and Chandra, M. (2014). Adsorbent modification and activation methods and adsorbent regeneration: Biomass-derived biosorbents for metal ions sequestration. *Journal of Environmental Chemical Engineering*, **2:** 239-259.

Laftah W. A., Hashim S., and Ibrahim A. N. (2011). Polymer hydrogels: A review. *Polymer Plastic Technology*, **50:** 1475–1486.

Lakshmi, V. (2011). M. Tech. (Agril. Engg) Thesis, Department of Soil and Water Engineering, UAS, Dharwad, Karnataka.

Lanthong, P., Nuisin, R. and Kiatkamjornwong, S. (2006). Graft copolymerization, characterization, and degradation of cassava starch-g-acrylamide/itaconic acid superabsorbents. *Carbohydrate Polymers*, ***66*(2):** 229-245.

Li D., Yang P. and Han Y. (2004). Application effects of super absorbent polymers on grape cultivation. In G. H. Huang & S. P. Luis (Eds.), *Land and Water Management Decision Tools and Practices,* 798–803.

Li, Z. and Liu, S. (2007). Influence of slag as additive on compressive strength of fly ash-based geopolymer. *Journal of Materials in Civil Engineering*, **19:** 470–474.

Liang, S., Guo, X., Feng, N. and Tian, Q. (2009). Application of orange peel xanthate for the adsorption of Pb^{2+} from aqueous solutions. *Journal of Hazardous Material*, **170**: 425-429.

Liu, F., Wu, J., Chen, K. and Xue, D. (2010). Morphology Study by using scanning electron microscopy. *Science, Technology, Applications and Education,***3**: 1781-1792.

Liu, Y. and Chan-Park, M. (2009). Hydrogel based on interpenetrating polymer networks of dextran and gelatin for vascular tissue engineering. *Biomaterials* **30(2):**196–207.

Lu, S., Bai, S., Zhu, L. and Shan, H. (2009). Removal mechanism of phosphate from aqueous solution by coal fly ash. *Journal of Hazardous Materials* **161:** 95-101.

Luo, Y., Wei, Q., Xu, F., Chen, Y., Fan, L. and Zhang, C. (2009). Assembly, characterization and swelling kinetics of Ag nanoparticles in PDMAAg-PVA hydrogel networks. *Material Chemical. Physics*, **118(2-3):** 329-336.

Ma, J., Li, X. and Bao, Y. (2015). Advances in cellulose-based superabsorbent hydrogels. *Journal of Materials in Civil Engineering*, ***5*(73):** 59745-59757.

Mahdavinia, G., Massoumi, B., Jalili, K. and Kiani, G. (2012). Effect of sodium montmorillonite nanoclay on the water absorbency and cationic dye removal of carrageenan-based nanocomposite superabsorbents. *Journal of Polymer Research*, **19(9):** 1–13.

Mahmoudian M. and Ganji F. (2017). Vancomycin-loaded HPMC micro-particles embedded within injectable thermosensitive chitosan hydrogels. *Progamme Biomaterials*, **6:** 49–56.

Mamun Hossain S. A. A., Wang L. X., Chen T. T., and Li Z. H. (2017). Leaf area index assessment for tomato and cucumber growing period under different water treatments. *Plant Soil Environment*, **63(1)**: 461–467.

Martens P., Bryant S. and Anseth K. (2003). Tailoring the degradation of hydrogels formed from multivinyl poly (ethylene glycol) and poly (vinyl alcohol) macromers for cartilage tissue engineering. *Biomacromolecules*, **4:** 283–292.

Meng, Y. and Ye, L. (2017). Synthesis and swelling property of superabsorbent starch grafted with acrylic acid/2-acrylamido-2-methyl-1-propanesulfonic acid. *Journal Science Food Agricultural*, **97(11):** 3831-3840.

Merkel, K., Rydarowski, H., Kazimierczak, J. and Bloda, A. (2014). Processing and characterization of reinforced polyethylene composites made with lignocellulosic fibres isolated from waste plant biomass such as hemp composition. *Journal of Engineering*, **67:** 138-144.

Mikkelsen, R. (1994). Using hydrophilic polymers to control nutrient release. *F*ertilizer *Research*, **38:** 53-59.

Mikkelsen, R., Behel, A. and Williams, H. (1993). Addition of gel-forming hydrophilic polymers to nitrogen fertilizer solutions. *Fertilizer Research*, **36:** 55– 61.

Mishra, R., Datt, M., Pal, K. and Banthia, A. (2008). Preparation and characterization of amidated pectin based hydrogels for drug delivery system. *Journal Material Science: Mater Med*, **19:** 2275–2280.

Moghimi E., Fathi P., Toashih V., and Moez Ardalan M. (2011). Impact of perlite on water use efficiency and some growth components in wheat (cultivar of zarrin). *Journal of Water and Irrigation Management,* **1(2):** 31-42.

Mohamood, N., Zainuddin, N., Ahmad, M. and Tan, S. (2018). Preparation, optimization and swelling study of carboxymethyl sago starch (CMSS)–acid hydrogel. *Journal of Chemical Science*, **12:** 1–10.

Mohan, Y., Vimala, K., Thomas, V., Varaprasad, K., Sreedhar, B., Bajpai, S. and Raju, K. (2010). Controlling of silver nanoparticles structure by hydrogel networks. *Journal of Colloidal International Science.*, 3**42(1):** 73-82.

Mohanty, K., Das, D. and Biswas, M. (2005). Adsorption of phenol from aqueous solutions using activated carbons prepared from *Tectona grandis* sawdust by zinc chloride activation. *Chemical Engineering Journal,* **(115):** 121–131.

Mondal, U.K. (2011). CRIDA Annual Report (2010-11), *Central Research Institute for Dryland Agriculture, Hyderabad.*

Muna, M., Mugendi, D., Kung'u, J., Mugwe, J. and Bationo, A. (2016). *Effects of organic and mineral fertilizer inputs on maize yield and soil chemical properties in a maize cropping system in Meru South District, Kenya*. 190–192.

Naeini, A., Adeli, M. and Vossoughi M. (2010). Poly (citric acid)-block-polyethylene glycol) copolymers - new biocompatibility hybrid materials for Nano medicine. *Nano medicine: Nanotechnology, Biology, and Medicine*, **6:** 556–562.

Nagahama K., Ouchi T. and Ohya Y. (2008). Temperature-induced hydrogels through self-assembly of cholesterol-substituted star PEG-b-PLLA copolymers: an injectable scaffold for tissue engineering. *Advanced Function Materials*, **18:** 1220–1231.

Naja G., Mustin C., Volesky B. and Berthelin J. (2005). A high resolutions titrator; a new approach to studying binding sites of microbial biosorbents. *Water Research* **39:** 579-596.

Namazi, H. and Jafarirad, S. (2011). Investigation on some physicochemical properties of guest-conjugated and -incorporated hybrid organic/inorganic linear-dendritic Nano carriers. *Journal Polymer Research,* **18:** 1431–1440.

Naohara, R; Narita, K and Ikeda-Fukazawa T (2017) Change in hydrogen bonding structures of a hydrogel with dehydration. *Chemical Physical chemistry Lett,***670:** 84–88.

Nayak S., Lee H., Chmielewski J. and Lyon L. (2004). Folate-mediated cell targeting and cytotoxicity using thermoresponsive microgels. *Journal of American Chemical Society*,**126:** 10258–10259.

Nazarli, H.; Zardashti, M; Darvishzadeh, R. and Najafi, S. (2010). the effect of water stress and polymer on water use efficiency, yield and several morphological traits of sunflower under greenhouse condition. *Journal of Agriculture and Biology.* **2:** 53-58.

Niazuddin M., Talukder M., Shirazi. and Hye M. (2002). Response of maize to irrigation and nitrogenous fertilizer. *Bangladesh Journal of Agricultural Science*, **29(2):** 283-289.

Njoku, V., Islam, M.A., Asif, M. and Hameed, B (2014). Utilization of sky fruit husk agricultural waste to produce high quality activated carbon for the herbicide bentazon adsorption. *Journal of Chemical Engineering*, **251:** 183–191.

Nnadi, F. and Brave, C. (2013). Environmentally friendly superabsorbent polymers for water conservation in agricultural lands, **1(5):** 94–98.

Nyoro, J., Kirimi, L. and Jayne, T. (2010). Competitiveness of Kenyan and Ugandan maize production: Challenges for the future *Working Paper 10, Egerton University, Tegemeo Institute, Nairobi.*

Ogutunde, P., Friesen, N., van de Giesen, H. and Savenije, G. (2006). Hydro climatology of the Volta River Basin in West Africa: Trends and variability from 1901 to 2002. *Physical Chemistry Earth*, **31:** 1180–1188.

Okamoto K., Wang H., Ijyuin T., Fujiwara S., Tanaka K. and Kita H. (1999). Pervaporation of aromatic/non-aromatic hydrocarbon mixtures through crosslinked membranes of polyimide with pendant phosphonate ester groups, *Journal of Membrane Science,* **157:** 97–105.

Omidian H. and Park K. (2010) Introduction to hydrogels. In: Ottenbrite RM (ed) Biomedical applications of hydrogels handbook. *Springer, London*, 1–16.

Omri, A., Benzina, M. and Ammar, N. (2013). Preparation, modification and industrial application of activated carbon from almond shell. *Journal of engineering Chemical*, **19:** 2092–2099.

Orosz, F., Jakab, S., Losak, T. and Slezak, K. (2009). Effect of fertilizer application to sweet corn (Zea mays) grown on sandy soil. *Journal of Environmental Biology*, **30:** 933–938.

Pal K. and Pal S (2006). Development of porous hydroxyapatite scaffolds. *Journal of Material sand Manufacturing Processes,* **21:** 325-820.

Pandey, A. and Negi, S. (2015). Removal of chromium (VI) from aqueous medium using chemically modified banana peels as efficient low adsorbent. *Journal of Bioresource Technology*, **192:** 115.

Papita, S. (2010). Assessment on the removal of methylene Blue Dye using Tamarid Fruit Shell as Bio sorbent. *Springer Science and Business Media,* **213:** 287-299.

Parikh, S. and Chorover, J. (2005). FT-IR spectroscopic study of biogenic Mn oxide formation by Pseudomonas putida GB-1. *Journal of Geomicrobiology*, **22:** 207-218.

Parvathy, P. and Jyothi, A. (2012). Synthesis, characterization and swelling behavior of superabsorbent polymers from cassava starch-graft-poly(acrylamide). *Starch-Starke*, ***64*(3):** 207-218.

Parvathy, P., Jyothi, A., John, K. and Sreekumar, J. (2014). Cassava Starch Based Superabsorbent Polymer as Soil Conditioner: Impact on Soil Physico-Chemical and Biological Properties and Plant Growth. *Clean-Soil Air Water*, ***42*(11):** 1610-1617.

Passerini, N., Albertici, B., Perissuti, B. and Rodriguez, L. (2006). evaluation of melt granulation and ultrasonic spray congealing as techniques to enhance the dissolution of praziquantel. *International Journal of Pharmaceutical*, **318:** 92-102.

Pourjavadi, A. and Kurdtabar, M. (2007). Collagen-based highly porous hydrogel without any pyrogen: Synthesis and characteristics. *European Polymer Journal*, **43:** 877-889.

Ravichandran, P., Shantha, K., Panduranga, G. and Rao, K. (1997). Preparation, swelling characteristics and evaluation of hydrogels for stomach specific drug delivery. *International Journal of Pharmacy*, **154:** 89–94.

Rimmer, S. (2011). Biomedical Hydrogels: Biochemistry, manufacture and medical applications. Materials. Cambridge. *Woodhead Publishing Limited.*

Rowley J., Madlambayan G. and Mooney, D. (1999). Alginate hydrogels as synthetic extracellular matrix materials. *Biomaterials*, **20:** 45–53.

Rudzinski W. E., Dave A. M., Vaishnav U. H., Kumbar S. G., Kulkarni A. R., and Aminabhavi T. M. (2002). Hydrogels as controlled release devices in agriculture. *Designed Monomers and Polymers*, **5:** 39-65.

Sakiyama, T.; Chu, C.; Fujii, T. and Yano, T. (1993). influence of hydrogel on growth and yield of maize seedlings in sandy soil. *journal of applied polymer science*, 2021: 50.
Sannino, A., Demitri, C. and Madaghiele, M. (2009). Biodegradable cellulose-based hydrogels: Design and applications. *Materials*, ***2*(2):** 353–373.

Sannino, A., Madaghiele, M., Conversano, F., Mele, G., Maffezzoli, A., Netti, P., Ambrosio, L. and Nicolais, L. (2004). Cellulose derivative hyaluronic acid-based microporous hydrogels cross-linked through divinyl sulfone (DVS) to modulate equilibrium sorption capacity and network stability. *Biomacromolecules*, **5:** 92-96.

Santana, G., Lelis, R., Jaguaribe, E., Morais, R., Paes, J. and Trugilho, P. (**2017).** Development of activated carbon from bamboo (bambusa vulgaris) for pesticide removal from aqueous solutions. *Cerne*, **23:** 123–132.

Selling, G., Utt, K., Finkenstadt, V., Kim, S. and Biswas, A. (2015). Impact of Solvent Selection on Graft Co-polymerization of Acrylamide onto Starch. *Journal of Polymers and the Environment*, ***23*:** 294-301.

Sendur, Kumaran, S., Natarajan, S., Muthvel, I. and Sathiayamurthy, V. (2001). Efficacy of graded doses of polymers on processing quality of tomato. *Journal of Madras Agricultural*, **88:** 298-299.

Senna, A., do-Carmo, J., da-Silva, J. and Botaro, V. (2015). Synthesis, characterization and application of hydrogel derived from cellulose acetate as a substrate for slow-release NPK fertilizer and water retention in soil. *Journal of Environmental Chemical Engineering*, **3(2):** 996-1002.

Shah, B. and Jadav, P. (2012). Extractive efficacy of microwave synthesized zeolitic material for acephate equilibrium and kinetics. *Journal of the Serbian Chemical Society*, **1:** 146-146.

Shahbeig, H., Bagheri, N., Ghorbanian, S., Hallajisani, A. and Poorkarimi, S. (2013). A new adsorption isotherm model of aqueous solutions on granular activated carbon. *World Journal of Modelling and Simulation*, **9:** 243–254.

Shang J., Shao Z., and Chen X. (2008). Chitosan-based electroactive hydrogel. *Polymer*, **49(25):** 5520-5525.

Shi, Y., Li, J., Shao, J., Deng, S., Wang, R., Li, N., Sun, J., Zhang, H., Zheng, X., Zhou, D., Huttermann, A. and Chen, S. (2010). Effects of Stockosorb and Luquasorb polymers on salt and drought tolerance of. *Populus popularis Science of Horticulture,* **124:** 268-273.

Shoa-Hoseini, M., Farsi, M. and Khavari, K. (2007). Study effect of water deficit stress on yield and yield components if some corn hybrids using path analysis. *Majale danesh keshavarzi (In Persian),* **18(1):** 71–85.

Shooshtarian S., Abedi Koupai J., and Tehranifar A. (2011). Evaluation of application of superabsorbent polymers in green space of arid and semi-arid regions with emphasis on Iran. *Journal of Biodiversity and Ecological Sciences,* **1(2):** 258-269.

Silberbush, M., Adar, E. and De-malach, Y. (1993). Use of a hydrophilic polymer to improve water storage and availability to crops grown in sand dunes. i. corn irrigated by trickling. *Agricultural water management,* **23:** 303-313.

Silva, P., Sagoe, K. and Sirivivatnanon, V. (2007). Kinetics of geopolymerisation: Role of Al2O3 and SiO2. *Cement and Concrete Research,* **37:** 512–518.

Silverstein, R. and Bassler, G. Spectrometric Identification of Organic Compounds. *4th Edition.*

Singh R., and Singh A. (2013). Optimization of Reaction Conditions for Preparing Carboxymethyl Cellulose from Corn cobic Agricultural Waste, *Waste Biomass Valorization,* **4:** 129-137.

Sivalapan, S. (2006). Some benefits of treating a sandy soil with a cross-linked type polyacrylamide. *Australia Agricultural water management.*,**46:** 579-584.

Song, H., Wu, D., Zhang, R., Qiao, L., Zhang, S., Lin, S., & Ye, J. (2009). Synthesis and application of amphoteric starch graft polymer. *Carbohydrate Polymers*, **78(2):** 253-257.

Sorber J., Steiner G., Schulz V., Guenther M., Gerlach G., and Salzer R. (2008). Hydrogel-based piezoresistive pH sensors: Investigations using FTIR attenuated total reflection spectroscopic imaging. *Analytical Chemistry*, **80(8):** 2957-2962.

Stern, R. Merwe, A., Laker, M. and Shainberg, I. (1992). effect of soil surface treatments on runoff and wheat yields under irrigation. *A*gronomy *j*ournal, **84:** 114-119.

Sugumaran, P., Priya, S. Rauichandran, P. and Seshadri, S (2012). Production and characterization of activated carbon from banana empty fruit bunch and delonix regia fruit pod. *Journal of Sustainable Energy and Environment*, **3:** 125–132.

Tayel M. Y., and EL-Hady O. A. (1981). Super gel as a soil conditioner and its effects on some soil-water retentions. *Acta Horticulturae (ISHS),* **119(22)**: 247-256.

Teodorescu, M; Morariu, S; Bercea, M and Sacarescu L (2016) Viscoelastic and structural properties of poly(vinyl alcohol)/ poly(vinylpyrrolidone) hydrogels. *A*gronomy *j*ournal *of agriculture*, **6:** 39718–39727.

Thakur, S.; Chaudhary, J.; Kumar, V.; Thakur, V **(2019).** Progress in pectin-based hydrogels for water purification: Trends and challenges. *Journal Environmental. Management*., **238**: 210–223.

Thombare, N., Mishra, S., Siddiqui, M., Jha, U., Singh, D., and Mahajan, G. (2018). Design and development of guar gum-based novel, superabsorbent and moisture retaining hydrogels for agricultural applications. *Carbohydrate Polymer*, **185:** 169-178.

Tong-Chao, W., Li, W., Yan, W. and Jun-Zhong, W. (2007). Influence of bed-planting and strew mulching system on soil water and crop using of farmland. *Journal of Soil and Water Conservation*, **2:** 25–29.

Undie, U., Uwah, D., Attoe, E (2012). Effect of intercropping and crop arrangement of yield and productivity of late season maize/soybean mixtures in the humid environment of South Southern Nigeria. *Journal. Agricultural. Science.*, **4:** 37–50.

Ullah, F.; Othman, M.; Javed, F.; Ahmad, Z. and Akil, H. (2015). Classification, processing and application of hydrogels. *A review Material. Science Engineering*, **57:** 414–433.

Uz, B., Sabit, E., Demiray, E. and Erta, E. (2008). analyzing the soil texture effect on promoting water holding capacity by polyacrylamide international meeting on soil fertility land management and agroclimatology, *turkey*, 209-215.

Van Vlierberghe, S., Dubruel, P., Schacht, E. (2011). Biopolymer-based hydrogels as scolds for tissue engineering applications. *A review Biomacromolecules*, **12:** 1387–1408.

Varaprasad, K., Raghavendra, G.M., Jayaramudu, T., Yallapu, M., Sadiku, R. (**2017)**. A mini review on hydrogels classification and recent developments in miscellaneous applications. *Material. Science Engineering*, **79:** 958–971.

Varaprasad, K; Mohan, Y; Ravindra, S; Reddy, N; Vimala, K; Monika, K; Sreedhar, B. and Raju, K. (2010). Hydrogel-silver nanoparticle composites: A new generation of antimicrobials. *Journal of Applied Polymer Science*, **115:** 1199-1207.

Vazdani F, Alahdadi A, Akbari G, and Behbahani M. (2008). effect of super absorbent polymer (terawatt a200) and different levels of drought stress on soybean yield and yield components. *Research in agriculture and horticulture and construction*, 75-78.

Vazdani, F.; Allahdadi, I and Akbari, G. (2007). impact of superabsorbent polymer on yield and growth analysis of soybean (*g*lycine max l.) under drought stress condition. *Pakistan journal of biological science,* 1**0:** 4190-4196.

Viera, R., Filho G., Assuncao R., Meireles C., Vieira J. and Oliveira G. (2007). Synthesis and characterization methylcellulose from sugar cane bagasse cellulose. *Carbohydrate Polymers*, **67:** 182-189.

Vimala, K., Sivudu, K., Mohan, Y., Sreedhar, B. and Raju, K. (2009). Controlled silver nanoparticles synthesis in semi-hydrogel networks of poly(acrylamide) and carbohydrates. A rational methodology for antibacterial application. *Carbohydrate. Polymer,* **75(3):** 463-471.

Volkamar, K. and Chang, C. (1995). Influence of hydrophilic gel polymers on water relations, growth and yield of barley and canola. *Canadian Journal of Plant Science,* **75:** 605-611.

Wallace A., and Wallace G. A. (1986). Effect of polymeric soil conditioners on emergence of tomato seedlings. *Soil Science,* **141(5):** 321-323.

Wang, C. and Chen, C. (2005). Physical properties of the crosslinked cellulose catalyzed with Nano titanium dioxide under UV irradiation and electronic field. *Applied Catalysis A: General*, **293:** 171-179.

Wang, J. and Ye, L. (2015). Structure and properties of polyvinyl alcohol/polyurethane blends. *Composite Part B-Engineering*, ***69*:** 389-396.

Wang, L., Zhang J., and Wang A. (2008). Removal of methylene blue from aqueous solution using chitosan-g-poly (acrylic acid)/ montmorillonite superadsorbent nanocomposite. *Colloids and Surfaces: Physicochemical and Engineering Aspects,* **322**(1)**:** 47-53.

Watson, D. (1956). Leaf growth in relation to crop yield. Ed. F.L. Milthorpe, Butterworths, *Scientific Publications London*, 178-191.

Wei, Y. and Durian, D. (2014). Rain water transport and storage in a model sandy soil with hydrogel particle additives. *The European Physical Journal*, **37**(**97):** 1-11.

Wingerson, A. and Richard, C. (2002). Method of treating lignocellulosic biomass to produce cellulose, http://www.patentstorm.us/patents/6419788-description.html, US. Patent Issued on July 16.

Witono, J., Noordergraaf, I., Heeres, H. and Janssen, L. (2014). Water absorption, retention and the swelling characteristics of cassava starch grafted with polyacrylic acid. *Carbohydrate Polymers*, ***103*:** 325-332.

Woodhouse, J. and Johnson, M. (1991). Effect of superabsorbent polymers on survival and growth of crop seedlings. *Agricultural Water Management*, ***20*(1):** 63–70.

Wu D., Wang T., Lu B.; Xu X., Cheng S., and Jiang X. (2008). Fabrication of supramolecular hydrogels for drug delivery and stem cell encapsulation. *Langmuir*, **24(18):** 10306-10312.

Xiang, Y. and Chen, D. (2007). Preparation of a novel pH-responsive silver nanoparticle /poly(HEMAPEGMA- MAA) composite hydrogel. *European Polymer Journal*, **43(10):** 4178-4187.

Yazdani, F., Allahdadi, I. and Akbari, G. (2007). Impact of superabsorbent polymer on yield and growth analysis of soybean (*Glycine max* L.) under drought stress condition. *Pakistan Journal of Biology Sciences*, **10:** 4190-4196.

Yazdani-Pedram, M., Retuert, J. and Quijada, R. (2000). Hydrogels based on modified chitosan, 1 Synthesis and swelling behavior of poly(acrylic acid) grafted chitosan. Macromol. *Applied Surface Science*, **201(9):** 923-930.

Yeasmin, M. and Mondal, M. (2015). Synthesis of highly substituted carboxymethyl cellulose depending on cellulose particle size. *International Journal of Biological Macromolecules*, **80:** 725-731.

Yokoyama, F., Masada, I., Shimamura, K., Ikawa, T. and Monobe, K. (1986). Morphology and structure of highly elastic poly(vinyl alcohol) hydrogel prepared by repeated freezing-and-melting., 264 (1986). *Colloid Polymer Science*, **264:** 505–601.

Zain, G., Nada, A., El-Sheikh, M., Attaby, F. and Waly, A. (2018). Superabsorbent hydrogel based on sulfonated-starch for improving water and saline absorbency. *International Journal Biological Macromolecular*, **115:** 61-68.

Zhang, W., Liu, B. and Song, J. (2005). Effects of super-absorbent polymers on the physical and chemical properties of soil following different wetting and drying cycles. *Soil Use and Management*, **26:** 253–260.

Zhao, Y., Cai, C., Luo, Y. and He, Z. (2004). FTIR Spectra of the M(EDTA)n-Complexes in the Process of Sol-Gel Technique. *Journal of Superconductivity*, **17:** 383–387.

Zheng, Y., Xie, Y, and Wang, A. (2012). Rapid and wide pH-independent ammonium-nitrogen removal using a composite hydrogel with three-dimensional networks. *Chemical Engineering Journal*, ***179*****:** 90-98.

Zhiming, F.; Dengwei, L. and Yuehong, Z. (2007). Water requirements and irrigation scheduling of spring maize using GIS and crop wet model in Beijing-Tianjin- hebei region. *Chinese Geographical Science*, **17:** 56–62.

Zhu, S., Wang, J., Yan, H., Wang, Y., Zhao, Y., Feng, B., Duan, K. and Weng, J. (2017). An injectable supramolecular self-healing bio-hydrogel with high stretch ability, extensibility and ductility, and a high swelling ratio. *Journal of Material Chemistry*, **5:** 7021.

APPENDICES

Appendix 1A: IR bands functional groups analysis of HCE-1and HCE-2

HCE-1 superabsorbent hydrogel		**HCE-2 superabsorbent hydrogel**	
Absorption $\bar{\upsilon}$ (cm^{-1})	**Functional group**	**Absorption $\bar{\upsilon}$ (cm^{-1})**	**Functional group**
3339.83	N-H stretching vibration	3385.99	-OH broad stretch vibration
2934.62	C-H asymmetric stretch of CH, CH_2 and CH_3	3283.04	-OH normal polymeric stretch
2376.19	CN aromatic secondary amide stretching	3258.12	H-bonding asymmetric strong interaction
2312.61	CN aromatic secondary amide bending	1568.87	$-COO^-$ symmetric stretching in ester
1590.99	$-COO^-$ in activated carbon	1411.73	-OH phenol bending
1400.43	-COOH acid	1257.68	-CN aromatic primary amide stretching
1386.05	-OH stretching vibration of phenol		
1341.42	CN stretching of tertiary amine		
1216.22	C-O stretching vibration of phenol		
1110.31	C-O alkyl ether stretching		
1073.54	CN stretching of primary amine		
994.15	C-H vinyl out of plane bending		
917.67	OH bending		
851.62	$C - O - O^-$ in aromatic ether		
703.05	H bond deformation vibration		

Appendix 1B: IR bands functional groups in HCG-1 and HCG-2 before and after crosslinking

HCG-1super hydrogel before cross linking		**HCG-2super hydrogel after cross linking**	
Absorption $\bar{\upsilon}$ (cm^{-1})	**Functional group**	**Absorption $\bar{\upsilon}$ (cm^{-1})**	**Functional group**
3342.01	OH alcohol bending vibration	3383.57	OH broad stretch vibration
2934.73	CH asymmetric stretching of CH,CH_2 and CH_3	3252.05	OH normal polymeric stretch
1591.34	COO^- on salt	2965.95	CH asymmetric stretching of CH,CH_2 and CH_3 lignin
1400.28	COO^- on acid	2316.68	CN stretching vibration
1341.99	C-O stretching vibration of ether	2106.68	CN bending vibration
1216.44		1639.48	COO^-v-bending asymmetric
1110.56	Alkyl substituted C-O ether stretch	1527.37	COO^-asymetric bending
1073.17	C-O-C stretch of ring ethers	1409.08	OH phenol bending
994.01	Vinyl C-H out of plane bend	1255.84	Aromatic ether stretching
917.63	Vinylidene C-H out of plane bend	1117.67	Secondary alcohol C-O stretching
702.86	H- bond deformation	745	C-H out of plane bending
		620	Alcohol OH out of plane bend

Appendix 1C:IR bands functional groups of HLE-1 and HLE-2 before and after crosslinking

HLE-1 **super hydrogel before cross linking**		HLE-2 **super hydrogel after cross linking**	
Absorption $\bar{\upsilon}$ (cm^{-1})	**Functional group**	**Absorption $\bar{\upsilon}$ (cm^{-1})**	**Functional group**
3329.83	NH secondary amide stretching	3948.89	OH stretch vibration
2934.52	C-H asymmetric stretch of CH_3	3909.17	OH stretch vibration
1591.45	Aromatic ring stretch	3787.88	NH-NH_2 dimeric stretching
1399.95	Tertiary alcohol OH bending.	3371.58	Bonded N-H/ C-H/ OH stretching
1341.35	Primary OH in plane bending	2350.81	CN
1215.77	CN aromatic secondary stretch	1989.08	
1110.52	Cyanate –OCN stretch	1947.42	
1073.28	CN primary amine stretch	1577.76	NH primary amide bending
994.05		1383.61	OH phenol bending
917.56		1205.20	C-O phenol stretching
701.72	OH in alcohol out of plane bending	1079.83	CN primary amide stretching
618.45		885	C-O-O-C peroxide stretching
		737	C-H out of plane bending
		671	Alcohol OH out of plane bend

Appendix 1D: IR bands functional groups analysis of uncrosslinked HLG-1 and crosslinked HLG-2 superabsorbent hydrogel.

HLG-1 **before cross linking**		HLG-2 **after cross linking**	
Absorption $\bar{\upsilon}$ (cm^{-1})	**Functional group**	**Absorption $\bar{\upsilon}$ (cm^{-1})**	**Functional group**
3790.34	Isolated OH groups stretching	3338.55	OH stretching alcohol
3410.95	H bonded OH stretching	2934.41	CH asymmetric stretching of CH_3
2104.20	CN bending	1706.30	C=O stretch in acid
1528	COO^- stretching	1591.67	Aromatic ring stretch
1256.32	C-O stretching in alcohol	1399.85	OH tertiary bend alcohol
1120.37	OH secondary stretching	1339.36	Primary OH in plane bending
745.75	C-H out of plane bending	1323.24	OH in secondary plane bending
619.96	OH out of plane bend	1291.93	Vinylidene CH in plane bend
483.18		1215.96	C-O stretching in alcohol
		1110.39	Alkyl substituted ether C-O stretch
		1073.19	Ethers large rings C-O stretching
		994.20	C-O stretch bend
		918.14	C-H out of plane bend
		851.53	Aromatic C-O-O- stretch

Appendix 2A: Powdered diffraction pattern of HCE-1

Pos. [°2Th.]	Height [cts]	FWHM [°2Th.]	d-spacing [Å]	Rel. Int. [%]
18.2776	2.82	1.3318	4.85394	13.30
20.6536	4.08	0.0010	4.30060	19.23
26.6761	21.19	0.1417	3.34179	100.00
36.3732	0.75	0.5668	2.47006	3.56
43.5976	4.75	0.0010	2.07605	22.42
43.5976	4.75	0.0010	2.07605	22.42
44.5816	2.33	0.8701	2.03248	11.01
49.9608	0.91	0.5668	1.82553	4.28
54.9256	1.00	0.0900	1.67169	4.72
59.8388	1.40	0.3779	1.54564	6.58
67.9326	0.69	1.1520	1.37872	3.25

Appendix 2B: Powdered diffraction pattern of HCE-2

Pos. [°2Th.]	Height [cts]	FWHM [°2Th.]	d-spacing [Å]	Rel. Int. [%]
11.8470	2.68	0.5196	7.47028	18.83
17.7405	2.13	0.5077	4.99966	14.97
20.8544	2.37	0.2598	4.25965	16.63
23.8173	4.23	0.8848	3.73603	29.76
25.7176	5.37	0.0010	3.46412	37.76
26.6128	14.23	0.2834	3.34959	100.00
30.8411	12.03	0.5786	2.89933	84.58
35.8816	2.67	0.0010	2.50276	18.75
36.5877	1.01	0.2952	2.45607	7.10
39.4568	1.50	0.3660	2.28384	10.55
40.3393	0.29	0.2834	2.23589	2.07
43.5602	6.13	0.3779	2.07774	43.08
44.5773	2.72	0.3542	2.03267	19.10
49.9096	1.00	0.0900	1.82728	7.03
50.3780	0.08	0.5077	1.81139	0.57
53.0176	1.00	0.0900	1.72726	7.03
54.8056	1.00	0.0900	1.67506	7.03
54.9303	0.41	0.9446	1.67156	2.86
59.9211	0.76	0.3660	1.54372	5.37
67.6639	0.68	0.3188	1.38469	4.77
68.1947	0.83	0.3600	1.37406	5.83

Appendix 2C: Powdered diffraction pattern of HCG-1

Pos. [°2Th.]	Height [cts]	FWHM [°2Th.]	d-spacing [Å]	Rel. Int. [%]
20.8687	16.93	0.1417	4.25677	38.69
26.6541	31.11	0.1417	3.34450	71.09
36.5169	2.28	0.2834	2.46067	5.20
39.3736	1.00	0.0900	2.28847	2.29
42.5176	43.76	0.0010	2.12625	100.00
43.6252	5.29	0.1692	2.07480	12.10
50.0978	5.01	0.2362	1.82086	11.44
54.8622	0.55	0.5668	1.67347	1.25
59.9552	1.24	0.4723	1.54292	2.84
68.0151	1.64	1.1520	1.37725	3.74

Appendix 2D: Powdered diffraction pattern of HCG-2

Pos. [°2Th.]	Height [cts]	FWHM [°2Th.]	d-spacing [Å]	Rel. Int. [%]
18.2137	8.13	0.4723	4.87084	30.98
20.5625	4.12	2.0106	4.31945	15.69
21.5932	1.00	0.2407	4.11556	3.81
25.4853	26.25	0.1889	3.49517	100.00
26.6426	11.41	0.1653	3.34592	43.46
28.5071	11.10	0.2125	3.13117	42.26
33.0364	1.09	0.2598	2.71151	4.17
34.8843	9.10	0.2362	2.57200	34.66
36.8669	1.02	0.5668	2.43811	3.87
38.0914	2.25	0.2598	2.36250	8.58
40.1942	3.31	0.2834	2.24362	12.60
43.5754	3.07	0.3779	2.07705	11.68
53.3707	2.61	0.2834	1.71666	9.94
54.8096	1.11	0.4251	1.67495	4.21
56.0142	1.44	0.3779	1.64175	5.48
60.1722	0.94	0.5668	1.53787	3.60
62.8803	0.92	0.7557	1.47800	3.51
69.2729	0.33	0.7557	1.35641	1.24
77.1118	0.39	0.9216	1.23588	1.49

Appendix 2E: Powdered diffraction pattern of HLE-1

Pos. [°2Th.]	Height [cts]	FWHM [°2Th.]	d-spacing [Å]	Rel. Int. [%]
15.9638	20.84	0.0834	5.55191	15.38
16.8095	46.63	0.1889	5.27442	34.42
21.2143	105.28	0.2125	4.18819	77.71
23.5951	24.26	0.2834	3.77070	17.91
27.8810	135.48	0.2125	3.20005	100.00
29.7747	93.77	0.2362	3.00070	69.22
31.2002	30.82	0.2362	2.86677	22.75
32.5360	6.41	0.5668	2.75207	4.73
33.6581	11.54	0.3779	2.66284	8.52
35.9475	18.84	0.5668	2.49832	13.91
38.2456	1.00	0.2724	2.35333	0.74
38.6056	14.69	0.2790	2.33221	10.84
41.7850	15.44	0.3779	2.16182	11.39
42.5979	11.84	0.2612	2.12242	8.74
44.4235	20.26	0.3779	2.03935	14.95
45.4573	12.48	0.2526	1.99535	9.21
49.4946	8.14	0.2204	1.84163	6.01
57.4962	5.26	0.6912	1.60159	3.88

Appendix 2F: Powdered diffraction pattern of HLE-2

Pos. [°2Th.]	Height [cts]	FWHM [°2Th.]	d-spacing [Å]	Rel. Int. [%]
18.2155	8.19	0.4723	4.87036	26.86
21.4692	7.36	0.1889	4.13904	24.14
25.5185	30.50	0.1889	3.49069	100.00
26.0113	7.22	0.2362	3.42566	23.66
26.6769	13.27	0.1889	3.34169	43.49
27.8384	6.64	0.1653	3.20485	21.77
28.5245	12.00	0.2125	3.12931	39.35
29.2860	1.28	0.2834	3.04964	4.19
33.0486	2.65	0.2125	2.71054	8.69
34.9086	9.50	0.2598	2.57026	31.15
36.8661	0.84	0.5668	2.43816	2.77
38.1798	2.47	0.2834	2.35724	8.10
40.1958	3.19	0.2598	2.24354	10.47
43.6660	3.78	0.4251	2.07295	12.40
53.4245	2.44	0.3779	1.71506	7.99
54.8823	1.12	0.5668	1.67290	3.66
56.0554	1.65	0.5196	1.64065	5.41
60.1990	0.87	0.5668	1.53725	2.85

Appendix2G: Powdered diffraction pattern of HLG-2

Pos. [°2Th.]	Height [cts]	FWHM [°2Th.]	d-spacing [Å]	Rel. Int. [%]
18.2155	8.19	0.4723	4.87036	26.86
21.4692	7.36	0.1889	4.13904	24.14
25.5185	30.50	0.1889	3.49069	100.00
26.0113	7.22	0.2362	3.42566	23.66
26.6769	13.27	0.1889	3.34169	43.49
27.8384	6.64	0.1653	3.20485	21.77
28.5245	12.00	0.2125	3.12931	39.35
29.2860	1.28	0.2834	3.04964	4.19
33.0486	2.65	0.2125	2.71054	8.69
34.9086	9.50	0.2598	2.57026	31.15
36.8661	0.84	0.5668	2.43816	2.77
38.1798	2.47	0.2834	2.35724	8.10
40.1958	3.19	0.2598	2.24354	10.47
43.6660	3.78	0.4251	2.07295	12.40
53.4245	2.44	0.3779	1.71506	7.99
54.8823	1.12	0.5668	1.67290	3.66
56.0554	1.65	0.5196	1.64065	5.41
60.1990	0.87	0.5668	1.53725	2.85
62.8408	0.77	0.9216	1.47761	2.53

Appendix 2H: Powdered diffraction pattern of HLG-2

Pos. [°2Th.]	Height [cts]	FWHM [°2Th.]	d-spacing [Å]	Rel. Int. [%]
43.6231	4.38	0.4608	2.07317	100.00

Appendix 3A: The effect of amount of lemon juice (citric acid) on the percentage swelling of 2.0 g HLG-2 and HLE-2

Volume CA ml	0.9	1.8	3.6	5.4	7.2	9
Swelling % HLG-2	380.23 ± 0.38^{e}	610.23 ± 2.57^{d}	730.33 ± 0.71^{a}	860.67 ± 0.65^{b}	790.83 ± 1.54^{c}	760.83 ± 1.34^{b}
Swelling % HLE-2	280.90 ± 0.27^{e}	330.93 ± 0.71^{d}	680.10 ± 0.10^{a}	830.23 ± 0.76^{b}	955.03 ± 0.21^{c}	960.03 ± 0.65^{b}

Appendix 3B: The effect of amount of activated charcoal on the percentage swelling of 2.0 g HCG-2 and HCE-2

Amount of AC used (g)	1	2	4	6	8	10
Swelling % HCG-2	390.43±0.15^{e}	620.40±0.92^{c}	830.57±0.21^{a}	1020.13±0.75^{b}	910.63±0.76^{d}	850.63±0.76^{d}
Swelling % HCE-2	370.63±0.06^{e}	590.13±0.57^{d}	780.50±1.02^{a}	860.33±1.03^{b}	830.13±0.74^{c}	730.50±12.02^{a}

Appendix 3C: The effect of amount of maleic acid on the percentage swelling of 2.0 g HLG-2, HCG-2, HCE-2 HLE-2 hydrogel immersed in 500 mL of distilled water and swelling period of 24 hours

Amount of MA used (g)	1.25	2.5	3.75	5.0	6.25	7.5
Swelling % HLG-2	380.33±5.55^{e}	560.00±7.55^{d}	990.33±2.52^{a}	950.67±3.51^{b}	855.33±6.51^{c}	810.01±3.51^{c}
Swelling % HCG-2	430.67±6.03^{e}	1120.33±5.51^{d}	960.67±2.52^{a}	710.00±4.58^{b}	620.00±4.00^{c}	610.01±4.21^{c}
Swelling % HCE-2	330.33±8.50^{e}	720.00±7.55^{d}	830.00±3.61^{a}	1070.33±3.51^{b}	510.33±2.52^{c}	495.05±2.51^{c}
Swelling % HLE-2	490.33±8.62^{e}	680.00±4.58^{d}	920.33±5.13^{a}	720.67±4.51^{b}	630.67±3.51^{c}	620.48±3.51^{c}

APPENDIX 3D: The effect of swelling time on the percentage swelling of 2.0 g HLG-2, HCG-2, HCE-2 HLE-2 hydrogel prepared at optimum conditions when immersed in 500 mL of distilled water

Time in hours	0.5	1.0	2	4	6	12	24
Swelling % HLG-2	315.07±1.74^{d}	455.53±1.19^{b}	670.77±0.90^{a}	730.77±0.61^{c}	910.30±1.08^{d}	880.87±0.38^{b}	860.87±0.38^{b}
Swelling % HLE-2	305.63±1.02^{e}	455.50±0.95^{c}	685.90±0.85^{a}	845.87±0.38^{b}	925.20±0.95^{d}	885.87±0.38^{b}	845.87±0.38^{b}
Swelling % HCE-2	220.87±1.50^{e}	348.27±0.71^{b}	425.53±0.80^{a}	684.37±1.16^{c}	850.80±0.62^{d}	1090.80±0.70^{d}	1090.80±0.70^{d}
Swelling % HCG-2	330.43±1.08^{e}	580.73±0.42^{b}	835.80±0.56^{a}	970.13±0.21^{c}	1240.80±0.70^{d}	1255.80±0.70^{d}	1230.80±0.70^{d}

Appendix 4A: The effect of hydrogel dosage on percentage moisture content at flowering stage (50days)

Dosage of hydrogel kg/ha	Control Mean±SD	HCE-2 Mean±SD	HCG-2 Mean±SD	HLE-2 Mean±SD	HLG-2 Mean±SD
15	63.43±0.06^{e}	71.60±0.10^{b}	73.97±0.12^{b}	67.53±0.06^{a}	68.90±0.10^{a}
30	63.60±0.20^{e}	76.20±0.17^{c}	79.33±0.15^{a}	72.53±0.25^{b}	74.27±0.21^{d}
45	64.03±0.15^{e}	84.10±0.17^{b}	86.60±0.10^{a}	80±0.78^{c}	82.70±0.20^{d}
60	64.57±0.25^{e}	91.80±0.30^{b}	93.20±0.10^{a}	85.47±0.31^{c}	88.20±0.17^{d}

Appendix 4B: Effect of growth period on plant height using HCE-2, HCG-2, HLE-2 and HLG-2 hydrogels at different doses

Days	Control Mean±SD	HCE-2 Mean±SD	HCG-2 Mean±SD	HLE-2 Mean±SD	HLG-2 Mean±SD
15 kg/ha of hydrogel was applied					
15	4.2 ±0.15^{d}	5.00 ± 0.10^{c}	6.57 ± 0.21^{a}	5.80 ± 0.10^{b}	4.53 ± 0.15^{d}
30	38.43±0.15^{e}	48.43 ±0.31^{d}	71.63 ±0.15^{a}	66.67 ±0.15^{b}	54.80 ±0.10^{c}
45	143.73±0.42^{e}	162.90 ±0.27^{b}	159.77 ±0.45^{c}	164.03 ±0.31^{a}	153.83 ±0.45^{d}
60	140.60±0.53^{d}	203.53 ±0.25^{b}	192.93 ±0.25^{c}	208.40 ±0.20^{a}	208.03 ±0.21^{a}
30 kg/ha of hydrogel was applied					
15	4.27±0.15^{c}	7.10±0.20^{ab}	7.47±0.15^{a}	6.73±0.15^{b}	6.83±0.15^{b}
30	38.53±0.21^{e}	59.8±30.25^{d}	76.87±0.15^{a}	69.8±30.35^{b}	61.63±0.21^{c}
45	143.37±0.25^{e}	174.23±0.25^{a}	168.57±0.25^{c}	170.47±0.21^{b}	157.63±0.35^{d}
60	140.30±0.20^{e}	208.57±0.25^{d}	216.50±0.27^{b}	218.67±0.38^{a}	211.47±0.31^{c}
when 40 kg/ha of hydrogel was applied					
15	4.10±0.20^{b}	8.27±0.21^{a}	8.53±0.15^{a}	8.50±0.10^{a}	8.23±0.06^{a}
30	38.30±0.20^{e}	61.57±0.25^{d}	80.50±0.20^{a}	73.63±0.15^{b}	63.53±0.15^{c}
45	143.63±0.25^{e}	179.27±0.15^{a}	172.63±0.25^{c}	174.33±0.12^{b}	168.47±0.35^{d}
60	140.27±0.15^{e}	220.30±0.20^{c}	239.27±0.15^{a}	233.67±0.15^{b}	218.27±0.21^{d}
60 kg/ha of hydrogel was applied					
15	4.27±0.15^{b}	8.63±0.15^{a}	8.50±0.20^{a}	8.37±0.25^{a}	8.47±0.21^{a}
30	38.30±0.20^{e}	65.50±0.30^{d}	85.53±0.25^{a}	75.43±0.15^{b}	66.30±0.20^{c}
45	143.60±0.20^{d}	182.23±0.21^{b}	200.60±0.46^{a}	201.10±0.30^{a}	173.30±0.20^{c}
60	140.27±0.21^{e}	223.30±0.20^{c}	240.47±0.25^{a}	235.23±0.15^{b}	220.57±0.15^{d}

Means across the row that do not share a letter are significantly different, SD= standard deviation.

Appendix 4C: Effect of growth period on number of leaves using HCG-2, HLE-2, HLG-2 and HCE-2 hydrogels at different dosages.

Days	**Control Mean±SD**	**HCE-2 Mean±SD**	**HCG-2 Mean±SD**	**HLE-2 Mean±SD**	**HLG-2 Mean±SD**
15 kg/ha of hydrogel was applied					
15	4.00±0.00^{b}	4.67±0.58^{ab}	5.67±0.58^{a}	5.33±0.58^{ab}	4.33±0.58^{ab}
30	7.00±1.00^{b}	10.67±0.58^{a}	11.67±0.58^{a}	10.67±0.58^{a}	11.33±0.58^{a}
45	10.6±70.58^{a}	11.67±0.58^{a}	12.00±1.00^{a}	11.67±0.57^{a}	12.00±1.00^{a}
60	11.67±0.58^{c}	12.00±1.00^{bc}	14.00±0.00^{a}	13.67±0.58^{ab}	12.00±1.00^{bc}
30 kg/ha of hydrogel was applied					
15	4.00±0.00^{a}	4.67±0.58^{a}	5.67±0.58^{a}	5.33±0.58^{a}	5.00±1.00^{a}
30	7.00±1.00^{b}	10.00±1.00^{a}	11.67±0.58^{a}	10.67±0.58	11.67±0.58^{a}
45	10.67±0.58^{a}	11.67±0.58^{a}	12.00±1.00^{a}	11.67±0.58^{a}	11.00±1.00^{a}
60	11.67±0.58^{a}	12.67±0.58^{a}	13.67±0.58^{a}	13.00±1.00^{a}	12.00±1.00^{a}
45 kg/ha of hydrogel was applied					
15	4.00±0.00^{b}	5.33±0.58^{ab}	6.67±0.58^{a}	6.33±0.58^{a}	5.67±0.58^{a}
30	7.00±1.00^{c}	9.33±0.58^{b}	11.67±0.58^{a}	11.00±1.00^{ab}	11.00±1.00^{ab}
45	10.67±0.58^{a}	12.00±1.00^{a}	12.67±0.58^{a}	11.67±0.58^{a}	12.00±1.00^{a}
60	11.67±0.58^{a}	12.00±1.00^{a}	13.00±1.00^{a}	12.67±0.58^{a}	11.67±0.58^{a}
60 kg/ha of hydrogel was applied					
15	4.00±0.00^{c}	5.67±0.58^{ab}	6.67±0.58^{a}	6.00±0.00^{ab}	5.33±0.58^{b}
30	7.00±1.00^{b}	10.67±0.58^{a}	11.67±0.58^{a}	11.00±0.00^{a}	10.33±0.58^{a}
45	10.67±0.58^{a}	11.33±0.58^{a}	12.00±1.00^{a}	11.67±0.58^{a}	11.00±0.00^{a}
60	11.67±0.58^{a}	12.33±0.58^{a}	13.00±1.00^{a}	12.00±0.00^{a}	11.67±0.58^{a}

Means across the row that do not share a letter are significantly different, SD= standard deviation

Appendix 4D: Effect of the hydrogels HCG-2, HLE-2, HLG-2 and HCE-2 on leaf area index (cm^2) at different dosage

Days	Control Mean±SD	HCE-2 Mean±SD	HCG-2 Mean±SD	HLE-2 Mean±SD	HLG-2 Mean±SD
15 kg/ha of hydrogel was applied					
15	4.90±0.20^{c}	6.30±0.20^{ab}	6.77±0.25^{a}	6.23±0.15^{b}	5.97±0.15^{b}
30	10.57±0.25^{d}	16.67±0.15^{c}	18.90±0.20^{a}	17.70±0.20^{b}	16.17±0.32^{c}
45	37.03±0.25^{d}	45.87±0.15^{b}	50.23±0.45^{a}	43.57±0.25^{c}	44.33±0.42^{c}
60	50.20±0.40^{d}	59.57±0.32^{c}	63.47±0.35^{a}	60.03±0.31^{c}	61.27±0.25^{b}
30 kg/ha of hydrogel was applied					
15	4.90±0.20^{c}	8.93±0.15^{a}	9.47±0.15^{a}	9.07±0.25^{a}	7.87±0.25^{b}
30	10.57±0.25^{d}	16.63±0.15^{c}	20.33±0.31^{a}	19.50±0.20^{b}	16.50±0.30^{c}

45	37.03±0.25^{c}	51.13±0.42^{b}	52.43±0.25^{a}	51.67±0.21^{ab}	51.33±0.35^{b}
60	50.20±0.40^{e}	64.57±0.25^{d}	68.50±0.30^{a}	65.33±0.15^{c}	66.40±0.20^{b}
45 kg/ha of hydrogel was applied					
15	4.90±0.20^{d}	8.87±0.38^{c}	11.03±0.25^{a}	9.60±0.17^{b}	8.33±0.25^{c}
30	10.57±0.25^{d}	32.20±0.10^{b}	33.37±0.25^{a}	31.30±0.20^{c}	32.37±0.15^{b}
45	37.03±0.25^{d}	56.30±0.20^{c}	59.27±0.21^{a}	58.40±0.56^{b}	55.87±0.21^{c}
60	50.20±0.40^{e}	77.07±0.25^{c}	79.63±0.15^{a}	77.90±0.27^{b}	75.53±0.31^{d}
60 kg/ha of hydrogel was applied					
15	4.90±0.20^{c}	11.47±0.15^{b}	16.10±0.27^{a}	11.70±0.20^{b}	11.27±0.15^{b}
30	10.57±0.25^{d}	32.90±0.17^{c}	35.37±0.25^{a}	34.00±0.27^{b}	32.53±0.25^{c}
45	37.03±0.25^{d}	63.70±0.20^{b}	67.93±0.15^{a}	63.57±0.21^{b}	62.80±0.27^{c}
60	50.20±0.40^{d}	82.33±0.15^{b}	88.63±0.15^{a}	82.77±0.32^{b}	81.50±0.20^{c}

Means across the row that do not share a letter are significantly different, SD= standard deviation

Appendix 4E: Effect of dosage on dry matter accumulation in grams when HCG-2, HLE-2, HLG-2 and HCE-2 hydrogels were applied

Days	**Control Mean±SD**	**HCE-2 Mean±SD**	**HCG-2 Mean±SD**	**HLE-2 Mean±SD**	**HLG-2 Mean±SD**
15 kg/ha of hydrogel was applied					
15	0.43±0.06^{c}	1.60±0.10^{b}	1.97±0.12^{a}	1.57±0.06^{b}	1.90±0.10^{a}
30	1.60±0.20^{e}	17.20±0.17^{c}	19.33±0.15^{a}	18.53±0.25^{b}	15.27±0.21^{d}
45	9.03±0.15^{e}	53.10±0.17^{b}	57.60±0.10^{a}	51.67±0.78^{c}	46.70±0.20^{d}
60	50.57±0.25^{e}	78.80±0.30^{b}	86.20±0.10^{a}	76.47±0.31^{c}	62.20±0.17^{d}
Harvest	78.23±0.40^{e}	110.37±0.21^{b}	115.90±0.30^{a}	93.60±0.36^{c}	80.53±0.31^{d}
30 kg/ha of hydrogel was applied					
15	0.43±0.06^{d}	1.73±0.06^{c}	2.07±0.06^{a}	1.83±0.06^{bc}	2.00±0.10^{ab}
30	1.60±0.20^{e}	23.70±0.10^{c}	43.03±0.21^{a}	29.17±0.06^{b}	21.60±0.10^{d}
45	9.03±0.15^{e}	72.17±0.15^{b}	86.60±0.10^{a}	68.17±0.15^{c}	59.60±0.20^{d}
60	50.57±0.25^{e}	93.43±0.15^{b}	111.70±0.10^{a}	83.57±0.15^{c}	77.40±0.10^{d}
Harvest	78.23±0.40^{e}	125.70±0.10^{b}	145.47±0.21^{a}	115.57±0.25^{c}	102.47±0.15^{d}
45 kg/ha of hydrogel was applied					
15	0.43±0.06^{c}	1.87±0.06^{b}	2.17±0.06^{a}	2.00±0.10^{ab}	2.10±0.10^{a}
30	1.60±0.20^{e}	28.43±0.15^{c}	48.53±0.32^{a}	43.77±0.12^{b}	24.60±0.10^{d}
45	9.03±0.15^{e}	98.73±0.15^{c}	118.77±0.15^{a}	111.43±0.15^{b}	61.30±0.30^{d}
60	50.57±0.25^{e}	127.63±0.21^{c}	171.77±0.15^{a}	153.63±0.12^{b}	96.60±0.20^{d}
Harvest	78.23±0.40^{e}	181.60±0.20^{c}	222.53±0.21^{a}	211.60±0.20^{b}	150.50±0.20^{d}
60 kg/ha of hydrogel was applied					

15	0.43±0.06^{c}	1.97±0.12^{ab}	2.07±0.15^{a}	1.83±0.06^{ab}	1.70±0.10^{b}
30	1.60±0.20^{e}	42.50±0.20^{c}	50.80±0.27^{a}	38.87±0.35^{b}	31.40±0.20^{d}
45	9.03±0.15^{e}	108.47±0.15^{b}	128.47±0.21^{a}	106.93±0.25^{c}	88.57±0.31^{d}
60	50.57±0.25^{e}	131.47±0.25^{c}	173.60±0.10^{a}	156.63±0.25^{b}	101.53±0.31^{d}
Harvest	78.23±0.40^{e}	186.33±0.25^{c}	225.77±0.15^{a}	219.40±0.10^{b}	155.37±0.35^{d}

Means across the row that do not share a letter are significantly different, SD= standard deviation

Appendix 4F: Effect of dosage on crop growth rate (g/m^2/day) when HCG-2, HLE-2, HLG-2 and HCE-2 hydrogels were applied

Days	**Control Mean±SD**	**HCE-2 Mean±SD**	**HCG-2 Mean±SD**	**HLE-2 Mean±SD**	**HLG-2 Mean±SD**
15 kg/ha of hydrogel was applied					
0 – 15	2.13±0.12^{d}	3.17±0.06^{c}	4.00±0.10^{a}	3.73±0.15^{ab}	3.67±0.06^{b}
15 – 30	3.13±0.06^{d}	10.47±0.15^{c}	12.70±0.10^{a}	11.47±0.21^{b}	10.53±0.21^{c}
30 – 45	13.53±0.31^{e}	19.23±0.12^{c}	21.30±0.20^{a}	20.30±0.17^{b}	16.30±0.10^{d}
45 – 60	4.60±0.30^{c}	6.33±0.21^{b}	7.67±0.15^{a}	6.53±0.12^{b}	6.53±0.25^{b}
30 kg/ha of hydrogel was applied					
0 – 15	2.13±0.12^{d}	4.07±0.15^{bc}	4.60±0.10^{a}	3.93±0.06^{c}	4.30±0.10^{b}
15 – 30	3.13±0.06^{d}	14.33±0.25^{b}	16.73±0.15^{a}	14.30±0.20^{b}	11.33±0.25^{c}
30 – 45	13.53±0.31^{d}	23.30±0.10^{b}	24.90±0.20^{a}	22.83±0.35^{b}	19.57±0.21^{c}
45 – 60	4.60±0.30^{d}	6.27±0.15^{c}	7.60±0.17^{a}	6.93±0.15^{b}	6.07±0.15^{c}
45 kg/ha of hydrogel was applied					
0 – 15	2.13±0.12^{c}	4.37±0.06^{b}	5.00±0.17^{a}	4.63±0.15^{b}	4.30±0.10^{b}
15 – 30	3.13±0.06^{e}	23.73±0.15^{a}	20.47±0.15^{b}	19.50±0.27^{c}	18.50±0.27^{d}
30 – 45	13.53±0.31^{d}	27.37±0.32^{a}	26.53±0.21^{b}	26.37±0.12^{b}	22.50±0.20^{c}
45 – 60	4.60±0.30^{e}	9.40±0.20^{c}	10.40±0.27^{b}	11.50±0.20^{a}	8.47±0.21^{d}
60 kg/ha of hydrogel was applied					
0 – 15	2.13±0.12^{c}	4.53±0.25^{b}	5.50±0.27^{a}	4.60±0.20^{b}	4.47±0.21^{b}
15 – 30	3.13±0.06^{d}	24.37±.21^{a}	21.63±0.25^{b}	21.27±0.15^{b}	19.07±0.15^{c}
30 – 45	13.53±0.31^{d}	29.17±0.15^{c}	30.50±0.20^{b}	31.37±0.21^{a}	28.63±0.31^{c}
45 – 60	4.60±0.30^{e}	10.40±0.20^{c}	12.53±0.21^{a}	11.60±0.30^{b}	9.47±0.31^{d}

Means across the row that do not share a letter are significantly different, SD= standard deviation

Appendix 5A: The effect of dosage (kg/ha) of hydrogels on number of maize cobs per plant

Dosage(kg/ha)	Control Mean±SD	Number of cobs per plant obtained when varied dose of the hydrogels were applied			
		HCE-2 Mean±SD	HCG-2 Mean±SD	HLE-2 Mean±SD	HLG-2 Mean±SD
15	1.00±0.00[a]	1.33±0.58[a]	2.00±0.00[a]	1.67±0.58[a]	1.67±0.58[a]
30	1.00±0.00[a]	1.67±0.58[a]	2.33±0.58[a]	1.67±0.58[a]	1.33±0.58[a]
45	1.00±0.00[b]	2.00±0.00[a]	2.33±0.58[a]	2.00±0.00[a]	1.67±0.58[ab]
60	1.00±0.00[b]	2.00±0.00[a]	2.33±0.58[a]	2.00±0.00[a]	1.67±0.58[ab]

Means across the row that do not share a letter are significantly different, SD= standard deviation

Appendix 5B: The effect of dosage (kg/ha) of hydrogels on number of grains per cob

Dosage(kg/ha)	Control Mean±SD	Number of grains per cob obtained when varied dose of the hydrogels were applied			
		HCE-2 Mean±SD	HCG-2 Mean±SD	HLE-2 Mean±SD	HLG-2 Mean±SD
15 kg / ha	225.33±5.55[e]	286.00±7.55[d]	394.33±2.52[a]	367.67±3.51[b]	335.33±6.51[c]
30 kg / ha	229.67±6.03[e]	336.33±5.51[d]	448.67±2.52[a]	406.00±4.58[b]	388.00±4.00[c]
45 kg / ha	226.33±8.50[e]	388.00±7.55[d]	607.00±3.61[a]	441.33±3.51[b]	420.33±2.52[c]
60 kg / ha	230.33±8.62[e]	397.00±4.58[d]	607.33±5.13[a]	455.67±4.51[b]	419.67±3.51[c]

Means across the row that do not share a letter are significantly different, SD= standard deviation

Appendix 5C: The effect of dosage (kg/ha) of hydrogels on girth of the cob (cm)

Dosage (kg/ha)	Control Mean±SD	Mean girth of the cob (cm) obtained when varied dose of the hydrogels were applied			
		HCE-2 Mean±SD	HCG-2 Mean±SD	HLE-2 Mean±SD	HLG-2 Mean±SD
15	4.30±0.20[e]	5.77±0.15[c]	7.40±0.20[a]	6.60±0.20[b]	5.23±0.06[d]
30	4.37±0.06[d]	6.77±0.15[c]	8.37±0.25[a]	7.33±0.06[b]	6.50±0.10[c]
45	4.20±0.10[e]	7.53±0.15[d]	10.70±0.10[a]	9.33±0.15[b]	8.40±0.10[c]
60	4.00±0.10[e]	7.90±0.10[d]	10.77±0.06[a]	9.40±0.20[b]	8.40±0.10[c]

Means across the row that do not share a letter are significantly different, SD= standard deviation

Appendix 5D: The effect of dosage (kg/ha) of hydrogels on cob length (cm)

Dosage (kg/ha)	Control Mean±SD	Mean cob length (cm) obtained when varied dose of the hydrogels were applied			
		HCE-2 Mean±SD	HCG-2 Mean±SD	HLE-2 Mean±SD	HLG-2 Mean±SD
15	10.33±0.15^{d}	12.30±0.20^{c}	14.70±0.10^{a}	13.13±0.15^{b}	13.33±0.06^{b}
30	10.50±0.10^{d}	16.23±0.12^{b}	17.80±0.10^{a}	15.33±0.25^{c}	15.30±0.17^{c}
45	10.17±0.06^{e}	17.13±0.15^{d}	20.40±0.10^{a}	18.80±0.10^{b}	18.40±0.10^{c}
60	10.27±0.06^{d}	18.10± 0.27^{c}	22.10±0.10^{a}	18.80±0.17^{b}	18.43±0.12^{bc}

Means across the row that do not share a letter are significantly different, SD= standard deviation

Appendix 5E: The effect of dosage (kg/ha) of hydrogels on cob grain weight per cob (g)

Dosage (kg/ha)	Control Mean±SD	Mean grain weight(g) per cob obtained when varied dose of the hydrogels were applied			
		HCE-2 Mean±SD	HCG- Mean±SD 2	HLE Mean±SD	HLG-2 Mean±SD
15	60.23±0.38^{e}	136.23±2.57^{d}	170.33±0.71^{a}	144.67±0.65^{b}	139.83±1.54^{c}
30	60.90±0.27^{e}	143.93±0.71^{d}	194.10±0.10^{a}	162.23±0.76^{b}	140.03±0.21^{c}
45	60.43±0.15^{e}	202.40±0.92^{c}	222.57±0.21^{a}	194.13±0.75^{b}	148.63±0.76^{d}
60	60.63±0.06^{e}	257.13±0.57^{d}	279.50±1.02^{a}	242.33±1.03^{b}	173.13±0.74^{c}

Means across the row that do not share a letter are significantly different, SD= standard deviation

Appendix 5F: The effect of dosage (kg/ha) of hydrogels on weight of the cob (g)

Dosage (kg/ha)	Control Mean±SD	Mean weight(g) of the cob obtained when varied dose of the hydrogels were applied			
		HCE-2 Mean±SD	HCG- Mean±SD 2	HLE-2 Mean±SD	HLG-2 Mean±SD
15	136.10±0.82^{e}	263.00±0.27^{c}	292.23±0.86^{a}	285.77±0.35^{b}	207.67±0.60^{d}
30	136.33±0.38^{e}	288.07±0.45^{b}	302.10±0.36^{a}	286.10±0.62^{c}	232.77±0.45^{d}
45	136.50±0.30^{e}	298.87±0.40^{c}	308.57±0.21^{b}	311.37±0.49^{a}	233.80±0.62^{d}
60	136.40±0.36^{e}	363.00±0.56^{c}	376.13±0.76^{a}	367.00±0.20^{b}	279.13±0.25^{d}

Means across the row that do not share a letter are significantly different, SD= standard deviation

Appendix 5G: The effect of dosage (kg/ha) of hydrogels on percentage shelling

Dosage (kg/ha)	**Control Mean±SD**	**Mean percentage shelling obtained when varied dose of the hydrogels were applied**			
		HCE-2 Mean±SD	**HCG-2 Mean±SD**	**HLE-2 Mean±SD**	**HLG-2 Mean±SD**
15	44.75±0.21^{d}	51.33±0.31^{c}	58.43±0.47^{b}	50.40±0.17^{a}	49.13±0.31a
30	44.37±0.31^{e}	58.93±0.67^{d}	64.07±0.61^{c}	56.90±0.10^{a}	55.43±0.40^{b}
45	44.30±0.40^{e}	67.20±0.10^{d}	72.70±0.56^{a}	62.17±0.32^{c}	59.63±0.45b
60	44.70±0.17^{e}	70.43±0.31^{d}	76.47±0.21^{a}	65.03±0.38^{c}	62.23±0.15^{b}

Means across the row that do not share a letter are significantly different, SD= standard deviation

Appendix 6A: The effect of dosage (kg/ha) of hydrogels on grain yield (kg/ha)

Dosage (kg/ha)	**Control Mean±SD**	**Mean grain yield (kg/ha) obtained when varied dose of the hydrogels were applied**			
		HCE-2 Mean±SD	**HCG-Mean±SD 2**	**HLE-2 Mean±SD**	**HLG-2 Mean±SD**
15	415.17±3.82^{e}	1362.83±5.58^{c}	1855.67±4.38^{a}	1589.60±3.05^{b}	1165.43±4.62^{d}
30	430.43±4.82^{e}	1478.07±7.40^{d}	1930.77±5.46^{a}	1670.37±5.71^{b}	1415.00±3.25^{c}
45	460.07±11.59^{e}	1620.53±2.91^{c}	2138.83±3.13^{a}	1845.03±7.44^{b}	1380.73±2.65^{d}
60	495.33±7.80^{e}	1780.13±3.42^{c}	2272.83±3.72^{a}	1905.80±3.44^{b}	1448.93±3.97^{d}

Means across the row that do not share a letter are significantly different, SD= standard deviation

Appendix 6B: The effect of dosage (kg/ha) of hydrogels on stover yield (kg/ha)

Dosage (kg/ha)	Control Mean±SD	Mean stover yield (kg/ha) obtained when varied dose of the hydrogels were applied			
		HCE-2 Mean±SD	HCG-Mean±SD 2	HLE-2 Mean±SD	HLG-2 Mean±SD
15	1917.43±1.35 e	3191.57±4.84 a	2717.93±2.06 c	2787.53±3.15 b	2152.23±4.23 d
30	1917.23±0.31 e	3253.50±4.05 a	2819.77±0.45 d	2887.70±2.57 b	2848.63±2.21 c
45	1917.83±0.25 e	3360.07±2.97 b	3472.50±2.92 a	3033.87±2.39 c	2962.33±3.85 d
60	1917.43±0.95 e	3391.33±2.81 b	3662.83±3.98 a	3078.73±1.96 d	3085.50±0.66 c

Means across the row that do not share a letter are significantly different, SD= standard deviation

Appendix 6C: The effect of dosage (kg/ha) of hydrogels on cob yield (kg/ha)

Dosage (kg/ha)	Control Mean±SD	Mean cob yield (kg/ha) obtained when varied dose of the hydrogels were applied			
		HCE-2 Mean±SD	HCG-Mean±SD 2	HLE-2 Mean±SD	HLG-2 Mean±SD
15	260.90 ± 1.81^{e}	556.53 ± 1.32^{d}	770.40 ± 1.21^{a}	785.67 ± 0.50^{b}	745.60 ± 0.98^{c}
30	289.83 ± 1.16^{e}	689.80 ± 1.05^{c}	950.67 ± 0.80^{a}	895.40 ± 0.96^{b}	796.87 ± 0.31^{d}
45	301.47 ± 1.62^{e}	815.60 ± 1.20^{d}	1045.90 ± 1.28^{a}	1020.67 ± 1.12^{b}	850.27 ± 1.32^{c}
60	316.37 ± 1.05^{e}	962.73 ± 1.27^{d}	1150.53 ± 1.12^{a}	1108.67 ± 1.06^{b}	918.43 ± 1.15^{c}

Means across the row that do not share a letter are significantly different, SD= standard deviation

Appendix 6D: The effect of dosage (kg/ha) of hydrogels on biological yield (kg/ha

Dosage (kg/ha)	**Control Mean±SD**	**Mean biological yield (kg/ha) obtained when varied dose of the hydrogels were applied**			
		HCE-2 Mean±SD	**HCG-Mean±SD 2**	**HLE-2 Mean±SD**	**HLG-2 Mean±SD**
15	2989.07±1.74^{d}	4441.53±1.19^{b}	4956.77±0.90^{a}	4055.77±0.61^{c}	3988.30±1.08^{d}
30	2987.63±1.02^{e}	4675.50±0.95^{c}	5110.90±0.85^{a}	4718.87±0.38^{b}	3916.20±0.95^{d}
45	2988.87±1.50^{e}	4829.27±0.71^{b}	5295.53±0.80^{a}	4721.37±1.16^{c}	4086.80±0.62^{d}
60	2987.43±1.08^{e}	4928.73±0.42^{b}	5455.80±0.56^{a}	4779.13±0.21^{c}	4203.80±0.70^{d}

Means across the row that do not share a letter are significantly different, SD= standard deviation

Appendix 6E: The effect of dosage (kg/ha) of hydrogels on harvest index (%)

Dosage (kg/ha)	Control Mean±SD	Mean harvest index (%) obtained when varied dose of the hydrogels were applied			
		HCE-2 Mean±SD	HCG-Mean±SD 2	HLE-2 Mean±SD	HLG-2 Mean±SD
15	13.43±0.25^{e}	30.53±0.40^{d}	37.20±0.46^{a}	29.83±0.25^{b}	29.23±0.55^{c}
30	14.167±0.25^{e}	31.533±0.51^{d}	37.467±0.25^{a}	31.333±0.25^{b}	31.767±0.42^{c}
45	15.333±0.32^{e}	33.300±0.20^{d}	40.667±0.21^{a}	33.433±0.32^{b}	33.267±0.25^{c}
60	16.43±0.40^{e}	36.53±0.31^{d}	41.50±0.27^{a}	34.60±0.36^{b}	34.40±0.20^{c}

Means across the row that do not share a letter are significantly different, SD= standard deviation